The role of mRNA translational regulation in models of hepatotoxicity

Thesis submitted for the degree of

Doctor of Philosophy

at the University of Leicester

by

Kate Marie Dudek, BSc.

MRC Toxicology Unit

University of Leicester

September 2013

ABSTRACT

The role of mRNA translational regulation in models of hepatotoxicity

Kate Marie Dudek

Over the past few years translational regulation has been shown to be critical, particularly in cases of cellular stress where it can elicit a rapid, efficient response at the protein level. It was, therefore, hypothesised that changes in mRNA translation might play an important role in compound-induced hepatotoxicity and that identifying such changes would provide a more complete understanding of the molecular mechanisms of such toxicity.

The translational profiling technique frequently used for *in vitro* samples was modified slightly to enable its use with *in vivo* samples and, it revealed that, in cases of acute, compound-induced hepatotoxicity more mRNAs showed a change at the translational level than at the transcriptional level. This suggested that the liver was acting rapidly at the translational level to alter protein activity following toxic insult. One mRNA that exhibited translational repression was selected for further investigation. Following compound-induced hepatotoxicity, *Dio3* demonstrated no change at the mRNA level, but a significant reduction in protein, thus, it was hypothesised that the translational repression of *Dio3* was the predominant factor regulating the reduction in protein. Furthermore, it was proposed that due to the involvement of *Dio3* in maintaining thyroid hormone levels, this was an important feedback mechanism by which the liver, upon early signs of damage, was acting rapidly to maintain its own energy equilibrium, avoiding global disruption of the hypothalamic-pituitary-thyroid axis.

miRNAs have been identified as translational regulators; however, there was no evidence that the translational repression of *Dio3* was miRNA-mediated. Global hepatic miRNA expression analysis did however, reveal that miRNAs appeared to mediate large networks important in the cellular response to compound-induced liver injury. Furthermore, by correlating miRNA and translational profiling data sets from the same models, it was possible to identify specific functionally-relevant miRNA-mRNA interactions. miRNA expression profiling was extended to the plasma of rats treated with one of the hepatotoxic compounds. A subset of miRNAs were differentially expressed following treatment and these appeared to mediate pathways involved in hepatic fibrosis and stellate cell activation, suggesting that they might function as predictive biomarkers following compound-induced hepatotoxicity.

The work presented in this thesis has expanded the existing data available for a number of models of compound-induced hepatotoxicity to encompass global changes in both mRNA translation and miRNA expression. It has shown that mRNA translation, regardless of how it is regulated, plays an important role in the dynamic response of the liver to cellular stress induced by hepatotoxic compounds.

ACKNOWLEDGEMENTS

Over the past five years I have been very fortunate in being able to work with a range of people who have offered support, encouragement and advice. In fact it is difficult to know where to start in terms of thanking the necessary colleagues, friends and relations.

First of all, a big thank you to my supervisors, Professor Timothy Gant and Professor Andrew Smith. Tim took a chance on me at the start and gave me the opportunity to pursue this (at what has certainly seemed at times, crazy) idea. Without your encouragement, support and ideas I would not be where I am. Andy took me on board when Tim left for pastures new, with the main aim being to sort out the logistics of getting to the end. However, he proved a source of great knowledge and advice and always had an open door for discussion, so I am very grateful for all he has done.

I have been privileged to work with many people over the last five years, all of whom have helped in some way, be it through technical advice, practical help or simply providing a friendly ear and words of comfort and support. I would like to thank Mr David Read for his help obtaining histopathological images, Mr Pete Willan who helped me in my mad panic to complete a last animal study with one day to spare on our project licence, and all the other people who have helped throughout the years. Thanks to Dr Fiona Sewell, a friend from my undergraduate days who was only ever an email away and has offered so much encouragement and advice to me, particularly over the last few months. Particular mention to three special ladies who propped me up, fed me coffee and wine (not simultaneously!) and have become good friends; Joan Riley, Jinli Luo and Carolyn Jones. Thank you for your practical help and your emotional support, especially to you Carolyn, who has really had to live the ups and downs of the last few months with me. I am forever grateful.

For some people a simple thank you does not seem sufficient. Emma Marczylo, I literally would not be at this stage were it not for you. For all you have done, for your friendship, support, loyalty and endless practical assistance I thank you!

I am also fortunate to have an amazingly strong support network of friends and family, all who have offered endless encouragement and love over the past five years. Mum, Dad, Jane, Nan, Mick and Annette; you never doubted me and for that I thank you. Likewise my friends have been amazing, even if the idea of chopping up rat livers for a job continually bemuses them, so I would also like to thank Keely, Sarah and Barry.

Finally, to my Tom, for being my husband and my best friend. For your endless loyalty, belief, support and love. You believed I could do this when I had serious doubts, you wiped the tears away, made me laugh, did so many small things that meant I could get to this point (you even cooked most of our dinners for the past five months!) I thank you from the bottom of my heart.

I dedicate this thesis to all my friends and family. I could not have done it without you.

LIST OF CONTENTS

LIST OF TABLES

LIST OF FIGURES

LIST OF ABBREVIATIONS

µl	Microlitre
µM	Micromolar
Abc	ATP-binding cassette
ADR	Adverse drug reaction
aFGF	Acidic fibroblast growth factor
AhR	Aryl hydrocarbon receptor
ALT	Alanine transaminase
AO	Arachis oil
APS	Ammonium persulphate
AST	Aspartate aminotransferase
ATP	Adenosine triphosphate
BRCA1	Breast cancer-associated protein 1
BSA	Bovine serum albumin
CAR	Constitutive androstane receptor
CCl_4	Carbon tetrachloride
Cel	*Caenorhabditis elegans*
CIP	Calf intestinal alkaline phosphatase
CNS	Central nervous system
CO_2	Carbon dioxide
CT	Cycle threshold
Cy-3	Cyanine-3
Cy-5	Cyanine-5
Cyp	Cytochrome P450
D1	Dio1 protein
D2	Dio2 protein
D3	Dio3 protein
Dio1	Iodothyronine deiodinase type I
Dio2	Iodothyronine deiodinase type II
Dio3	Iodothyronine deiodinase type III
Dio3os	Dio3 opposite strand
DMEM	Dulbecco's Modified Eagle Medium
DMSO	Dimethyl sulfoxide
DNA	Deoxyribonucleic acid
Dnmt	DNA methyltransferase
Dpm	Disintegrations per minute
DTT	Dithiothreitol
EDTA	Ethylenediaminetetraacetic acid
eEF	Eukaryotic elongation factor
EGF	Epidermal growth factor
eIF	Eukaryotic initiation factor
ER	Endoplasmic reticulum
eRF	Eukaryotic response factor
EtOH	Ethanol
FCS	Foetal calf serum

FOXO TF	Forkhead box class O transcription factors
G	Griseofulvin
Gapdh	Glyceraldehyde 3-phosphate dehydrogenase
GTFs	General transcription factors
GTP	Guanosine triphosphate
H	Hour
H & E	Haematoxylin and eosin
HD	High dose
Ip	Intraperitoneal
IPA	Ingenuity pathway analysis
IRE	Iron-responsive element
IRES	Internal ribosome entry site
LNA	Locked nucleic acid
lncRNAs	long non-coding RNAs
Lowess	Locally weighted scatterplot smoothing
M	Molar
m^7G	7-methyl-guanosine
MEEBO	Mouse exonic evidence based oligonucleotide
met-$tRNA_i$	methionine-loaded initiator tRNA
Mg	Miligram
$MgCl_2$	Magnesium chloride
min	Minute
MIQE	Minimum Information for Publication of Quantitative Real-Time PCR Experiments
miRNA	microRNA
mM	Milimolar
MRC	Medical Research Council
mRNA	Messenger RNA
MTS	3-(4,5-dimethylthiazol-2-yl)-5-(3-carboxymethoxyphenyl)-2-(4-sulfophenyl)-2H-tetrazolium
Na	Sodium
NaCl	Sodium chloride
NaOAC	Sodium acetate
NaOH	Sodium hydroxide
NTC	Non template control
ORF	Open reading frame
PABP	Poly (A)-binding protein
PBS	Phosphate buffered saline
PCR	Polymerase chain reaction
piRNA	Piwi-interacting RNA
PNACL	Protein Nucleic Acid Chemistry Laboratory
PredTox	Predictive Toxicology
pre-miRNA	Precursor miRNA
pre-mRNA	Precursor mRNA
pri-miRNA	Primary miRNA
PXR	Pregnane-X receptor
qRT-PCR	quantitative Reverse transcription-PCR
RIA	Radioimmunoassay

RIN	RNA integrity number
RISC	RNA-induced silencing complex
RNA	Ribonucleic acid
RT	Room temperature
-RT	Reverse transcription reaction excluding reverse transcriptase
rT3	Reverse T3
RXR	Retinoid X receptor
s	Second
SDS	Sodium dodecyl sulfate
SEM	Standard error of the mean
Sesn1	Sestrin1
siRNA	Short interfering RNA
Smarce1	SWI/SNF related, matrix associated, actin dependent regulator of chromatin, subfamily e, member 1
SMCE1	Smarce1 protein
SMEs	Small and medium enterprises
SNPs	Single nucleotide polymorphism
SSC	Saline-sodium citrate
sumo	Small ubiquitin-related modifier
T2	3,3'-diiodothyronine
T3	3,5,3'-triiodothyronine
T4	Thyroxine
TATA	(A/T) A (A/T) (TATA box)
TBE	Tris/Borate/EDTA
TBP	TATA box binding protein
TBST	Tris buffered saline
T_C	Transcription
TH	Thyroid hormone
T_L	Translation
TNFα	Tumour necrosis factor alpha
TR/RXR	Thyroid hormone receptor/retinoid X receptor
TRH	Thyrotropin-releasing hormone
Tris-HCl	Tris(hydroxymethyl)aminomethane-hydrochloric acid
tRNA	Transfer RNA
TSH	Thyroid-stimulating hormone
UTR	Untranslated region
UV	Ultraviolet
V	Vehicle
XRE	Xenobiotic response element
ΔΔCT	Delta delta CT

CHAPTER 1: INTRODUCTION

1.1 THE LIVER

The liver is the largest internal organ, constituting between 2.5 – 5% of the body mass of both rodents and humans. Its functions are widespread and include metabolism of carbohydrates, fat, hormones and natural and synthetic chemicals; and synthesis of fibrinogen and bile acids. Blood is supplied to the liver via the hepatic portal vein (approximately 80%) and the hepatic artery (approximately 20%) (Lautt and Greenway, 1987), which together with the bile duct comprise the portal triad. The rich blood supply to and from the liver (blood exits through the hepatic vein to the vena cava), means that the liver is the first site of exposure for many ingested chemicals.

1.1.1. The structure of the liver

The liver is comprised of adjoining lobules. Whilst hepatocytes constitute approximately 60% of the liver (Weibel et al., 1969), the remainder is comprised of other cells, including endothelial cells, bile canniculi cells, kupffer cells and Ito cells (Fig. 1.1).

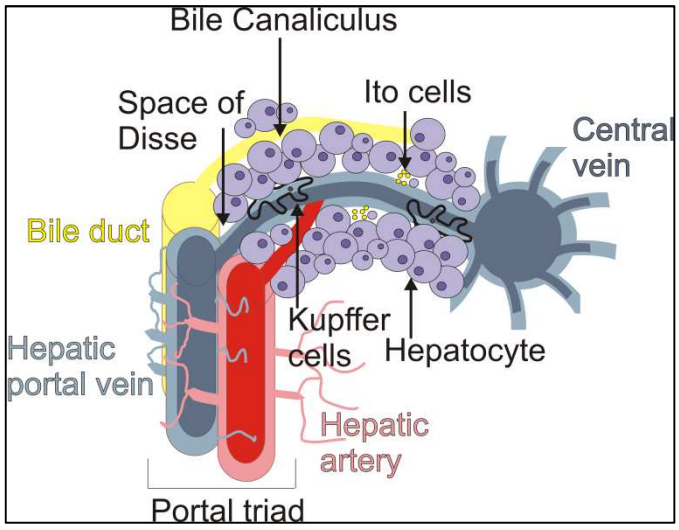

Fig. 1.1. Organisation of the liver lobule.

The region closest to the portal triad is called the periportal zone (I) and it is generally here that hepatocytes arise by division. With age they move closer to the central vein, to an area known as the centrilobular zone (III). The hepatocytes in this zone are less well protected from reactive oxygen species than those in the periportal zone and are supplied by blood lower in oxygen and nutrients (Popp and Cattley, 1991). Despite this most biotransformation occurs in zone III, thus processes such as oxidation, reduction and hydrolysis take place here, rendering hepatocytes in this zone more susceptible to damage (Greaves, 2012). The fat storing cells of Ito are located in the space of Disse (Suematsu and Aiso, 2001). These cells are the main fibrinogenic cells in the liver, they produce cytokines and prostaglandins in response to toxic stimuli and thus, are an essential part of the mechanism in responding to hepatic damage and initiating regeneration (Flisiak, 1997). Ito cells are identical to the stellate cells identified by Kupffer in 1876 (Aterman, 1986). Following damage to the liver the normally quiescent stellate cells lose vitamin A and are transformed into proliferative, fibrogenic myofibroblasts (Friedman, 2000; Hui and Friedman, 2003). Fibrosis is a tightly regulated reversible process, however, without intervention it can lead to irreversible liver cirrhosis (Friedman, 2000). Thus, early identification of fibrosis, through the monitoring of stellate cell activation, can serve as a useful warning and prevent more lasting liver damage. Kupffer cells are phagocytic and are located on the endothelial cells. They appear to have a dual phenotype during fibrinogenesis and repair (Friedman, 2005). During liver injury they promote proliferation and apoptosis and assist in matrix formation, whereas with recovery they cease to support the activated stellate cells and switch to promoting matrix degradation (Duffield et al., 2005). An absence of Kupffer cells has been shown to increase the susceptibility of mice to drug-induced liver injury (Ju et al., 2002), thus inferring a major protective role for these cells.

Bile ducts are responsible for bile transport. They form the bile canaliculi, which are in direct contact with the hepatocytes, enabling bile secretion. If bile secretion is inhibited, any biliary constituents that are normally released into the intestine for excretion are retained in the liver and blood, thus leading to the development of hyperbilirubinemia or cholestasis (Greaves, 2012). Cholestasis is a major symptom of compound-induced liver injury and can occur with and without observable hepatocyte damage (Padda et al., 2011). Cholestasis is essentially a disruption in bile production, it can be caused directly by a compound, or by its metabolites, or by an auto-immunological response to the compound. This makes identification of the underlying toxic mechanism very difficult.

1.1.2. The liver and metabolism

Phase I metabolism in the liver requires a catalytic agent. Whilst alcohol dehydrogenase, mono-oxygenases and esterases are sometimes recruited, the most common catalysts are the cytochrome P450 (Cyp) enzymes. This family of genes are structurally conserved and have been identified in plants and bacteria as well as humans and rodents (Danielson, 2002). The Cyp enzymes contain an iron protoporphyrin IX group, which selectively activates oxygen and thus catalyses a set of reactions including hydroxylation, oxidation, dealkylation and reduction (Jeffery, 1991). These reactions involve the addition of a functional group, such as –OH, to a compound, meaning a conjugate can be added during phase II metabolism. In some cases compounds will interact with the Cyp enzymes and either over-induce their activity or inhibit their function. This is a major cause of negative compound interactions. Examples of compounds that are detrimental to Cyp functions are Ethylene, CCl_4 and Halothane. These react with the iron moiety and either inhibit haem synthesis, or in severe cases destroy the Cyp enzymes (Kyle and Farber, 1991). Phase II metabolism involves the addition of a water-soluble conjugate to the phase I metabolised compound. This can occur via mechanisms including, but not limited to glucuronidation, sulphation and acetylation, all of which require enzyme activation and are used for the metabolism of endogenous substrates, such as steroids, hormones, or neurotransmitters, and exogenous compounds, such as drugs (Jeffery, 1991). Once this step is complete the remaining metabolites are exported from the liver via excretion. Excretion occurs via the urine or via the bile (Jeffery, 1991); if the metabolised compound is between 300 and 450 Da it is too large to pass through the glomerular filtrate in the kidney and thus will be excreted in the bile. Toxic compounds that do pass into the kidneys can cause additional nephrotoxicity, hence the reason why nephro- and hepatotoxicity sometimes occur simultaneously. As discussed in section 1.1.1, a disruption in bile flow can lead to cholestasis, which can cause the accumulation of compounds to toxic levels. Some hepatotoxic compounds block excretion via the bile ducts, causing bile acid to collect, potentially leaking into, and thus damaging, the surrounding hepatocytes. The thiazolidinediones are thought to cause toxicity through this type of mechanism (Funk et al., 2001; Snow and Moseley, 2007). The Abc family of genes are heavily implicated in compound excretion via the bile (Jonker et al., 2009).

1.1.3. Hepatic injury

The liver plays a fundamental role in the metabolism of any compound that enters the body. This renders it prone to insult or injury from toxic compounds or metabolites. Fortunately, hepatocytes are highly adaptive and the liver has a remarkable regeneration capability. Following a 2/3 hepatectomy of a rodent liver, restoration of liver mass is virtually complete 7 - 10 days after the procedure (Michalopoulos, 2007; Yin et al., 2011). However, this is an adaptive response, and if the toxic insult is sufficiently severe irreparable damage is observed. Examples of compound-induced cellular insult are provided in Table 1.1. Due to the production of reactive oxygen species, the liver is also susceptible to conditions such as viral hepatitis, non-alcoholic steatohepatitis and hepatocellular carcinoma (Shin et al., 2013; Zhu et al., 2012). However, as this thesis explores genetic regulation in response to compond-induced hepatotoxicity, the summary provided in Table 1.1 is limited to histopathological symptoms of xenobiotic exposure. Many of the insults occur in combination and the onset of some can result in an increased susceptibilty to damage induced by different means. For example, microvesicular steatosis sensitises mice to Fas-mediated hepatocyte apoptosis (Feldstein et al., 2003). Furthermore, some agents, such as safrole and ponceau MX, cause changes to the liver that are excaberated over time, eventually resulting in long-term toxicity and hepatic carcinogenicity (Crampton et al., 1977).

Table 1.1. Types of cellular injury observed with compound-induced hepatotoxicity.

Cellular injury	Histopathological/clinical symptoms (Greaves, 2012)	Compound(s)
Steatosis (fatty change)	Lipid containing cytoplasmic vacuoles (microvesicular) → "Foamy" appearance Large single vacuoles (macrovesicular) → Displaced nucleus	Valproic acid (Fromenty et al., 1997) Carbon tetrachloride (Kubota et al., 2013; Rao et al., 1997) Pyrrolizidine (Fox et al., 1978)
Hypertrophy/hyperplasia	Cellular proliferation Margination of chromatin Round eosinophilic cytoplasmic inclusions Increased metabolising enzyme activity	Phenobarbital (Jones et al., 1993) Mitemcinal (GM-611) (Hayashi et al., 2008) Ibuprofen (Bendele et al., 1993)
Peroxisomal proliferation	PPARα and PPARγ activation Increased catalase activity	Cl-924 (hypolipidemic) (Walker et al., 1996) Methapheniline (Reznik-Schuller and Lijinsky, 1983) Ibuprofen (Bendele et al., 1993)
Necrosis	Eosinophilic hepatocytes Congestion and inflammation	Acetaminophen (Antoine et al., 2009; Davidson and Eastham, 1966) Thioacetamide (Porter et al., 1979; Shirai et al., 2013) Ethanol (Cohen and Nagy, 2011) Carbon tetrachloride (Kubota et al., 2013) Dimethylnitrosamine (George et al., 2001; Jezequel et al., 1987)
Apoptosis (single cell necrosis)	Cell shrinkage and fragmentation Phagocytosis Increased hepatic enzyme levels	Cocaine (Cascales et al., 1994) Cycloheximide (Alessenko et al., 1997; Ito et al., 2006) Mitomycin C (Castaneda and Kinne, 1999)
Inflammation	Aggregates of cells (often cluster around necrotic hepatocytes) Vascular Dilation Intranuclear inclusions Granulomas	Thioacetamide (Hsu et al., 2012) Glyburide (Saw et al., 1996) Atorvastatin (Walsh and Rothwell, 1999)
Chronic inflammation (chronic hepatitis)	Inflammatory infiltrate (composed of lymphocytes and plasma cells) Erosion of limiting plate Collapse of reticulin, extending fibrous strands	Sulfonamide (Tonder et al., 1974) Oxyphenisatin (Reynolds et al., 1971) Chlorpromazine (Russell et al., 1973) Nitroimidazole (Ersoz et al., 2001)

Table 1.1. continued

Cellular injury	Histopathological/clinical symptoms (Greaves, 2012)	Compound(s)
Mallory bodies	Homogenous dense intracytoplasmic bodies Enlarged hepatocytes Accumulation of cytokeratins 8 and 18	Griseofulvin (Fortier et al., 2010; Knasmuller et al., 1997) Ethanol (Crawford, 2012)
Cirrhosis *(regenerative hyperplasia)*	Fibrosis Nodular lesions	Ethanol (Crawford, 2012) Thioacetamide (chronic) (Li et al., 2002; Nuber et al., 1980)
Porphyrin pigments	Red-browm pigment globules in bile canaliculi Small granules in hepatocytes and Kupffer cells Portal tract inflammation Activation of stellate cells, increasing fibrosis	Griseofulvin (Knasmuller et al., 1997; Zatloukal et al., 2007) Hexachlorobenzene (Ockner and Schmid, 1961) Dideoxycytidine (DDC) (Zatloukal et al., 2007) 3-[(arylthio)ethyl]sydnone (TTMS) (Stejskal et al., 1975)
Cholestasis	Accumulation of bile pigments in the bile caniculi (bile plugs) Disruption of hepatocyte junctions	Griseofulvin (Gant et al., 2003) Chlorpromazine (Akerboom et al., 1991) α-Naphthylisothiocyanate (Greaves, 2012; Richards et al., 1982)

Examples of compounds that induce the histopathological/clinical symptoms associated with the different types of cellular injury.

1.1.4. Adverse drug reactions

The presentation of one or more of the symptoms listed in Table 1.1 can cause a drug to fail during the development phase. In fact, along with cardiotoxicity, hepatotoxicity is one of the major reasons why drugs fail the testing process (Ferri et al., 2013; Williams, 2006), often at huge cost to the pharmaceutical industry (Paul et al., 2010). Although a clear testing structure is in place for any new candidate drug (Fig. 1.2), drug-induced liver injury remains the main cause of drug withdrawal from the market (Williams, 2006) and it cannot always be predicted during pre-clinical testing.

Adverse drug reactions (ADRs) were first categorised by the World Health Organisation in 1972 as "A response to a drug that is noxious and unintended and occurs at doses normally used in man for the prophylaxis, diagnosis or therapy of disease, or for modification of a physiological function" (WHO, 1972). Originally ADRS were classified into three main categories; augmented, idiosyncratic and chemical (Park et al., 1998); however this terminology has now been extended to encompass four distinct types. Type A ADRs can often be predicted from the pharmacology or chemical structure of a drug or its metabolites and show a dose response. Type B, or idiosyncratic, ADRs are not predictable and can show large inter-patient variability and no dose response. Type C ADRs are associated with long-term exposure and can usually be predicted, and type D ADRs are delayed reactions that occur after termination of treatment (Stachulski et al., 2013). Type B (idiosyncratic) ADRs are a problem due to the unpredictability, they can occur due to the formation of toxic metabolites, which can demonstrate either on-target or off-target effects. The Cyp enzymes are particularly prone to forming toxic metabolites and subsequently ADRs. Cyp2d6 is involved in the metabolism of many drugs, including, but not limited to, opioids (Kirchheiner et al., 2007), β-blockers (Andrade, 2013) and anti-cancer therapeutics such as Tamoxifen (Zafra-Ceres et al., 2013). However, the large number of genetic polymorphisms of Cyp2d6 dramatically alter how efficiently the enzyme is able to metabolise its target drug (Zhou, 2009).

Although it may not prove possible to ever predict every potential ADR, elucidating the molecular basis of current hepatoxins provides a better understanding of the underlying mechanisms of toxicity. One frequently studied hepatotoxin is Acetaminophen. Widely used as an analgesic, Acetaminophen can cause necrosis (Table 1.1), in some cases after only a single dose (Williams, 2006). Acetaminophen toxicity is the most common form of acute liver injury in the United Kingdom (Chun et al., 2009), and is thought to be due to the production of reactive metabolites, including N-acetyl-p-benzoquinoneimine (Nelson, 1990). Insufficient

clearance of this metabolite results in oxidative stress, through the depletion of glutathione and the production of excessive oxygen radicals (Davis et al., 1974). Using Acetaminophen overdose as a model, molecular biologists have been able to investigate changes in gene regulation, from the transcript level to the protein level, thus obtaining a more comprehensive understanding of the mechanism underlying its toxicity (Ruepp et al., 2002). Furthermore, recent work has investigated nucleic acid changes in the plasma and serum following Acetaminophen treatment with the aim of identifying novel bioamrkers of drug-induced hepatotoxicty (Antoine et al., 2009; Fannin et al., 2010; Starkey Lewis et al., 2012).

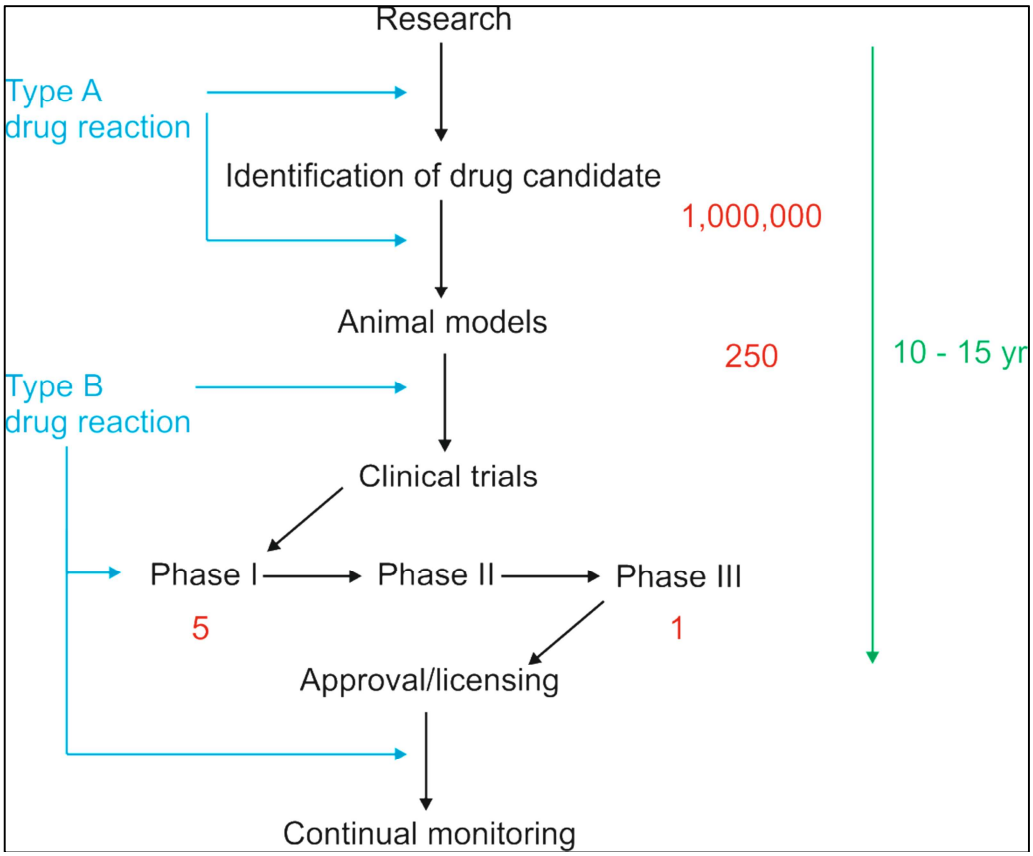

Fig. 1.2. The process of drug development. Red numbers denote approximate numbers of novel compounds that enter each stage of testing (values taken from Understanding Animal Research (http://www.understandinganimalresearch.org.uk/)).

1.2. MODEL SYSTEMS

As described in section 1.1.3 many compounds can cause hepatotoxicity. Some, such as Acetaminophen, are generally well tolerated and non-toxic when administered at pharmaceutical doses, but cause profound toxicity following overdose (Larson et al., 2005). Others fail during the development process (Fig. 1.2) because of significant side effects. Finally, there are some compounds that do not fail at any of the pre-clinical test stages, but cause pronounced toxicity (usually idiosyncratic ADR) in a subset of patients. Thus, there are a number of reasons why the molecular mechanisms of compound-induced hepatotoxicity need to be better understood. Firstly, so that compounds that fail during development can be identified as early in the process as possible, thus reducing the large financial and time costs involved (Paul et al., 2010). Secondly, to prevent and treat overdose and unexpected adverse toxicities in susceptible patients.

The work presented in this thesis used a range of models of compound-induced hepatotoxicity. Two of these (the Griseofulvin-treated mouse and the Thioacetamide-treated rat) are commonly used models of hepatotoxicity, implemented widely by the research community to better understand the molecular basis of such toxicity. Due to the known species differences in the reponse to toxic stimuli (Cunningham, 2002; Koufaris and Gooderham, 2013), using mouse and rat model systems was advantageous. A further example of compound-induced hepatotoxicity came courtesy of the Predictive Toxicology (PredTox) consortium. Rather than using known hepatotoxins, this consortium was established to investigate compounds that had themselves failed during the development process. Data mining and sharing, through the establishment of a consortium such as this, is regarded as a useful tool for obtaining an improved mechanistic understanding of toxicity (Park et al., 2011). Furthermore, the use of compounds that had failed at a late stage in development, meant they could still serve a useful purpose, despite not reaching the clinic. Each of the models is described in more detail in sections 1.2.1-1.2.3.

1.2.1. Griseofulvin

Griseofulvin was originally developed as an anti-fungal treatment, and was used most frequently in the treatment of athlete's foot (Gupta et al., 1994). When given orally to mice, it produces symptoms resembling those seen in patients with erythropoeitic protoporphyria-associated liver disease (Gant et al., 2003; Knasmuller et al., 1997). The histopathological signs of hepatotoxicity following Griseofulvin treatment include cholestasis, mallory body formation and porphyrin deposits (Table 1.1). Griseofulvin inhibits the final enzyme in the haem biosynthesis pathway, thus leading to the toxic accumulation of porphyrins (Fig. 1.3). Whilst the underlying biochemistry for Griseofulvin-induced toxicity is known and hepatic gene changes at the transcriptional level are well characterised (Gant et al., 2003), genetic regulation at the translational level has not yet been explored. Thus, this model was selected for the investigation of translational regulation in response to compound-induced hepatotoxicity.

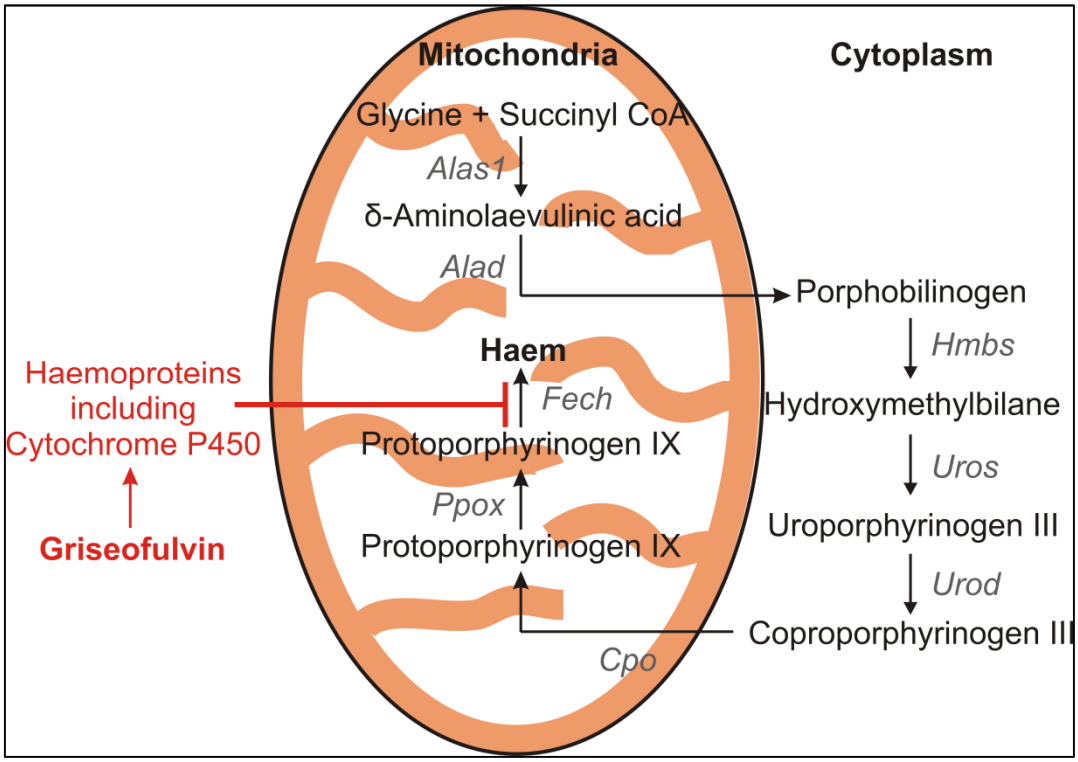

Fig. 1.3. The haem biosynthesis pathway. Major regulatory genes are marked in italics. *Alas1*=δ-Aminolevulinic acid synthase 1, *Alad*=δ-Aminolevulinic acid dehydratase, *Hmbs*= Hydroxymethylbilane synthase, *Uros*=Uroporphyrinogen III synthase, *Urod*=Uroporphyrinogen III decarboxylase, *Cpo*=Coproporphyrinogen oxidase, *Ppox*=Protoporphyrinogen IX oxidase, *Fech*=Ferrochelatase.

1.2.2. Thioacetamide

The Thioacetamide-treated rat was first identified as a model of hepatotoxicity by Gupta in 1956 (Gupta, 1956) and it is now well-established (Mehendale, 2005), not least because the histopathogical output closely mimics that seen in humans with chronic liver disease (Oren et al., 1996). The toxicity of Thioacetamide is due to metabolite formation. Cyp2e1, catalyses its activation, first to Thioacetamide-sulfoxide and then to the toxic metabolite Thioacetamide-disulfoxide (Chilakapati et al., 2005). Chronic treatment with Thioacetamide causes cirrhosis, and even acute, short-term treatment can cause pronounced necrosis and inflammation (Table 1.1). In the work presented in this thesis, the Thioacetamide-treated rat proved useful as an additional model of hepatotoxicity, supplementing and verifying the findings from the PredTox model. This was particularly important because of limited sample availiability from the consortium. Like the Griseofulvin model, changes at the translational level following treatment with Thioacetamide have not been reported to date and so this model was also selected for the investigation of translational regulation in response to compound-induced hepatotoxicity.

1.2.3. PredTox

The InnoMed PredTox consortium was set up in 2005 with a view to reducing the financial and time restraints caused by the extensive testing required for any new drug candidate (Paul et al., 2010). It comprised 15 pharmaceutical companies, 2 small and medium enterprises (SMEs) and 3 universities, and was formed under EU Framework Program 6. The members of the consortium sought to develop genomic biomarkers for the early detection of drug-induced toxicity. Male Wistar rats received pharmacologically-active doses of 14 compounds that had failed in development due to hepato- and/or nephrotoxicity. Samples taken from rats treated with each of the compounds were subject to various analyses, which included conventional toxicological techniques, such as clinical chemistry and histopathology; and newer ‘omics methods, such as transcriptomics and proteomics (see Chapter 2, section 2.1.3). This work resulted in the publication of a set of study reports summarising the data (Boitier et al., 2011; Matheis et al., 2011b; Suter et al., 2011). The consortium provided liver samples from the most severely hepatotoxic compounds, which enabled additional data sets to be generated.

1.3 GENE EXPRESSION

The gene expression pathway encompasses transcription, translation and post-translational modifications, including folding of the completed polypeptide chain to form an active protein (Fig. 1.4). Each of these steps are critical for determination of the phenotypic output of the cell, and are thus tightly regulated. This enables the cell to respond rapidly to changing conditions or toxic stimuli. It is vital to understand these steps at the molecular level in order to fully elucidate mechanisms of toxicity.

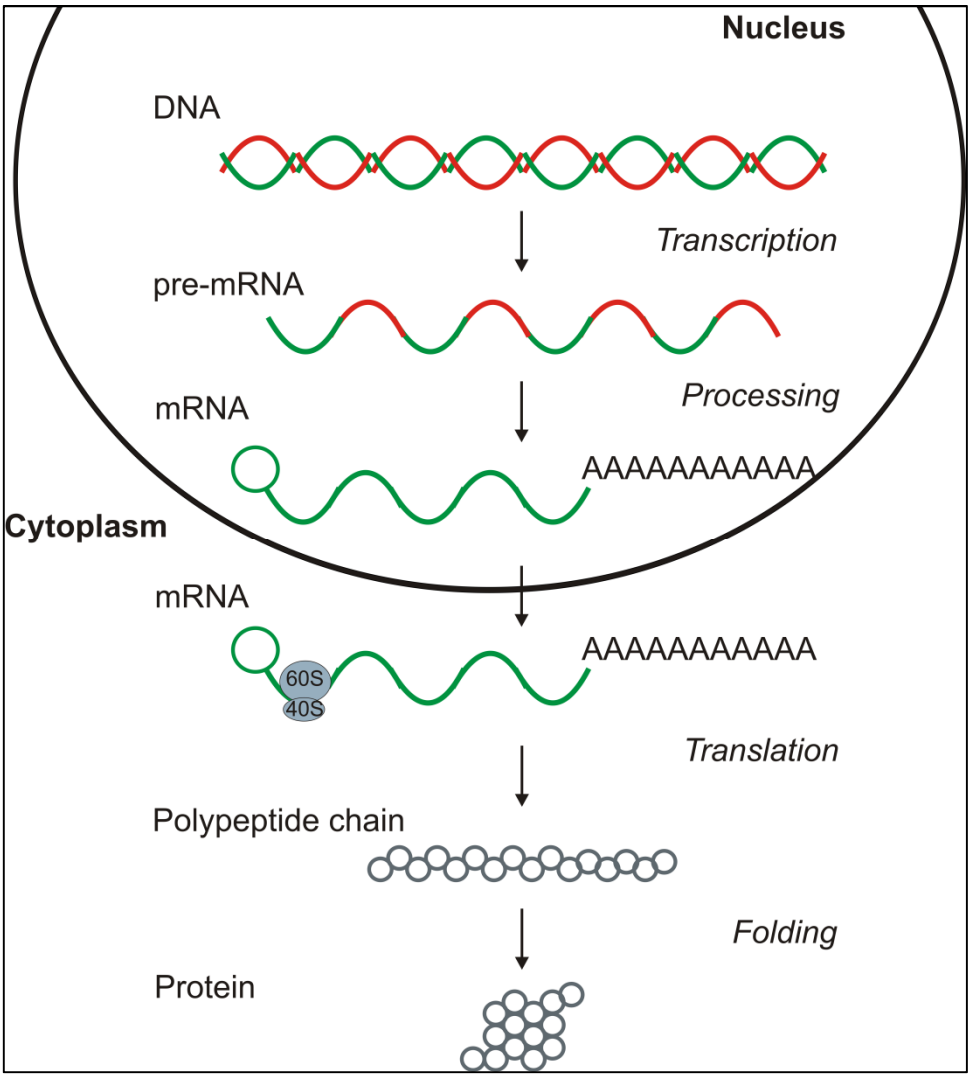

Fig. 1.4. The gene expression pathway.

1.3.1. Transcription

1.3.1.1 Process of transcription

The first step in the pathway is transcription. This is where, through the binding of helicase enzymes, double stranded DNA molecules undergo a conformational change, enabling RNA polymerase to bind and a complementary RNA strand to be produced. There are three eukaryotic polymerases, first identified in 1969 (Roeder and Rutter, 1969), each of which is responsible for transcribing different types of RNA. RNA polymerase I transcribes 18S and 28S ribosomal RNA, RNA polymerase II transcribes protein coding mRNAs and miRNAs, and RNA polymerase III transcribes tRNA and 5S rRNA (Thomas and Chiang, 2006).

mRNA transcription is a five step process involving pre-initiation, initiation, promoter clearance, elongation and termination. For transcription to occur the RNA polymerase requires a promoter site. This core region is located approximately 30 nucleotides upstream of the transcription start site (Carninci et al., 2006). The most well characterised example is the TATA (A/T) A (A/T) (TATA box) sequence (Hames and Hooper, 2000). A pre-initiation complex is formed through the successful recruitment of RNA polymerase and general transcription factors (GTFs) to the TATA box. These GTFs include TFIIA, TFIIB, TFIID, TFIIE, TFIIF and TFIIH (Baumann et al., 2010), which are recruited sequentially. TFIID contains TATA box binding protein (TBP) and TFIIB interacts with, and stabilises, TFIID; thus TFIID and TFIIB are critical for the recognition of the promoter region by the pre-initiation complex (Butler and Kadonaga, 2002). Once RNA polymerase II, TFIIA, TFIIE and TFIIH have been recruited the resulting complex is ready to begin transcribing the gene. TFIIH is a large multicomponent protein that has ATPase-dependent helicase activity, which allows the promoter to open and phosphorylates the carboxy-terminal domain of RNA polymerase II (Compe and Egly, 2012). The release of RNA polymerase II from the complex signals the start of the elongation phase of transcription. The process of transcription initiation (including pre-initiation, initiation and promoter clearance) is shown in Fig. 1.5. The RNA polymerase then proceeds along the DNA strand, and using complementary base pairing, produces an RNA molecule with an identical sequence to the coding DNA strand. The strand continues to elongate until a terminator region is reached, where the hydrogen bonds linking the RNA and DNA molecules break, releasing the newly synthesised complementary RNA molecule.

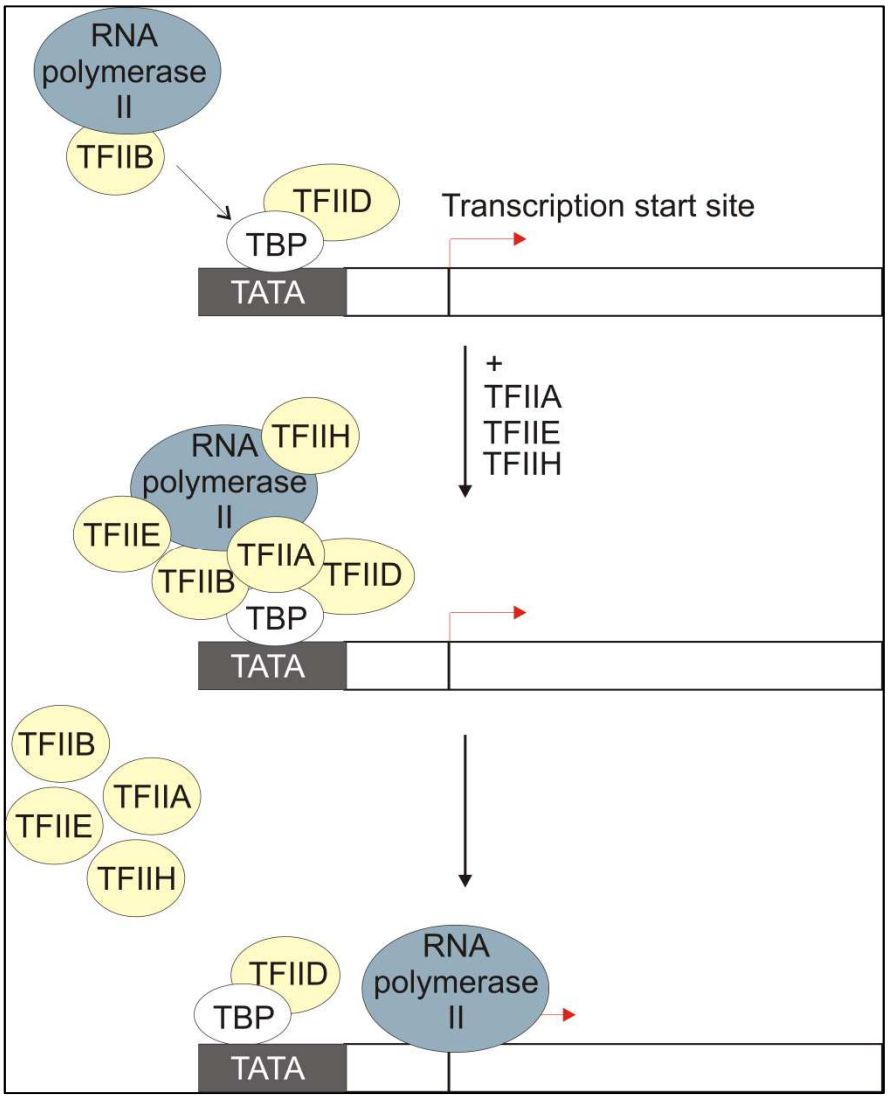

Fig. 1.5. Transcription initiation. The initiation complex is formed by the binding of RNA polymerase II and a set of GTFs to the TATA promoter region, which is located approximately 30 nucleotides upstream of the transcription start site.

The resulting primary transcript encodes at least one gene, which can be either protein coding or non-protein coding. Protein coding transcripts are strands of precursor mRNA (pre-mRNAs) which undergo further processing to form mature mRNAs, which are exported to the cytoplasm and undergo translation to form proteins. Non-protein coding genes often have a regulatory role and include species such as miRNAs and lncRNAs (see sections 1.3.2.2.1 and 1.3.2.2.3). Alternatively some genes that do not code for specific proteins, play an accessory role in the protein assembly machinery.

A series of processing steps are required for the pre-mRNAs to form complete mRNAs and encode proteins. First a 7-methyl-guanosine (m^7G) cap is added to the 5' end of the pre-mRNA strand (Shatkin, 1976). This happens very early during processing (Salditt-Georgieff et al., 1980) and, in addition to promoting the initiation of translation (Shatkin et al., 1976), the cap structure increases stability and prevents pre-mRNA degradation by exonucleases (Furuichi et al., 1977). The m^7G cap is added via the activity of three enzymes; RNA triphosphatase, RNA guanylytransferase and RNA (guanine-7)-methyltransferase (McCracken et al., 1997), which remove the terminal 5' phosphate, add a G residue to the diphosphate 5' end, and add a methyl group to the N-7 position of the guanine ring (Hames and Hooper, 2000). The next processing step is polyadenylation, where up to 250 adenine (A) residues are added to the 3' end of the molecule, forming a poly(A) tail. This reaction is catalysed by poly(A) polymerases, using ATP as a precursor (Hames and Hooper, 2000). The poly(A) tail further stabilises the pre-mRNA and increases the efficiency of translation (Eckmann et al., 2011). The final step in the process is splicing. This is where intron regions are identified and excised from the pre-mRNA strand and the exons are ligated together (Pandya-Jones, 2011). Splicing is catalysed by the spliceosome (Wahl et al., 2009) and results in a functional mRNA strand that can undergo translation. Furthermore, it is during splicing that, through either exon removal or retaining of introns, alternative splice variants are formed. Thus a range of functionally distinct proteins can be synthesised from a single gene transcript (Hames and Hooper, 2000). A summary of these three processing steps is shown in Fig. 1.6.

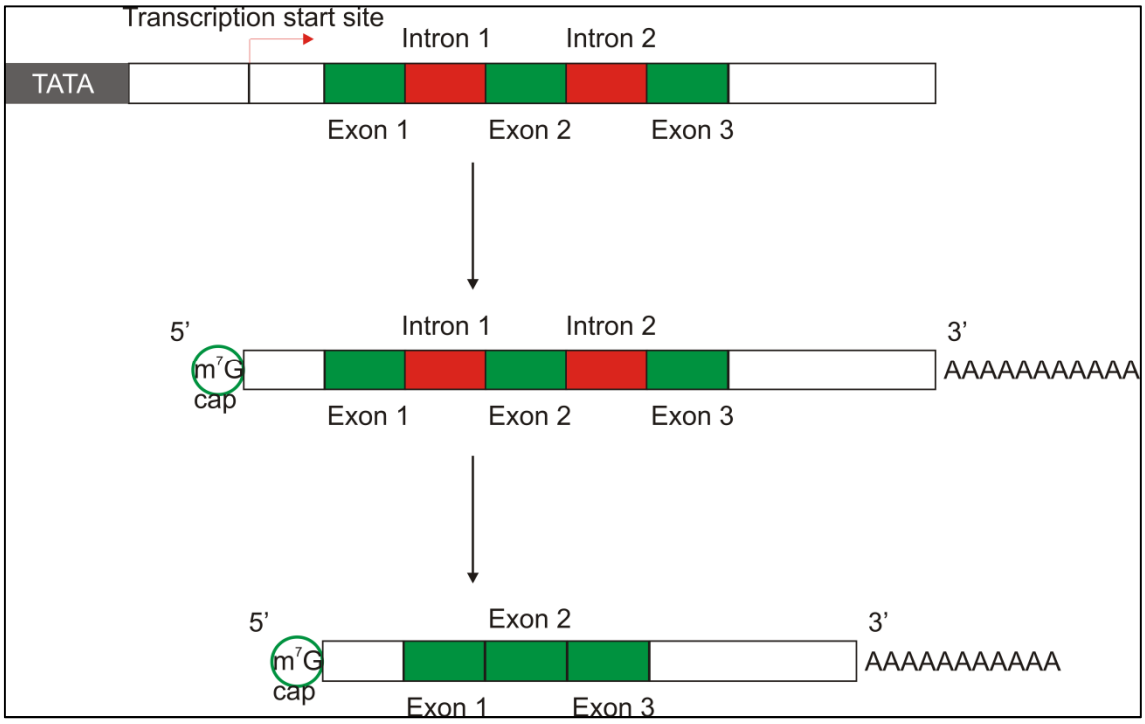

Fig. 1.6. Processing of pre-mRNA. The pre-mRNA is further processed prior to translation. A 5' m^7G cap is added first, then the 3' end undergoes cleavge and the additon of a poly(A) tail. This tail is a repeating sequence of approximately 200 adenines. Finally the intronic regions are removed and the exons are spliced together.

1.3.1.2 Regulation of transcription

Transcription factors are heavily involved in the stress resonse pathway, they bind to promoter regions of specific genes and are fundamental to regulation at the transcriptional level. They can be recruited within minutes and activate many proteins (Christmann and Kaina, 2013). Some of the most widely studied transcription factors include p53, breast cancer-associated protein 1 (BRCA1) and NF-κB. p53 is activated during DNA replication arrest or double strand breaks, it regulates a large number of genes involved in DNA repair and apoptosis (Polyak et al., 1997). BRCA1 interacts with p53 and is phosphorylated upon DNA damage (Tibbetts et al., 2000). BRCA1 is also associated with RNA polymerase II, thus functioning as a transcriptional co-activator (Anderson et al., 1998). NF-κB is activated by the IκB-kinase complex following DNA double strand breaks (Christmann and Kaina, 2013; Habraken and Piette, 2006). Transcription factors can act locally, or distally; they frequently function in combination with other factors and are highly cell-type specific (Dunham et al., 2012). To demonstrate just how complex genetic regulation can be, in addition to regulating many genes at the transcriptional level, transcription factors can themselves be regulated at the post-translational level. An example of this is seen with the liver-specific family of Forkhead box class O (FOXO) transcription factors (Tikhanovich et al., 2013).

During compound metabolism, transcription factors regulate the activity of both the Cyp enzymes and the transporters responsible for excretion in the final stage of the process. Recently documented examples include Cyp2b, Cyp2c and Cyp3a, which are induced by Pregnane-X receptor (PXR) (Mota et al., 2011), and the membrane transporters Abcc2, Abcc3, Abcg5, Abcg8, Slco1a1 and Slco1a4, which are induced by both PXR and constitutive androstane receptor (CAR) (Roques et al., 2013). The aryl hydrocarbon receptor (AhR) is a transcription factor specifically involved in the response to xenobiotics via its interaction with the xenobiotic response element (XRE) (Hao and Whitelaw, 2013). The complexity of transcriptional regulation is further demonstrated by the fact that during drug metabolism, in addition to binding to XREs, the AhRs, PXRs and CARs also interact with FOXO transcription factors to regulate energy metabolism (Konno et al., 2008).

Enhancer elements can also regulate transcriptional activity. They act from a distance, of up to a megabase (Nobrega et al., 2003), to regulate their target and thus, alter gene expression (West and Fraser, 2005). The long-range activity of enhancer elements, means they regularly exert off target effects on neighbouring genes (Butler and Kadonaga, 2001).

A further type of transcriptional regulation involves epigenetic mechanisms. Epigenetic modifications cause changes in transcription without altering the underlying DNA sequence, examples include DNA methylation and histone modifications (Cedar and Bergman, 2009; Suzuki and Greally, 2013). DNA methylation occurs when the methyl group of S-adenosyl methionine is transferred to the 5-position of cytosine, mainly within CpG islands (Bird, 2002; Miller et al., 1974). DNA methylation levels can alter with the increased presence of toxic metabolites (Li et al., 2013), suggesting a role for DNA methylation in toxicological processes. Furthermore, the DNA methyltransferases, Dnmt1, Dnmt3a and Dnmt3b, can act as co-repressors alongside transcription factors, to silence gene expression (Brenner et al., 2005; Fuks et al., 2001; Robertson et al., 2000). Histones are a family of proteins that assemble across a DNA strand in nucleosomes to form chromatin and thus exert a protective effect (Kornberg and Lorch, 1992). The structure of chromatin comprises eight histone molecules complexed with about 150 base pairs of DNA (Kornberg, 1977). Histone proteins can undergo a series of different post-translational modifications including acetylation, ubiquitylation, methylation, phosphorylation and sumoylation, each of which can alter the interaction between the complex of histone proteins and DNA, thereby regulating transcription (Shahbazian and Grunstein, 2007).

1.3.2. Translation

1.3.2.1 Process of translation

Translation comprises three key steps; initiation, elongation and termination, which result in the construction of a complete polypeptide chain. The first step in the process, initiation, is thought not only to be the most complex step (Filipowicz et al., 2008), but also the rate-limiting step (Gingras et al., 1999) and is, thus of fundamental importance.

Initiation of translation usually begins with recognition of the m^7G 5' cap by the eukaryotic initiation factor (eIF) eIF4F complex (Filipowicz et al., 2008). This complex contains eIF4E, which binds directly to the m^7G cap; eIF4A, which is a DEAD-box (Asp-Glu-Ala-Asp) RNA helicase; and eIF4G, which is a scaffold protein. Interaction of eIF4G with another initiation factor, eIF3, facilitates the recruitment of the 40S ribosomal subunit. eIF4G also interacts with poly (A)-binding protein (PABP), which binds to the 3' poly A tail, bringing the 5' and 3' ends of the mRNA together to form a circular loop (Wells et al., 1998). This results in increased stability and enables the regulatory factors located within the 3' untranslated region (UTR) to assist in initiating translation (Gebauer and Hentze, 2004). Translational efficiency is further enhanced by the synergistic activities of the 5' cap and 3' poly (A) tail (Gallie, 1991). The 43S-preinitiation complex is formed by the recruitment of additional initiation factors, including eIF2, which is coupled to GTP and methionine-loaded initiator tRNA (met-$tRNA_i$). The eIF4A is thought to unwind secondary structures in the 5' UTR, enabling the 43S complex to bind and scan the mRNA strand until an AUG start codon is reached. The met-$tRNA_i$ base pairs with the AUG codon in the ribosomal peptidyl (P)-site, forming the 48S complex. eIF5 is then recruited and catalyses the hydrolysis of eIF2-bound GTP; the energy generated enables the release of the initiation factors and the joining of the 60S ribosomal subunit (Blagden and Willis, 2011; Gebauer and Hentze, 2004). With the successful binding of the 60S ribosomal subunit, the 80S ribosome is formed and elongation proceeds. This process of cap-dependent initiation is responsible for approximately 90% of eukaryotic mRNA translation (Blagden and Willis, 2011) and is represented in Fig. 1.7. An alternative form of initiation is cap-independent, or internal ribosome entry site (IRES)-mediated translation. This type of translation initiation is more frequently observed in conditions of cellular stress (Spriggs et al., 2008) and involves the 40S ribosomal subunit binding directly to a highly structured IRES within the 5' UTR of the target mRNA (Blagden and Willis, 2011).

Elongation of translation proceeds via the activities of eukaryotic elongation factor (eEF)1A and possibly the initiation factor eIF5 (Saini et al., 2009). The exact role of eIF5 is unclear, but

eEF1A is thought to direct a met-$tRNA_i$ molecule to the ribosomal acceptor aminoacyl (A)-site, where codon recognition triggers further GTP hydrolysis, enabling binding (via peptide bonds) of the anticodon of the met-$tRNA_i$ to the ribosome. GTP hydrolysis causes a conformational change allowing movement of the met-$tRNA_i$ and mRNA, further catalysed by recruitment of elongation factor eEF2. eEF1A is released and recycled and further met-$tRNA_i$ molecules are recruited (Dever and Green, 2012). With each anticodon triplet that binds the protein chain is elongated via peptide bonds. Translation termination occurs when a stop codon is reached, in a reaction catalysed by eukaryotic response factors (eRFs) 1 and 3 (Zhouravleva et al., 1995). The exact mechanism of stop codon recognition remains elusive (Dever and Green, 2012). However, it is at this stage that the ribosomal subunits dissociate and the polypeptide chain is released (Filipowicz et al., 2008).

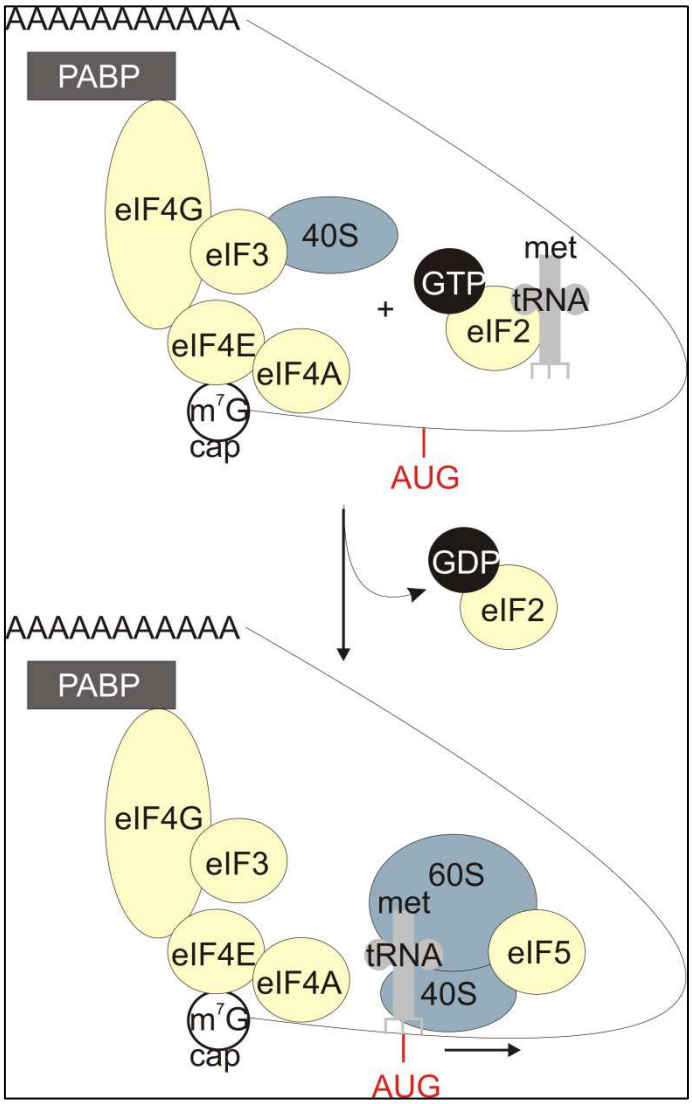

Fig. 1.7. Translation initiation. The 43S pre-initiation complex is formed by recruitment of the eIF4F complex to the 5' m^7G cap of the mRNA. The scaffold protein eIF4G, in combination with eIF3 facilitates recruitment of the 40S ribosomal subunit, which scans the mRNA strand until a start codon is reached. met-$tRNA_i$ binds to the AUG start codon and eIF2-bound GTP is hydrolysed, generating energy. With this energy the 60S ribosomal subunit is recruited and elongation can proceed.

1.3.2.2 Regulation of translation

As with all genetic regulation, translational regulation is a complex process. Most translational regulation occurs at the initiation phase (Sonenberg and Hinnebusch, 2009). In certain situations the global rate of protein synthesis is reduced following damage, but particular mRNAs are more efficiently translated as part of the stress response mechanism (Spriggs et al., 2010). It is suggested that in these instances translation initiation switches to being IRES-mediated (Powley et al., 2009). A further example of translational regulation is reinitiation, whereby the 40S ribosomal subunit, instead of dissociating at the terminator complex with the 60S subunit, remains bound to the mRNA strand and resumes scanning until another start codon is reached (Kozak, 1992). Reinitiation is an inefficient process resulting in reduced protein production (Kozak, 2005). It is observed during conditions of amino acid starvation when eIF2 is phosphorylated by a kinase protein. This phosphorylation prevents the hydrolysis of GTP and causes met-tRNA$_i$ to accumulate; as a result some of the 40S subunits bypass the closest AUG codons and are rendered susceptible to reinitiation (Kozak, 2005). Phosphorylation of eIF2 can also cause defects in metabolism and the transcriptional activation of stress response genes (Sonenberg and Hinnebusch, 2009). Translation initiation can be further regulated by mRNA binding proteins. These bind to the 5' end of the strand and prevent the recruitment of the ribosomal complex (Muckenthaler et al., 1998). One of the most well characterised examples is the interaction between ferritin and the iron-responsive element (IRE). They have a protective function, whereby if a cell is subject to oxidative stress the translation of ferritin is repressed by the recruitment of the IRE to the 5' strand of the mRNA (Gray and Hentze, 1994). An additional blocking mechanism occurs when RNA-binding proteins interact, causing tethering of the 3' and 5' ends, although this mechanism has predominantly been explored in *Drosophila melanogaster* to date (Cho et al., 2005).

Whilst less common, translational regulation can also occur at the elongation step. An example of this is frameshifting where the ribosome is induced to shift to an alternative overlapping reading frame (Matsufuji et al., 1995; Namy et al., 2004). Frameshifting is a form of recoding that results in the synthesis of two or more polypeptides (Gesteland and Atkins, 1996). The main objective of programmed frameshifting is to regulate polyamine levels and maintain telomeres (Namy et al., 2004). Non-programmed frameshift mutations have been reported in cancer, cystic fibrosis and hypertrophic cardiomyopathy (Chung et al., 2011; Iannuzzi et al., 1991; Xu et al., 2013), amongst other conditions, demonstrating the importance of understanding the molecular basis of this form of regulation. An alternative form of translational regulation during the elongation step is ribosomal pausing. This is where reduced

chaperone availability causes a build up of ribosomes within the first 50 codons (Liu et al., 2013). Interestingly this has been observed in cases of proteotoxic stress, where misfolded proteins accumulate (Liu et al., 2013), thus this regulatory mechanism could also be involved when compound-induced hepatotoxicity causes a build up of toxic metabolites.

A final mechanism of translational regulation involves non-coding RNA species, such as microRNAs (miRNAs), long non-coding RNAs (lncRNAs), short interfering RNAs (siRNAs) and piwi-interacting RNAs (piRNAs), all of which generally repress translation. As the research into these specific RNA species has grown, it is becoming more evident that they play a predominant role in regulating the expression of a large number of genes. In fact, in certain cases this form of RNA-mediated control is the primary determinant of gene expression (Bottley et al., 2010; El Gazzar and McCall, 2010; Greenman et al., 2007). Thus, miRNAs, lncRNAs, siRNAs and piRNAs are discussed in more detail below.

1.3.2.2.1 miRNAs

Since their discovery in 1993 (Lee et al., 1993; Wightman et al., 1993), there has been tremendous interest in the structure, function and behaviour of microRNAs (miRNAs). They have been experimentally demonstrated to play a role in a range of physiological and pathophysiological conditions including cancer (Baer et al., 2013), heart disease (Fiedler and Thum, 2013), obesity and liver disease (Hsu and Ghoshal, 2013) and, furthermore, miRNAs have been implicated in hepatotoxicity (Koufaris et al., 2012; Pogribny et al., 2007; Zhang and Pan, 2009).

Primary miRNA transcripts (pri-miRNAs) of up to and over 10,000 nucleotides are transcribed within the nucleus, usually by polymerase II promoters (Lee et al., 2004), although in some cases polymerase III promoters are used (Borchert et al., 2006). Polymerase II promoters usually contain toxicologically significant enhancer regions indicating a role for miRNAs in response to xenobiotics and cellular stress (Taylor and Gant, 2008). The transcripts are cleaved by the RNase III enzyme Drosha to form precursor miRNA stem-loops (pre-miRNAs) of approximately 70-100 nucleotides, which are transported to the cytoplasm via Exportin 5. Once in the cytoplasm, a second RNase III enzyme, Dicer, cleaves the pre-miRNA to form the mature miRNA duplex, comprised of the guide (miRNA) strand and an alternative (miRNA*) strand, each approximately 18-23 nucleotides long. This miRNA:miRNA* duplex unwinds and the guide strand is incorporated into the RNA-induced silencing complex (RISC), where it binds to the 3’ UTR of its target mRNA and initiates either translational repression or mRNA degradation (Taylor and Gant, 2008). Fig. 1.8 summarises this process. It is important to note

that the miRNA*can originate from either the 3' or 5' strand. These miRNA* strands were generally thought to be degraded and thus less involved in downstream regulation (Carthew and Sontheimer, 2009). However, as work has developed it has become clear that some of the miRNA* do have important functional roles, for example following cellular stress (Ro et al., 2007). Thus to avoid confusion regarding functional relevance and nomenclature most names within miRBase have now been updated so that miRNAs are named according to whether they are derived from the 3' or the 5' strand. For example, miR-1-3p is derived from the 3' strand, whilst mir-1-5p is derived from the 5' strand.

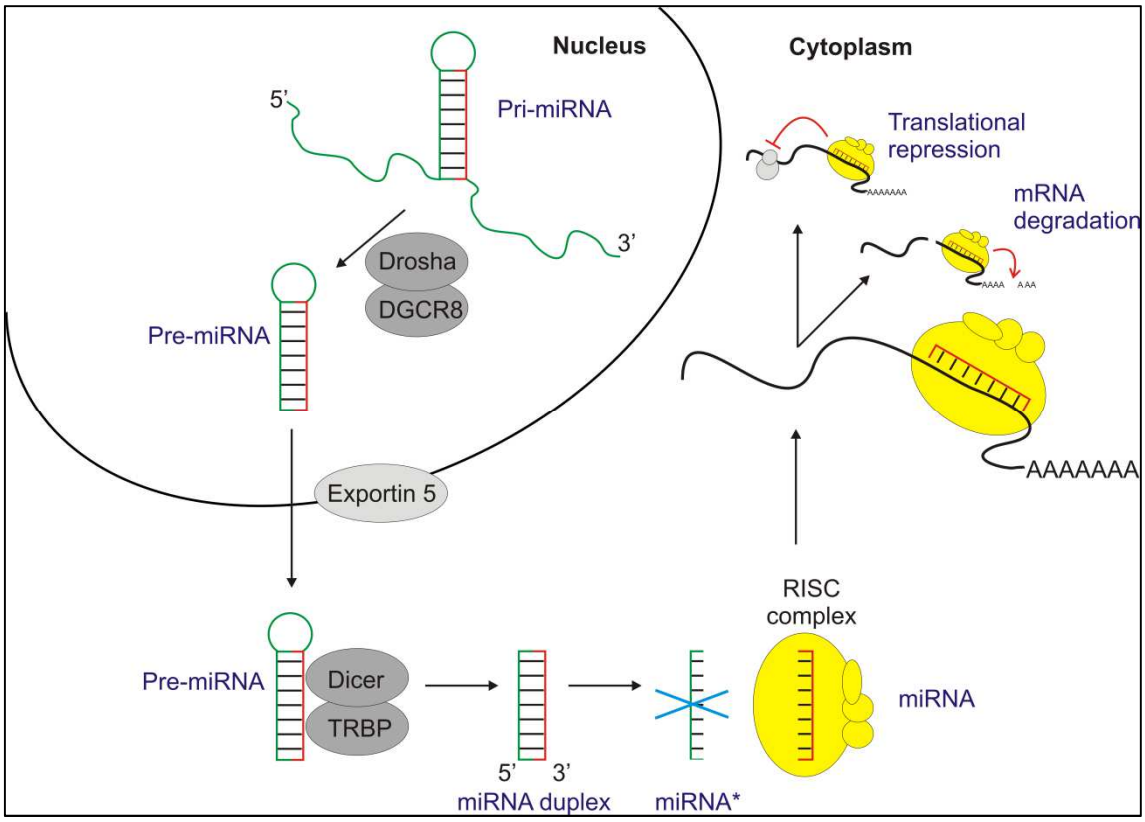

Fig. 1.8 Biosynthesis of miRNA molecules. Pri-miRNAs are transcribed in the nucleus and cleaved by Drosha, together with its partner protein DGCR8, to form pre-miRNAs. These pre-miRNAs are exported to the cytoplasm by Exportin 5 and further cleaved by Dicer, together with its partner protein TRBP, to produce the miRNA:miRNA* duplex. The duplex unwinds and the guide strand (miRNA) is incorporated into the RISC complex. The alternative strand (miRNA*) is usually degraded. The RISC complex binds to the 3' UTR of the target mRNA and initiates either translational repression or mRNA degradation.

1.3.2.2.2 miRNA-mediated regulation

Many studies have investigated the mechanism of miRNA-mediated post-transcriptional regulation. The initial, widely accepted hypothesis was that miRNAs bind to the 3' UTR of a target mRNA and cause either mRNA degradation or translational repression, depending on the nature of the miRNA-mRNA interaction. The general consensus was that binding with perfect complementarity triggered endonucleolytic cleavage and mRNA degradation (Jones-Rhoades et al., 2006), whilst binding via a short 6-8 nucleotide "seed" region induced translational repression (Bartel, 2004; Hutvagner and Zamore, 2002). Plant miRNAs predominantly bind with perfect complementarity to their target mRNAs and therefore mRNA degradation is the main mechanism of miRNA-mediated regulation (Jones-Rhoades et al., 2006; Rhoades et al., 2002). In contrast, successful binding of the core "seed" region appears to be sufficient for mammalian miRNAs to exert their effects (Filipowicz et al., 2008; Pritchard et al., 2012; Wang, 2013). There is much debate in the literature regarding the predominant mechanism of miRNA-mediated regulation in mammals. Some *in vitro* and *in vivo* studies have suggested that translational repression is the predominant mechanism. For example, Meijer *et al* used an *in vitro* model to show that miRNAs bind to eIF4A2, which is involved in translation initiation (Fig. 1.7), thus initiation is blocked and the translational repression machinery is activated (Meijer et al., 2013); and Djuranovic *et al* used an *in vivo* system to demonstrate that, whilst deadenylation and decay of target mRNA occurred, they were secondary to translational repression (Djuranovic et al., 2012). Indeed, a cyclic process has been proposed, whereby the binding of a miRNA to its target induces translational repression, which leads to poly(A) tail destabilisation and mRNA degradation, further repressing translation (Omer et al., 2009). In contrast, other *in vitro* studies have reported that mRNA degradation is the primary event (Beilharz et al., 2009; Guo et al., 2010), although there are limited *in vivo* studies to support this hypothesis.

miRNA studies have also revealed further levels of complexity to miRNA-mediated post-transcriptional regulation. In 2008, miR-10a was found to bind to the 5' UTR of some targets and the 3' UTR of others, causing enhancement of repression and relief from repression, respectively (Orom et al., 2008). It has also been reported that miRNAs can switch between repression and activation of mRNA targets depending on the phase of the cell cycle (Vasudevan et al., 2007), and can regulate alternative non-coding RNA species (Liang et al., 2013). Furthermore, the transcription of miRNAs themselves can be tightly regulated. DNA methylation and histone modifications have been shown to affect miRNA expression (Lujambio et al., 2010; Weber et al., 2007), and changes in both DNA methylation status and miRNA

expression are observed following exposure to environmental toxins (Hou et al., 2012). Some miRNAs have also been found to exist as part of a negative feedback loop, within which they are transcribed from the transcription factors that they themselves regulate (Li and Carthew, 2005; Seggerson et al., 2002). Finally, the fact that the binding of the short seed region is sufficient for miRNAs to exert their effect (Filipowicz et al., 2008; Pritchard et al., 2012; Wang, 2013) also means that each one is predicted to target many different mRNAs, which are usually diverse in function (Lim et al., 2005); and, that one mRNA can be targeted by a number of different miRNAs depending on the physiological situation. Whilst miRNAs often exist in clusters, or families, there is contrasting research on whether or not these function as part of common regulatory pathways (Abbott et al., 2005; Shukla et al., 2011a).

Therefore, miRNA-mediated mRNA regulation is complex and likely to depend upon a range of factors, including the number and extent of miRNA changes, the target mRNAs, the cell type, the cellular environment, and the number and positioning of miRNA binding sites, each of which will be unique to the particular conditions under investigation (Filipowicz et al., 2008; Huntzinger and Izaurralde, 2011).

1.3.2.2.3 lncRNAs

It has been demonstrated that over three quarters of the mammalian genome is transcribed (Djebali et al., 2012). One of the most common, yet poorly understood RNA species, are the lncRNAs (Derrien et al., 2012). First identified in 2005 by the FANTOM consortium (Carninci et al., 2005; Maeda et al., 2006), there are now known to be many hundreds in the mammalian genome (Carpenter et al., 2013; Guttman et al., 2009; Rinn and Chang, 2012), many of which have been catalogued by the ENCODE consortium (Derrien et al., 2012). Whilst the function of many lncRNAs remains unclear, the fact that they assmeble into complexes with proteins and other RNA species (Guttman and Rinn, 2012; Rinn and Chang, 2012), suggests a fundamental role in the genetic regulatory pathway; specifically at the translational level (Johnsson et al., 2013). One example is antisense Uchl1, a lncRNA located in the brain, which binds to a protein coding mRNA within a partially overlapping region on the sense strand and increases protein synthesis at the post-transcriptional stage (Carrieri et al., 2012). Some lncRNAs are derived from the transcription of pseudogenes, by transcription factors, such as TNFα (Rapicavoli et al., 2013), which further supports a role for them in the genetic regulation pathway. The identification of lncRNAs as regulatory molecules in cancer development and progression (Johnsson et al., 2013; Tsai et al., 2011), means that work exploring these RNA species is expanding very rapidly and, furthermore, recent studies have suggested a role for them in

maintaining signaling network feedback loops, particularly during the inflammatory response (Carpenter et al., 2013; Rapicavoli et al., 2013). One of the physiological signs of compound-induced hepatotoxicity is inflammation and, in responding to damage the liver must maintain control of critical regulatory feedback mechanisms. Thus, there is the potential for lncRNAs to be involved in compound-induced hepatotoxicity.

1.3.2.2.4 Endogenous siRNAs

siRNAs are produced from long double-stranded RNA transcripts derived from repetitive or transposable elements (Carthew and Sontheimer, 2009; Okamura and Lai, 2008). Initially endogenous siRNAs were thought to be unique to plants, however, they have now been observed in *Caenorhabditis elegans* and *Drosophila melanogaster*, as well as mouse embryonic stem cells and human skin (Xia et al., 2013). Like miRNAs they form an association with the RISC complex, however, unlike miRNAs they require near perfect complementarity to their target molecule prior to exerting a physiological effect (Carthew and Sontheimer, 2009). siRNAs have not been widely studied in the case of human disease, but their identification has led to the development of chemically synthesised double-stranded siRNA molecules experimentally induced to interfere with the function of endogenous genes (Fire et al., 1998). Due to the high degree of complementarity this RNA interference mechanism is highly specific (Rao et al., 2009) and is now being utilised in the cancer field (Ghafouri-Fard, 2012). However, in developing these species as therapeutic agents, care has to be taken from a toxicological viewpoint that the observed “off-target” effects (Borchert et al., 2006; Jackson et al., 2006) are limited or controlled.

1.3.2.2.5 piRNAs

Piwi-interacting RNAs (piRNAs) are another form of small regulatory species. They are germline specific and known to be involved in transcriptional regulation as well as transgenerational epigenetics, functioning to maintain germline stability (Bortvin, 2013).

1.3.3 Post-translational protein modifications

1.3.3.1 Protein folding

Following translation it is necessary for the polypeptide chain to undergo a conformational change to form a three-dimensional folded active structure (Anfinsen, 1972). The native conformation of a protein is determined by its amino acid sequence (Anfinsen, 1973). Within the cell, folding is a continual process catalysed by the presence of a group of structurally distinct molecular chaperones (Lee and Tsai, 2005). The importance of accurate protein folding is highlighted in neurodegenerative diseases, which are clinically characterised by accumulations of misfolded protein aggregates (Selkoe, 2003; Stefani and Rigacci, 2013). These aggregates cause profound cellular dysfunction. Thus, correct protein folding is critical for the successful production of functionally viable proteins.

1.3.3.2 Post-translational regulation

Post-translational modifications include structural changes, such as the addition of disuphide bonds, or proteolytic cleavage and/or the addition of a biochemical functional group to the completed peptide chain. Such modifications are either vital for full functionality, or implemented to increase the functional properties of the protein, or regulate its activity. Functional groups include large moieties such as lipids and carbohydrates, or smaller moieties such as phosphate and acetate, both of which alter protein activity. Proteins such as ubiquitin and small ubiquitin-related modifier (sumo) can also function as regulators, their addition causes protein degradation or repression. Phosphorylation involves the addition of a phosphate group, which either activates or inhibits the activity of a protein (Burnett and Kennedy, 1954). Abnormal phosphorylation is a major cause of human disease (Cohen, 2001). Acetylation involes the addition of an acetyl group to the peptide chain and occurs in up to 80% human proteins (Hwang et al., 2010). Protein hyperacetylation has been demonstrated in cases of alcoholic liver disease (Fritz et al., 2012) and deacetylation excaberates Acetaminophen-induced hepatotoxicity (Lu et al., 2011). Ubiquitination involves the addition of a ubiquitin group, and usually marks a protein for degradation by the 26S proteasome (Jung and Grune, 2013). This is a tightly regulated event useful for irreversibly inactivating proteins that are no longer required, however, when this process is disrupted diseases such as cancer, neurodegeneration and metabolic disorders can arise (Sakamoto, 2002). Sumoylation is a reversible process, involving the addition of sumo to regulate expression of a target. It is implicated in various forms of stress including oxidative stress and heat shock (Golebiowski et

al., 2009; Zhou et al., 2004). Furthermore, sumoylation appears to alter protein solubility, thus defects can lead to the formation of toxic aggregates (Krumova et al., 2011).

One particular group of proteins particularly susceptible to post-translational modification are the histones. As mentioned in section 1.3.1.2, histone modifications are a type of epigenetic regulation that result in changes in the rate of gene transcription. Protein modifications can include acetylation, methylation, phosphorylation, glycosylation, sumoylation, ubiquitination and adenosine diphosphate ribosylation (Hou et al., 2012). Acetylation, whereby an acetyl group is added from acetyl-coenzyme A to a lysine side chain within the N-terminal tail (Sterner and Berger, 2000); and methylation, whereby one or more methyl groups are added to the nitrogen of the guanidinium group (Klose and Zhang, 2007) are the two modifications most affected by environmental chemicals (Hao and Whitelaw, 2013). Such modifications act to activate and/or repress translation.

1.3.4 Alternative genetic regulation

The process of genetic regulation is by no means straightforward. As already discussed there are many regulators, which exert their effects at each stage of the gene expression pathway, many of which can interact with one another, further increasing the complexity of the pathway. Alternative forms of regulation also exist, including gene-environment interactions and individual genetic polymorphisms, such as SNPs (Nachman, 2001). Furthermore, some compounds will cause the development of immunological reactions, such as hypersensitivity. These sorts of reactions are challenging to manage because they frequently have latent onset and can be caused by a variety of mechanisms (Lochmatter et al., 2009; Mayorga et al., 2013).

1.4 HYPOTHESIS

Does mRNA translation have a role in the response of the liver to compound-induced hepatotoxicity?

1.5 AIMS

All of the model systems utilised in this work have been well studied at the transcriptional level, and this has provided valuable mechanistic insights into the processes involved in hepatotoxicity. However, over the past few years translational regulation has also been shown to be critical, particularly in cases of cellular stress where it can elicit a rapid, efficient response at the protein level. It could therefore be hypothesised that changes in mRNA translation also play an important role in compound-induced hepatotoxicity. Identifying such changes will provide a more complete understanding of the molecular mechanisms of such toxicities. In turn this may help to identify adverse toxicities early in the drug/compound development process, and prevent and treat overdose and unexpected adverse toxicites in susceptible patients.

Thus the aims of this work were to:

- Identify mRNA-regulated toxic mechanisms specific to compound-induced hepatotoxicity.
- Adapt the existing translational profiling technique (predominantly used with *in vitro* samples) to make it more amenable for the analysis of *in vivo* samples.
- Apply mRNA translational profiling techniques to liver samples taken from models of compound-induced hepatotoxicity.
- Further explore physiologically relevant mRNAs that demonstrate translational regulation.
- Perform miRNA profiling on liver samples taken from models of compound-induced hepatotoxicity.
- Identify putative interactions between mRNAs that are undergoing translational regulation and miRNAs that are differentially expressed following treatment.
- Perform miRNA profiling on plasma samples taken from rats treated with the hepatotoxic compound Thioacetamide.

CHAPTER 2: MATERIALS AND METHODS

Unless otherwise stated all reagents were purchased from Sigma (Poole, UK).

2.1 ANIMAL MODELS

All in-house animal work was carried out in accordance with the Animals Scientific Procedures Act (1986) under project licence PPL 80/2126 and personal licence PIL 80/10347.

2.1.1 Griseofulvin-treated mouse

BALB/c mice were bred in-house and were housed in negative pressure isolators at 21°C with a 12 h light-dark cycle. At approximately 6 weeks of age, 7 days prior to commencement of the study, 20 mice were put onto a Rat and Mouse No. 1 maintenance (RMI) fine ground diet. After acclimatisation the diet was switched to one containing either vehicle-only (2% (w/v) arachis oil), n=10, or 2% arachis oil with 1% (w/w) Griseofulvin, n=10. This dose selection was based on the literature and prior work performed within the group (De Matteis and Rimington, 1963; Gant et al., 2003).

To assess food consumption the food hoppers were weighed daily. This showed that the different groups were consuming approximately equal amounts of food. Mice were weighed every three days; any animal whose weight fell below 80% that of the control animals, or displayed symptoms of distress, was removed from the study. On this basis one of the Griseofulvin treated mice was removed on day 17 of the study.

After 5 days of treatment, half of the animals from each treatment group were anaesthetised using isofluorane. Blood was withdrawn via cardiac puncture and was immediately transferred into lithium/heparin tubes (Vetlab Supplies, Pulborough, UK). Following centrifugation (16,100g, 4°C, 5 min) the plasma was collected and stored at -80°C. Organs were perfused *in situ* with PBS containing cycloheximide (100 µg/ml) and animals were sacrificed using cervical dislocation under terminal anaesthesia. Organs were harvested, immediately snap frozen in liquid nitrogen and stored at -80°C. The remaining animals from each group underwent the same procedure after treatment for 22 days.

2.1.2 Thioacetamide-treated rat

Male Wistar rats (300 – 350g) were sourced from Charles River (Margate, UK). They were housed in negative pressure isolators at 21°C with a 12 h light-dark cycle. After 1 week acclimatisation, animals received a single dose, via the intraperitoneal (ip) route, of vehicle-only (0.9% (v/v) saline) (n=6), or Thioacetamide, dissolved in 0.9% (v/v) saline to final doses of 50 mg/kg (n=6), 100 mg/kg (n=6) or 150 mg/kg (n=6). These doses were selected as they fell below the threshold for overt toxicity (Kucera et al., 2011; Mangipudy et al., 1995b).

24 h after dosing, half of the animals from each treatment group were anaesthetised using isofluorane. Blood was withdrawn via the descending vena cava and immediately transferred into lithium/heparin tubes. Following centrifugation (16,100g, 4°C, 5 min) the plasma was collected and stored at -80°C. Organs were perfused *in situ* with PBS containing cycloheximide (100 µg/ml) and animals were sacrificed using decapitation under terminal anaesthesia. Organs were harvested, sections were taken for histological analysis and the remainder was immediately snap frozen in liquid nitrogen and stored at -80°C. The remaining animals from each group underwent the same procedures 48 h after treatment.

A scaled down version of this study was repeated using a single time point (24 h) and a single dose (100 mg/kg). Animals received vehicle-only (0.9% (v/v) saline) (n=3), or 100 mg/kg Thioacetamide (n=3) and were sacrificed and processed as described above. This was to obtain non-heparinased plasma for the profiling of circulating miRNAs. Heparin is a potent inhibitor of downstream reverse transcription reactions (Johnson et al., 2003). Although a lithium chloride precipitation has been shown to remove heparin in some instances (del Prete et al., 2007), this method was not suitable for the very small yields of RNA obtained from plasma samples. Thus, extra plasma samples were generated as described above, except the blood was collected into potassium/EDTA tubes (Sarstedt, Leicester, UK). EDTA is the anticoagulant of choice for plasma miRNA quantification (Zampetaki and Mayr, 2012).

2.1.3 Predictive Toxicology study

The original Innomed PredTox project consortium investigated 14 proprietary drug compounds that had failed during preclinical development and 2 reference toxic compounds; gentamicin and troglitazone (Table 2.1).

Table 2.1. PredTox study compounds

FP6 Study Name	Compound sponsor	Toxicity		Histopathology
		Hepatotoxic	Nephrotoxic	
FP001RO	Roche	✓		Cholestasis
FP002BI	Boehringer Ingelheim		✓	Necrosis
FP003SE	Serono	✓		Cholestasis
FP004BA	Bayer	✓		Necrosis
FP005ME	Merck	✓		Necrosis
FP006JJ	Roche	✓		Steatosis
FP007SE	Boehringer Ingelheim	✓	✓	Cholestasis/necrosis
FP008AL	Altana	✓		Hypertrophy
FP009SF	Ref. compound Gentamicin		✓	Necrosis
FP010SG	Ref. compound Troglitazone	✓		Hypertrophy
FP011OR	Organon	✓		Hypertrophy
FP012SV	Servier	✓		Hypertrophy
FP013NO	Novartis	✓	✓	Hypertrophy
FP014SC	Bayer Schering Pharma	✓		Necrosis
FP015NN	Novo Nordisk	✓		Necrosis
FP016LY	Lilly		✓	Hypertrophy

Male Wistar rats were dosed orally with either vehicle-only, or a low dose or high dose of each compound. Doses were determined for each compound individually based on pre-existing data. The aim was to achieve target organ toxicity 2 weeks after exposure. However, in order for the development of toxicity to be monitored 3 time-points were selected; 2 days (animals received a single dose on day 1 and were sacrificed on day 2, n=5); 4 days (animals received a daily dose for 3 days and were sacrificed on day 4, n=5); and 15 days (animals received a daily dose for 14 days and were sacrificed on day 15, n=5).

Clinical observations and weight measurements were recorded, and urine samples were collected, throughout the study. At the time of completion serum, plasma, liver and kidney samples were collected and stored at -80°C. Various analyses of the biological samples were then performed as depicted in Fig. 2.1.

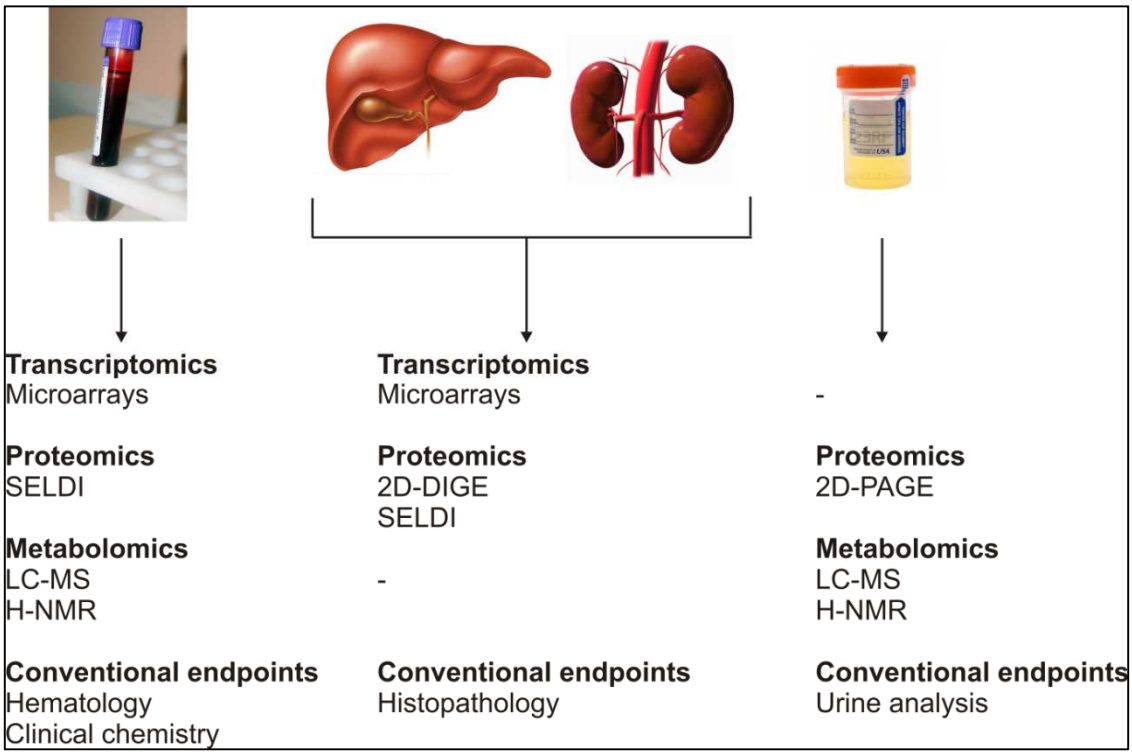

Fig. 2.1. Overview of the analyses performed by the PredTox consortium. The consortium used both newer 'omics technologies and conventional toxicological methods on blood, urine and tissue (liver and kidney) samples in an attempt to generate a comprehensive understanding of the underlying toxicological mechanisms. Adapted from (Suter et al., 2011).

The technical details relating to the various analyses that were performed are described in detail elsewhere (Suter et al., 2011). Study conditions were kept as constant as possible between the different sponsors. The principal findings and outcomes from these studies are presented as research papers (Boitier et al., 2011; Matheis et al., 2011a; Suter et al., 2011). Following the preliminary analysis that was performed by the consortium members, those compounds that caused the most pronounced hepatotoxicity were selected for further study. The consortium kindly provided liver samples from animals within each group. Further details, where available, on each of these 5 compounds are provided in Table 2.2.

Table 2.2. The properties of the five PredTox compounds selected for further study.

FP6 study name	Official name	Structure	Proposed High Dose	Proposed Low Dose	Target Organs	Chemical Class	Pharmacological Class
FP004BA	(+)-(1R)-1-[4-(4-fluorophenyl)-2,6-diisopropyl-5-propyl-pyridin-3-yl]ethanol	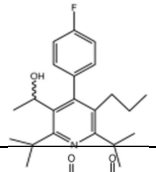	100 mg/kg	20 mg/kg	liver, kidney	4-Phenyl-pyridine	Glucagonreceptor antagonist
FP005ME	1-(2-trifluoromethoxyphenyl)-2-nitroethanone	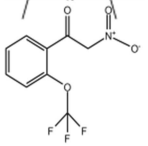	350 mg/kg	15 mg/kg	liver	Carbonylnitromethanes	Carbonylnitromethanes
FP007SE	-	-	1000 mg/kg	100 mg/kg	kidney, liver	-	-
FP013NO	-	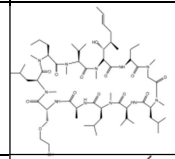	-	-	-	Cyclosporin derivative	-
FP014SC	Tetraethyl[(3-hydroxy-2-pyridyl)-amino]-methanediphosphonate	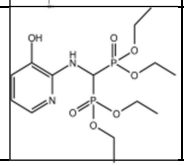	1120 mg/kg	280 mg/kg	liver	Bisphosphonate	Inhibitor of osteoclast activity

(-) denotes areas where information was not provided by the compound sponsor.

2.2 CELL CULTURE

2.2.1 Cell lines and culture conditions

One mouse liver cell line and three rat liver cell lines were used throughout the course of this work.

The Hepa 1-6 mouse hepatoma liver cell line was acquired from the MRC Toxicology Unit. These cells were cultured in Dulbecco's Modified Eagle Medium (DMEM), supplemented with 4.5 g/L glucose, 4 mM L-glutamine, 0.04 mM phenol red, 1 mM Na pyruvate and 10% (v/v) foetal calf serum (FCS) (Life Technologies, Paisley, UK).

The FAO and H4IIE rat hepatoma liver cell lines and RLE rat hepatocyte cell line were acquired from the MRC Toxicology Unit. All were cultured in DMEM, supplemented with 4.5g/L glucose, GlutaMAX™ (4 mM L-Alanyl-L-glutamine), 0.04 mM phenol red, 1 mM sodium pyruvate, 10% (v/v) FCS and 1% (v/v) non-essential amino acids (Life Technologies, Paisley, UK).

Cells were incubated at 37°C in a 5% CO_2 humidified atmosphere. Media was replaced every other day and cells were passaged when they reached >90% confluency.

2.2.2 Passaging of cells

Media was aspirated and cells were washed twice with PBS. To detach cells 1X trypsin/EDTA solution (0.05g/L trypsin and 0.02g/L EDTA) in PBS was added to the cell culture vessel and cells were incubated at 37°C for approximately 5 min. Media was then added (10X volume of trypsin solution) to inactivate the trypsin. Cells were transferred to a universal and pelleted by centrifugation (200g, RT, 3 min). The supernatant was aspirated; cells were resuspended in fresh media and plated in new culture vessels at the required density.

2.3 RNA PROCESSING

2.3.1 RNA extraction: tissue samples

Approximately 70 mg pieces of frozen liver tissue were cut using a sterile blade on a steel block cooled on dry ice. It was critical to keep the liver frozen during handling so as to maintain the integrity of the RNA. The frozen liver was placed in a 2 ml tube and homogenised in 1 ml Tri reagent using an Ultra-Turrax T8 (IKA, Germany) in 40 s bursts until completely homogenised. Following incubation at RT for 5 min, 200 µl 1-Bromo-3-chloropropane was added. The tubes were shaken vigorously, vortexed for 10 s, and incubated at RT for a further 3 min. The tubes were centrifuged (12,000g, 4^{o}C, 15 min) and the upper aqueous phase was transferred to a 1.5 ml tube. An equal volume (600 µl) of isopropanol was added and the tubes were vortexed for 10 s and incubated at RT for 10 min. RNA was pelleted by centrifugation (12,000g, 4^{o}C, 10 min) and the supernatant was discarded. Pellets were washed twice with 1 ml cold 75% (v/v) EtOH. All traces of EtOH were removed using a gel loading tip and pellets were air dried at RT for approximately 10 min. RNA pellets were resuspended in an appropriate volume of ultra pure (18 MΩ) water. The quantity and quality of RNA was measured as described in sections 2.3.3 and 2.3.4 and RNA was stored at -80°C until required.

2.3.2 RNA extraction: cell samples

Cells were grown until 90% confluent and media was aspirated. Cells were washed twice with PBS and then lysed directly in the cell culture vessel using Tri reagent. 1 ml Tri reagent was used for each well of a 6 well-plate. The lysate was transferred to a 2 ml tube, incubated at RT for 5 min and the RNA was extracted as described in section 2.3.1.

2.3.3 Quantification and quality control

RNA was quantified using a Nanodrop-1000 spectrophotometer (ThermoFisher Scientific, Loughborough, UK). RNA was deemed suitable for downstream work if the $OD_{260/280}$ was between 1.8 and 2.1 and the $OD_{260/230}$ was > 1.5. If the ratios were low the RNA was re-precipitated as described in section 2.3.3.1 to remove any contaminants.

2.3.3.1 Re-precipitation of RNA

The volume of RNA was made up to 100 µl with ultra pure (18 MΩ) water. 100 µl of acid-phenol : chloroform (1 : 1) was added and samples were vortexed for 10 s. Following centrifugation (12,000g, 4^{o}C, 10 min) the upper aqueous phase was transferred to a 1.5 ml tube. To ensure maximum recovery a further 100 µl ultra pure (18 MΩ) water was added to

the acid-phenol : chloroform mix, vortexed for 10 s and centrifuged (12,000g, 4°C, 15 min). The aqueous phase was added to the aqueous phase acquired from the first centrifugation. Samples were precipitated in 1/10th volume of 3 M NaOAc (pH5.2) and 2.75X 100% EtOH at -20°C overnight. RNA was pelleted by centrifugation (12,000g, 4^{o}C, 10 min) and the supernatant was discarded. Pellets were washed twice with 1 ml cold 75% (v/v) EtOH. All traces of EtOH were removed using a gel loading tip and pellets were air dried at RT for approximately 10 min. RNA pellets were resuspended in an appropriate volume of ultra pure (18 MΩ) water. The quantity and quality of RNA was measured as described in sections 2.3.3 and 2.3.4. This re-precipitation consistently improved the $OD_{260/280}$ and $OD_{260/230}$ ratios. RNA was stored at -80°C until required.

2.3.4 Quality assessment of RNA

To check that RNA was not degraded, samples were analysed using either agarose gel electrophoresis or a 2100 Bioanalyser (Agilent Technologies, Santa Clara, CA).

2.3.4.1 RNA quality: Agarose gel

A 1% (w/v) agarose gel was prepared by dissolving agarose in 1X Tris/Borate/EDTA (TBE) buffer. The gel was cast and left to set whilst samples were prepared. RNA was diluted to a concentration of 1 µg/µl in ultra pure (18 MΩ) water. 2 µl of each diluted sample was mixed with 3 µl RNA loading buffer (50% (v/v) glycerol, 1 mM EDTA, 0.25% (w/v) xylene cyanol and 0.25% (w/v) bromophenol blue). 2 µl of a 0.24 - 9.5 Kb RNA ladder (Life Technologies, Paisley, UK) was also mixed with 3 µl loading buffer; this was run alongside the samples as a size marker. The samples and ladder were loaded and the gel was electrophoresed at 60 V for approximately 1 h in 1X TBE buffer. The gel was removed and stained in 1X TBE containing 0.01% (v/v) ethidium bromide at RT for 20 min. Following de-staining in 1X TBE at RT for 5 min, the gel was scanned using a BioDoc-It™ Imaging system (Ultra-Violet Products Ltd., Cambridge, UK). Non-degraded RNA showed prominent 18S and 28S ribosomal bands (Fig. 2.2 A), whilst degraded RNA resulted in a smear (Fig. 2.2 B).

2.3.4.2 RNA quality: Bioanalyser

A more recent, alternative method of assessing RNA quality is through the use of a 2100 Bioanalyser and RNA 6000 Nano kit from Agilent. The Bioanalyser works through the use of a specially designed chip; once samples are loaded onto the chip an integrated electrical circuit is formed. The charged RNA particles are electrophoretically driven through a sieving polymer

matrix on a voltage gradient. Smaller fragments move faster than larger fragments and all are visually detected using laser-induced fluorescent signals.

The RNA 6000 Nano kit was used according to the manufacturer's instructions. Briefly, the chip was primed with a gel-dye mix (65 µl gel, 1 µl dye), and 5 µl of RNA marker was added to each well. Samples were diluted to concentrations of between 50 ng/µl and 500 ng/µl. 1 µl of each sample was loaded onto the prepared chip. 1 µl of an RNA ladder was loaded alongside the samples. The prepared chip was vortexed for 1 min and loaded into the Bioanalyser. Each run took approximately 30 min. The software generated visual outputs, including a virtual gel, similar to that seen when running an agarose gel, and an electropherogram (Fig. 2.2 C). Each sample was also allocated an RNA integrity number (RIN) score. The closer to 10 the RIN score was, the better the quality of the RNA. A score of ≥ 8 was deemed suitable for downstream work. Degraded RNA resulted in a smear on the gel and a low RIN score (Fig. 2.2 D).

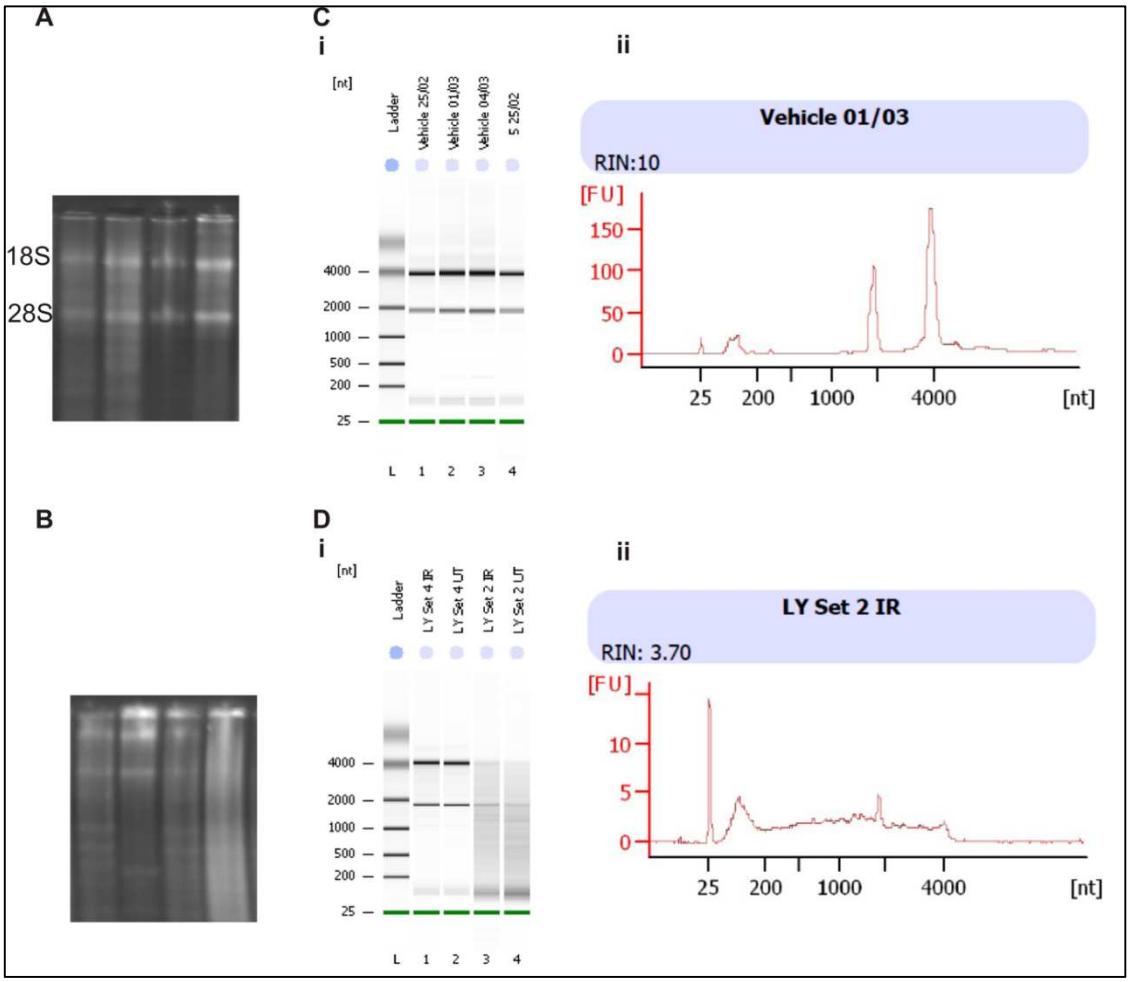

Fig. 2.2. Agarose gel electrophoresis and Bioanalyser ouput images. (**A**) Agarose gel image from non-degraded RNA samples, bands correlate to the 18S and 28S ribosomal subunits. (**B**) Agarose gel image from degraded RNA samples; no 18S or 28S ribosomal bands are evident. (**C**) Bioanalyser gel image (**i**) and electropherogram (**ii**) from non-degraded RNA samples, bands and peaks correspond to the 18S and 28S ribosomal subunits. The ratio between the 2 ribosomal peaks is used to calculate the RIN score. In the example shown here each sample had a RIN of ≥ 9. (**D**) Bioanalyser gel image (**i**) and electropherogram (**ii**) from degraded RNA sample (gel lanes 3 and 4); no 18S or 28S ribosomal bands or peaks are evident and the RIN scores are low.

2.4 DNA PROCESSING

2.4.1 DNA extraction

DNA was extracted using a DNeasy Blood and Tissue kit (Qiagen, Venlo, Netherlands), according to the manufacturer's instructions. Briefly, approximately 25 mg of frozen liver tissue was ground to a powder in liquid nitrogen using a pestle and mortar on dry ice. The ground sample was transferred to a 1.5 ml tube. 180 µl buffer ATL and 20 µl proteinase K were added and the tubes were vortexed for 10 s, prior to incubation at 56°C for 1 h. 200 µl buffer AL was added and tubes were vortexed for 10 s. 200 µl 100% EtOH was added and tubes were vortexed for 10 s. The entire volume was transferred to a DNeasy spin column. Columns were centrifuged (6000g, RT, 1 min) and washed sequentially with 500 µl buffer AW1 and 500 µl buffer AW2. DNA was eluted using buffer AE; 200 µl was added to the spin column filter and incubated at RT for 1 min. Centrifugation (6000g, RT, 1 min) recovered the DNA. To maximise DNA yield a further 200 µl buffer AE was added to the spin column and the incubation and centrifugation were repeated as described above.

2.4.2 Quantification and quality control

DNA yield and purity were assessed using a Nanodrop-1000 spectrophotometer (ThermoFisher Scientific, Loughborough, UK). DNA was deemed suitable for downstream work if the $OD_{260/280}$ was between 1.7 and 2.0.

2.5 PROTEIN PROCESSING

2.5.1 Protein extraction: tissue samples

Approximately 80 mg of frozen liver tissue was ground to a powder in liquid nitrogen using a pestle and mortar on dry ice. The ground sample was transferred to a 1.5 ml tube. 800 µl lysis buffer (50 mM Tris-HCl (pH 7.4), 150 mM NaCl, 1% (v/v) NP-40, 0.25% (w/v) Na deoxycholate and 5mM EDTA) and 1% (v/v) protease inhibitor cocktail was added (volume of lysis buffer and protease inhibitor cocktail were adjusted according to sample weight; 10 µl lysis buffer/mg tissue/1 µl protease inhibitor cocktail). Samples were passed through a 25 gauge needle 5-10 times to facilitate lysis and incubated on ice for approximately 60 min, with regular vortexing. Samples were centrifuged (15,600g, 4°C, 30 min) and the supernatants (containing protein) were transferred to 1.5 ml tubes.

2.5.2 Protein extraction: cell samples

Cells were grown until 90% confluent and media was aspirated. Cells were washed twice with PBS and lysed directly in the cell culture vessel using lysis buffer (50 mM Tris-HCl (pH 7.4), 150 mM NaCl, 1% (v/v) NP-40, 0.25% (w/v) Na deoxycholate and 5mM EDTA) and 1% (v/v) protease inhibitor cocktail was added. 500 µl lysis buffer and 5 µl protease inhibitor cocktail were used for each well of a 6 well-plate. Cells were detached using a cell scraper and the lysate was transferred to a 1.5 ml tube. Samples were centrifuged (15,600g, 4°C, 30 min) and the supernatants were transferred to 1.5 ml tubes.

2.5.3 Quantification

Protein concentration was determined using a Bradford assay (Bradford, 1976). An increased presence of protein stabilises the Coomassie Brilliant Blue dye and results in a higher A_{595nm} reading. Thus, the absorbance at A_{595nm} is directly proportional to the amount of protein and a standard curve can be used to calculate unknown protein concentrations. Bio-rad Protein Assay (Bio-rad, Hertfordshire, UK) was used according to the manufacturer's instructions. Briefly, protein standards were prepared using bovine serum albumin (BSA) at concentrations of 1 mg/ml, 0.75 mg/ml, 0.5 mg/ml, 0.25 mg/ml and 0.1 mg/ml. 20 µl of each standard, in duplicate, and 20 µl of each unknown sample, in triplicate, was transferred to a 1.5 ml tube. Bio-rad Protein Assay dye reagent was diluted 1 in 5 with water and filtered through No.1 Whatman filter paper (Whatman, UK) prior to use. 1 ml of diluted, filtered reagent was added to each of the standards and unknown samples. Tubes were vortexed for 10 s and incubated at RT for 15 min. A_{595nm} was recorded for each standard and unknown sample. The absorbance readings from each standard were used to plot a standard curve (Fig. 2.3) from which the concentration of the unknowns could be calculated. If the readings from the unknown samples were outside the range of the standard curve they were diluted in ultra pure (18 MΩ) water and re-assayed.

2.6 MICROARRAY MANUFACTURE

Microarrays were printed in-house using an inkjet style ArrayJet Ultra-Marathon II microarray printer (ArrayJet, Roslin, Scotland). This microarrayer was designed for the high-throughput printing of a large number of microarrays. When loaded to its maximum capacity, the ArrayJet could print 1000 slides simultaneously (Fig. 2.4). This print run would take approximately 5 days.

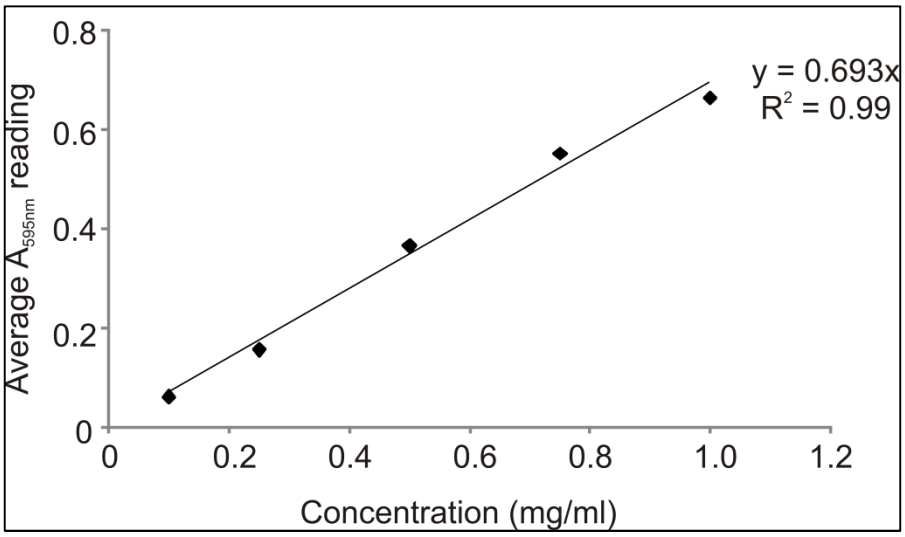

Fig. 2.3. Example of a Bradford assay standard curve. BSA standards were used to generate a standard curve for protein quantification. The concentration of an unknown protein sample could be calculated by dividing the average absorbance (A_{595nm}) by the slope of the line of best fit.

Fig. 2.4. The Arrayjet Microarray printer. Image taken immediately prior to a print run. The ArrayJet is loaded with 48 384-well plates (containing the probes for printing), and 1000 slides. Software is operated through the attached computer.

2.6.1 MEEBO microarrays

To investigate changes in mRNA expression a Mouse Exonic Evidence-Based Oligonucleotide (MEEBO) probe set was used. The probes were developed by a group of researchers from Stanford Functional Genomics Facility, with collaborators from Rockefeller, Basel, and the Stowers Institute. Produced commercially by Illumina, they were supplied, dried-down, in 384-well plates (Life Technologies, Paisley, UK). The probe set consisted of 38,784 70-mer probes designed to provide complete coverage of the mouse genome. Probes were resuspended to a concentration of 10 µM in printing buffer (3X SSC, 1.5 M Betaine and 30% (v/v) ethylene glycol) prior to use. A control plate was printed and intensity values were used to check the quality of the printed microarrays (Appendix I).

2.6.2 miRNA microarrays

To investigate changes in miRNA expression a miRNA probe set from Exiqon was used (Exiqon, Vedbaek, Denmark). Profiling of miRNAs is complicated by their short length and closely-related sequences (Wark et al., 2008). To overcome these issues, the Exiqon probes incorporate locked nucleic acid (LNA)-modified bases. LNA probes contain a "locked" ribose ring on the backbone, connecting the 2' oxygen to the 4' carbon, thus providing higher annealing affinities and increasing thermal stability between probes. When tested alongside other miRNA microarray platforms, the Exiqon probe set demonstrated increased specificity (Sah et al., 2010).

The majority of the work described in this thesis was performed when miRNA profiling was in its infancy, using one of the earlier Exiqon probe sets. The first probe set printed in-house contained approximately 1500 probes and corresponded to version 8.1 of miRBase. The current version of miRNase, version 20, was released in June 2013, and the latest probe set from Exiqon contains approximately 3100 probes. This demonstrates the speed at which the field has developed. The probes were supplied, dried down, in 384-well plates and were resuspended to a concentration of 20 µM in printing buffer (3X SSC, 1.5 M Betaine and 30% (v/v) ethylene glycol) prior to use. Frequently highly expressed miRNAs (miR-122, miR-21 and let-7d) were used to check for variability between print batches (Appendix II).

2.7 QUANTITATIVE RT-PCR

Quantitative Reverse Transcription-PCR (qRT-PCR) uses a fluorescent dye (SYBR® Green), which only emits fluorescence when bound to double-stranded DNA (i.e. a PCR product). Specific primers are used to amplify a particular region, or sequence of interest, and thus, the time

taken for the amount of fluorescent signal to reach a defined level (the cycle threshold, CT) is a measure of the abundance of that gene within a sample. An endogenous control gene is run alongside the gene of interest so that discrepancies in the reverse transcription stage or errors in pipetting can be removed by normalisation. It is important that the endogenous control is carefully selected for each individual experiment, as it should remain constant across all samples. This may mean that different controls are selected for use with different samples or experiments (Lardizabal et al., 2012).

2.7.1 Reverse transcription

RNA was extracted and quantified as described in section 2.3. Samples of sufficient quality (RIN score ≥ 8) were reverse transcribed using a high-capacity RNA to cDNA kit (Life Technologies, Paisley, UK), according to the manufacturer's instructions. Briefly, the RNA was diluted to a concentration of 2 µg in 9 µl ultra pure (18 MΩ) water and added to a reaction comprising of 10 µl 2X RT buffer and 1 µl 20X RT enzyme mix. Negative controls in which the RT enzyme was replaced with 1 µl ultra pure (18 MΩ) water were set up alongside. Any amplification from these negative controls would indicate genomic DNA contamination as no reverse transcription should take place. Reactions were mixed and incubated at 37°C for 1 h. This was followed by a denaturation step at 95°C for 5 min, and a hold at 4°C for at least 2 min. cDNA was stored at -20°C until required.

2.7.2 PCR

PCR was performed using a Power SYBR® Green kit (Life Technologies, Paisley, UK), according to the manufacturer's instructions. Briefly, cDNA and negative controls (-RT) from the reverse transcription reaction (section 2.7.1) were diluted 1 in 20 with ultra pure (18 MΩ) water. 1 µl diluted cDNA was added to a mix containing 12.5 µl 2X Power SYBR® Green reagent and 450 nM of forward and reverse primers in a MicroAmp® Optical 96-well reaction plate (Life Technologies, Paisley, UK). The Power SYBR® Green is a proprietary all-in-one reagent composed of SYBR® Green dye, a blend of dTTPs and dUTPs, AmpliTaq Gold® DNA polymerase and a passive reference dye (ROX™) to minimise non-specific fluctuations in fluorescence. Negative controls contained 1 µl of the diluted negative control reverse transcription reactions (-RT), and non-template controls (NTCs) contained 1 µl ultra pure (18 MΩ) water in the place of cDNA. Each 25 µl reaction was prepared in triplicate. Plates were centrifuged (453g, RT, 5 min) and loaded into an Applied Biosystems® 7500 Fast Real-Time PCR system (Life Technologies, Paisley, UK). The PCR protocol began with activation of the Taq polymerase; 50°C for 2 min, 95°C for 5 min. This was followed by 40 cycles of denaturing (95°C, 15 s) and

annealing/extending (60°C, 1 min). Finally a melt curve analysis was performed; 95°C for 30 s, 60°C for 15 s, increased to 95°C at 0.1°C/s.

2.7.3 Primer efficiency check and qRT-PCR quality control

The sequence of each mRNA of interest, excluding introns, was downloaded from Ensembl Genome browser (http://www.ensembl.org/index.html) and exon-spanning primers were designed using Primer Express, version 2.0. These primers were checked for specificity using Primer Blast (http://www.ncbi.nlm.nih.gov/tools/primer-blast/), and secondary structure or primer-dimer formation using the design tool in Sigma. All primers were purchased from Sigma (Poole, UK).

Primer efficiency was assessed for each primer pair prior to use. This is in accordance with the MIQE guidelines (Bustin et al., 2009). A calibration curve was generated by reverse transcribing RNA (as described in section 2.7.1) and performing PCR on serial 10-fold dilutions of the resulting cDNA (2 µg – 20 pg equivalent RNA input). Primers were used at a concentration of 450 nM. Log_{10}[RNA input (pg)] was plotted against CT value (Fig. 2.5). PCR (primer) efficiency was calculated as ($10^{-1/slope}$) and percentage primer efficiency as 100 x ($10^{-1/slope}$-1). A slope of -3.32 gives an efficiency of 100%; at this percentage the amount of product doubles for each cycle of PCR. Efficiencies of 90-110% were deemed suitable for use in the $2^{-\Delta\Delta CT}$ relative expression calculation. These checks also confirmed that the equivalent of 100 ng RNA input was suitable for subsequent qRT-PCR analysis.

Primer sequences and efficiencies are provided in Appendix III.

2.7.4 Data analysis

Provided there was only a single melt curve peak and no amplification with the negative control or NTC samples, the raw CT values were extracted and the $2^{-\Delta\Delta CT}$ method was used to determine whether there were any changes in relative expression between samples (Fig. 2.6). β-Actin was used as the endogenous control.

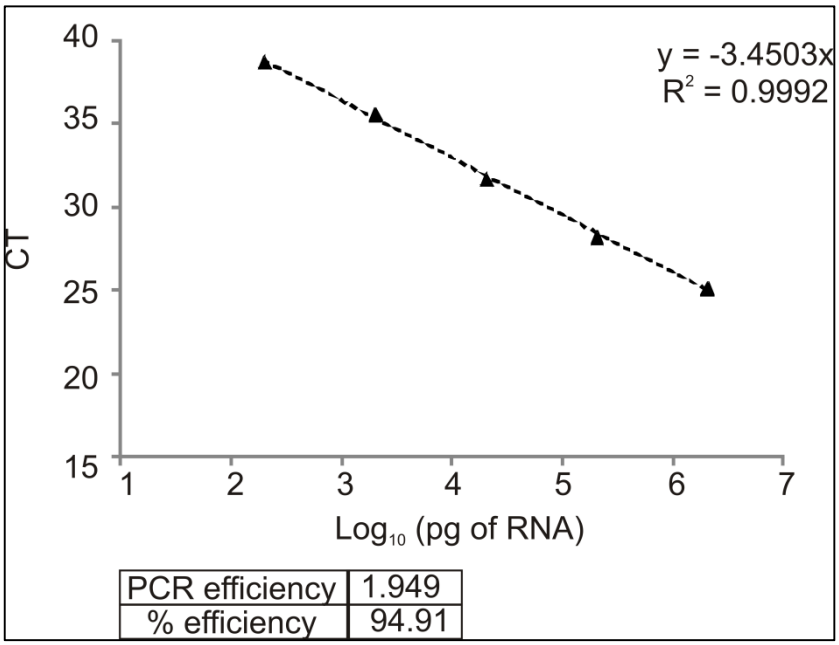

Fig. 2.5. Example of a PCR amplification curve. PCR was performed on serial 10-fold dilutions of cDNA. This plot was used to calculate the PCR (primer) efficiency ($10^{-1/slope}$) and percentage (primer) efficiency (100 x ($10^{-1/slope}$-1)) of each primer pair. In this case the efficiency of the primers (*Dio3*) was 95%, thus the product increased by 1.95X every PCR cycle.

1. CT (mRNA of interest) – CT (endogenous control) = ΔCT
2. ΔCT (compound-treated sample) – ΔCT (vehicle-treated sample) = ΔΔCT
3. Fold change in expression between compound-treated sample and vehicle-treated sample = $2^{-\Delta\Delta CT}$

Fig. 2.6. Calculation of relative changes in expression using the $2^{-\Delta\Delta CT}$ method.

2.8 WESTERN BLOTTING

Protein was extracted and quantified as described in section 2.5. 30-40 µg protein was mixed 1:1 with 2X sample buffer (100 mM Tris-HCl (pH 6.8), 100 mM DTT, 25% (v/v) glycerol, 2% (w/v) SDS, 0.01% (w/v)) and denatured at 95°C for 5 min. Protein samples were separated at 80 V for 1.5 h on a 10% acrylamide gel (1.5 M Tris-HCl (pH 8.8), 10% (w/v) SDS, 10% (w/v) APS, 0.07% (v/v) TEMED), and transferred to 0.45 µm nitrocellulose membrane (GE Healthcare, Buckinghamshire, UK) via electrotransfer at 100 V for 1 h in chilled blotting buffer (39 mM glycine, 48 mM Tris, 20% (v/v) methanol). Successful transfer was confirmed using a ponceau red stain (0.1% (w/v) ponceau, 5% (v/v) acetic acid). Membranes were blocked at RT for 1 h with 10% non-fat dry milk (Marvel) in TBST (Tris buffered saline, with 0.05% Tween-20) and incubated at 4°C overnight with the appropriate primary antibody (Table 2.3) in 5% Marvel in TBST. Membranes were washed at RT in TBST (5 x 5 min) and incubated with the appropriate horseradish peroxidase-conjugated secondary antibody (Table 2.3) at RT for 2 h. Membranes were washed at RT in TBST (5 x 5 min) and visualised using ECL™ Western Blotting detection reagents (GE Healthcare, Buckinghamshire, UK). Where possible, to check for equal loading, membranes were stripped in stripping buffer (62.5 mM Tris-HCl (pH 6.8), 2% (w/v) SDS, 100 mM β-mercaptoethanol) at 50°C for 30 min with occasional agitation, re-blocked, probed with a control antibody and subsequent secondary antibody, and visualised as described above. Bands were quantified using the gel analysis function of ImageJ software (http://rsb.info.nih.gov/ij).

Table 2.3. Antibodies used for Western blotting.

Primary antibody	Species	Dilution	Supplier	Secondary antibody	Dilution	Supplier
Dio3	Rabbit	1:1000	Novus Biologicals	Goat IgG-HRP	1:1000	Santa Cruz
Smarce1 (Baf57)	Rabbit	1:2000	Millipore	Goat IgG-HRP	1:2000	Santa Cruz
Gapdh	Rabbit	1:40,000	Sigma	Goat IgG-HRP	1:40,000	Santa Cruz
β-Actin	Rabbit	1:500	Millipore	Goat IgG-HRP	1:2000	Santa Cruz
β-Tubulin	Goat	1:100	Santa Cruz	Donkey IgG-HRP	1:2000	Santa Cruz

Optimum working dilution and antibody supplier are shown.

CHAPTER 3: APPLICATION OF GLOBAL mRNA TRANSLATIONAL PROFILING TECHNIQUES TO MODELS OF HEPATOTOXICITY

3.1 SUMMARY

In cases of acute, compound-induced hepatotoxicity a number of mRNAs showed a change in their translational activity. A greater proportion of mRNAs were regulated at this level than at the transcriptional level. Such changes are likely to result in a change in protein expression. It can therefore be hypothesised that by implementing changes at a level beyond transcription, the liver is able to instigate a rapid response to the toxic insult, thereby preventing lasting cellular damage. This hypothesis is supported by the literature, where other examples of gene regulation occurring solely at the translational level have been demonstrated, for example in the CNS. It thus follows that rapid changes in mRNA translation could be an effective way for dynamic organs, such as the liver, to rapidly alter protein expression following a toxic insult.

3.2 INTRODUCTION

3.2.1 Translational regulation

Measuring gene expression change as a marker of cell damage is a well established technique. Gene expression levels can be measured for all genes simultaneously using genomics methodologies such as microarrays. For small numbers of genes and for microarray validation, qRT-PCR is used. Methodologies such as these can identify specific gene changes and disrupted molecular pathways following cellular injury.

Controlling gene expression requires a number of key steps from RNA transcription to post-translational modifications of the completed polypeptide chain. Regulatory effects are seen transcriptionally, and pre- and post-translationally, for example, through mRNA and protein stability and degradation. These processes are described in more detail in Chapter 1, section 1.3. Initially, most work on gene regulation explored transcriptional changes in expression, as this was considered the predominant stage at which control occurred. It is now understood, however, that changes at the translational level may be of equal, if not greater, physiological and toxicological importance due to the speed with which new protein can be generated (Sonenberg and Hinnebusch, 2009). Consequently research in this area is attracting considerable interest.

Translational responses are essential within the CNS, where cells require rapid variation in their metabolic activity (Bottley et al., 2010; Le Quesne et al., 2010). Regulation at this level

enables a faster, more flexible response to cellular stress because the need to transport newly synthesised mRNAs to make more protein is avoided (Le Quesne et al., 2010). Such responses can also be specific to certain mRNAs. For example, in cases of temperature shock and DNA damage, where the majority of mRNA translation is shut down but a few key mRNAs increase their rates of translation, enabling the cell to deal with the additional stress (Spriggs et al., 2010). Furthermore, translational efficiency has been found to be the single best predictor of protein levels, whereas changes in mRNA abundance explain only approximately 40% of the variability (Schwanhausser et al., 2011). Furthermore, in certain cases translational regulation is the sole determinant of protein expression (Bottley et al., 2010; Moreno et al., 2012). Therefore, it is a key area to explore when trying to understand the molecular mechanisms underlying cellular responses to toxic insult.

Translation occurs through a process of ribosomal recruitment; the 40S and 60S ribosomal subunits bind in turn to the mRNA strand and elongation proceeds through the action of the eIF4F eukaryotic initiation complex (Gebauer and Hentze, 2004; Sonenberg and Hinnebusch, 2009). This process is described in more detail in Chapter 1, section 1.3.2.1 and is summarised in Fig. 3.1. Actively translated mRNAs will have a large number of ribosomes attached; those that are less active, and thus undergoing less efficient translation, will have fewer ribosomes attached. Coupling this process with genomics methodologies allows a global assessment of the translational activity of mRNAs following cellular stress. Furthermore, by combining these data with that obtained from transcriptional studies a comprehensive overview of the gene regulatory processes used by the cell to adapt to, and recover, from stress can be elicited. This approach has demonstrated a role for both transcriptional and translational regulation in many pathophysiological states such as apoptosis (Bushell et al., 2006), hypoxia (Thomas and Johannes, 2007) and amino acid starvation (Smirnova et al., 2005).

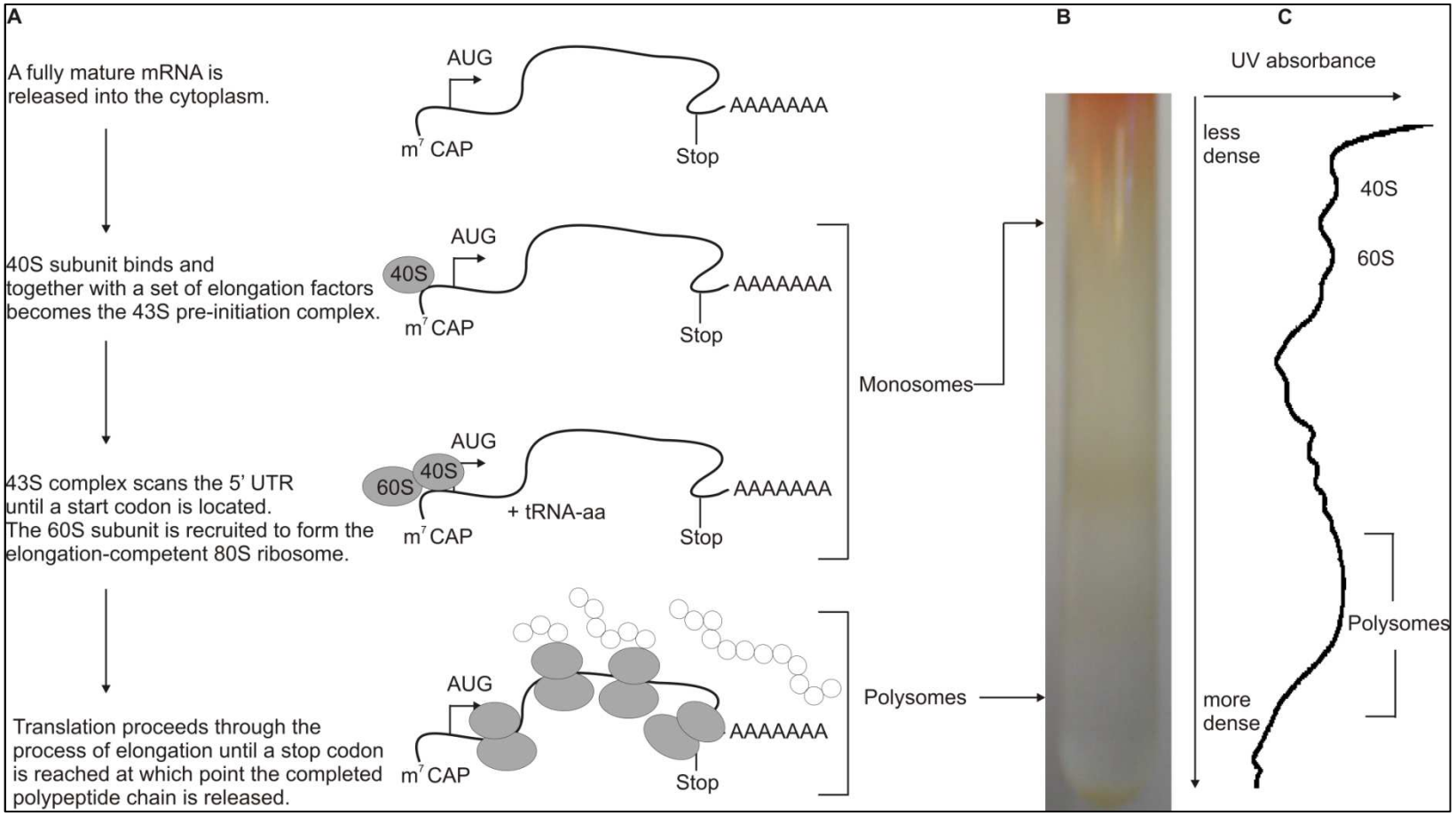

Fig. 3.1. Overview of translation initiation and RNA fractionation. (**A**) Key steps in translation initiation. Recruitment of the first ribosomal units to a mRNA forms a monosome. Once translation begins further ribosomes are recruited forming polysomes. The more ribosomes that a mRNA is associated with, the more dense that mRNA will be. (**B**) Sucrose density gradient. Those mRNAs that are more actively translated (more dense) will be located towards the bottom of the sucrose density gradient, whereas those that are less actively translated (less dense) will be located towards the top of the gradient. (**C**) UV trace of fractionation. Enables identification of peaks corresponding to (and thus fractions containing) the monosomes and the polysomes.

3.2.2 Translational profiling

The challenge with investigating translational regulation has always been that, rather than measuring the total amount of a given mRNA present within one sample and comparing this to the total amount in another sample, translational analysis requires measurement of a change in activity rate, i.e. how efficiently an mRNA undergoes post-transcriptional processing. This involves a fractionation step to separate the monosomes from the polysomes. Early ribosomal association studies were performed using *in vivo* samples in the mid-late 1960s and early 1970s (Jackson et al., 1964; Scornik, 1973). These two groups performed sucrose density gradient fractionation of rat liver samples and were amongst the first to investigate the separation of RNA samples according to ribosomal density. Scornik was also the first to include a 260nm trace of the gradient undergoing fractionation. This vastly improved the ability to accurately separate the monosomal from the polysomal species. In recent years, the translational profiling of *in vitro* rather than *in* vivo samples has become more widespread, leading to the development of a robust method described by Johannes and Sarnow (Johannes and Sarnow, 1998). These *in vitro* studies have been highly informative, particularly when investigating specific processes, such as cell death (Bushell et al., 2006), or cancer cell lines (Bates et al., 2012; Young et al., 2012). However, the use of *in vivo* samples remains important, particularly when attempting to model the kinetics of a xenobiotic across an entire organ or animal, as is the case here in models of hepatotoxicity.

3.2.3 Hepatotoxicity

Liver disease is a major health burden in the developed world (Vernon et al., 2011; Wang et al., 2012c). In the UK, liver disease ranks among the top five causes of death annually and, unlike the rest of Europe, rates are continuing to increase (Murray et al., 2013). There are a range of aetiologies of liver disease, including cancer, hepatitis C, alcoholic liver disease, obesity, and drug-induced injury. Furthermore, overt hepatotoxicity is the main reason for drug withdrawal both during development and from the market (Williams, 2006). Many of the same clinical features such as fibrosis, cholestasis and apoptosis are seen across the different types of liver disease and toxicity (Wang et al., 2012c), thus the delivery of a sub-toxic dose of a known hepatotoxin can provide a useful *in vivo* model system for investigating the underlying molecular mechanisms involved in hepatotoxicity.

3.3 AIM

To adapt existing translational profiling techniques, which are predominantly used with *in vitro* samples, for use with *in vivo* liver samples; and subsequently apply these techniques to samples taken from models of compound-induced hepatotoxicity.

3.4 MATERIALS AND METHODS

3.4.1 Animal models

The animal models used for the work described in this chapter were the Griseofulvin-treated mice and the PredTox compound-treated rats.

Animals were maintained and treated as described in Chapter 2, section 2.1.1 and 2.1.3.

3.4.2 Cell culture

Cells were grown and maintained as described in Chapter 2, section 2.2.

3.4.2.1 Determination of cell viability

3.4.2.1.1 MTS Assay

The MTS, or AQ_{ueous} One Solution Cell Proliferation, Assay (Promega, Madison, USA) is a colorimetric-based technique whereby viable cells are able to convert MTS tetrazolium compound (3-(4,5-dimethylthiazol-2-yl)-5-(3-carboxymethoxyphenyl)-2-(4-sulfophenyl)-2H-tetrazolium) into formazan. The formazan product can be detected by absorbance measurement at A_{490nm} and is directly proportional to the metabolic activity of the cells.

3.4.2.1.2 CellTiter Blue® Assay

The CellTiter Blue® Assay (Promega, Madison, USA) is an alternative measure of cell viability. Metabolically active cells convert resazurin to resorufin and thus generate a fluorescent signal. The Ex_{560nm}/Em_{590nm} intensity is directly proportional to cell viability.

3.4.2.2 Assessment of cell viability following Griseofulvin treatment using the MTS Assay and CellTiter Blue® Assay

These two assays followed a similar protocol. Cells were plated at a density of 20,000 cells/ml in 96 well-plates, incubated at 37 °C overnight to adhere, and then treated with increasing doses of Griseofulvin, dissolved in 0.1% (v/v) DMSO. A search of the literature was conducted to determine suitable doses (Kim et al., 2011; Rathinasamy et al., 2010; Rebacz et al., 2007). As

such, cells were dosed at 0.1 µM, 0.5 µM, 1 µM, 5 µM, 10 µM, 50 µM, 75 µM, 100 µM, 150 µM and 200 µM (n=8). The first column (1) contained cells in normal media and column 2 contained cells treated with 0.1% DMSO as a control. Cells were incubated at 37°C for 72 h and cell viability was determined using the AQ_{ueous} One Solution Cell Proliferation Assay and the CellTiter Blue® Assay according to the manufacturer's instructions. Briefly, 20 µl of the appropriate reagent was added to each well of the 96 well-plate and the plates were incubated at 37°C for 3 h. The absorbance (A_{490nm}), or fluorescence (Ex_{560nm}/Em_{590nm}) was measured using a Perkin Elmer Victor X4 plate reader (Perkin Elmer, Cambridge, UK). For each dose the measured value was normalized to, and expressed as a relative percentage of, the DMSO control reading.

3.4.2.3 Treatment of Hepa cells with Griseofulvin

Hepa 1-6 liver cells were plated into 6 well-plates at a density of 20,000 cells/ml. They were incubated at 37 °C overnight to adhere and then treated in duplicate with either 5 µM or 10 µM Griseofulvin in 0.1% (v/v) DMSO, or 0.1% (v/v) DMSO as a vehicle-only control. After 72 h, half of the cells were harvested into Tri reagent for RNA extraction and half were harvested into lysis buffer, plus protease inhibitor cocktail, for protein extraction, as described in Chapter 2, sections 2.3.2. and 2.5.2, respectively.

3.4.3 Sucrose Density Gradient Fractionation

3.4.3.1 Preparation of sucrose gradients

Solutions of 10%, 20%, 30%, 40% and 50% (w/v) sucrose in gradient buffer (300 mM NaCl, 15 mM $MgCl_2$, 15 mM Tris-HCl (pH 7.5), 2mM DTT and 100 µg/ml cycloheximide) were prepared. 2 ml of the 50% sucrose solution was added to a centrifuge tube and incubated at -80°C for a minimum of 30 min until frozen. 2 ml of the 40% sucrose solution was added to the same tube on top of the frozen 50% layer and tubes were returned to the freezer for a minimum of 30 min. This process was repeated with the 30%, 20% and 10% sucrose solutions and gradients were stored at -80°C until required. On the day of use gradients were removed from the freezer and allowed to equilibrate to RT prior to loading of the samples.

3.4.3.2 Preparation of samples (tissue)

Approximately 150 mg of liver tissue was ground to a powder in liquid nitrogen using a pestle and mortar on dry ice. The ground sample was then lysed in lysis buffer (15 mM Tris-HCl (pH 8.0), 300 mM NaCl, 15 mM $MgCl_2$, plus inhibitors (1 mg/ml heparin, 100 µg/ml cycloheximide

and 80 U RNAsin)). Lysis was allowed to proceed on ice for approximately 60 min, with regular vortexing. Samples were then centrifuged (15,600g, 4°C, 5 min) and supernatants were loaded onto gradients (prepared as described in section 3.4.3.1).

3.4.3.3 Preparation of samples (cell)

Hepa 1-6 liver cells were grown until approximately 70% confluent in 15 cm plates. Two plates were maintained for each sample. 200 µl cycloheximide (diluted to a concentration of 100 µg/ml in PBS) was added to each plate and the plates were incubated at 37°C for 5 min. Upon removal from the incubator, plates were nestled into a tray of ice, media (+ cycloheximide) was removed and 10 ml PBS-cycloheximide (100 µg/ml final concentration cycloheximide) was added. Cells were scraped and collected into chilled 50 ml falcons. Plates were rinsed with a further 5 ml PBS-cycloheximide and this was added to the chilled falcon. Falcons were centrifuged (515g, 4°C, 4 min) and the supernatant was discarded. Pellets were resuspended in 1 ml PBS-cycloheximide and transferred to 1.5 ml tubes. Tubes were centrifuged (800g, 4°C, 1 min) and the supernatant was removed. Pellets were resuspended in 1 ml ice cold lysis buffer (300 mM NaCl, 15 mM $MgCl_2$, 15 mM Tris-HCl (pH 7.5), 1% (v/v) Triton X-100 plus inhibitors (2mM DTT, 100 µg/ml cycloheximide and 500 U SUPERase-In)), left on ice to lyse for 1 min and then centrifuged (15,600g, 4°C, 1 min). Supernatants were loaded onto gradients (prepared as described in section 3.4.3.1).

3.4.3.4 Preparation of samples including EDTA and excluding cycloheximide

To produce example gradients where all polysomes were dissociated, additional gradients, prepared in the absence of cycloheximide and presence of EDTA, were performed using Hepa cells. The cells were prepared as described in section 3.4.3.3 with the exclusion of the cycloheximide step. In addition, cycloheximide was excluded from the lysis buffer and $MgCl_2$ was replaced with EDTA (300 mM NaCl, 15 mM EDTA, 15 mM Tris-HCl (pH 7.5), 1% (v/v) Triton X-100, plus inhibitors (2mM DTT and 500 U SUPERase-In)).

3.4.3.5 Fractionation of sucrose gradients

Gradients were ultra centrifuged (182,000g, 4°C, 2 h) in a Beckman ultracentrifuge using a SW40 rotor. 65% (w/v) sucrose in water containing 50 mg bromophenol blue was used in combination with a Harvard syringe pump system to fractionate each gradient into 10-16 individual 1 ml fractions. These fractions were collected into tubes containing 1 ml Tri reagent and stored at -80°C until RNA extraction.

3.4.3.6 RNA extraction

RNA was extracted from each fraction (prepared as described in section 3.4.3.5), using Tri reagent according to the manufacturer's instructions (Chapter 2, section 2.3). To ensure maximum purity, RNA was re-precipitated at -20°C overnight in 1/10th volume of 3 M NaOAc (pH 5.2) and 2.75X 100% EtOH. RNA was pelleted by centrifugation (12,000g, 4^{o}C, 10 min) and the supernatant was discarded. Pellets were washed twice with 1 ml cold 75% (v/v) EtOH. All traces of EtOH were removed using a gel loading tip and pellets were air dried at RT for approximately 10 min. RNA pellets were resuspended in an appropriate volume of ultra pure (18 MΩ) water. The quantity and quality of RNA was measured as described in Chapter 2, sections 2.3.3 and 2.3.4.

3.4.4 Verification of monosomal/polysomal regions

3.4.4.1 UV trace

A UV recorder was used to measure the absorbance (A_{254}) of the gradients during fractionation. The sensitivity of the detector was adjusted according to the starting quantity of material. With cell samples a sensitivity of 1 was typically employed, with liver samples this was increased to 2.

3.4.4.2 Gel electrophoresis

An equal volume of RNA from each fraction was mixed with 3 µl RNA loading buffer (50% (v/v) glycerol, 1 mM EDTA, 0.25% (w/v) xylene cyanol and 0.25% (w/v) bromophenol blue), loaded onto a 1% (w/v) agarose gel and electrophoresed as described in Chapter 2, section 2.3.4.1.

3.4.4.3 Micro dot blotting: 40S, 60S and β-Actin

An equal volume of RNA from each fraction was mixed with 12 µl denaturing buffer (59% (v/v) deionised formamide, 24% (v/v) formaldehyde, 0.14M MOPS) and dot blotted onto MagnaGraph nylon transfer membrane (Labtech International, East Sussex, UK) using a MicroGrid II automated microarrayer (Digilab, Marlborough, USA). Membranes were cross-linked with 120 mJ/cm^2 UV for 60 s and pre-hybridised in hybridisation buffer (50% (v/v) deionised formamide, 6X SSC, 5X Denhardt's solution, 1% (w/v) SDS) at 42°C for 3 h. A probe, derived from a PCR product to the coding region of β-Actin, was labelled with ^{32}P-αdCTP using *E. coli* Klenow fragment (for exact protocol see Appendix IV). Simultaneously, probes complementary to the 40S and 60S ribosomal subunits were end-labelled with ^{32}P-γATP (Appendix IV). Radioactive incorporation was measured by scintillation counting. 1x10^6

dpm/ml probe was added to the pre-hybridised membranes and hybridised at 42°C for 48 h. The hybridised dot blots were washed in solutions of increasing stringency (wash 1: 2X SSC, 0.1% (w/v) SDS (2 x 5 min washes), wash 2: 1X SSC, 0.1% SDS (2 x 5 min washes), wash 3: 0.1X SSC, 0.1% SDS (2 x 15 min washes), all performed at 42°C), visualised using autoradiography and quantified using ImageQuant TL (v2003.03).

3.4.4.4 Northern blotting: β-Actin

A 5 µl aliquot of RNA from each fraction was added to 15 µl of a slightly different denaturing buffer (66% (v/v) deionised formamide, 23% (v/v) formaldehyde, 1X MOPS (0.2 M MOPS (pH 7.0)) and 4 µl gel loading buffer (95% (v/v) formamide, 1 mM EDTA, 0.01% (w/v) bromophenol blue and 0.01% (w/v) xylene cyanol)). Samples were denatured at 65°C for 15 min, snap cooled on ice and then loaded onto a denaturing agarose gel (1% (w/v) agarose, 14% (v/v) formaldehyde in 1X MOPS, 80 mM NaOAc and 10 mM EDTA). Electrophoresis proceeded at 15 V overnight in 1X MOPS. The following day RNA was transferred from the gel to MagnaGraph nylon transfer membrane (Labtech International, East Sussex, UK) by capillary transfer (10X SSC). The membrane was first cross-linked (as described in section 3.4.4.3) and then transferred to methylene blue staining solution (0.02% (w/v) methylene blue, 0.3 M NaOAc (pH 5.2). Washing in distilled water revealed the 18S and 28S ribosomal RNA bands, which were marked on the membrane prior to hybridisation. Staining solution was removed by washing in 1X SSC, 1% (w/v) SDS and then ultra pure (18 MΩ) water. The membranes were pre-hybridised in hybridisation buffer (50% (v/v) deionised formamide, 6X SSC, 5X Denhardt's solution, 1% (w/v) SDS) at 42°C for 3 h. Labelling of β-Actin with ^{32}P-αdCTP, hybridisation, washing, visualisation and quantification proceeded as described in section 3.4.4.3.

3.4.5 Translational profiling using microarrays

3.4.5.1 Purification and pooling of fractions

Each gradient was sub-pooled into 4 groups corresponding to monosomes, light polysomes, medium polysomes and heavy polysomes according to ribosomal density (Fig. 3.2). Equal volumes of individual fractions were taken to give a final yield of approximately 10 µg RNA for each pooled sample. An example of the worksheet used to calculate required volumes is provided in Appendix V. The pooled sample was re-precipitated and resuspended in 10 µl ultra pure (18 MΩ) water as described in section 3.4.3.6.

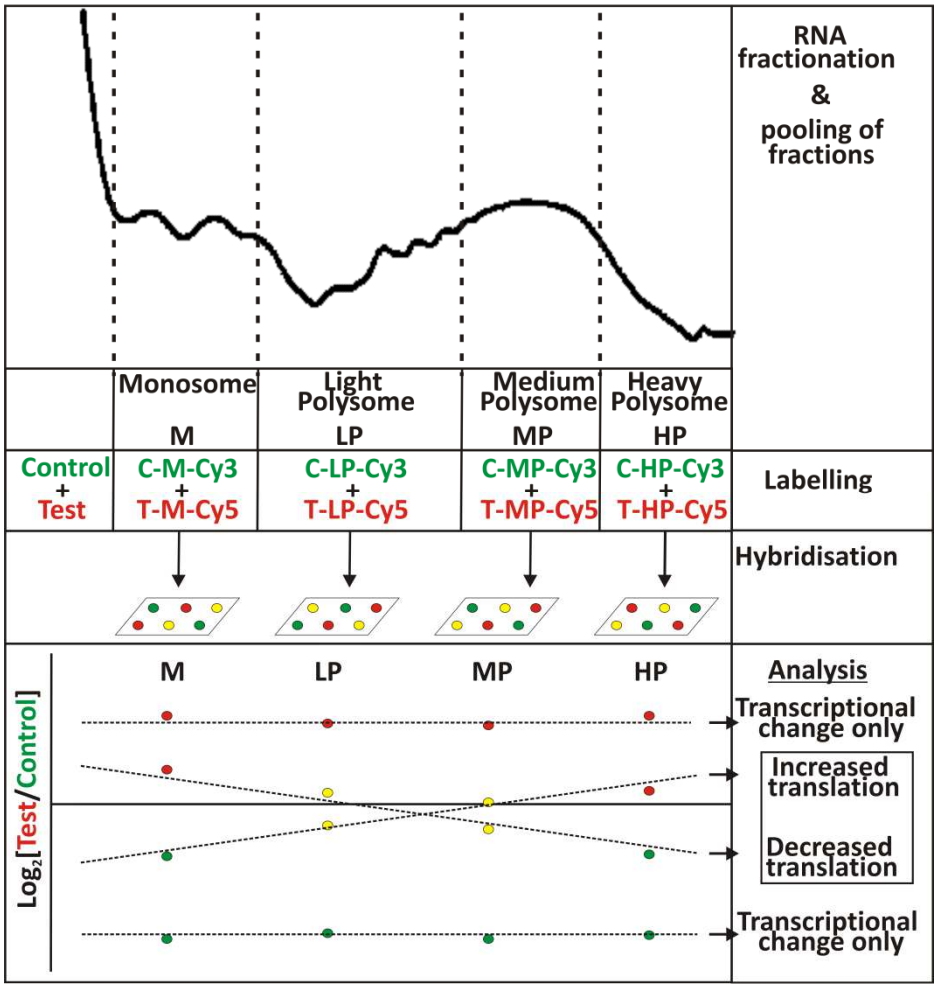

Fig. 3.2. Translational profiling of liver samples using microarrays. RNA from the livers of control (vehicle-treated) and test (compound-treated) animals was fractionated by sucrose density centrifugation and sub-pooled into four fractions: monosome (M), light polysome (LP), medium polysome (MP) and heavy polysome (HP). Each of the four control (C) fractions were labelled with Cy3 and hybridised against each of the four corresponding test (T) fractions labelled with Cy5. The statistical significance of differences between C and T in each of the four fractions was calculated using a reverse labelled two-tailed T-Test (Zhang and Gant, 2004). All data with four *p* values > 0.05 were rejected. Linear regression analysis showed movement of mRNAs through the gradient and enabled differentially translated and transcribed mRNAs to be identified. Reverse labelling reactions (T sub-pools labelled with Cy3 and C sub-pools labelled with Cy5) were also performed and incorporated into the analysis (image adapted from (Dudek et al., 2013)).

3.4.5.2 Reverse transcription, labelling and hydrolysis

A direct labelling method was used to label fractionated RNA. This meant that flurophore-conjugated nucleotides were incorporated directly during the reverse transcription step. The RNA was first primed with 1 µl oligo $dT_{23}N_2$ (8µg/µl) and 1 µl random pentadecamers (10 nmol/µl) (both from Sigma, Poole, UK) via incubation at 70°C for 10 min. Samples were reverse transcribed in a reaction comprising 4 µl 5X First strand buffer (Life Technologies, Paisley, UK), 0.5 µl dNTPs (0.5 mM dATP, 0.5 mM dGTP, 0.5 mM dCTP and 0.2 mM dTTP) (Kapa Biosystems, USA), 0.02 M DTT (Invitrogen, Paisley, UK), 200 U Superscript III (Invitrogen, Paisley, UK), 40 U RNAsin (Promega Madison, USA) and 2 µl of the appropriate dUTP- conjugated Cy-3 or Cy-5 dye (25 nmol/µl) (GE Healthcare, Buckinghamshire, UK), via incubation at 50°C for 2 h. Any remaining RNA was hydrolysed with 0.01 M EDTA (pH 8.0), 0.2% (w/v) SDS and 0.2 M NaOH to a final reaction volume of 50 µl and incubated at 70°C for 10 min. Reactions were neutralised with 1 M Tris-HCl (pH 7.0) and purified using Microcon YM-30 columns (Millipore, Billerica, USA). All labelling reactions were performed in duplicate, incorporating a dye swap technique for n=5 pairs of samples.

3.4.5.3 Hybridisation and scanning

Dye incorporation and cDNA yield was assessed using a Nanodrop-1000 Spectrophotometer (Nanodrop Technologies). Equal concentrations of the relevant Cy-3 labelled and Cy-5 labelled samples were combined, 1 µl tRNA (4 mg/ml in ultra pure (18 MΩ) water) was added to reduce the possibility of non-specific binding during hybridisation, and samples were denatured at 95°C for 5 min prior to loading onto a MEEBO microarray, containing 70-mer oligonucleotide probes (Life Technologies, Paisley, UK). Microarray design and printing is described in Chapter 2, section 2.6. Hybridisation was performed at 42°C overnight (for a minimum of 16 h). For each gradient a sub-pool of control (vehicle-treated) monosomal fractions was hybridised against the equivalent sub-pool of test (compound-treated) monosomal fractions on one microarray, the sub-pool of control light polysomal fractions was hybridised against the sub-pool of test light polysomal fractions on a second microarray, and so forth for each sub-pool. This is shown schematically in Fig. 3.2.

Following hybridisation, slides were washed at RT in solutions of increasing stringency (wash 1: 1X SSC, 0.03% (w/v) SDS for 5 min, wash 2: 0.2X SSC for 3 min, wash 3: 0.05X SSC for 3 min), dried by centrifugation (200g, RT, 4 min) and scanned on a 4200A Axon scanner (Molecular Devices, Sunnyvale, CA).

3.4.5.4 Data analysis

The scanned microarray images were analysed with GenePix Pro 5.0 to generate raw data files, which were normalised using Lowess and tested for statistical significance using a reverse labelled T-Test as previously described (Zhang and Gant, 2004). Lowess normalisation uses locally weighted regression to smooth scattered data (Quackenbush, 2002). Those mRNAs in which none of the $\log_2$ values across the gradient were statistically significant (all four *p* values > 0.05) were excluded from further analysis. There were a maximum of four $\log_2$ (test/control) values for the remaining mRNAs, which corresponded to the proportional representation within each sub-pool of fractions. By calculating the linear regression, or degree of slope, across the $\log_2$ values for each sub-pool of fractions (monosomes, light polysomes, medium polysomes and heavy polysomes), it was possible to determine any translational change. mRNAs that were present in increasingly higher amounts across the gradient had positive slopes (≥ +0.1) and represented mRNAs that were more efficiently translated. These mRNAs had a greater representation in the heavy polysomes of the treated samples. mRNAs that were present in smaller amounts across the gradient had negative slopes (≤ -0.1) and represented mRNAs that were less efficiently translated. These mRNAs had a greater representation in the polysomes of the control (vehicle-treated) samples. In addition, by averaging the 4 values across the gradient a measure of transcriptional activity could be calculated. If there was a consistent change, but no overall movement, i.e. an average $\log_2$ value of ≥ ±0.5, but a slope value that fell between +0.09 and -0.09, then a transcriptional, rather than a translational change, was the most likely regulatory event for that mRNA.

3.4.5.5 Canonical pathway analysis

Throughout the course of this work two pathway analysis packages were used. Those mRNAs altered in translational efficiency following Griseofulvin treatment were analysed using the Gene Set Analysis toolkit (available at http://bioinfo.vanderbilt.edu/webgestalt) (Zhang et al., 2005). The mRNAs altered in response to treatment with PredTox compound FP014SC were analysed using Ingenuity IPA software for pathway analysis (Ingenuity® Systems, www.ingenuity.com). Both packages identified canonical pathways in which a significant ($p \leq 0.05$) number of mRNAs were deregulated following treatment. This highlighted mRNAs of particular physiological relevance.

3.4.6 Validation of microarray results

3.4.6.1 Quantitative RT-PCR of fractionated RNA

Changes in translational efficiency of mRNAs of particular interest were further validated using qRT-PCR. The same sub-pools of fractions were used and, as with the translational microarray profiling, a worksheet was used to calculate the equal volume of each fraction required to produce a final sub-pooled concentration of RNA (for qRT-PCR analysis 200 ng was used) (Appendix VI). The pooled RNA was reverse transcribed using a High Capacity RNA-to-cDNA kit (Life Technologies, Paisley, UK), as described in Chapter 2, section 2.7.1. The efficiency of all primers was tested as described in Chapter 2, section 2.7.3 and PCR was performed using the *Power* SYBR®Green PCR Master Mix (Life Technologies, Paisley, UK) and an Abi Prism® 7000 Sequence Detection System as described in Chapter 2, section 2.7.2. The proportional representation of a mRNA within each pooled set (monosomes, light polysomes, medium polysomes and heavy polysomes) was calculated as a percentage of the total gradient. This provided a measure of the movement of the mRNA across the gradient and was, therefore, used to validate the changes seen with treatment following microarray translational analysis.

qRT-PCR was also used to analyse transcriptional regulation using total RNA samples. Method was as described in Chapter 2, section 2.7. Statistically significant differences were calculated using a two-tailed Student's T-Test.

3.4.6.2 Western Blotting: SMCE1

Protein was extracted and quantified as described in Chapter 2, section 2.5. To assess whether alterations in the translational efficiency of *Smarce1* were having a downstream effect on protein levels, a polyclonal antibody against the SMARCE1 protein (SMCE1, also known as Baf57) was used (Millipore, Billerica, USA). Western blotting was performed as described in Chapter 2, section 2.8. Ponceau red stain was used to identify any obvious discrepancies in the loading of protein samples, due to difficulties obtaining a suitable loading control. Statistically significant differences were calculated using a two-tailed Student's T-Test.

3.5 RESULTS

3.5.1 Determination of *in vitro* Griseofulvin doses

Although the majority of the work described in this chapter was performed using *in vivo* samples, having the same model situation represented in an *in vitro* system proved useful for method development and further validation of results. Results from the two cell viability assays are presented in Fig. 3.3. A low and a high dose were selected for further work. The low dose (5 µM) caused an approximate 15% reduction in the viability of Hepa 1-6 liver cells, whilst the high dose (10 µM) caused up to a 60% reduction in cell viability. Readings were comparable across both assays. These doses were selected as it was between 5 µM and 10 µM that the largest change in overall cell survival was seen (Fig. 3.3).

Early evidence that these doses were inducing a physiological response within the cells came from quantification of RNA and protein yields. Yields from each Griseofulvin-treated sample were normalised to the yields from vehicle-treated samples, harvested at the same time. With increasing dose there was reduced RNA and protein recovery (Fig. 3.4). This suggests the Griseofulvin was having a negative effect on the ability of the cells to make more RNA and protein, indicating they were suffering stress, and this was enhanced in a dose-dependent manner.

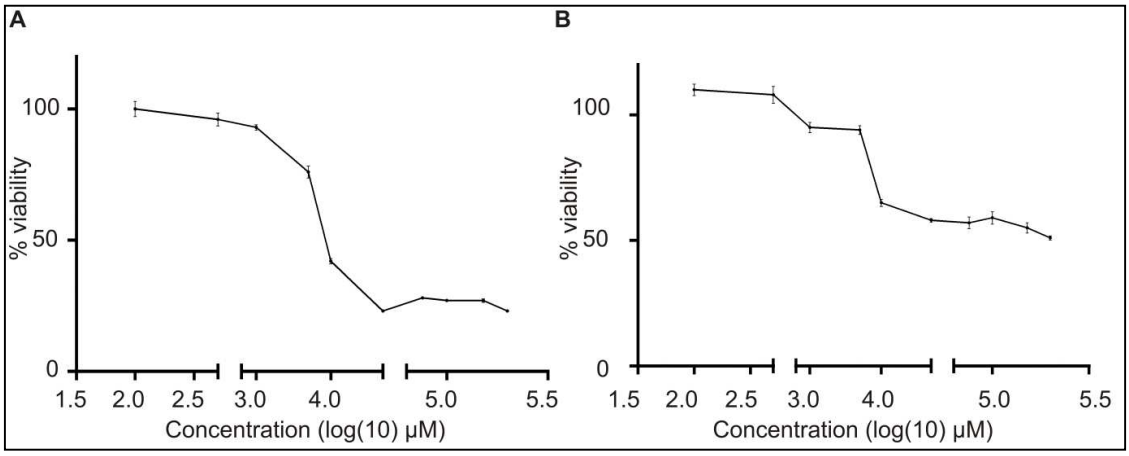

Fig. 3.3. Cell viability assays enabled determination of suitable dosing concentrations for treating Hepa 1-6 cells with Griseofulvin. (**A**) CellTiter Blue® assay and (**B**) MTS assay. Data represents mean ± SEM. Hepa 1-6 cells were treated with a range of Griseofulvin concentrations (0.1 µM – 200 µM) n=8, or vehicle-only control (0.1% DMSO) n=8, for 72 h.

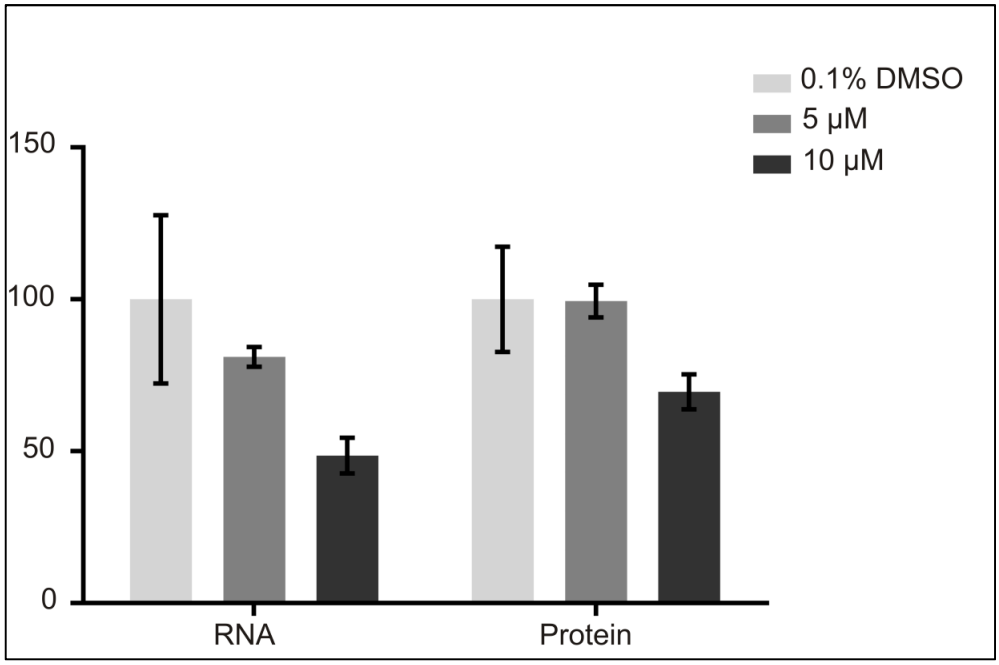

Fig. 3.4. RNA and protein yields were reduced following treatment with Griseofulvin. Hepa 1-6 cells were treated with 5 µM and 10 µM Griseofulvin for 72 h (n=3). Yields were normalised to those obtained from cells treated with the vehicle-only control (n=3). Data represents mean ± SEM.

3.5.2 Adaptation of translational profiling technique for use with *in vivo* samples

The first problem to overcome when performing translational profiling on *in vivo* tissues was maintaining the integrity of the polysome complexes and RNA within the samples. Samples were ground with a pestle and mortar on dry ice using liquid nitrogen to ensure that they were kept frozen. They were then gently lysed in buffer containing the inhibitors heparin and RNasin to inhibit any RNases and prevent RNA degradation. Cycloheximide was added to the lysis buffer to lock the mRNA/ribosomal complex in place, thereby preventing the ribosomes from detaching from the polypeptide chain and, thus, functioning to stall translation. This inhibits protein biosynthesis by blocking the elongation phase of translation (Warner et al., 1966).

During fractionation of cell samples the 254nm UV trace clearly demonstrated the location of the monosomal and polysomal regions. Indeed, individual ribosomes can be observed within the polysomal region of *in vitro* samples (Fig. 3.5 A). Although such high resolution was not possible with the *in vivo* liver samples, even with the loading of a smaller quantity of starting material onto the gradient, separation of the monosomal and polysomal regions was still observed (Fig. 3.5 B).

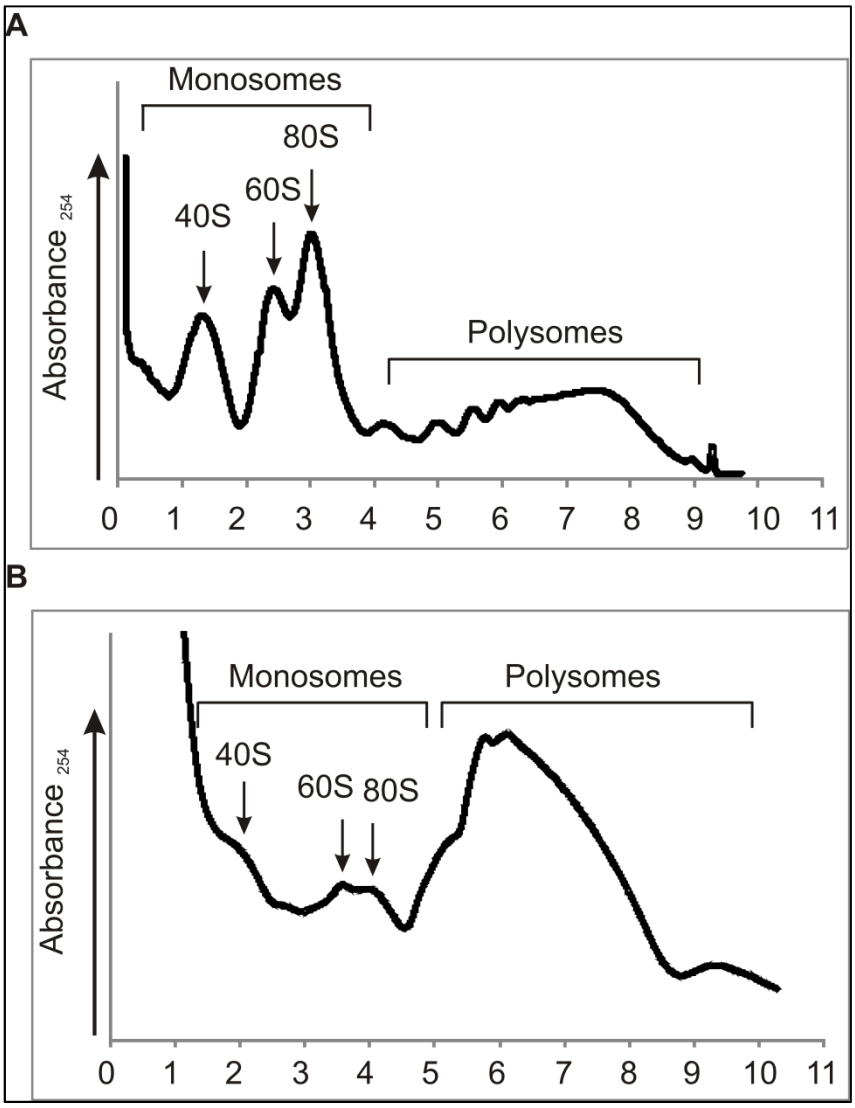

Fig. 3.5. UV absorbance traces recorded during sucrose density fractionation indicate separation of the monosomal and polysomal regions. (**A**) Example of a trace from fractionated untreated Hepa cells, grown to 70% confluency, harvested and lysed in the presence of cycloheximide, and fractionated. The absorbance was recorded at a sensitivity of 1. (**B**) Example of a trace from a fractionated vehicle-only (0.9% saline) treated rat liver sample. Liver tissue was lysed in the presence of cycloheximide and fractionated. The absorbance was recorded at a sensitivity of 2. The 40S subunit is recruited to the mature mRNA first, followed by the 60S subunit to form the 80S complex. Together these represent the monosomes, whilst later peaks represent the polysomes.

To enable accurate sub-pooling of monosomes and polysomes a number of techniques, including gel electrophoresis, micro dot blotting and Northern blotting, were employed in combination with the UV absorbance trace. An example of how the UV traces, RNA concentrations and radiolabelled membranes were used to identify the monosomal and polysomal regions is provided in Fig. 3.6. The ribosomal subunits, 40S and 60S, indicated the beginning of the monosomal fractions, whilst β-Actin (a highly actively translated mRNA within many cells and tissues) revealed the location of the polysomal region. In addition, fractionation of gradients in the absence of cycloheximide and presence of EDTA caused the ribosomes to detach from the polypeptide chain and disassociated the 80S ribosome complexes back into unbound 40S and 60S subunits. This further confirmed the location of the monosomal and polysomal regions (Fig. 3.6).

In the example gradient shown in Fig. 3.6 the monosomal pool consisted of fractions 1 – 5. This encompassed the recruitment of the 40S and 60S subunits (fractions 2 and 4, respectively) to form the 80S complex, and was prior to the increase in β-Actin expression, evident from fraction 6 onwards. In addition, following inclusion of EDTA in the gradient, the highest RNA concentrations and the majority of the β-Actin signal were present in fractions 1 – 5, providing further evidence that this was the monosomal region. The polysomal region, identified as such by its higher proportional representation of β-Actin, comprised fractions 6 – 11.

Relatively small shifts in translational activity were expected. Therefore, to enable detection of these more subtle translational changes it was decided to split the polysomal region into three further sub-pools (designated light, medium and heavy polysomes). These are shown in Fig. 3.2. The light polysomes consisted of those fractions where the trace was beginning to indicate the individual ribosomes (fractions 6 and 7 in Fig. 3.6); the medium polysomes were indicated by the highest β-Actin signal intensity and plateauing of the UV trace (fractions 8 and 9 in Fig. 3.6); and the heavy polysomes were at the very end of the gradient, where β-Actin intensity remained high, but the A_{254} was beginning to reduce (fractions 10 and 11 in Fig. 3.6).

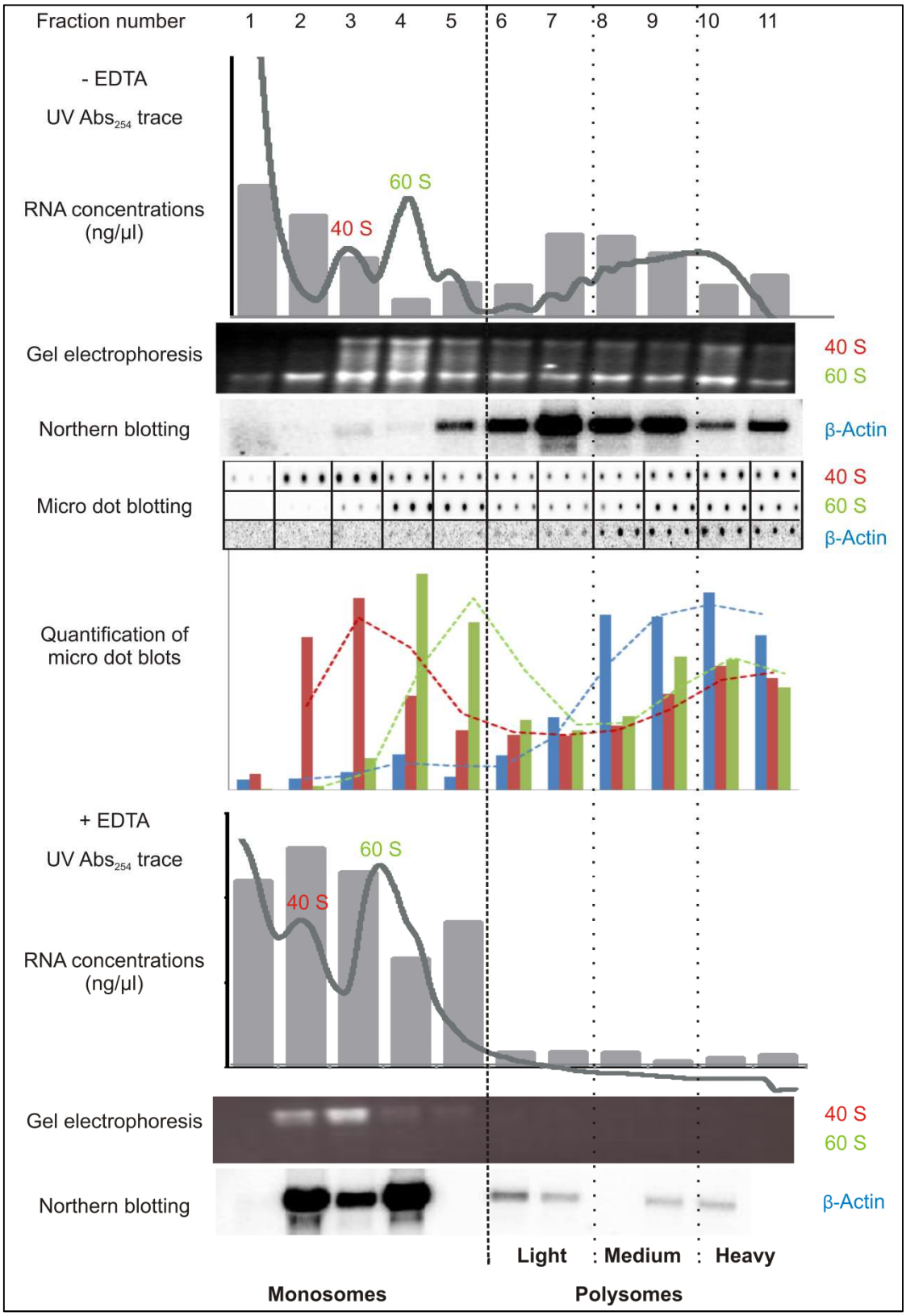

Fig. 3.6. Combining methods enabled accurate determination of the monosomal and polysomal regions following fractionation. The 40S and 60S subunits represent the monosomal region, whilst β-Actin (a translationally active mRNA) represents the polysomal region. In the presence of EDTA the polysomes were dissociated, resulting in a shift of the RNA and β-Actin to the early (monosomal) fractions.

As discussed in section 3.4.5.4 and shown in Fig. 3.2, microarray analysis was then performed on the pooled fractions. Control monosomes were hybridised against treated monosomes, control light polysomes against treated light polysomes, and so forth for each sub-pool of fractions. Upon completion the $\log_2$ value of treated/control was calculated for each mRNA in each sub-pool of fractions, enabling movement of particular mRNAs across the gradient to be calculated. Differences between $\log_2$ values were calculated and where significant in at least one of the sub-pools ($p \leq 0.05$), linear regression analysis across the gradient was calculated. By also averaging the $\log_2$ values across the gradient, changes in transcriptional activity could be identified concurrently.

This technique was applied to two different model systems of hepatotoxicity.

3.5.3 Model 1: Griseofulvin-treated mice

The Griseofulvin-treated mouse is a well characterised model of hepatotoxicity, already implemented within our group (Gant et al., 2003). Griseofulvin is an anti-fungal treatment, most commonly used in the treatment of athletes' foot (Gupta et al., 1994). When given orally to mice it produced changes in the liver similar to those observed in patients with erythropoietic protoporphyria-associated liver failure, including inflammation, fibrosis and cholestasis (Knasmuller et al., 1997). Early evidence of liver injury was seen after treatment for 5 days, and by 22 days there was pronounced hepatotoxicity (Gant et al., 2003). This was concurrent with a large number of transcriptional changes in the cytochrome p450 genes and disruption of the steroid biosynthesis pathway (Gant et al., 2003). The 22 day time point was selected for further work as by this stage inflammation was high and there was maximum accumulation of protoporphyrin.

3.5.3.1 Translational changes following treatment with Griseofulvin

Following treatment with Griseofulvin for 22 days, 219 mRNAs showed a change at the translational level (Fig. 3.7). These were grouped according to whether they were translationally increased or repressed, and whether this was concurrent with (60 mRNAs, Fig. 3.7 A), opposite to (28 mRNAs, Fig. 3.7 B), or without (131 mRNAs, Fig. 3.7 C) a transcriptional change. A final category consisted of those mRNAs that demonstrated a transcriptional change only (79 mRNAs, Fig. 3.7 D). Example mRNAs from each category are provided in Table 3.1.

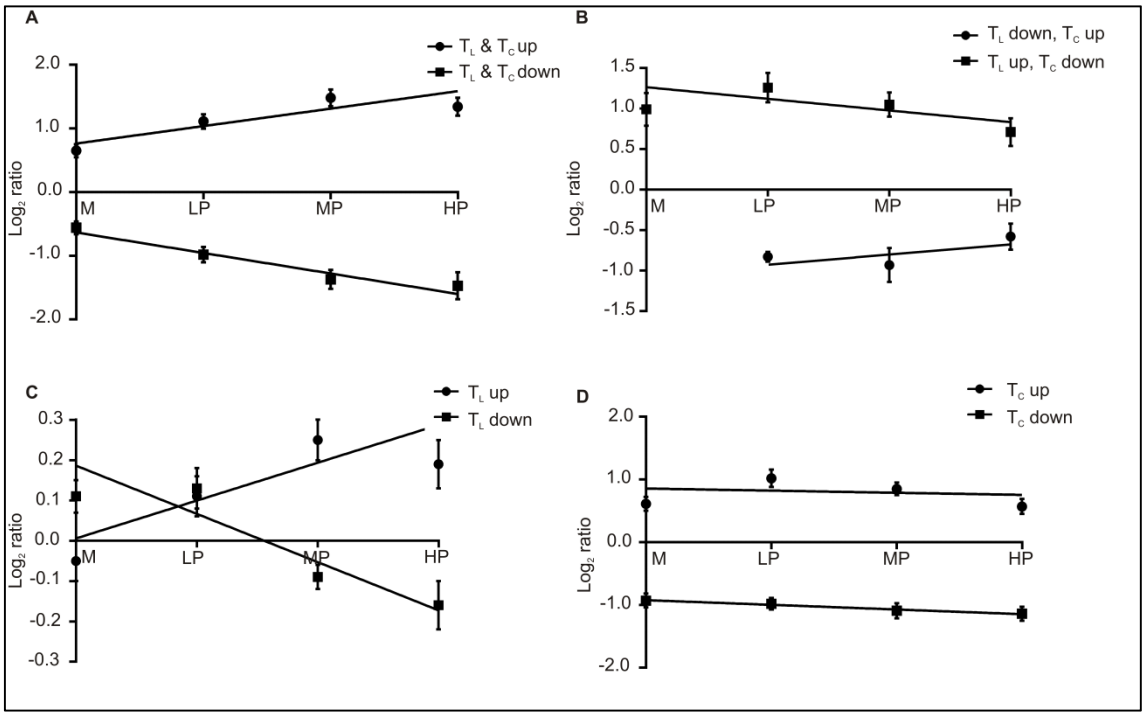

Fig. 3.7. Treatment with Griseofulvin induced changes in mRNA translation and abundance. All mRNAs that had at least one statistically significant $\log_2$ value (treated/control) were grouped according to the type of regulation they exhibited. (**A**) mRNAs demonstrating concordant translational and transcriptional regulation (60); (**B**) mRNAs demonstrating opposing translational and transcriptional regulation (28); (**C**) mRNAs demonstrating regulation at the translational level only (131); (**D**) mRNAs demonstrating regulation at the transcriptional level only (79). Values in brackets denote number of mRNAs within each group and plotted values represent the mean ± SEM for each category. Mice were placed on a diet of 1% Griseofulvin in 2% arachis oil or 2% arachis oil for 22 days (n≥4).

Table 3.1. Significant mRNA changes in the livers of mice treated with Griseofulvin.

Regulation	Name	Fold change				Ave T_C change	Log_2 ratio				Slope	*p* value			
		M	LP	MP	HP		M	LP	MP	HP		M	LP	MP	HP
Concordant	Gsta1	1.42	**1.72**	**2.89**	**2.62**	**2.16**	0.506	**0.781**	**1.530**	**1.392**	**0.34**	0.057	0.135	**0.009**	**0.008**
	Smarce1	0.82	0.79	**0.68**	**0.68**	**0.74**	-0.285	-0.344	**-0.554**	**-0.565**	**-0.11**	0.214	**0.022**	**0.008**	**0.039**
Opposing	2310051D06Rik	**1.6**	**2.0**	**1.6**	1.1	**1.60**	**0.715**	**0.999**	**0.691**	0.197	**-0.19**	**0.025**	**0.001**	**0.035**	**0.013**
	Mapk1	-	**0.46**	**0.40**	**0.71**	**0.52**	-	**-1.108**	**-1.325**	**-0.497**	**0.31**	-	**0.037**	**0.007**	0.142
Translational	Dbi	1.0	**1.4**	**1.6**	1.3	1.32	0.038	**0.532**	**0.655**	0.322	**0.31**	0.833	0.176	**0.034**	0.154
	Prm3	0.9	0.8	**0.7**	**0.6**	0.76	-0.166	-0.319	**-0.496**	**-0.654**	**-0.16**	0.171	0.106	0.185	**0.042**
Transcriptional	Cyp2c29	**2.3**	**2.6**	**2.5**	**2.0**	**2.34**	**1.195**	**1.380**	**1.331**	**0.968**	-0.07	**0.048**	0.054	**0.021**	**0.024**
	Fabp1	**0.3**	**0.5**	**0.3**	**0.4**	**0.38**	**-1.586**	**-1.076**	**-1.519**	**-1.455**	-0.01	**0.004**	0.291	**0.011**	**0.000**

A reduction in mRNA at the translational or transcriptional level is shown in green, an increase in red and a statistically significant *p* value in blue. Mice were placed on a diet of 1% Griseofulvin in 2% arachis oil or 2% arachis oil for 22 days (n≥4).

3.5.3.2 Canonical pathway analysis

The list of translationally regulated mRNAs was uploaded and analysed using the Gene Set Analysis toolkit (available at http://bioinfo.vanderbilt.edu/webgestalt) and significant ($p \leq 0.05$) canonical pathways were identified. These pathways were compared to those obtained from a different model system of erythropoietic protoporphyria; the Fech mouse. Balb/c$^{m1Pas/m1Pas}$ (Fech) mice have an SNP mutation in the ferrochelatase gene, which results in < 5% normal enzyme activity (Davies et al., 2005). As with Griseofulvin-treated mice, these mutant mice demonstrate physical manifestations of hepatotoxicity, including cholestasis and an accumulation of porphyrins. Whilst the mutant mouse model had a far larger spectrum of changes than the Griseofulvin-treated samples (unpublished data: E.L. Marczylo), a number of identical canonical pathways were affected in both model systems (Fig. 3.8). Of particular interest was the pathway "Metabolism of xenobiotics by cytochrome p450". Previous work with both models had identified the cyp genes as being highly associated with the development of hepatotoxicity (Davies et al., 2005; Gant et al., 2003).

The results from the pathway analysis provided support for use of the Griseofulvin-treated mouse as a model of cholestatic hepatotoxicity. Not only were the same significant canonical pathways identified as were seen following similar experiments with the Fech mouse, but those pathways were highly relevant to the observed histopathological signs of toxicity. The benefit of the Griseofulvin-treated mouse over the Fech ^{m1Pas} mouse model is that the relatively limited exposure of the animals to the toxin, in contrast to the presence of an inbred mutation from birth, means more of the genetic responses are due directly to the hepatotoxin, and not caused by secondary, compensatory effects.

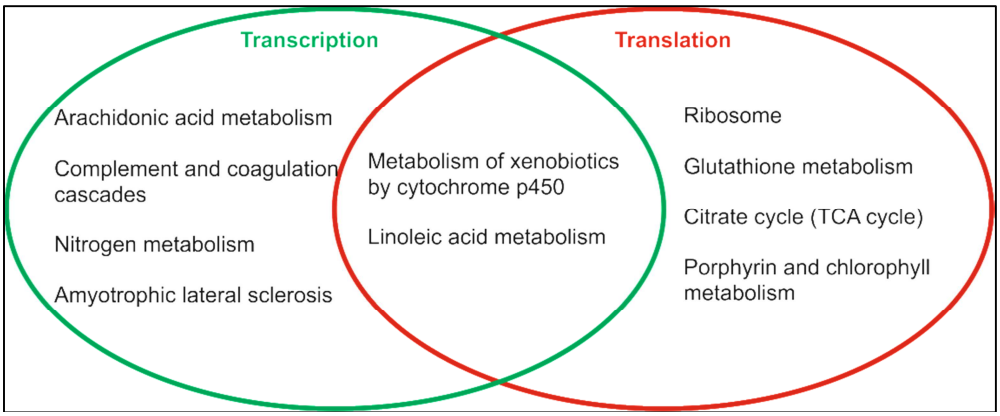

Fig. 3.8. Common pathways were significantly altered in two independent models of cholestatic hepatototoxicity. Profiling was performed on mice treated with Griseofulvin for 22 days and 8 week old Fech ^{m1Pas} mice. Common pathways are shown according to type of regulation.

3.5.3.3 Validation of microarray changes using qRT-PCR and Western blotting

SWI/SNF related, matrix associated, actin dependent regulator of chromatin, subfamily e, member 1 (*Smarce1*), also known as BAF57, was selected for further validation. *Smarce1* was of interest in this study since it was thought to be regulated by a number of the miRNAs perturbed in the liver following treatment with Griseofulvin.

Translational profiling revealed that this mRNA demonstrated regulation at the translational and potentially the transcriptional level (Table 3.1). The $\log_2$ values for *Smarce1* mRNA decreased across the gradient, signifying that this mRNA was present in increasingly smaller amounts and resulting in a negative slope value (-0.11). This indicated movement from the heavy polysomes towards the light polysomes and monosomes (Fig. 3.9 A) and was representative of less efficient translation. The average $\log_2$ value across the gradient was -0.4, indicating a small (1.4-fold) reduction in total *Smarce1* mRNA expression.

qRT-PCR confirmed the translational change (Fig. 3.9 B). The same movement of *Smarce1* mRNA from the heavy and medium polysomes towards the light polysomes and the monosomes was observed. qRT-PCR on total RNA indicated that there was no significant change in the level of *Smarce1* mRNA following treatment with Griseofulvin, suggesting limited transcriptional regulation (Fig. 3.9 C).

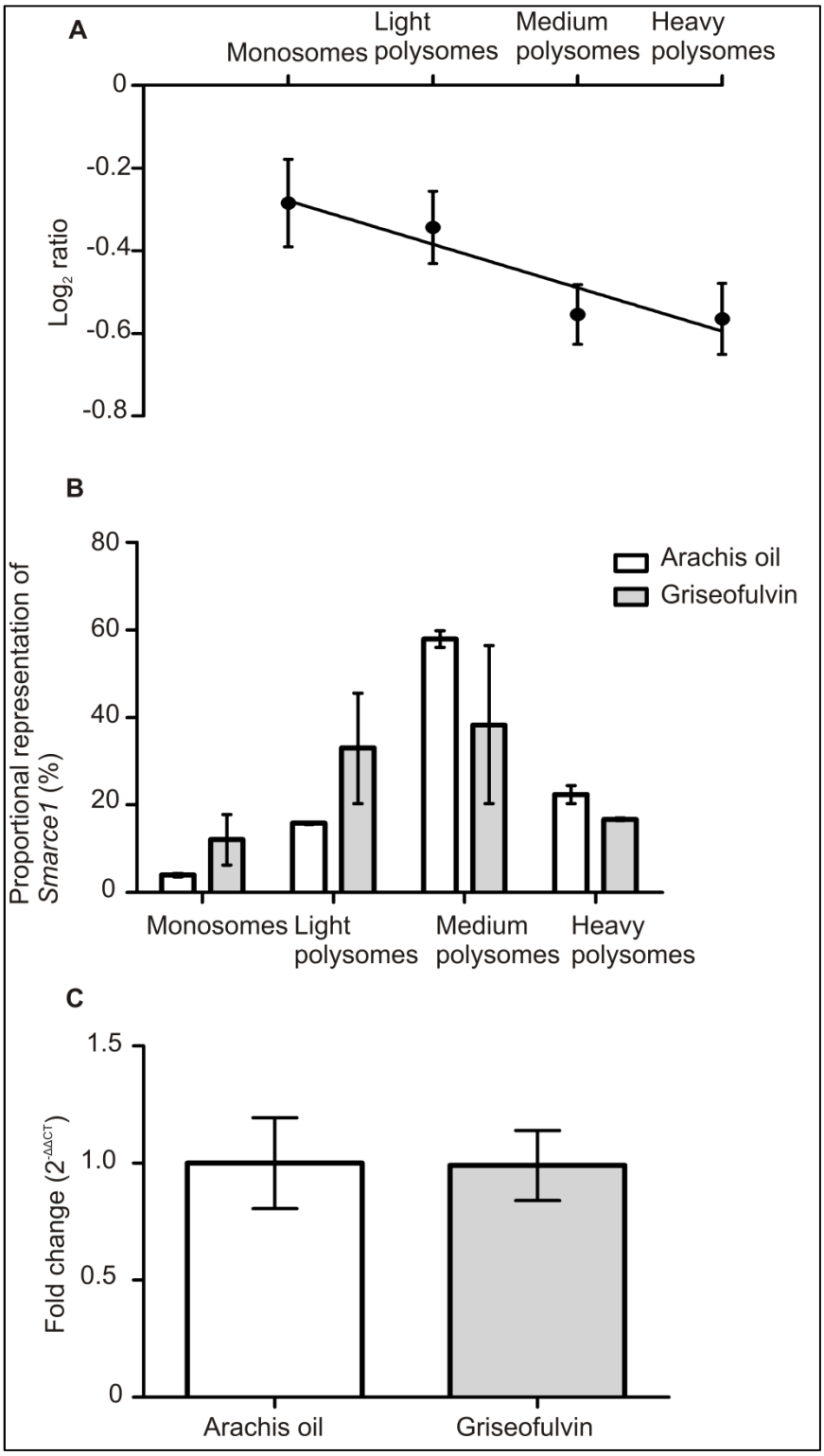

Fig. 3.9. *Smarce1* showed a change in translation following treatment with Griseofulvin, but only a limited change at the transcriptional level. (**A**) Translational profiling, (**B**) qRT-PCR of fractionated RNA, and (**C**) qRT-PCR of total mRNA. qRT-PCR data (total mRNA) were normalised to β-Actin and represent mean ± SEM. Mice were placed on a diet of 1% Griseofulvin in 2% arachis oil or 2% arachis oil for 22 days (n≥4).

To confirm that the reduced translation of *Smarce1* mRNA was having a downstream effect on SMCE1 protein levels, Western blot analysis was performed. Treatment with Griseofulvin for 22 days caused a significant (p = 0.00) reduction in SMCE1 (Fig. 3.10 A). Previous work had revealed a large number of transcriptional changes in the livers of mice treated with Griseofulvin for 5 days (Gant et al., 2003). Therefore, it was of interest to see whether there was a reduction in SMCE1 at an earlier time point. Following treatment for 5 days, a significant (p = 0.03) reduction in protein levels was seen (Fig. 3.10 B). This reduction was less pronounced than that seen at the 22 day time point, suggesting a time-dependent reduction in SMCE1 following Griseofulvin treatment.

Attempts were made to strip and re-probe the Western blots with an antibody against three standard controls; Gapdh, β-Actin and β-tubulin. However, all of these showed an apparent change at the protein level (Fig. 3.11). This is unsurprising since it has already been reported that common controls, such as Gapdh and β-Actin can have altered expression levels depending on the experimental condition, across human, mouse and rat studies (Frericks and Esser, 2008; Lardizabal et al., 2012; Radonic et al., 2004). Furthermore, in rodent studies Gapdh protein has already been shown to demonstrate reduced activity following toxic doses of Acetaminophen (Williams, 2006). Thus, selection of an appropriate reference gene is of critical importance and not straightforward (Amoako et al., 2013; Gebeh et al., 2012). As an alternative to using an antibody-based loading control, images of each membrane stained with ponceau red were used to confirm equal loading and these are shown alongside the Western blots in Fig. 3.10.

3.5.3.4 Levels of SMCE1 were also reduced in an in vitro model system

To investigate whether the change seen *in vivo* was also seen *in vitro*, Hepa 1-6 liver cells were treated with a sub-toxic dose of Griseofulvin, as determined using cell viability assays (section 3.4.2). The ability to replicate a result seen *in vivo* in a cell-culture based system has advantages, particularly with regards to further elucidating the molecular mechanisms involved in the *in vivo* situation. Western blot analysis revealed that SMCE1 was also reduced *in vitro* following treatment of cells with 5 µM and 10 µM Griseofulvin (Fig. 3.12). Although this reduction did not reach statistical significance (p = 0.29 and 0.31, respectively), the same trend was seen across the 3 replicates. There was no dose dependent effect; the average percentage reduction in SMCE1 at 10 µM was only 1% less than that at 5 µM (41% and 42% less protein than the vehicle-only control (0.1% DMSO), respectively).

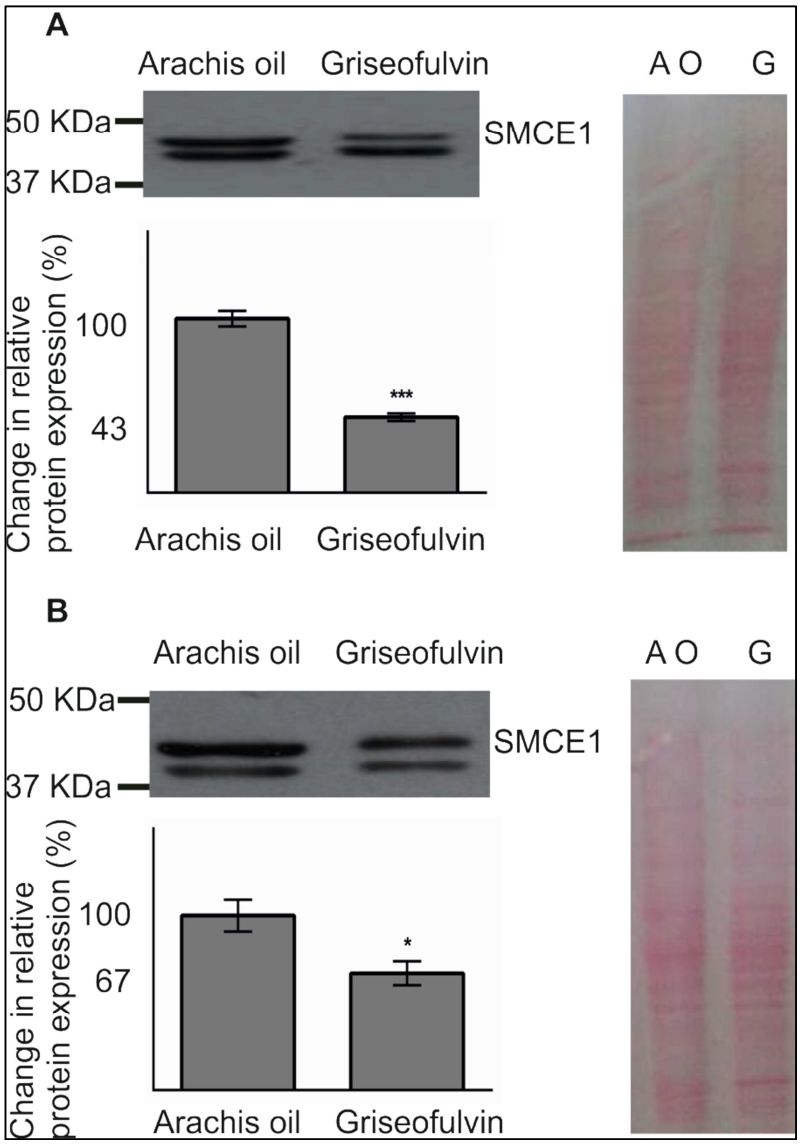

Fig. 3.10. SMCE1 was reduced following Griseofulvin treatment. (**A**) 22 d and (**B**) 5 d; [AO] Arachis oil, [G] Griseofulvin-treated. Representative blots are shown. Membranes were stained with ponceau red following transfer to demonstrate equal loading. Data represent mean ± SEM. * $p \leq 0.05$, *** $p \leq 0.001$ (T-Test). Mice were placed on a diet of 1% Griseofulvin in 2% arachis oil or 2% arachis oil for 22 days (n≥4).

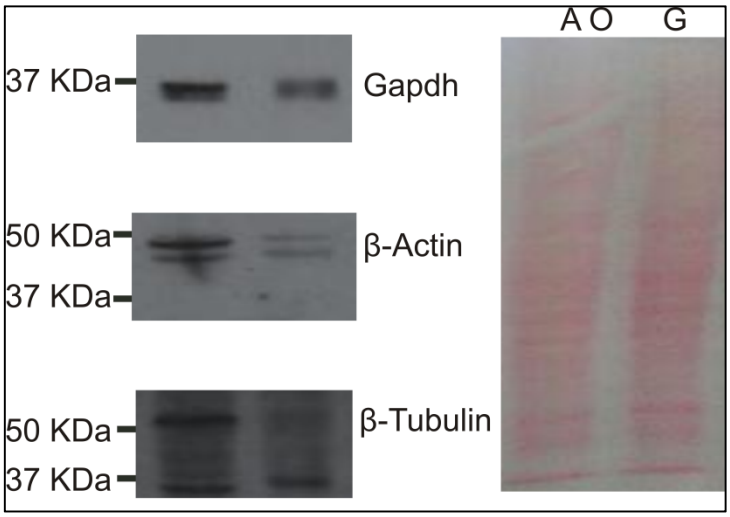

Fig. 3.11. The levels of three standard loading controls changed following treatment with Griseofulvin. [AO] Arachis oil, [G] Griseofulvin-treated. Representative blots are shown. Membranes were stained with ponceau red following transfer to demonstrate equal loading. (AO = Arachis oil (vehicle only control), G = Griseofulvin-treated). Mice were placed on a diet of 1% Griseofulvin in 2% arachis oil or 2% arachis oil for 22 days (n≥4).

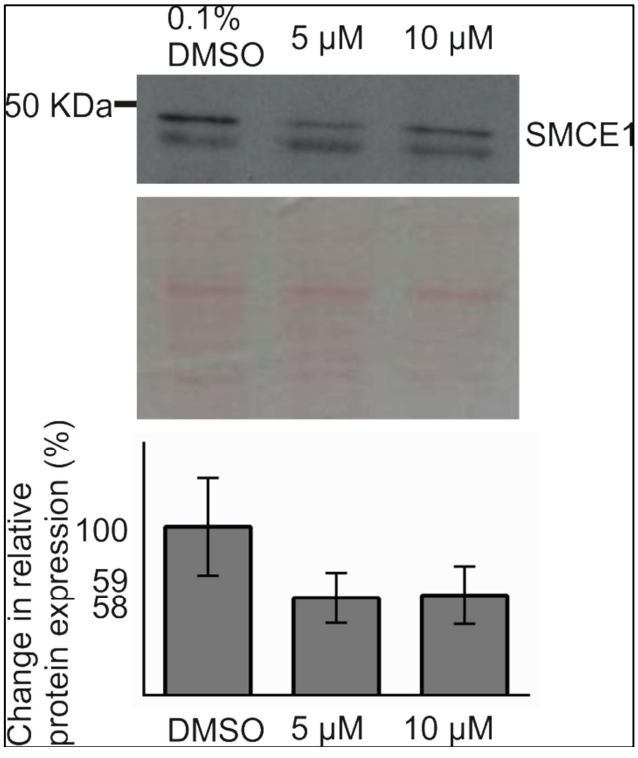

Fig. 3.12. SMCE1 was reduced following treatment with Griseofulvin in an *in vitro* system. A representative blots is shown. Membranes were stained with ponceau red following transfer to demonstrate equal loading. Hepa 1-6 cells were treated with 5 μM and 10 μM Griseofulvin for 72 h (n=3). Control cells were treated with vehicle-only (0.1% DMSO) (n=3).

3.5.4 Model 2: The PredTox model

The second model of hepatotoxicity that was used came courtesy of the InnoMed Predictive Toxicology consortium (Chapter 2, section 2.1.3). The consortium provided liver samples from the five studies that had caused the most pronounced toxicity in their preliminary analysis. Looking at the histopathological summaries (Table 3.2) the compound that caused the most severe clinical signs of hepatotoxicity (FP014SC) was selected for further analysis.

Table 3.2. Summary of the histopathological data for each of the PredTox compounds.

FP6 study name	Compound sponsor	Toxicological response within liver	Severity
FP005ME	Merck	Hepatocellular apoptosis Necrosis Peribiliary inflammation Fibrosis Bile duct proliferation and necrosis Hepatocellular hypertrophy	+
FP013NO	Novartis	Absence of hepatocellular glycogen deposits Increased fatty deposits	+
FP004BA	Bayer	Bile duct damage Hepatocyte necrosis Regenerative hyperplasia Inflammatory responses Cholestasis Fibrosis	++
FP007SE	Boehringer Ingelheim	Increased transamininases, ALP and bilirubin Pericholangitis with bile duct hyperplasia Cholestasis Inflammation Hepatocellular hypertrophy Vacuolation	++
FP014SC	Bayer Schering Pharma (formerly Schering)	Severe, acute necrotic liver injury Elevated liver transaminases Cholestasis Hepatocellular vacuolation and hypertrophy Regeneration and increased mitosis	+++

Severity levels; +++ > ++ > +.

FP014SC, or Tetraethyl[(3-hydroxy-2-pyridyl)amino]methanediphosphonate, is a bisphosphonate (chemical structure shown in Fig. 3.13). Originally identified as an inhibitor of osteoclast activity it was developed for use in the treatment of osteoporosis. Unfortunately the extent of hepatotoxicity ensured that it never entered the clinic. When used as a compound of interest in the PredTox study the allocated high dose was 1120 mg/kg, given via oral gavage (Chapter 2, Table 2.2).

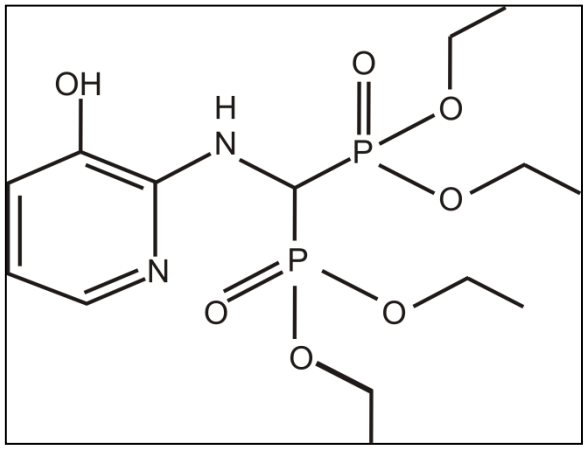

Fig. 3.13. Chemical structure of PredTox compound FP014SC. This compound caused the most pronounced hepatotoxicity of the five PredTox compounds selected for further study.

3.5.4.1 Translational changes following treatment with PredTox compound FP014SC

To perform translational profiling on the samples from the FP014SC study, the same microarray set was used as for the Griseofulvin-treated samples. Although this set was designed against the mouse, previous work from within our group had established that the microarrays showed excellent cross-species reactivity between mouse and rat (6 month research project undertaken by A. Paun, student of T.W. Gant). Following high dose treatment for 15 days, 447 mRNAs showed a change at the translational level (Fig. 3.14). These were grouped according to whether they were translationally increased or repressed, and whether this was concurrent with (47 mRNAs, Fig. 3.14 A), opposite to (34 mRNAs, Fig. 3.14 B), or without (366 mRNAs, Fig. 3.14 C) a transcriptional change. A final category consisted of those mRNAs that demonstrated a transcriptional change only (38 mRNAs, Fig. 3.14 D). Example mRNAs from each category are provided in Table 3.3.

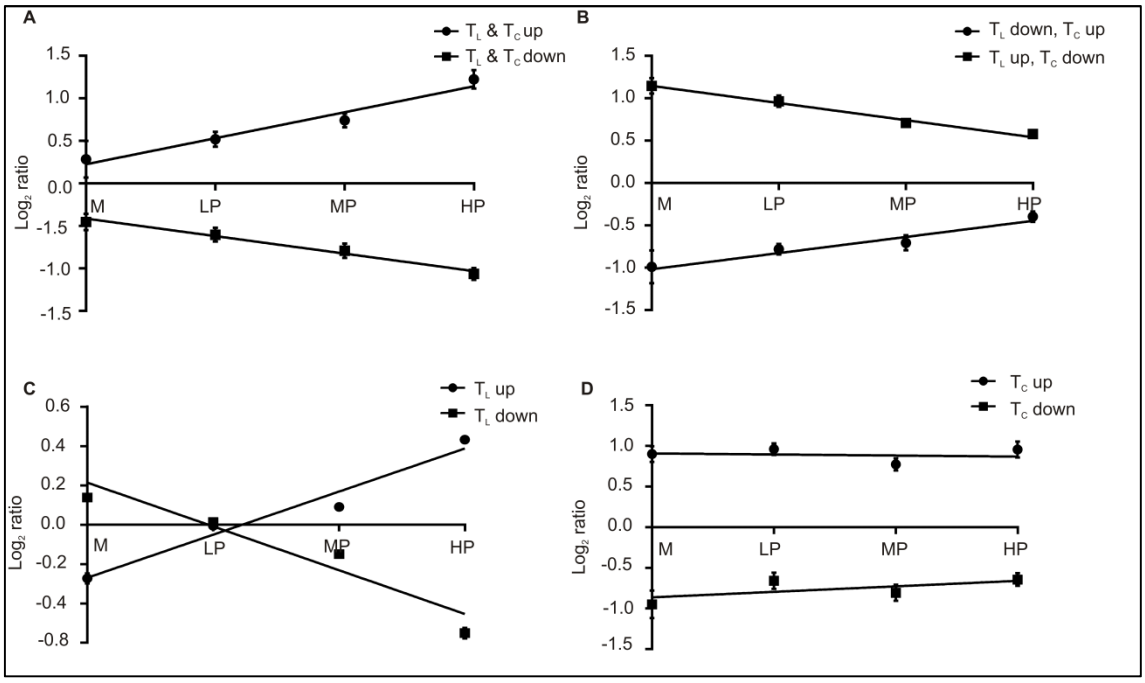

Fig. 3.14. Treatment with PredTox compound FP014SC induced changes in mRNA and abundance. All mRNAs that had at least one statistically significant $\log_2$ value (treated/control) were grouped according to the type of regulation they exhibited. (**A**) mRNAs demonstrating concordant translational and transcriptional regulation (47); (**B**) mRNAs demonstrating opposing translational and transcriptional regulation (34); (**C**) mRNAs demonstrating regulation at the translational level only (366); (**D**) mRNAs demonstrating regulation at the transcriptional level only (38). Values in brackets denote number of mRNAs within each group and plotted values represent the mean ± SEM for each category. FP014SC-treated rats received high dose FP014SC or vehicle-only treatment for 15 days (n=5).

Table 3.3. Significant mRNA changes in the livers of rats treated with PredTox compound FP014SC.

Regulation	Name	Fold change				Ave T_C	Log_2 Ratio				Slope	*p* value			
		M	LP	MP	HP	change	M	LP	MP	HP		M	LP	MP	HP
Concordant	Aldob	0.4	1.0	1.2	3.4	1.50	-1.379	0.023	0.284	1.759	**0.97**	0.130	0.833	0.045	0.014
	Dio3	0.8	0.7	0.6	0.4	0.59	-0.396	-0.602	-0.775	-1.508	**-0.35**	0.343	0.334	0.033	0.065
Opposing	Ptgdr	2.1	1.8	1.7	1.5	1.78	1.087	0.879	0.727	0.590	**-0.16**	0.146	0.127	0.004	0.086
	Serpina3n	0.4	-	0.7	0.9	0.66	-1.347	-	-0.435	-0.215	**0.39**	0.016	-	0.289	0.368
Translational	Sesn1	0.8	0.9	1.1	-	0.95	-0.260	-0.149	0.151	-	**0.21**	0.267	0.153	0.020	-
	Pin1	1.2	0.9	0.9	0.5	0.87	0.223	-0.181	-0.109	-0.940	**-0.34**	0.416	0.364	0.213	0.050
Transcriptional	Eef1a1	2.3	2.3	2.3	2.7	2.39	1.187	1.172	1.197	1.444	0.08	0.522	0.215	0.035	0.067
	Cyp2e1	0.5	0.6	0.5	0.7	0.60	-0.979	-0.676	-0.932	-0.458	0.13	0.045	0.010	0.018	0.057

A reduction in mRNA at the translational or transcriptional level is shown in green, an increase in red and a statistically significant *p* value in blue. FP014SC-treated rats received high dose FP014SC or vehicle-only treatment for 15 days (n=5).

3.5.4.2. Canonical pathway analysis

The complete list of mRNAs, identified as being translationally regulated, was submitted to GEO (accession number GSE38807).This data fulfilled the six main criteria required for a dataset to be judged MIAME-compliant (Brazma et al., 2001). The same list was uploaded to Ingenuity IPA software for pathway analysis (Ingenuity® Systems, www.ingenuity.com). This analysis identified 169 canonical pathways with 2 or more altered genes (Table 3.4).

A significant number of the identified canonical pathways were under the control of retinoid X receptor (RXR). These pathways are highlighted in red in Table 3.3. *Dio3* (Iodothyronine deiodinase type III) was selected for further validation since it was identified as an indirect regulator of RXR and demonstrated translational repression following treatment with FP014SC (Table 3.3). The regulation of *Dio3* (including the validation data) is explored in more detail in Chapter 4.

3.5.4.3 Validation of microarray changes using qRT-PCR

Sestrin 1 (*Sesn1*) was selected for further validation as an example of an mRNA that showed a subtle change in translational efficiency. Translational profiling revealed that this mRNA demonstrated regulation at the translational level only (Table 3.3). The $\log_2$ values for *Sesn1* mRNA increased across the gradient, indicating that this mRNA was present in increasingly higher amounts and resulting in a positive slope value (0.21). This indicated movement from the monosomes and light polysomes towards the medium polysomes (Fig. 3.15 A) and was representative of more efficient translation. It is important to note that this was a relatively small shift and there was no detectable *Sesn1* present in the heavy polysomal pool. This demonstrates the sensitivity of this technique for the identification of small, yet statistically significant, changes in translational efficiency. When averaged across the gradient, absolute mRNA levels were unchanged (mean fold change of 0.95), indicating no change at the transcriptional level.

qRT-PCR confirmed the translational change (Fig. 3.15 B). The same movement of *Sesn1* mRNA from the monosomes and light polysomes to the medium polysomes was observed.

Table 3.4. Canonical pathways significantly perturbed (2+ genes) following treatment with PredTox compound FP014SC.

Ingenuity Canonical Pathways	-log(*p*-value)	Genes
Fatty Acid Metabolism	8.71E+00	15
LPS/IL-1 Mediated Inhibition of RXR Function	2.67E+00	10
Production of Nitric Oxide and Reactive Oxygen Species in Macrophages	3.10E+00	10
Clathrin-mediated Endocytosis Signaling	2.99E+00	10
G-Protein Coupled Receptor Signaling	3.19E-01	9
mTOR Signaling	2.47E+00	9
Axonal Guidance Signaling	6.89E-01	9
Glucocorticoid Receptor Signaling	1.51E+00	9
Tryptophan Metabolism	2.81E+00	8
Protein Kinase A Signaling	8.34E-01	8
PPARα/RXRα Activation	2.11E+00	8
Metabolism of Xenobiotics by Cytochrome P450	3.18E+00	8
LXR/RXR Activation	3.15E+00	8
RAR Activation	2.11E+00	8
EIF2 Signaling	1.94E+00	8
Regulation of eIF4 and p70S6K Signaling	2.57E+00	8
Protein Ubiquitination Pathway	1.16E+00	8
PI3K Signaling in B Lymphocytes	2.14E+00	7
Role of Macrophages, Fibroblasts and Endothelial Cells in Rheumatoid Arthritis	6.13E-01	7
Molecular Mechanisms of Cancer	4.75E-01	7
Calcium Signaling	1.58E+00	7
Xenobiotic Metabolism Signaling	7.18E-01	7
Dopamine-DARPP32 Feedback in cAMP Signaling	1.71E+00	7
ERK/MAPK Signaling	1.47E+00	7
Acute Phase Response Signaling	1.67E+00	7
Valine, Leucine and Isoleucine Degradation	3.11E+00	6
CREB Signaling in Neurons	1.17E+00	6
B Cell Receptor Signaling	1.48E+00	6
Breast Cancer Regulation by Stathmin1	9.81E-01	6
Wnt β-catenin Signaling	1.19E+00	6
Bile Acid Biosynthesis	3.58E+00	6
Arachidonic Acid Metabolism	1.75E+00	6
RhoGDI Signaling	7.73E-01	5
Ephrin Receptor Signaling	7.94E-01	5
Huntington's Disease Signaling	5.30E-01	5
Purine Metabolism	3.30E-01	5
Linoleic Acid Metabolism	2.07E+00	5
Glycolysis/Gluconeogenesis	1.81E+00	5
Fatty Acid Elongation in Mitochondria	4.93E+00	5
Phospholipase C Signaling	4.68E-01	5
Actin Cytoskeleton Signaling	5.54E-01	5

Table 3.4. continued

Ingenuity Canonical Pathways	-log(*p*-value)	Genes
Atherosclerosis Signaling	1.33E+00	5
Sertoli Cell-Sertoli Cell Junction Signaling	7.45E-01	5
Semaphorin Signaling in Neurons	1.97E+00	4
NRF2-mediated Oxidative Stress Response	4.57E-01	4
P2Y Purigenic Receptor Signaling Pathway	8.48E-01	4
Tyrosine Metabolism	1.46E+00	4
Pyruvate Metabolism	1.62E+00	4
Human Embryonic Stem Cell Pluripotency	7.53E-01	4
GNRH Signaling	8.21E-01	4
Role of NFAT in Cardiac Hypertrophy	4.39E-01	4
Synaptic Long Term Potentiation	1.02E+00	4
Colorectal Cancer Metastasis Signaling	2.50E-01	4
Glioblastoma Multiforme Signaling	6.23E-01	4
PI3K/AKT Signaling	8.67E-01	4
PTEN Signaling	9.79E-01	4
Hereditary Breast Cancer Signaling	8.86E-01	4
Tight Junction Signaling	5.85E-01	4
IL-8 Signaling	4.91E-01	4
Glycerolipid Metabolism	1.05E+00	4
FXR/RXR Activation	1.25E+00	4
Inositol Phosphate Metabolism	6.16E-01	4
AMPK Signaling	7.37E-01	4
Mitochondrial Dysfunction	7.37E-01	4
Type II Diabetes Mellitus Signaling	9.06E-01	4
Ceramide Signaling	1.39E+00	4
Aldosterone Signaling in Epithelial Cells	5.79E-01	4
Amyotrophic Lateral Sclerosis Signaling	1.08E+00	4
Signaling by Rho Family GTPases	2.66E-01	4
Sphingosine-1-phosphate Signaling	9.26E-01	4
Germ Cell-Sertoli Cell Junction Signaling	5.73E-01	4
p38 MAPK Signaling	5.90E-01	3
Circadian Rhythm Signaling	1.84E+00	3
FGF Signaling	7.87E-01	3
Pentose and Glucuronate Interconversions	1.55E+00	3
GM-CSF Signaling	1.08E+00	3
Neuropathic Pain Signaling In Dorsal Horn Neurons	6.05E-01	3
iCOS-iCOSL Signaling in T Helper Cells	5.90E-01	3
PKCθ Signaling in T Lymphocytes	5.26E-01	3
Prostate Cancer Signaling	8.20E-01	3
Cyclins and Cell Cycle Regulation	8.43E-01	3
Aryl Hydrocarbon Receptor Signaling	4.01E-01	3
Small Cell Lung Cancer Signaling	9.44E-01	3

Table 3.4. continued

Ingenuity Canonical Pathways	-log(*p*-value)	Genes
Thyroid Cancer Signaling	1.44E+00	3
TR/RXR Activation	7.77E-01	3
Galactose Metabolism	1.47E+00	3
Non-Small Cell Lung Cancer Signaling	1.03E+00	3
Alanine and Aspartate Metabolism	1.55E+00	3
Dendritic Cell Maturation	3.04E-01	3
OX40 Signaling Pathway	7.66E-01	3
Cdc42 Signaling	2.93E-01	3
Type I Diabetes Mellitus Signaling	5.67E-01	3
Insulin Receptor Signaling	4.37E-01	3
Natural Killer Cell Signaling	6.05E-01	3
Oxidative Phosphorylation	3.68E-01	3
Role of Oct4 in Mammalian Embryonic Stem Cell Pluripotency	1.42E+00	3
Cardiac β-adrenergic Signaling	4.26E-01	3
fMLP Signaling in Neutrophils	5.75E-01	3
CCR3 Signaling in Eosinophils	5.33E-01	3
CXCR4 Signaling	3.30E-01	3
Paxillin Signaling	6.29E-01	3
LPS-stimulated MAPK Signaling	9.17E-01	3
Regulation of Actin-based Motility by Rho	7.87E-01	3
Rac Signaling	6.05E-01	3
p70S6K Signaling	4.76E-01	3
NGF Signaling	6.05E-01	3
Androgen and Estrogen Metabolism	8.32E-01	3
Sulfur Metabolism	2.38E+00	3
Fructose and Mannose Metabolism	1.30E+00	3
Renal Cell Carcinoma Signaling	9.58E-01	3
Hypoxia Signaling in the Cardiovascular System	1.00E+00	3
RhoA Signaling	2.58E-01	2
Neurotrophin/TRK Signaling	4.98E-01	2
ATM Signaling	6.71E-01	2
Arginine and Proline Metabolism	4.66E-01	2
Ubiquinone Biosynthesis	4.90E-01	2
Basal Cell Carcinoma Signaling	4.90E-01	2
Factors Promoting Cardiogenesis in Vertebrates	3.72E-01	2
Role of NANOG in Mammalian Embryonic Stem Cell Pluripotency	2.66E-01	2
Glioma Signaling	3.29E-01	2
Melatonin Signaling	4.74E-01	2
Urea Cycle and Metabolism of Amino Groups	1.01E+00	2
Estrogen-Dependent Breast Cancer Signaling	5.81E-01	2
p53 Signaling	3.39E-01	2
Bladder Cancer Signaling	3.61E-01	2

Table 3.4. continued

Ingenuity Canonical Pathways	-log(*p*-value)	Genes
Androgen Signaling	2.54E-01	2
Cell Cycle: G1/S Checkpoint Regulation	6.24E-01	2
Chronic Myeloid Leukemia Signaling	3.34E-01	2
Cell Cycle Regulation by BTG Family Proteins	9.42E-01	2
Pancreatic Adenocarcinoma Signaling	2.78E-01	2
PXR/RXR Activation	4.98E-01	2
HGF Signaling	3.09E-01	2
IL-1 Signaling	3.44E-01	2
Glutamate Receptor Signaling	6.13E-01	2
Butanoate Metabolism	5.81E-01	2
Telomerase Signaling	3.05E-01	2
Crosstalk between Dendritic Cells and Natural Killer Cells	3.55E-01	2
Cytotoxic T Lymphocyte-mediated Apoptosis of Target Cells	4.09E-01	2
Allograft Rejection Signaling	3.97E-01	2
Caveolar-mediated Endocytosis Signaling	4.58E-01	2
Virus Entry via Endocytic Pathways	3.55E-01	2
Neuroprotective Role of THOP1 in Alzheimer's Disease	8.48E-01	2
Fc Epsilon RI Signaling	2.91E-01	2
PDGF Signaling	4.82E-01	2
CD40 Signaling	5.52E-01	2
TNFR1 Signaling	7.24E-01	2
Angiopoietin Signaling	5.33E-01	2
Parkinson's Signaling	1.45E+00	2
Apoptosis Signaling	3.61E-01	2
Retinoic acid Mediated Apoptosis Signaling	5.52E-01	2
Citrate Cycle	1.08E+00	2
Activation of IRF by Cytosolic Pattern Recognition Receptors	5.52E-01	2
Dopamine Receptor Signaling	4.44E-01	2
CDK5 Signaling	3.72E-01	2
Regulation of IL-2 Expression in Activated and Anergic T Lymphocytes	4.23E-01	2
CD28 Signaling in T Helper Cells	2.40E-01	2
Agrin Interactions at Neuromuscular Junction	5.07E-01	2
FAK Signaling	3.72E-01	2
PAK Signaling	3.61E-01	2
Renin-Angiotensin Signaling	2.66E-01	2
Role of BRCA1 in DNA Damage Response	6.24E-01	2
Sphingolipid Metabolism	3.97E-01	2
Keratan Sulfate Biosynthesis	6.35E-01	2
Inositol Metabolism	2.41E+00	2
G Protein Signaling Mediated by Tubby	9.63E-01	2
14-3-3-mediated Signaling	2.26E-01	2
Starch and Sucrose Metabolism	5.07E-01	2

All mRNAs that showed movement across the gradient following translational profiling (447) were uploaded for pathway analysis to Ingenuity® IPA software. Those pathways under the control of retinoid X receptor are highlighted in red.

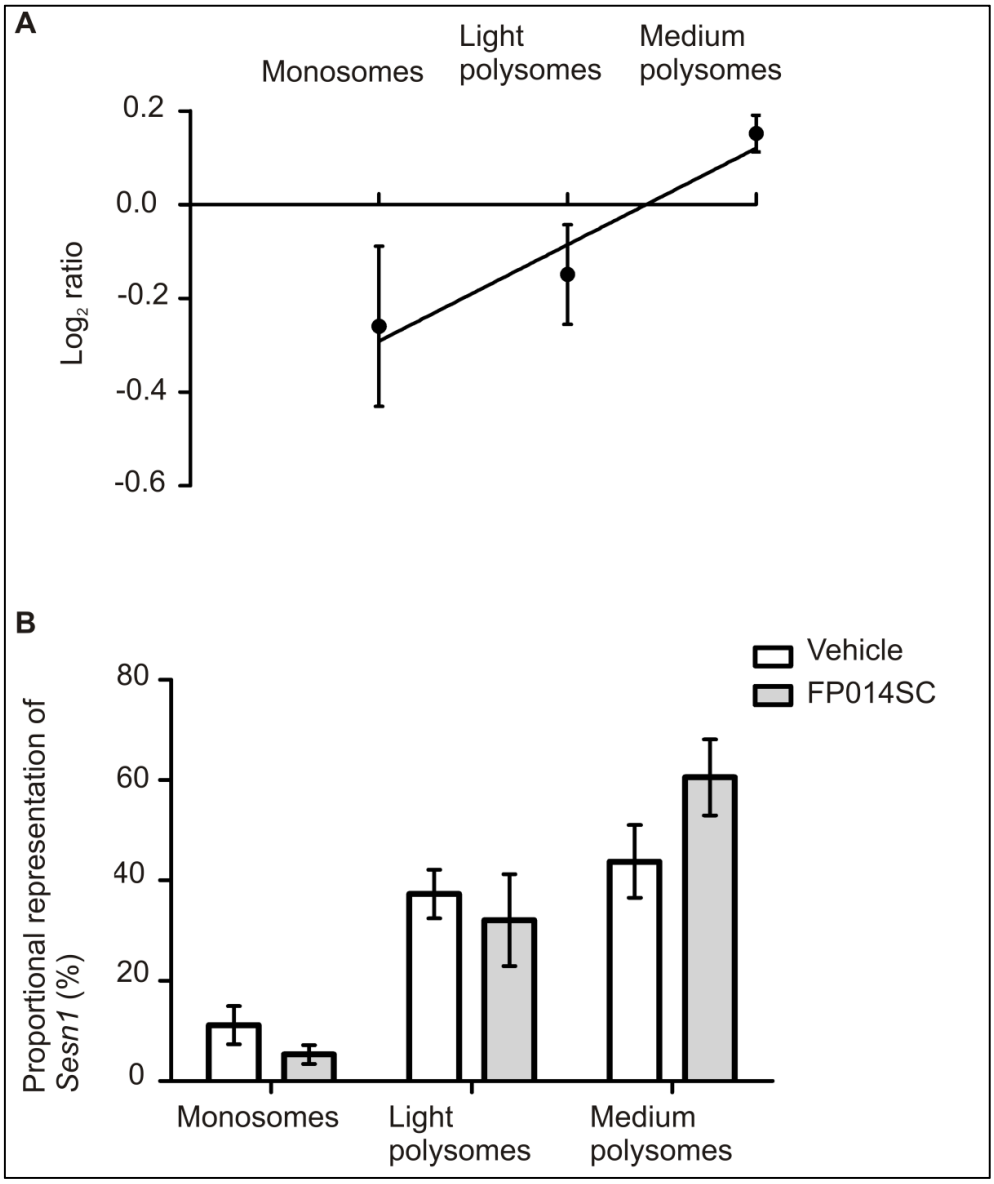

Fig. 3.15. *Sesn1* showed a change in translation following treatment with PredTox compound FP014SC. (**A**) Translational profiling, and (**B**) qRT-PCR of fractionated RNA. Data represent mean ± SEM. FP014SC-treated rats received high dose FP014SC or vehicle-only treatment for 15 days (n=5).

3.6 DISCUSSION

Recent research has indicated that gene expression changes regulated at the translational level are as, if not even more, important than transcriptional changes. The methodology and data described in this chapter support this hypothesis.

The importance of looking at the translatome, alongside the transcriptome and the proteome, in *in vivo* samples has been recently highlighted. Fu *et al* performed a study on fasted rats to investigate the effect of obesity (Fu et al., 2012). These authors demonstrated the benefit of translational analysis for dynamically active processes, such as short term food deprivation. The model systems used for the work described in this chapter (the Griseofulvin-treated mouse and the PredTox FP014SC-treated rat) are further examples of dynamic processes; the hepatic injury was fast to occur, but brief, and most changes were transient (Suter et al., 2011). In both model systems only early-stage, acute hepatotoxicity was investigated and, by the later time points in the PredTox studies, the histology and clinical chemistry results indicated that mechanisms of regeneration and increased cellular proliferation had been initiated (Boitier et al., 2011; Suter et al., 2011). The liver is well documented as having excellent repair capabilities (Jaeschke et al., 2012). Following short-term treatment with a range of hepatotoxins, including acetaminophen, thioacetamide, carbon tetrachloride and D-galactosamine, some degree of regeneration is observed (Mehendale, 2005). These compounds are all commonly used in rodent models of hepatotoxicity (Feng et al., 2007; Mangipudy et al., 1995a; Rocchi et al., 1973; Williams et al., 2004). Importantly, the effect is not unique to rodents; in cases of human drug overdose the liver is very efficient at implementing its own inbuilt repair mechanisms (Liu et al., 2004). Taken together, this provides further evidence that acute compound-induced hepatotoxicity is a dynamic process, involving temporary changes in genetic regulation. It has been widely reported that translational changes occur rapidly after cellular insult (Le Quesne et al., 2010), thus implying a role for translational regulation during dynamic responses to damage. It is unlikely that many mRNAs would undergo complete translational repression or activation; instead, those with a toxic or protective role would more likely be dynamically regulated in direct response to the extent of liver injury. This leads to the hypothesis that most mRNAs would demonstrate more subtle changes in translational activity following compound-induced hepatotoxicity.

The first study to combine sucrose density gradient fractionation with microarray analysis, thereby enabling the translational activity of hundreds of mRNAs to be investigated in parallel, was reported in 1999. Johannes *et al* identified mRNAs that were translated at a reduced rate

following removal of the 5' cap binding complex eIF4F (Johannes et al., 1999). Sucrose density fractionation was used to separate samples into actively and non-actively translated sub-pools, which were then hybridised against each other on a cDNA microarray. This study yielded dramatic results since the majority of mRNAs require eIF4F for successful translation. By artificially removing eIF4F the reduced translation of a large number of mRNAs would be anticipated. Less than 3% (200 out of 7000 mRNAs) remained translationally active, demonstrating not only the importance of the complex in translation, but also the validity of the technique. Subsequent work from other groups employed the same methods to study translational changes in a range of cellular conditions and toxic insults *in vitro* (Galban et al., 2003; Greenman et al., 2007; Grolleau et al., 2002; Vyas et al., 2009).

To investigate the effect of various hepatotoxic compounds on translation in an *in vivo* situation, it was necessary to optimise the translational profiling techniques for use with liver tissue samples. One published solution to the difficulties of performing translational profiling on *in vivo* samples was to utilise additional techniques, such as TRAP (translating ribosome affinity purification) (Helmy et al., 2012). However, the work presented in this chapter shows that by making small adjustments to the methodology, successful and robust translational profiling of *in vivo* liver samples, with improved resolution was possible. These adjustments included accurately determining the location of the monosomal and polysomal regions (Fig. 3.6), separating each gradient into four sub-pools and hybridising the sub-pools against each other. For example the monosome sub-pool from a compound-treated sample was hybridised against the monosome sub-pool from a vehicle-treated sample, and so forth (Fig. 3.2). An additional advantage of performing the translational profiling in this manner was the potential to simultaneously measure transcriptional regulation, generating a more comprehensive overview of the mechanisms involved in the response of the liver to compound-induced hepatotoxicity.

It should be noted that very recent work has utilised ribosomal profiling along with high-throughput sequencing (Gerashchenko et al., 2012; Reid and Nicchitta, 2012) as an alternative to microarray profiling. Whilst exciting and novel, this method is labour intensive, difficult and costly. The method described in this chapter is more cost-effective and can be applied to a wide range of samples.

In view of the transient nature of the insult it was important to accurately identify and separate the relevant fractions into four sub pools, representing monosomes and light, medium and heavy polysomes (Fig. 3.2). The major determinant of the monosomal region was

the appearance of the 40S and 60S subunits. With fractionation of cell samples, peaks representing recruitment of the 40S and 60S subunits were clearly visible on the UV trace (Fig. 3.5 A). When fractionating liver tissue samples these peaks showed reduced resolution (Fig. 3.5 B). Therefore, additional techniques were implemented to assist in determining the monosomal region (Fig. 3.6). Gel electrophoresis was used to ascertain which fractions contained 18S and 28S bands, this identified the location of the 40S and 60S subunits respectively. In addition micro dot blotting was used to measure the abundance of each of the subunits within each fraction. The monosomal fractions contained a greater proportion of 40S and 60S than the polysomal fractions. When liver samples were fractionated the polysomal region could be identified using the UV trace (Fig. 3.5 B). However, higher resolution was required in order to accurately split this region into light, medium and heavy polysome sub-pools. Northern blotting and micro dot blotting were used to measure the location and abundance of β-Actin. This is an example of a mRNA that is heavily translated within many cell and tissue types under a range of conditions. Therefore, it functioned well as a marker of the heavier polysomal fractions. To split the polysomal region into three sub-pools the abundance of β-Actin in each fraction was plotted. The highest levels of β-Actin represented the heavy polysome region, which comprised those mRNAs undergoing very active translation. The fractions immediately after the monosmal region, where the polysomal peak was evident, but the abundance of β-Actin was lower was the light polysomal region. mRNAs within these fractions would be minimally translationally active. Those fractions which fell between these two defined sub-pools were classed as the medium polysomes. Gradients that were performed in the presence of EDTA and absence of cycloheximide demonstrated complete ribosomal dissociation (Fig. 3.6). The majority of the β-Actin signal moved into the earlier fractions and there was very limited RNA in the later polysomal fractions. This, therefore, provided further evidence for the location of both the monosomal and polysomal regions.

These rigorous analyses were applied to each fractionated gradient. This demonstrated slight discrepancies between gradients meaning that each sub-pool did not always contain the same fractions. Through the implementation of these techniques the reproducibility of sub-pooling between gradients was improved. In contrast, alternative studies have pooled predefined regions consisting of the same fractions for every gradient (Galban et al., 2003; Jiang et al., 2012). This makes assumptions about the consistency of RNA fractionation between gradients, which, as found in this study, may not always be appropriate. It is therefore important to fully validate the correct location of the monosomal and polysomal regions within each individual

gradient so that sub-pooling is accurate and equivalent ribosomal populations are correctly compared.

The experimental design meant that the use of standard normalisation approaches was appropriate, thus reducing the chance of normalisation errors during the subsequent mathematical analysis of the microarray results. This was a further benefit of the proposed translational profiling technique. The normalisation of microarray-based data is essential due to the many sources of systemic variation (Yang et al., 2002). These include dye bias (Brownstein, 2006), differences in sample labelling and hybridisation efficiency, and even external factors such as laboratory climate and humidity (Fare et al., 2003). Most of the widely-used microarray normalisation techniques, for example, Quantile and Lowess, rely on two assumptions; firstly, that only a small number of mRNAs will be altered in any particular condition, and secondly that where changes are present they will be normally distributed (Bolstad et al., 2003; Quackenbush, 2002). Whilst this holds true for most transcriptional microarray profiling, the experimental design of most translational profiling methodologies means that these two conditions are rarely met. For example, the use of an experimental design whereby a polysomal sub-pool is hybridised against a monosomal sub-pool from the same gradient (Spriggs et al., 2008). In this instance, most mRNAs will demonstrate a change in expression, due to very few having equal representation across the entire gradient. Thus the standard methods of local and global normalisation are not appropriate. Instead, between chip normalisation is avoided and a more complex rank based significance testing is applied to remove within chip sources of error (data currently being prepared for publication as a manuscript: N. Burgoyne and T Sbarrato). Alternatively, a pooled polysomal sample is sometimes hybridised against total RNA (Davidson et al., 2009; Liu et al., 2012). Total RNA is likely to be more similar in composition to the polysomal pool than the monosomal pool is; enabling the application of standard methods of normalisation. However, in this chapter, to ensure the greatest similarity between hybridised samples, control monosomes were compared to test monosomes and control polysomes were compared to test polysomes. In this scenario, the two normalisation criteria are fully met; most mRNAs remain unchanged and those that do demonstrate a normal distribution of fold change. This allows the accurate implementation of standard normalisation techniques to account for extrinsic variation. Other groups have used a similar experimental design of hybridising test polysomes against control polysomes to avoid the need for more complex bioinformatic analysis (Fu et al., 2012; Galban et al., 2003; Jiang et al., 2012).

Following normalisation, linear regression analysis was performed on the four normalised log_2 ratios for each mRNA to identify movement through the gradient (Fig. 3.2). A positive regression value (≥ +0.1) indicated more efficient translation and a negative value (≤ -0.1) indicated translational repression. In addition, a consistent change in either direction (i.e. all four sub-pools showing an average log_2 value ≥ ±0.5), represented a transcriptional change. This generated a more accurate and complete view of movement across the gradient and allowed transcriptional changes to be measured alongside translational changes. Alternative experimental designs in the literature have involved the sub-pooling of larger single polysomal regions (Fu et al., 2012; Galban et al., 2003; Jiang et al., 2012). Polysomes were defined as either all fractions with 3 or more ribosomes (Fu et al., 2012), or a predefined region (fractions 6 – 10) (Jiang et al., 2012) or (fractions 5 – 11) (Galban et al., 2003) within each gradient. The former of these methods relies on high resolution UV traces to determine individual ribosome recruitment. The resolution obtained from *in vivo* samples is too low to identify individual ribosomes (Fig. 3.5 B) and, therefore, this method was unsuitable for use with *in vivo* liver samples. Moreover, both Fu *et al* and Jiang *et al* limited profiling to those mRNAs undergoing active translation (i.e. those present in a single large polysome sub-pool) (Fu et al., 2012; Jiang et al., 2012). Such methods cannot measure transcriptional changes or the more subtle translational changes expected during dynamic *in vivo* responses. Whilst Galban *et al* did include a monosomal pool (fractions 1 and 2), they discarded fractions 3 and 4 in every instance (Galban et al., 2003). Thus, although this enables the analysis of both transcriptional and translational changes, the resolution and accuracy of such an approach is reduced compared to the use of four sub-pools that encompass the entire gradient.

Splitting each gradient into four sub-pools and performing the bioinformatic analysis as described above did indeed increase resolution and enable identification of more subtle changes in translational efficiency. This is supported by the validation of Sestrin1 (*Sesn1*). *Sesn1* mRNA showed a movement from the monosomes and light polysomes towards the medium polysomes (Fig. 3.14 A and B), indicating increased translational activity following treatment with FP014SC. *Sesn1* is involved in combating oxidative stress following DNA damage (Kopnin et al., 2007) and, is thought to regulate the "guardian of the genome", p53, during genotoxic stress (Hay, 2008). Therefore, a protective role during compound-induced hepatotoxicity is possible. The change across the gradient, although statistically significant, was small and did not progress into the heavy polysomes. Had the gradient been divided into two broad pools this potentially physiologically-relevant, functionally protective change may not have been observed.

Further evidence for the success of this improved translational profiling approach was demonstrated by the detection of other functionally-relevant pathway and individual mRNA changes in an independent *in vivo* model of compound-induced hepatotoxicity. Following treatment with Griseofulvin, which inhibits the final enzyme in the haem biosynthetic pathway and leads to the toxic accumulation of porphyrins (see Chapter 1, section 1.2.1), physiologically-relevant pathways, including "Metabolism of xenobiotics by cytochrome p450" and "Porphyrin metabolism" (Fig. 3.8) were identified as significantly enriched in those mRNAs showing altered regulation. Of particular interest was the translational repression of SWI/SNF related, matrix associated, actin dependent regulator of chromatin, subfamily e, member 1 (*Smarce1*). *Smarce1* mRNA showed movement from the heavy and medium polysomes towards the light polysomes and monosomes (Fig. 3.9 A and B), which indicated reduced translational activity following treatment with Griseofulvin. This resulted in reduced SMCE1 protein (Fig. 3.10), suggesting that the translational repression was reducing protein synthesis. *Smarce1* mRNA is heavily involved in transcriptional repression and activation of genes through chromatin remodelling (Hah et al., 2010). The SWI/SNF complex has been widely studied in regards to its role in cancer progression (Decristofaro et al., 2001; Reisman et al., 2009; Roberts and Orkin, 2004). Members of the complex have been shown to function as tumour suppressors (Reisman et al., 2009) and, intriguingly, tumour cell lines have tested negative for SMCE1 protein (Decristofaro et al., 2001). In both the mutant Balb/c$^{m1Pas/m1Pas}$ (Fech) mouse and the Griseofulvin-treated mouse, the accumulation of protoporphyrin and progressive hepatobiliary injury will, over time, lead to the development of adenomas and adenocarcinomas (Davies et al., 2005; Gant et al., 2003; Libbrecht et al., 2003). Whilst only used acutely in this study, Griseofulvin leads to tumour development if given chronically over a period of time (Knasmuller et al., 1997), and thus, a reduction in SMCE1 levels might be a very early indicator of neoplastic development. This means that *Smarce1* is potentially a very interesting candidate for further study, particularly as the majority of previous work has focused on its transcriptional regulation (Gong et al., 2012; Hah et al., 2010). In this study there was limited evidence that acute treatment with Griseofulvin was causing a transcriptional change in *Smarce1* mRNA (Fig. 3.9 C). It will next be investigated whether *Smarce1* mRNA contains binding sites for any of the miRNAs that are altered in expression following Griseofulvin treatment. Any identified putative mRNA-miRNA interactions will further highlight the success and value of translational profiling. The Griseofulvin-induced reduction of SMCE1 was further analysed in an *in vitro* mouse liver cell line (Fig. 3.12), in the hope that an *in vitro* model could be used to further validate miRNA-mediated *Smarce1* mRNA translational regulation.

In addition to assessing the effectiveness of the translational profiling method, the two models of hepatotoxicity used throughout this chapter highlight the importance of identifying mRNA species that are translationally regulated during dynamic processes, such as acute compound-induced hepatotoxicity. Transcriptional analysis can generate a list of altered mRNAs, which may have a downstream effect on protein levels. However, a number of key changes may be missed by neglecting to also analyse samples at a level beyond transcription, i.e. at the translational level. Following treatment with Griseofulvin, more mRNAs demonstrated translational regulation than transcriptional regulation (219 versus 167) (Fig. 3.7). This imbalance was even more pronounced following treatment with the PredTox compound FP014SC (447 versus 144) (Fig. 3.14). When a rapid change is required by the cell, to deal with particularly toxic stimuli, the transcriptional regulatory step may be by-passed altogether (Bottley et al., 2010; El Gazzar and McCall, 2010; Greenman et al., 2007). The predominance of translational changes thus highlights the acute nature of the insult and suggests that the liver was responding rapidly to the additional cellular stress to maintain homeostasis.

3.7 CONCLUSION

Translational profiling is becoming a more widely-used technique for studying gene expression changes at a level beyond transcription. Whilst extensively used with *in vitro* systems, the most common methods have rarely been applied *in vivo*. Simple modifications to the well-established technique of translational profiling (Johannes and Sarnow, 1998) enabled hepatic mRNA translation to be profiled at a global level *in vivo*, with improved resolution. The profiling results from two distinct models of compound-induced hepatotoxicity revealed that many more mRNAs were altered at the translational compared to the transcriptional level. Many of these translational changes would have been missed if transcriptional analysis had been performed in isolation. Subsequent validation at the protein level further emphasised the importance and physiological relevance of translational regulation in the response to, and recovery from, toxic insult.

Performing translational profiling experiments, such as these, gives rise to a large number of further questions and hypotheses. Chapter 4 describes the detailed investigation into one of the interesting mRNAs identified by polysome profiling and Chapter 5 explores the role of miRNA-mediated post-transcriptional regulation in compound-induced hepatotoxicity.

CHAPTER 4: DECREASED TRANSLATION OF *DIO3* mRNA IS ASSOCIATED WITH COMPOUND-INDUCED HEPATOTOXICITY.

4.1 SUMMARY

Chapter 3 identified *Dio3* as a gene that not only exhibited specific translational repression following compound-induced hepatotoxicity, but also had a functional role in a number of relevant canonical pathways. *Dio3* is one of a set of three deiodinases responsible for maintaining thyroid hormone (TH) levels. Western blot analysis indicated that the translational repression correlated well with reduced *Dio3* protein (D3) levels. This reduction was enhanced over time and with increasing dose. It was also conserved across different test compounds. Northern blotting and qRT-PCR revealed that there was no reduction in *Dio3* mRNA, suggesting that the translational repression of *Dio3* was the predominant factor regulating D3 protein expression following liver damage. Localised disruptions in TH levels in the liver and plasma were also observed. It is proposed that changes in TH levels induce a reduction in the rate of *Dio3* translation, which results in decreased D3 production. This may be an important mechanism by which the liver, upon early signs of damage, can act rapidly to maintain its own energy equilibrium, thereby avoiding global disruption of the hypothalamic-pituitary-thyroid axis.

The majority of the work presented in this chapter has been published as a research paper in Biochemical Journal (Dudek et al., 2013).

4.2 INTRODUCTION

4.2.1 Identification of Dio3 as an mRNA of interest

As described in Chapter 3 the regulation of mRNAs at the translational level is of fundamental importance. This is evident across a range of cellular stresses, such as apoptosis and hypoxia (Bushell et al., 2006; Thomas and Johannes, 2007) and clinical conditions, including cancer and inflammation (Galban et al., 2003; Vyas et al., 2009). In cases of compound-induced hepatotoxicity the liver is required to instigate a rapid repair mechanism, thus limiting lasting, damaging effects. Having identified *Dio3* as an mRNA that, following treatment with FP014SC, not only showed an apparent change at the translational level, as revealed by translational profiling (Table 3.3), but also had a functional role in a number of related canonical pathways (Table 3.4), it was decided to further investigate this mRNA and its regulation.

4.2.2 Iodothyronine deiodinase, type III (*Dio3*)

Iodothyronine deiodinase (III), or *Dio3*, encodes an enzyme (D3) that is vital for TH regulation; the maintenance of TH levels throughout life is of fundamental importance. There are two major THs, thyroxine (T4), secreted by the thyroid gland, and its biologically active form, 3,5,3'-triiodothyronine (T3). In combination, these two molecules play a critical role during development, cellular proliferation and metabolic homeostasis (Hernandez et al., 2007; Lema and Nevitt, 2004; Paternostro and Meisami, 1994; Simonides et al., 2008; Simonides and van Hardeveld, 2008), and even transient disruptions in their levels can cause a wide number of transcriptional gene changes (Haddow et al., 1999; Oerbeck et al., 2007; Paquette et al., 2011). Prolonged deficiency causes growth retardation, impaired cognitive function and in severe cases infantile haemangioma (Boelen et al., 2006; Dentice et al., 2009; Huang et al., 2000). In addition to D3, there are two further deiodinases (D1 and D2). All three deiodinases are highly conserved throughout the vertebrate kingdom (Bianco et al., 2002).

Of the two THs, T4 is the most abundant; it is transported through the cellular membrane, via membrane transporters, before diffusion to the nucleus where it is converted to the more active T3, by D1 and D2 (Bianco, 2011). T3 and T4 function as part of a feedback loop to regulate secretion of thyroid-stimulating hormone (TSH) and thyrotropin-releasing hormone (TRH) (Fig. 4.1). Within each tissue additional feedback mechanisms exist so that if levels of T3 and T4 become too high, D3 is recruited from the plasma membrane (Baqui et al., 2003), and together with D1, converts T3 and T4 to the inactive metabolites, reverse T3 (rT3) and 3,3'-diiodothyronine (T2), respectively. T3 and T4 prevent the hypothalamus and pituitary gland from secreting more TRH and TSH as part of a negative feedback mechanism (Fig. 4.1). This is vital for the control of both the hypothalamic-pituitary-thyroid axis (Boelen et al., 2008; Hernandez et al., 2006) and TH levels throughout the body.

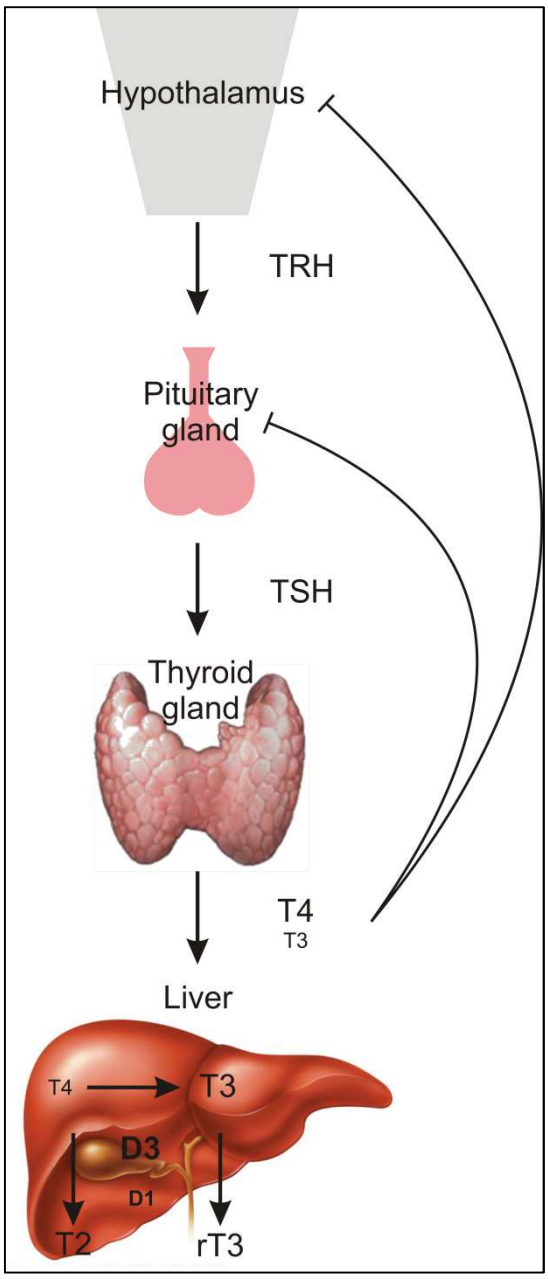

Fig. 4.1. Thyroid hormone regulation. The two THs, T3 and T4, closely control the hypothalamus-pituitary-thyroid axis through a negative feedback loop. If levels of T3 and T4 get too high D3 is recruited and converts the two THs to their inactive metabolites, rT3 and T2. This releases the inhibition of the hypothalamus and pituitary gland, meaning more TRH and TSH are released, enabling the systemic concentration of T3 and T4 to return to normal.

Dio3 shows particularly high expression in foetal and placental tissues (Bates et al., 1999; Galton et al., 1999; Huang et al., 2003), where it functions to protect the foetus from high levels of maternal TH. The majority of adult tissues demonstrate only low levels of *Dio3* mRNA, however, the rat brain maintains high D3 activity throughout life (Kaplan and Yaskoski, 1980). This data supports a functionally protective role for the enzyme, in this instance modulating TH levels within neurons. Furthermore, in some circumstances there is re-expression of *Dio3* in the adult, for example during proliferation and cell growth (Peeters et al., 2003). This has been demonstrated in a number of pathophysiological conditions including cancer, myocardial infarction and liver regeneration following partial hepatectomy (Huang et al., 2000; Kester et al., 2009; Wassen et al., 2002).

4.2.3 *Dio3* and translational regulation

Whilst much is known about the transcriptional regulation of *Dio3*, translational regulation has not been extensively investigated. Levels of *Dio3* are increased transcriptionally in the presence of THs (Hernandez, 2005), retinoic acid (Esfandiari et al., 1994) and growth factors (Hernandez et al., 1998), and reduced by growth hormones (Van der Geyten et al., 1999) and in hypothyroidism (Esfandiari et al., 1992). In addition, *Dio3* is part of a genomic imprinting region (Hernandez, 2005). Thus, the transcription of *Dio3* can also be regulated via differentially methylated regions (Charalambous and Hernandez, 2013). Currently no post-transcriptional regulation of *Dio3* has been identified, however, there is published data on *Dio2* that suggests this type of regulation is essential (Arrojo and Bianco, 2011). Within the brain, for example, translational regulation of *Dio2* is critical for the preservation of TH levels to prevent hypothyroidism, and increases in D2 activity far exceed transcriptional changes in *Dio2* mRNA (Peeters et al., 2001). Within the rat and human adult liver *Dio2* is not expressed (Croteau et al., 1996), however, *Dio3* is. It is, therefore, possible that in cases of increased cellular stress within the liver, such as that seen following compound-induced hepatotoxicity, this important mode of TH regulation could be controlled by *Dio3* rather than *Dio2*.

4.3 AIM

To further assess, and identify putative mechanisms for, the translational regulation of *Dio3* mRNA.

4.4 MATERIALS AND METHODS

4.4.1 Animal models

The animal models used for the work described in this chapter were the Thioacetamide-treated rats and the PredTox compound-treated rats.

Animals were maintained and treated as described in Chapter 2, section 2.1.2 and 2.1.3.

4.4.2 Determination of liver damage

4.4.2.1 Histopathology

Prior to performing any genomic-based analysis, sections (2 – 3 mm thick) were taken from the livers of rats treated with Thioacetamide or vehicle only and maintained in 10 % (v/v) neutral buffered formalin fixative. Sections were processed, stained and mounted by the imaging and pathology group at the MRC Toxicology Unit. Haematoxylin and eosin (H & E) staining was carried out using a Shandon Varistain machine (Thermo Fisher Scientific). Mounted slides were viewed using an Axiovert 200M (Zeiss, Cambridge, UK) and pictures taken using an Axiocam HR. Technical advice on viewing histology images was provided by Mr David Read.

The PredTox consortium had produced reports on each compound they investigated, and within these were key histopathological summaries.

4.4.2.2 Measurement of alanine transaminase and aspartate aminotransferase

To measure plasma activity of alanine transaminase (ALT) and aspartate aminotransferase (AST) kits from Sentinel Diagnostics (Alpha laboratories, Hampshire, UK) were used according to the manufacturer's instructions. Briefly, 100 µl plasma was mixed with 1 ml buffer 1 and incubated at 37°C for 1 min. 100 µl buffer 2 was added and after 1 min the A_{340nm} was recorded. The absorbance was measured a further 3 times (after 2, 3 and 4 min), and the ALT and AST activity was calculated by multiplying the average Δ absorbance/min by a fixed factor value (1905). Statistically significant differences were calculated using a one-way ANOVA with Dunnett's multiple comparison post hoc test.

4.4.3 Translational profiling

Translational profiling was performed as described in Chapter 3, section 3.4.5.

4.4.4 Validation of microarray results

4.4.4.1 Quantitative RT-PCR of fractionated RNA

A change in the translational efficiency of *Dio3* was further verified using qRT-PCR. The method was as described in Chapter 3, section 3.4.6.1.

4.4.4.2 Quantitative RT-PCR of total RNA

Liver RNA from animals treated with Thioacetamide or the PredTox compounds was extracted and quantified as described in Chapter 2, section 2.3. The RNA was DNase treated prior to undergoing reverse transcription, due to *Dio3* having only a single exon. Thus, to prevent genomic DNA contamination 10 µg RNA was incubated with Turbo DNase (Life Technologies, Paisley, UK) at 37°C for 1 h. The DNase was inactivated through re-extraction of the RNA, as described in Chapter 2, section 2.3.1. DNase-treated RNA was analysed by qRT-PCR as described in chapter 2, section 2.7. Statistically significant differences were calculated using a two-tailed Student's T-Test.

4.4.4.3 Western Blotting: D3

Protein was extracted and quantified as described in Chapter 2, section 2.5. To assess whether alterations in the translational efficiency of *Dio3* mRNA were having a downstream effect on protein levels, Western Blotting with a polyclonal antibody against D3 was used (Novus Biologicals, Littleton, CO). Anti-Gapdh was used to check for equal loading and for normalisation. Western blotting was performed as described in Chapter 2, section 2.8. The D3 antibody has previously been validated (Shukla et al., 2011b; Sittig et al., 2011) against the only other commercially available *Dio3* antibody (Huang et al., 2003). Statistically significant differences were calculated using a two-tailed Student's T-Test (2 group comparison) or a one-way ANOVA with Tukey's multiple comparison post hoc test (> 2 group analysis).

4.4.4.4 Northern blotting: Dio3

4.4.4.4.1 Construction of Dio3 probe for Northern blotting

Initial attempts were made to generate a PCR product from DNA extracted from one of the PredTox control rat liver samples using primers specific to *Dio3*. The DNA extraction method is described in Chapter 2, section 2.4. Primers were designed against the coding region of *Dio3* using Primer3 (http://frodo.wi.mit.edu/) and checked for specificity by performing a Blast search. All primer sequences are provided in Appendix III.

DNA was diluted to 10 ng in ultra pure (18 MΩ) water and added to a reaction comprising 10 µl 10X PCR buffer, 2 µl dNTP mix (10 mM), 50 mM $MgCl_2$, 1% (v/v) W1, 2.5 U Taq DNA polymerase (all Life Technologies, Paisley, UK) and 50 pmol forward and reverse primers. Reactions were denatured at 95°C for 5 min. This was followed by 30 cycles of denaturing (95°C, 30 s), and annealing and extending (52°C, (30 s), 72°C (1 min)), and a final incubation at 72°C for 5 min. Products were purified using a QIAquick PCR purification kit (Qiagen, Venlo, Netherlands) according to the manufacturer's instructions. Briefly, 100 µl PCR product was added to 500 µl buffer PB and applied to QIAquick spin column. Columns were centrifuged (16,100g, RT, 1 min) and washed with 750 µl buffer PE. Columns were centrifuged (16,100g, RT, 1 min) to remove residual buffer and DNA was eluted in 30 µl buffer EB.

Yields were low, so the PCR method was adjusted to include a touchdown approach (represented in Table 4.1) and the Taq from the kit was replaced with an industry gold standard, Kapa Taq DNA polymerase (Kapa Biosystems, USA).

Table 4.1. Parameters for touchdown PCR.

Stage	Temp (°C)	Time (min)	Temp (°C)	Time (min)	Temp (°C)	Time (min)	Cycles
1	95	5	65	2	72	2	1
2	95	0.5	63	2	72	2	1
3	95	0.5	61	2	72	2	1
4	95	0.5	59	2	72	2	1
5	95	0.5	57	2	72	2	1
6	95	0.5	55	2	72	2	35
7	95	0.5	55	2	72	5	1

The use of the touchdown approach and Kapa Taq DNA polymerase generated improved DNA yields, thus the PCR products were ligated into a pGEM®-T Easy vector System (Promega, Madison, USA), according to the manufacturer's instructions. Briefly, a 1:3 vector:insert ligation was set up in a reaction containing 5 µl 2X Rapid Ligation buffer, 1 µl pGEM®-T Easy vector and 1 µl DNA ligase. Ligation proceeded at 4°C overnight. The ligated DNA was transformed into competent cells (GeneCopoeia, Rockville, USA) using a heat shock protocol and spread onto agar plates. The colonies that grew were digested as appropriate and products were analysed on a gel. Unfortunately, the required insert was not present.

Thus, to obtain a usable product an open reading frame (ORF) *Dio3* clone was purchased from Genscript (NJ, USA), which came in a pDream2.1 / MCS vector (Fig. 4.2). When PCR was performed with this clone, using the touchdown approach (Table 4.1) and Kapa Taq DNA polymerase, the yield was greatly improved. Sequencing using an Applied Biosystems 3730 sequencer (performed by PNACL, University of Leicester) revealed that the resulting product had 99% similarity to *Dio3*.

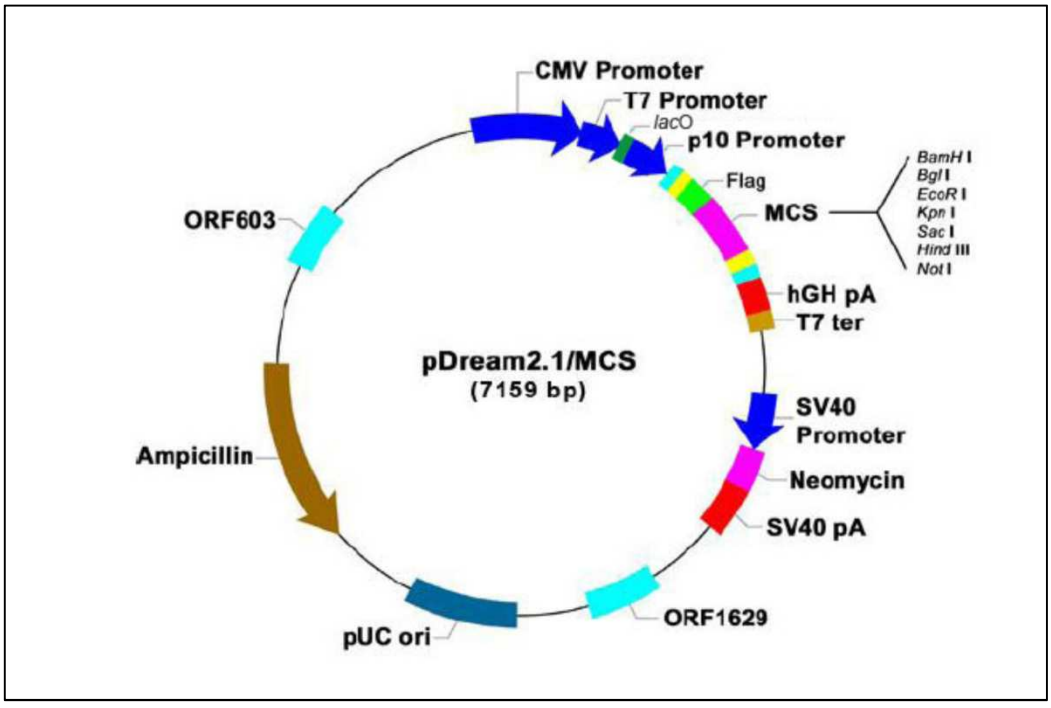

Fig. 4.2. pDream2.1 / MCS vector. This vector, containing a *Dio3* ORF clone, was used to produce a suitable probe for Northern blotting (taken from http://www.genscript.com/vector/SD0222-pDream2_1_MCS.html).

4.4.4.4.2 Hybridisation with radiolabelled Dio3 probe

The *Dio3* probe was radiolabelled with ^{32}P-αdCTP (Appendix IV) and Northern blotting was performed as described in Chapter 3, section 3.4.4.4.

4.4.5 Determination of T3 and T4 concentrations

Approximately 200 mg liver tissue and 200 µl plasma were sent on dry ice to the Laboratory of Comparative Endocrinology at the Catholic University of Leuven in Belgium. They measured the levels of T3 and T4 in both solid tissues and plasma samples using a series of highly sensitive and specific radioimmunoassay (RIAs) (Darras et al., 1990; Reyns et al., 2002). Statistically significant differences were calculated using a two-tailed Student's T-Test.

4.4.6 Cell culture

Cells were grown and maintained as described in Chapter 2, section 2.2.

4.4.6.1 Measurement of endogenous Dio3 mRNA and D3 protein levels

Cells were plated into 6 well-plates at a density of 20,000 cells/ml. They were incubated at 37°C overnight to adhere and harvested when they reached approximately 80% confluency. half of the cells were harvested into Tri reagent for RNA extraction and half were harvested into lysis buffer, plus protease inhibitor cocktail, for protein extraction, as described in Chapter 2, sections 2.3.2. and 2.5.2, respectively. qRT-PCR and Western blot analysis were performed as described in sections 4.4.4.2 and 4.4.4.3, respectively.

4.4.6.2 Induction of Dio3 mRNA/D3 protein in vitro

Literature searches were performed to identify known inducers of *Dio3* mRNA and/or D3 protein expression. The H4IIE cells were treated with retinoic acid (Esfandiari et al., 1994) and growth factors, EGF and aFGF (Hernandez et al., 1998).

4.4.6.2.1 Treatment of H4IIE cells with Retinoic acid

H4IIE cells were plated into two 6 well-plates at a density of 20,000 cells/ml. They were incubated at 37°C overnight to adhere and treated with 5 different doses of retinoic acid (Sigma, Poole, UK). Doses of 10 µM, 5 µM, 1 µM, 0.5 µM and 0.1 µM retinoic acid were prepared in 0.1% (v/v) DMSO. One well of the plate was treated with 0.1% (v/v) DMSO only as a vehicle-treated control. 48 h after treatment, cells from one plate were harvested into Tri reagent for RNA extraction, and from the other plate into lysis buffer, plus protease inhibitor

cocktail, for protein extraction. RNA and protein were extracted as described in Chapter 2, sections 2.3.2. and 2.5.2 respectively. qRT-PCR and Western blot analysis were performed as described in sections 4.4.4.2 and 4.4.4.3, respectively.

4.4.6.2.2 Treatment of H4IIE cells with EGF and aFGF

Rat EGF and mouse FGF acidic were purchased from Sigma (Poole, UK). As recommended by the manufacturer the EGF was reconstituted in 10 mM acetic acid, supplemented with 0.1% (w/v) BSA, and the aFGF was reconstituted in sterile PBS to a concentration of 100 µg/ml, supplemented with 0.1% (w/v) BSA. Cells were plated as described in section 4.4.6.2.1 and treated in triplicate with either 10 ng/ml EGF, 4 ng/ml aFGF or the vehicle only (acetic acid + 0.1% BSA and PBS + 0.1% BSA respectively). Approximately 9 h after treatment, cells from one plate were harvested into Tri reagent for RNA extraction, and from the other plate into lysis buffer, plus protease inhibitor cocktail, for protein extraction. RNA and protein were extracted as described in Chapter 2, sections 2.3.2. and 2.5.2 respectively. qRT-PCR and Western blot analysis were performed as described in sections 4.4.4.2 and 4.4.4.3, respectively.

4.5 RESULTS

4.5.1 Identification of Dio3 as a candidate for further study

4.5.1.1 Ingenuity analysis

As discussed in Chapter 3, following treatment with the PredTox compound FP014SC, 447 mRNAs demonstrated a change in translational efficiency (Chapter 3, Fig. 3.14), and these mRNAs were significantly enriched in 169 canonical pathways (Table 3.4). *Dio3* mRNA showed movement from the heavy polysomes to the monosomes following treatment with FP014SC, suggesting less efficient translation during compound-induced hepatotoxicity. Furthermore, *Dio3* appeared to have a regulatory role in the thyroid hormone receptor/retinoid X receptor (TR/RXR) activation pathway via its control of TH levels. The RXR-based canonical pathways are heavily involved during metabolic disruption, thus, it is hypothesised that *Dio3* might have an important role in the metabolic response to liver toxicity. The TR/RXR activation pathway is shown in Fig. 4.3; the other RXR-based pathways are highlighted.

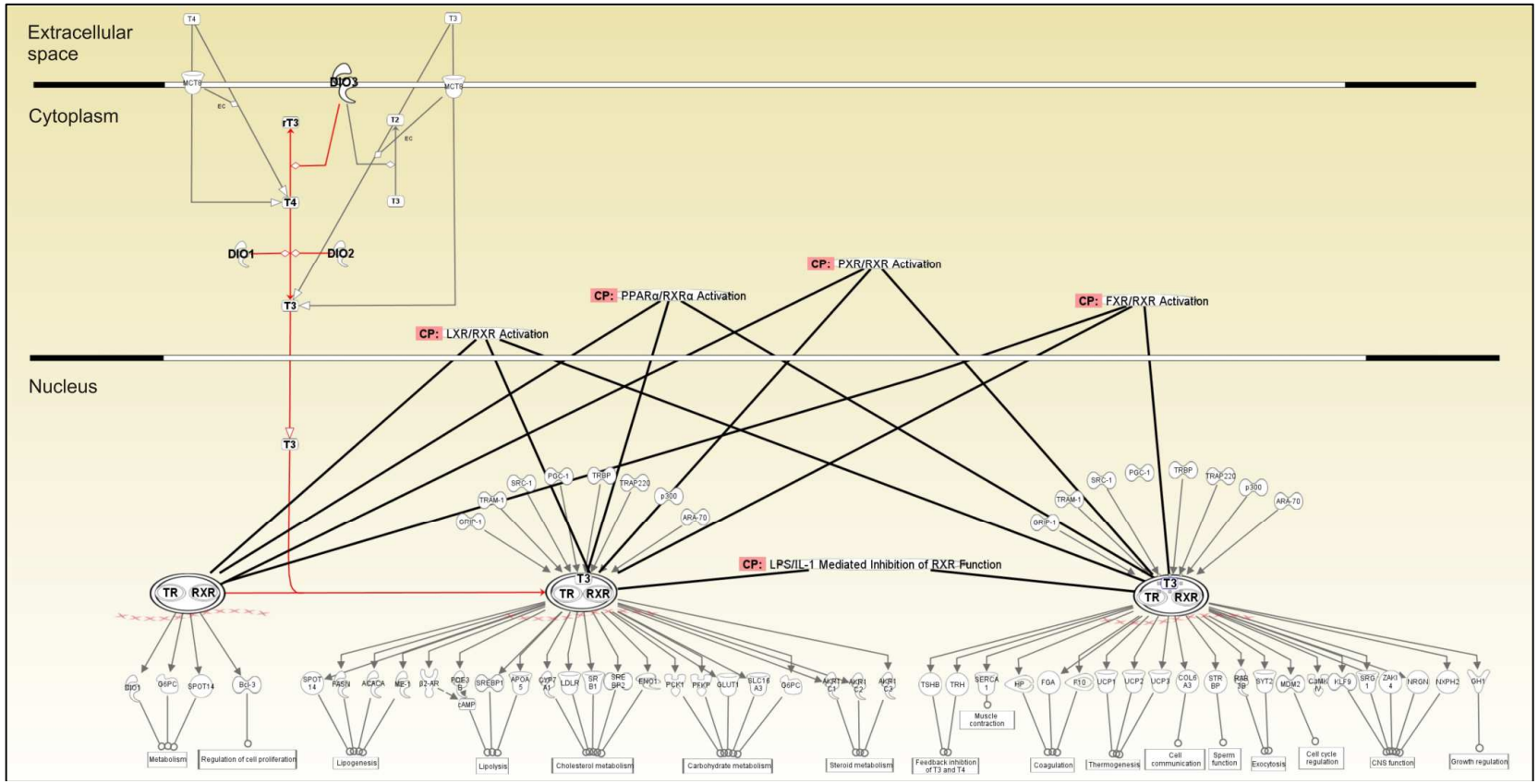

Fig. 4.3. *Dio3* has a regulatory role in the TR/RXR activation pathway. All mRNAs that demonstrated a change in translational efficiency were subject to pathway analysis using Ingenuity® IPA software. TR/RXR was identified as a key pathway. Associated RXR canonical pathways [CP] are also highlighted. *Dio3* plays a regulatory role in the TR/RXR pathway via its control of TH levels (pathway shown in red). Lines with arrows represent interactions between molecules, lines with circles represent interactions between molecules and processes, and solid black lines represent an interaction between a different canonical pathway and the TR/RXR activation pathway.

4.5.1.2 Validation of microarray change using qRT-PCR

qRT-PCR analysis was performed on the same pooled fractions that had undergone microarray analysis. This confirmed movement of *Dio3* mRNA across the gradient from the heavy polysomes towards the monosomes (Fig. 4.4), indicating reduced translational efficiency following treatment with FP014SC.

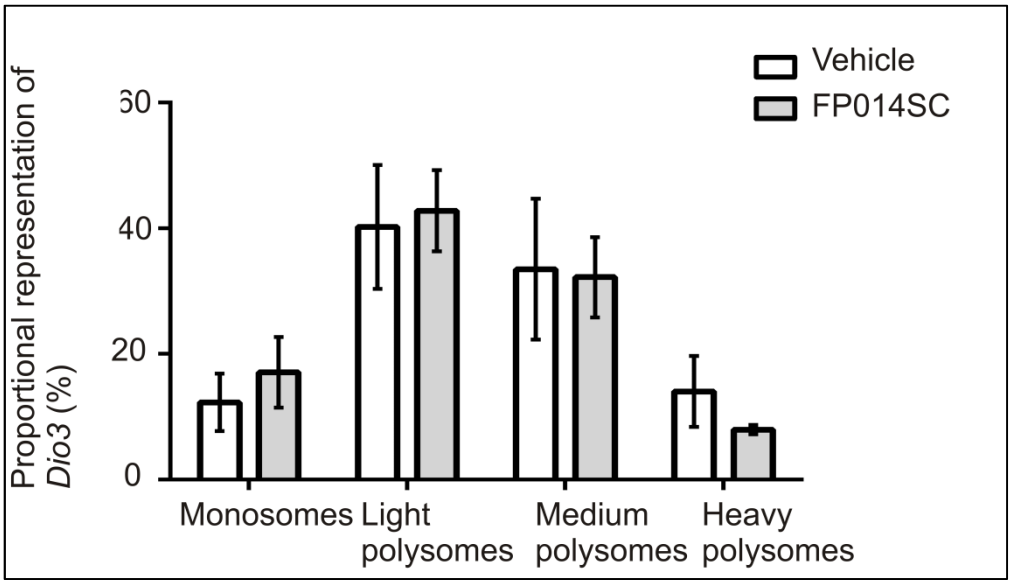

Fig. 4.4. qRT-PCR analysis demonstrated movement of *Dio3* mRNA from the heavy polysomes to the monosomes. This indicated a reduction in translational efficiency. FP014SC-treated rats received high dose FP014SC or vehicle-only treatment for 15 days (n=5).

4.5.2 Evidence that treatment with Thioacetamide provided a suitable additional model of hepatotoxicity in the rat

Prior work by the PredTox consortium had already indicated that the five compounds selected for further analysis in this study caused hepatic injury, as determined by their histopathology (Chapter 3, Table 3.2) and clinical chemistry (Suter et al., 2011). The PredTox model was supplemented with an additional model of toxicity, the Thioacetamide-treated rat model. This provided additional plasma samples and the opportunity to manipulate the experimental conditions as required. The rationale for choosing this model is discussed in detail in Chapter 1, section 1.2.2. To determine the degree of liver injury in the Thioacetamide-treated rats, plasma ALT and AST activity rates were measured 24 and 48 h after administration of a 100 mg/kg dose. Enzyme levels were increased by more than 10- (ALT) and 43- (AST) fold at 24 h following treatment with Thioacetamide (Fig. 4.5 A). Levels of both enzymes in the Thioacetamide-treated animals were lower at 48 h than at 24 h, reflecting the acute nature of the hepatic injury and subsequent initiation of repair mechanisms.

Clinical chemistry data were supported by histopathological analysis. Representative images from the livers of rats treated with the vehicle-only or highest dose (150 mg/kg) of Thioacetamide are shown in Fig. 4.5 B. The images from the Thioacetamide-treated livers demonstrated some fibrosis and inflammation; the hepatocytes had small dense nuclei and hepatocyte vacuolation [V], indicative of hepatocellular injury. However, there were also areas rich in hepatocytes forming parenchymal nodules, indicative of regenerative activity [R] after 48 h, concurrent with the decreased levels of serum transaminases.

The summary reports from the PredTox consortium revealed that ALT and AST levels were similarly increased following treatment with the selected compounds (Boitier et al., 2011; Matheis et al., 2011b; Suter et al., 2011). Representative data from the most severe hepatotoxic agent (FP014SC) is provided in Fig. 4.5 C. As with Thioacetamide treatment, the increase in ALT and AST activity rates was transient and levels had returned to close to those of vehicle-only treated controls by the day 15 time point. The PredTox compounds also induced a similar hepatic histopathology to that seen following treatment with the PredTox compounds, with common features including apoptosis, inflammation, cholestasis and regenerative repair (Chapter 3, Table 3.2).

The combined results of these analyses indicated that the Thioacetamide-treated rat showed similar clinical signs of hepatotoxicity to those observed in the PredTox compound-treated rats. Thus, confirming it was suitable for use as an additional model of compound-induced liver damage.

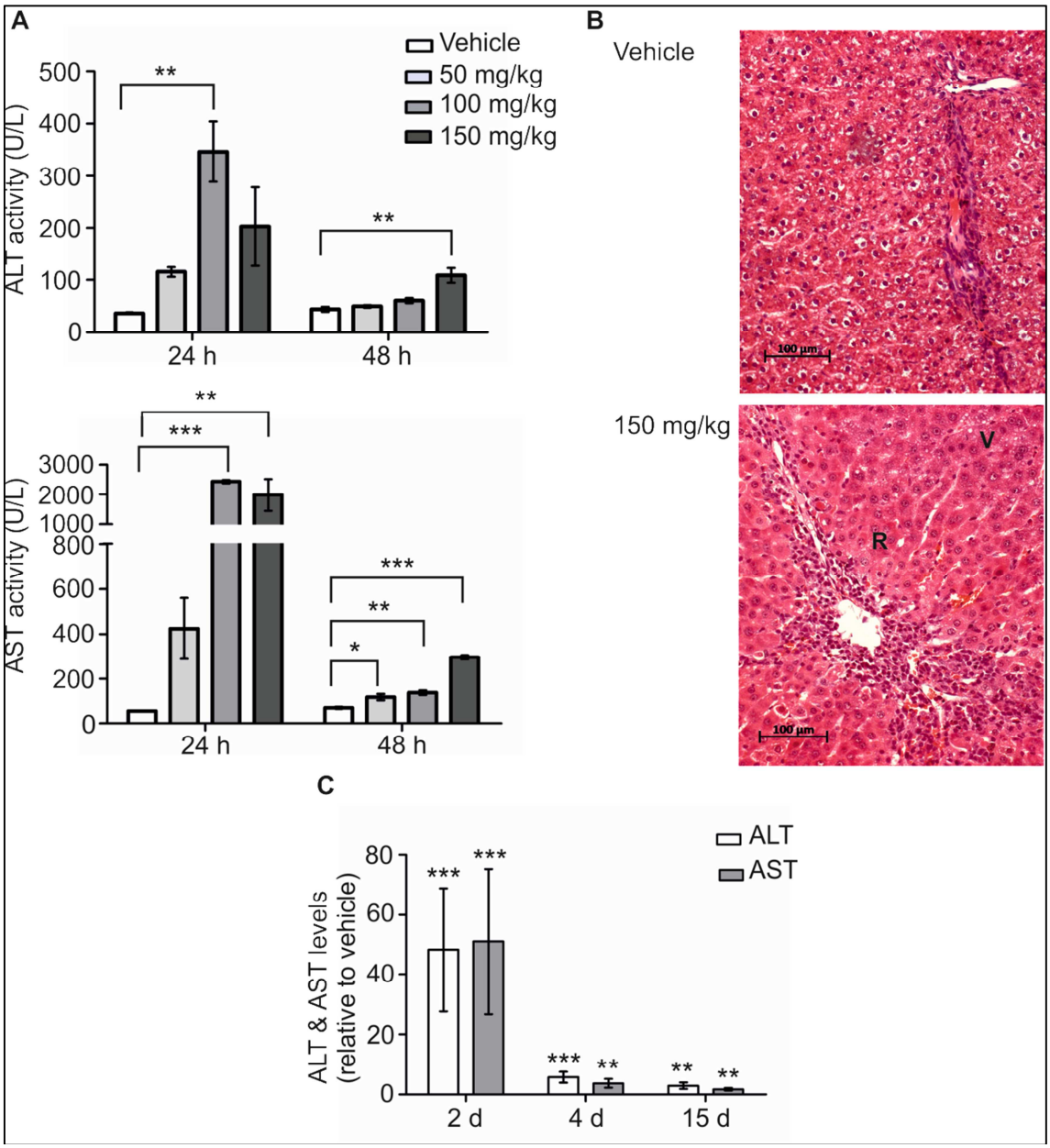

Fig. 4.5. Clinical chemistry and histopathology indicate hepatotoxicity following treatment with Thioacetamide or the PredTox compounds. (**A**) Plasma ALT and AST levels and (**B**) histopathological images following treatment with Thioacetamide; [V] denotes vacuolation, [R] denotes area of enhanced regenerative activity. (**C**) ALT and AST levels following treatment with FP014SC. Data represent mean ± SEM. * $p \leq 0.05$, ** $p \leq 0.01$, *** $p \leq 0.001$ (ANOVA + Dunnett's post hoc test). Thioacetamide-treated rats received 50 mg/kg, 100 mg/kg or 150 mg/kg Thioacetamide or vehicle-only (0.9% saline) treatment and were sacrificed after 24 h or 48 h (n=3 for all treatments/doses). FP014SC-treated rats received high dose FP014SC or vehicle-only treatment for up to 15 days (n=5 for all doses/time points).

4.5.3 The reduction in *Dio3* mRNA translation was complemented by a corresponding change in D3 protein levels

Dio3 protein (D3) levels were measured across all rat models (Thioacetamide treatment plus five PredTox compounds) by Western blotting. Following high dose treatment with Thioacetamide for 48 h, or FP007SE, FP004BA or FP014SC for 15 days a significant reduction in D3 was observed (Fig. 4.6 A-D). Furthermore, a similar trend was seen with the other PredTox compounds; FP005ME and FP013NO (Fig. 4.6 E & F), although they did not reach statistical significance.

4.5.4 D3 was reduced in both a dose- and time-dependent manner

When considering samples on an individual basis there was a correlation between extent of liver damage, according to clinical and histopathological grading, and reduction in D3 levels. This was particularly true of FP005ME; the averaged levels of D3 did not show a significant difference between the compound-treated (n=3) and vehicle-treated (n=3) samples. However, when considering the same samples individually, Western blot analysis revealed that the liver sample that showed the largest protein reduction (71%) following treatment, also had the most pronounced clinical signs of hepatotoxicity. Dose and time-course related responses were therefore explored. The Thioacetamide model was used to look for a dose-response reduction in D3 with more pronounced hepatotoxicity. Although the only significant reduction in D3 was observed following treatment at the highest dose (150 mg/kg), there was a small, but consistent change at the lower doses (Fig. 4.7 A). The PredTox compound that had caused one of the largest reductions in D3 following high dose treatment for 15 days (FP007SE) was initially used to measure time-related effects. The reduction in D3 was exacerbated over time, so that by day 15 levels were reduced by 85% (Fig. 4.7 B). A time-related increase in the extent of the down-regulation of D3 was also observed following treatment with the highest dose of FP004BA and FP014SC (Fig. 4.7 C & D).

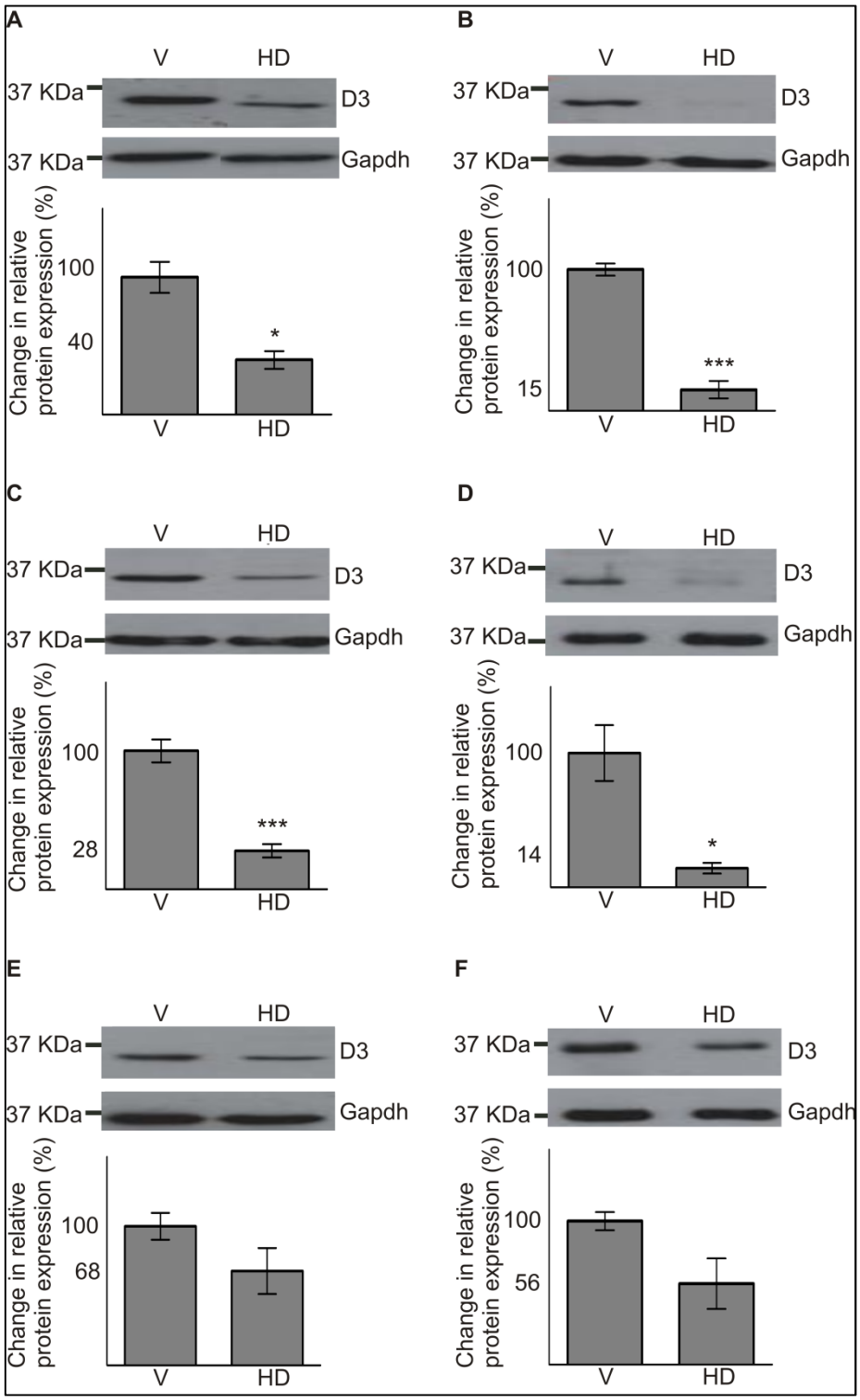

Fig. 4.6. D3 was down-regulated following compound-induced hepatotoxicity. (**A**) Thioacetamide, (**B**) FP007SE, (**C**) FP004BA, (**D**) FP014SC, (**E**) FP005ME and (**F**) FP013NO; [V] vehicle-only, [HD] high dose. Representative blots are shown. Western blot data was normalised to Gapdh and data represent mean ± SEM. * $p \leq 0.05$, *** $p \leq 0.001$ (T-Test). Thioacetamide-treated rats received 150 mg/kg Thioacetamide or vehicle-only (0.9% saline) treatment and were sacrificed after 48 h (n=3). PredTox compound-treated rats received high dose compound or vehicle-only treatment for 15 days (n≥3).

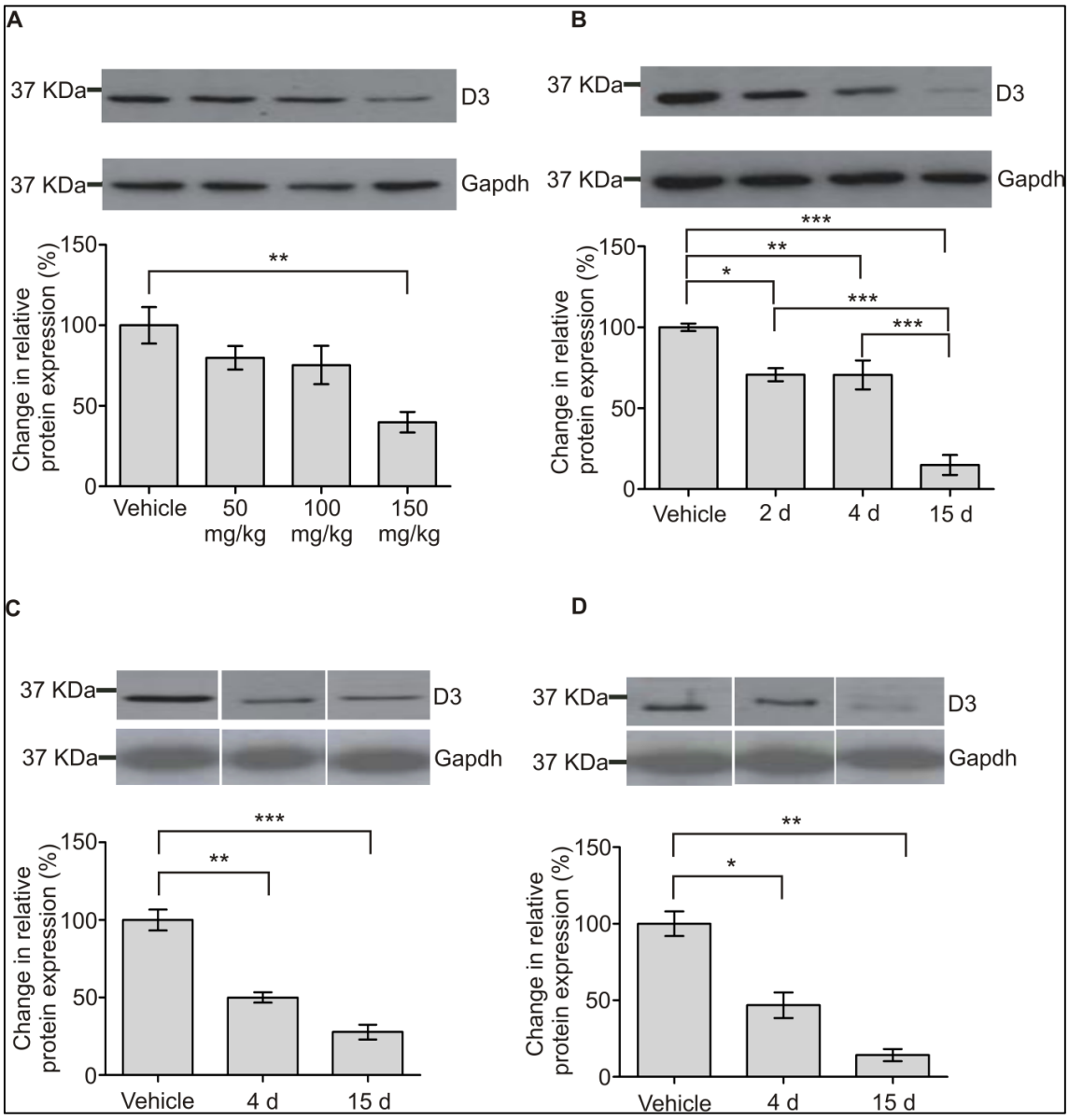

Fig. 4.7. D3 was down-regulated in both a dose- and time-dependent manner following compound-induced hepatotoxicity. (**A**) Thioacetamide, (**B**) FP007SE, (**C**) FP004BA and (**D**) FP014SC. Representative blots are shown. Western blot data was normalised to Gapdh and data represent mean ± SEM. * $p \leq 0.05$, ** $p \leq 0.01$, *** $p \leq 0.001$ (ANOVA + Tukey's post hoc test). Thioacetamide-treated rats received 50 mg/kg, 100 mg/kg or 150 mg/kg Thioacetamide or vehicle-only (0.9% saline) treatment and were sacrificed after 48 h (n=3 for all treatments/doses). PredTox compound-treated rats received high dose compound or vehicle-only treatment for up to 15 days (n≥3 for all doses/time points).

4.5.5 Changes in levels of Dio1, Dio2 and Dio3 mRNA

qRT-PCR using primers specific for *Dio1*, *Dio2* and *Dio3* was performed following treatment with Thioacetamide plus the three PredTox compounds that had caused a significant reduction in D3 protein.

Thioacetamide-treated rats demonstrated a non-significant down-regulation of *Dio1* mRNA (Fig. 4.8 A). Following treatment with the PredTox compounds, a down-regulation of *Dio1* mRNA was also seen with FP007SE or FP004BA, reaching statistical significance with FP004BA (Fig. 4.8 B & C). There was no change in expression following treatment with FP014SC (Fig. 4.8 D).

Although some *Dio2* mRNA expression was seen (Fig. 4.8), the CT values were very high. Thus, *Dio2* mRNA levels were bordering on the threshold of detection. In fact, the values from the FP007SE samples were beyond the limit of detection (Fig. 4.8 B). No significant change in *Dio2* expression was observed following treatment with Thioacetamide, FP004BA, or FP014SC (Fig. 4.8 A, C & D).

The levels of *Dio3* mRNA were also low; however, they remained consistently higher than the levels of *Dio2* mRNA. Thioacetamide-treatment caused a non-significant increase in *Dio3* mRNA (Fig. 4.8 A), whilst a significant increase in *Dio3* mRNA expression was observed following high dose treatment with FP007SE or FP004BA (Fig. 4.8 B & C). There was no change following treatment with FP014SC (Fig. 4.8 D).

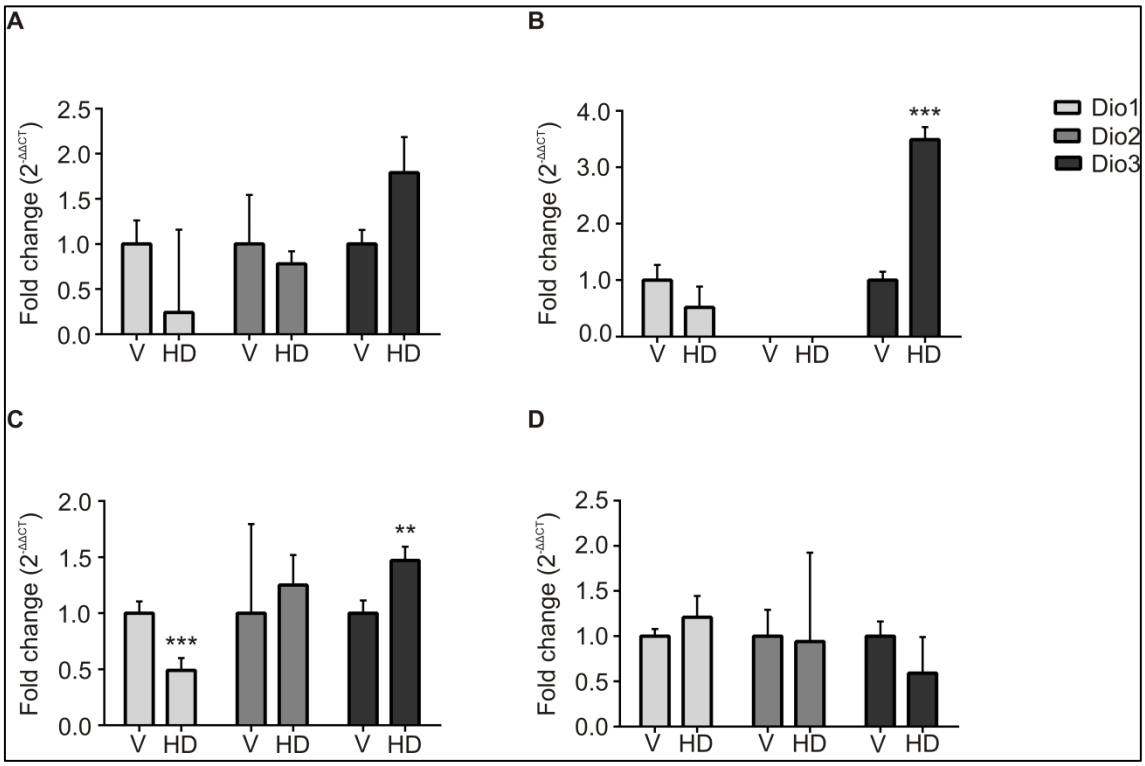

Fig. 4.8. qRT-PCR revealed some changes in the expression of the deiodinases following compound-induced hepatotoxicity. (**A**) Thioacetamide, (**B**) FP007SE, (**C**) FP004BA and (**D**) FP014SC; [V] vehicle-only, [HD] high dose. qRT-PCR data were normalised to β-Actin and represent mean ± SEM. ** $p \leq 0.01$, *** $p \leq 0.001$ (T-Test). Thioacetamide-treated rats received 150 mg/kg Thioacetamide or vehicle-only (0.9% saline) treatment and were sacrificed after 48 h (n=3). PredTox compound-treated rats received high dose compound or vehicle-only treatment for 15 days (n≥3).

4.5.6 Less Dio3 was recruited to the polysomes following compound-induced hepatotoxicity

As described in Chapter 3, section 3.4.3 sucrose density fractionation can be used to separate RNA into non-actively translated (monosomal) fractions and progressively more actively translated (light, medium and heavy polysomal) fractions. The relative proportion of a specific mRNA within each fraction can then be measured using Northern blotting and/or micro dot blotting. An increase in the abundance of *Dio3* mRNA in the monosomal and lighter polysomal fractions was observed following treatment with Thioacetamide, FP007SE or FP004BA (Fig. 4.9 A-C). Even though the FP014SC-treated samples were fractionated into a greater number of fractions than the samples from the other models, the same movement across the gradient was seen (Fig. 4.9 D). This movement across the gradient from the heavy polysomes towards the monosomes indicated that, following compound-induced hepatotoxicity, *Dio3* was less efficiently translated.

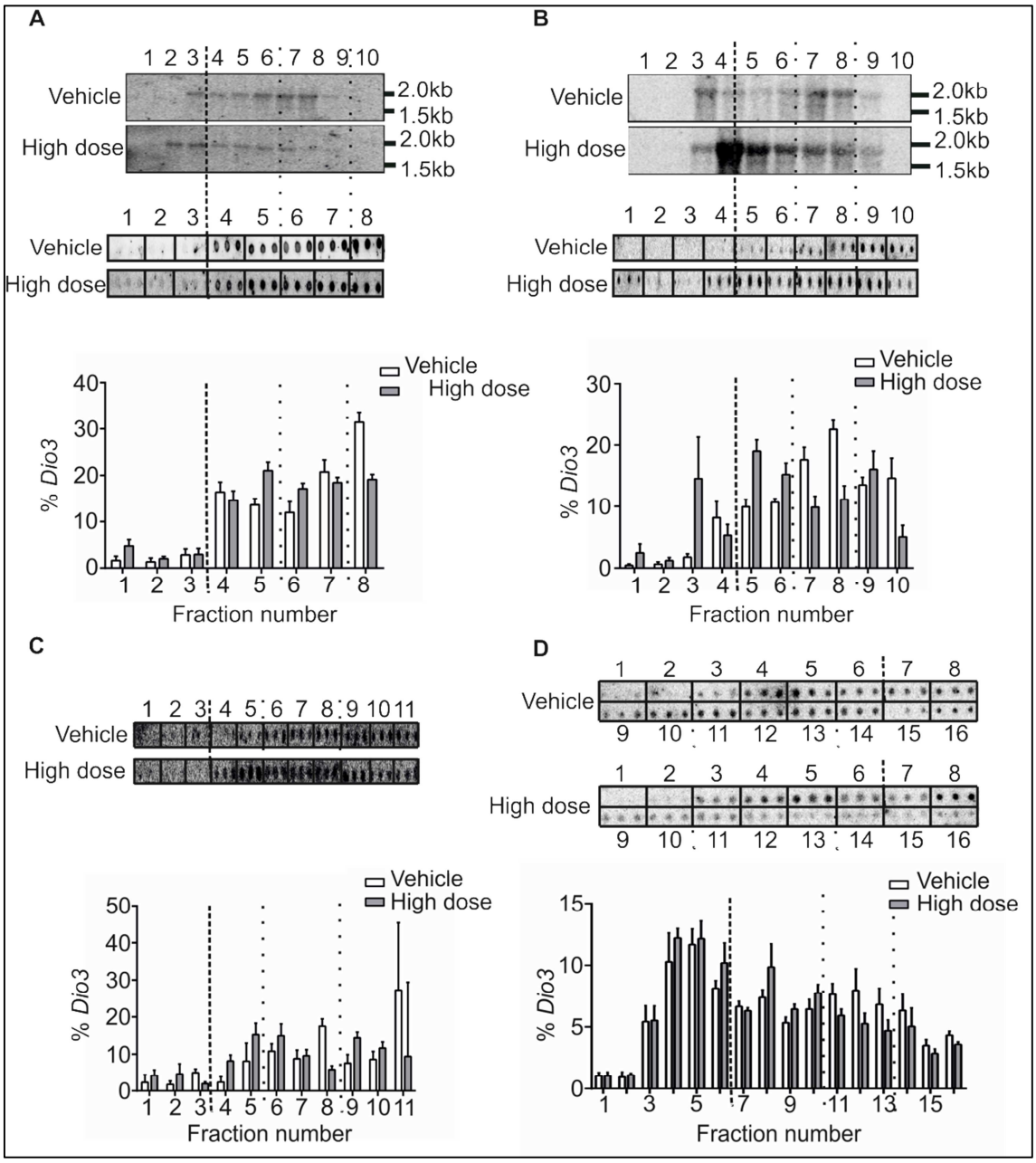

Fig. 4.9. Northern blotting and micro dot blotting confirmed movement of *Dio3* mRNA from heavy polysomes to monosomes following compound-induced hepatotoxicity. (**A**) Thioacetamide, (**B**) FP007SE, (**C**) FP004BA and (**D**) FP014SC. Representative blots are shown. The amount of *Dio3* within each fraction was calculated as a percentage of the total. Thioacetamide-treated rats received 150 mg/kg Thioacetamide or vehicle-only (0.9% saline) treatment and were sacrificed after 48 h (n=3). PredTox compound-treated rats received high dose compound or vehicle-only treatment for 15 days (n≥3). Dashed lines indicate location of monosomal and polysomal fractions.

4.5.7 The liver and plasma had reduced levels of T3 and T4 following compound-induced hepatotoxicity

Levels of T3 and T4 within the liver were measured following treatment with Thioacetamide, FP007SE, FP004BA or FP014SC (Fig. 4.10). Following treatment with Thioacetamide there was a reduction in T3 and T4 levels (Fig. 4.10 A). The reduction in T3 levels was significant 24 h after dosing, reduced by 73%. 48 h after dosing, levels of T3 were beginning to return towards those seen in the vehicle-treated controls. T4 levels were also reduced, although not to a statistically significant level, or to such an extent as T3 levels. In contrast to the T3 levels, however, the reduction in T4 was increased over time, from 25% at 24 h to 38% at 48 h.

Treatment with the PredTox compounds also induced a reduction in T3 and T4 levels. Treatment with FP007SE for 15 days caused a significant reduction in levels of T3 and T4, by 56% and 53%, respectively (Fig. 4.10 B). Treatment with FP004BA and FP014SC did not induce a statistically significant reduction in T3, although there was a trend for a reduction with FP004BA (Fig. 4.10 C and D). Both compounds induced a significant reduction in T4 levels, by 15% (FP004BA) and 29% (FP014SC) (Fig. 4.10 C & D).

The levels of T3 and T4 were also measured in the plasma of the Thioacetamide-treated rats (Fig. 4.11). Results were very similar to those observed in the liver. The reduction in T3 levels was largest and significant 24 h after dosing, with a 60% reduction. 48 h after dosing, levels of T3 were beginning to return towards those seen in the vehicle-treated controls. Although statistical significance was not reached, T4 levels also showed a trend for a reduction following treatment. This change was consistent across both time points, reduced by approximately 32%. Sample availability from the PredTox studies was limited, and did not allow measurement of T3 and T4 levels in the plasma.

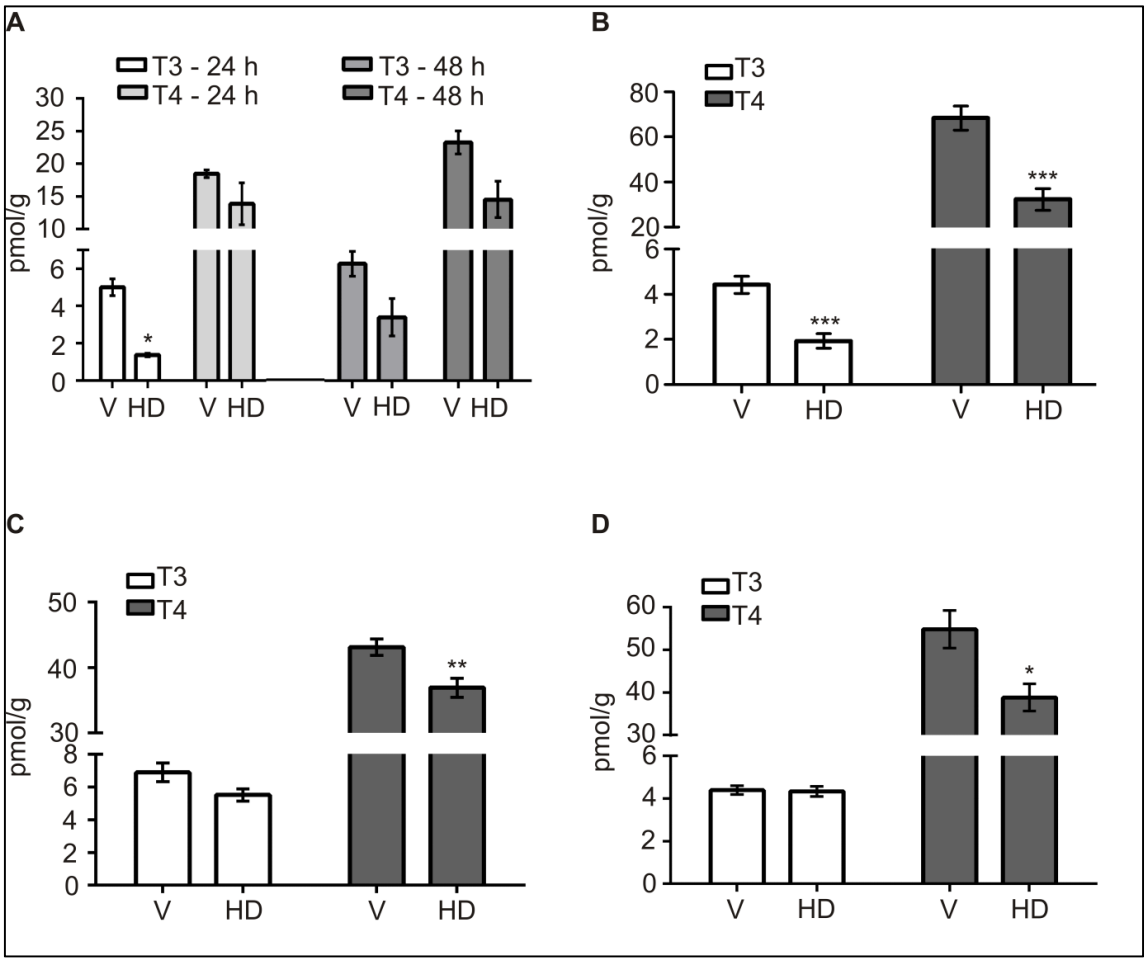

Fig. 4.10. RIAs revealed that T3 and T4 levels within the liver were reduced following compound-induced hepatotoxicity. (**A**) Thioacetamide, (**B**) FP007SE, (**C**) FP004BA and (**D**) FP014SC; [V] vehicle-only, [HD] high dose. Data represent mean ± SEM. * $p \leq 0.05$, ** $p \leq 0.01$, *** $p \leq 0.001$ (T-Test). Thioacetamide-treated rats received 150 mg/kg Thioacetamide or vehicle-only (0.9% saline) treatment and were sacrificed after 24 h or 48 h (n=3). PredTox compound-treated rats received high dose compound or vehicle-only treatment for 15 days (n≥3). Liver samples were sent to the Laboratory of Comparative Endocrinology at the Catholic University of Leuven in Belgium for T3 and T4 measurement.

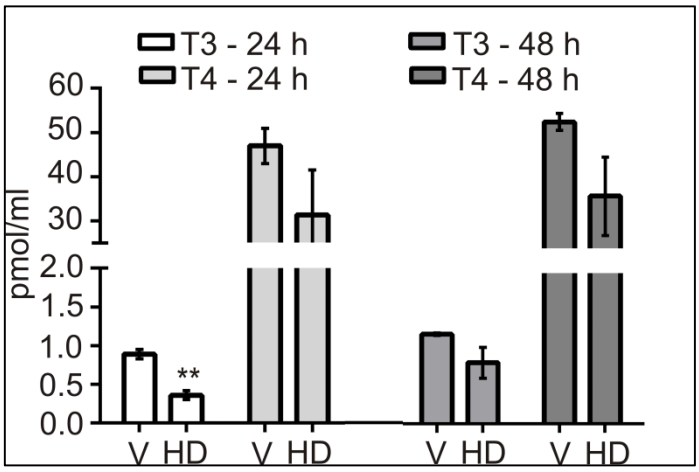

Fig. 4.11. RIAs revealed that T3 and T4 levels within the plasma were reduced following Thioacetamide-induced hepatotoxicity. Thioacetamide; [V] vehicle-only, [HD] high dose. Data represent mean ± SEM. ** $p \leq 0.01$ (T-Test). Thioacetamide-treated rats received 150 mg/kg Thioacetamide or vehicle-only (0.9% saline) treatment and were sacrificed after 24 h or 48 h (n=3). Plasma samples were sent to the Laboratory of Comparative Endocrinology at the Catholic University of Leuven in Belgium for T3 and T4 measurement.

4.5.8 Attempts to induce Dio3/D3 expression in an *in vitro* system were unsuccessful

4.5.8.1 Endogenous levels of Dio3 mRNA and D3 protein were low in three separate rat liver cell lines

As discussed in Chapter 3, it is advantageous to be able to model an *in vivo* system *in vitro*. Endogenous levels of *Dio3* mRNA and D3 protein and were low in three different rat liver cell lines (Fig. 4.12). Although the three cell lines did amplify sufficiently to produce CT values during qRT-PCR (Fig. 4.12 A), these values were very high (between 32 and 37). This is on the threshold of detection using qRT-PCR (Guthrie et al., 2008). There was considerably more endogenous *Dio3* mRNA in the *in vivo* rat liver samples than any of the cell lines. These low endogenous levels of *Dio3* mRNA correlated with low levels of D3 protein, which were also on the threshold of detection, even when three times more protein was loaded (Fig. 4.12 B). Although the RLE cell line appeared to contain more *Dio3* mRNA than the H4IIE cell line (Fig. 4.12 A), there was no visible band on the Western blot, indicating that this cell line contained no endogenous D3 protein (Fig. 4.12 B).

As a reduction in protein level following treatment was the desired outcome the protein had to be present at a sufficient level in the control (vehicle-treated) cells. Thus, it would not be possible to accurately measure a reduction in D3 following drug treatment in any of the three cell lines since the levels of D3 in the vehicle-treated samples were below, or on, the threshold of detection.

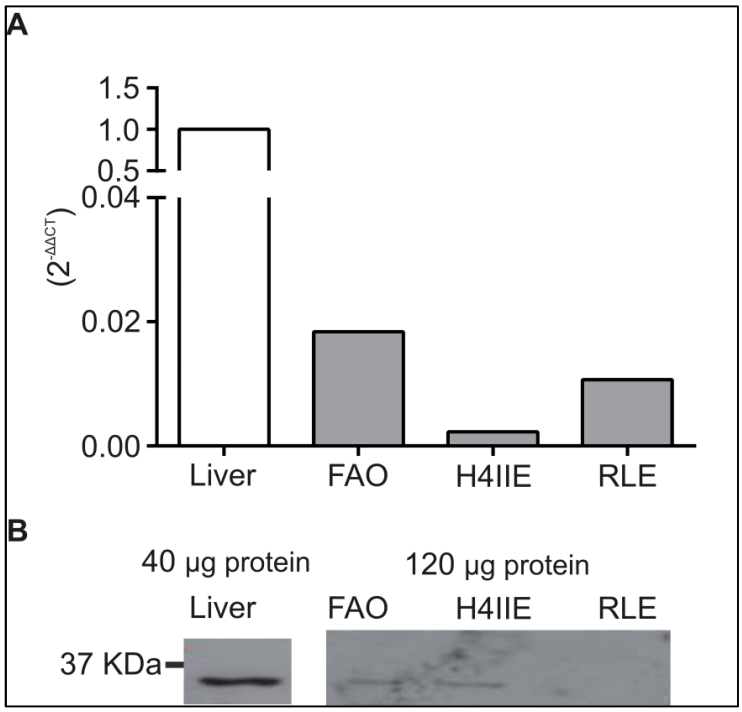

Fig. 4.12. Endogenous levels of *Dio3* mRNA and D3 protein in three independent rat liver cell lines were low. (**A**) qRT-PCR and (**B**) Western blot analysis were used to measure total *Dio3* mRNA and D3 protein levels respectively.

4.5.8.2 Retinoic acid treatment

D3 activity has been reported to increase up to 200-fold in astroglial cells in the presence of retinoic acid (Esfandiari et al., 1994). The fact that the RLE cells were epithelial and expressed no D3 protein, and the FAO cells grew in aggregates, suggested that the most amenable cells for future work were the H4IIE cells. These grew the most rapidly and were the easiest to maintain. Therefore, the H4IIE cells were incubated with increasing concentrations of retinoic acid in an attempt to increase expression of *Dio3*/D3 exogenously. At the mRNA level raw CT values remained high (between 32 and 35), with no statistically significant induction of *Dio3* mRNA (Fig. 4.13 A). Western blot analysis revealed a small concentration-dependent increase in D3 expression (Fig. 4.13 B). However, this was not comparable to the 60% enhancement seen by Esfandiari *et al* in brain cells, nor was it consistent enough for further experiments.

4.5.8.3 EGF and aFGF treatment

An alternative method for increasing activity of D3 is through the use of epidermal growth factor (EGF) and acidic fibroblast growth factor (aFGF) (Hernandez et al., 1998). Hernandez *et* al observed a substantial increase, not only in the activity of D3, but also in the levels of *Dio3* mRNA when culturing rat adipocytes in media containing 10 ng/ml EGF or 4 ng/ml aFGF. This was not replicated in the H4IIE cell line (Fig. 4.13 C & D). A small increase in mRNA levels was observed following treatment with aFGF. This was in agreement with Hernandez *et al*, who also observed that aFGF was the more potent of the growth factors (Hernandez et al., 1998). However, neither growth factor induced a statistically significant increase in *Dio3*/D3 in the H4IIE cells, at either the mRNA or protein level.

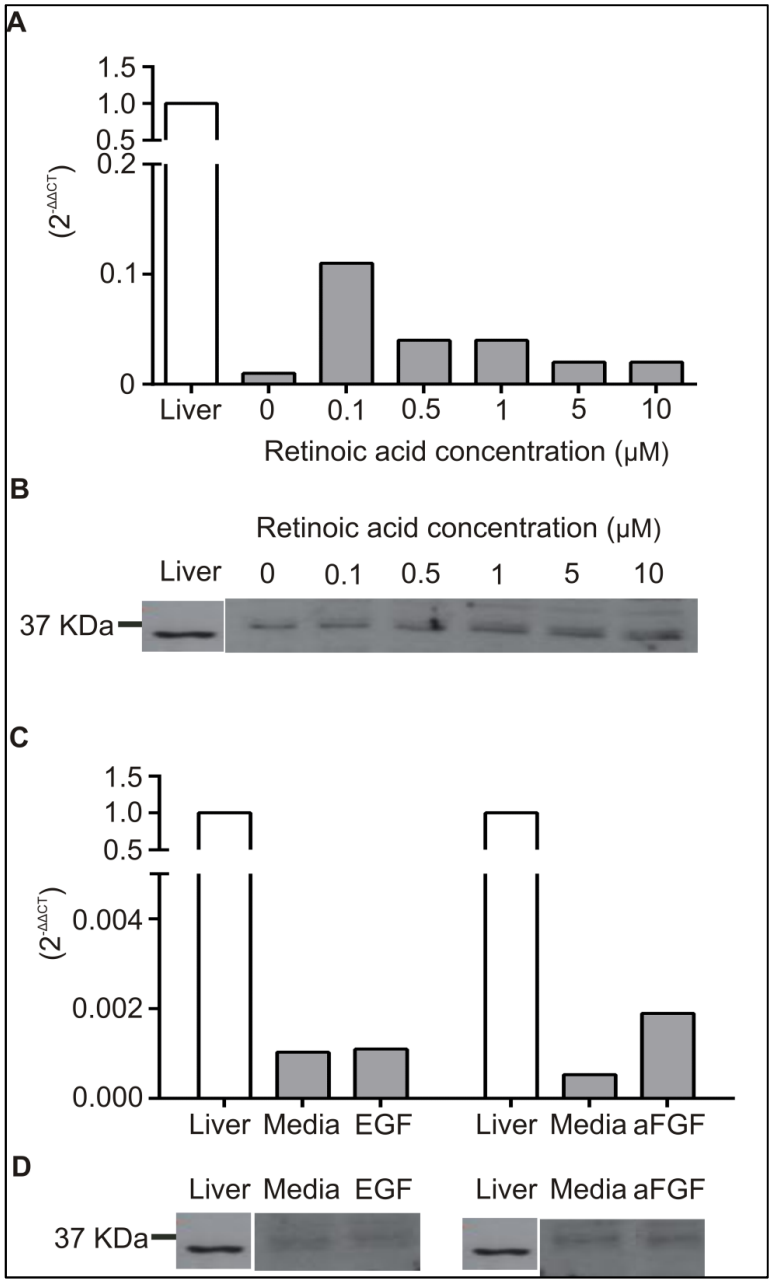

Fig. 4.13. Attempts to induce expression of *Dio3*/D3 in an *in vitro* system were unsuccessful. (**A**) and (**B**) retinoic acid; (**C**) and (**D**) EGF and aFGF. No significant change was seen either at the mRNA level (**A** & **C**) or the protein level (**B** & **D**). Cells were treated with increasing concentrations of retinoic acid in 0.1% DMSO and harvested after 48 h or with 10 ng/ml or 4 ng/ml aFGF and harvested after 9 h.

4.6 DISCUSSION

As described in Chapter 3 the regulation of mRNA translation provides a rapid and efficient means of adapting protein levels to respond to, protect against, and repair the damage caused by cellular stresses, such as liver injury. One of the mRNAs that showed a change in translational activity following compound-induced hepatotoxicity was *Dio3*. Furthermore, this mRNA had a functional role in a number of the deregulated canonical pathways. This chapter explored the regulation and role of *Dio3* in more detail and provides data to support the hypothesis that the translational repression of *Dio3* mRNA is an important mechanism by which D3 protein levels are reduced and the energy equilibrium of the liver is maintained, thus avoiding disruption of the hypothalamic-pituitary-thyroid axis.

Global genomic methods were used to investigate changes in translational activity following treatment with PredTox compound FP014SC (Chapter 3, section 3.5.3). The mRNAs that demonstrated a change were further analysed using Ingenuity pathway analysis. This revealed that *Dio3* might, via the control it exerts over TH levels, help to regulate the TR/RXR activation pathway (Fig. 4.3). There are a number of other RXR-associated metabolic pathways, also highlighted in Fig. 4.3, and thus, it was hypothesised that Dio3 might play a central role in the rapid response of the liver to compound-induced damage. The change in *Dio3* was therefore further validated using qRT-PCR and Western blotting. qRT-PCR confirmed that *Dio3* was less efficiently translated following treatment with FP014SC (Fig. 4.4), and Western blotting verified that this translational repression correlated with a reduction in D3 protein levels (Fig. 4.6).

In addition to further investigating the regulation of *Dio3* following treatment with FP014SC, it was decided to also look at whether this was a common response to compound-induced hepatotoxicity. Thus, D3 levels were analysed following treatment with the other PredTox compounds, plus an additional model system, the Thioacetamide-treated rat. Thioacetamide is most widely used as a model of cirrhosis in the liver following chronic dosing (Laleman et al., 2006; Trotta et al., 2013). It already has a link to TH regulation due to belonging to the family of thioamides, which are used clinically to treat hyperthyroidism (Fumarola et al., 2011; Locke, 1982). Due to its classification as a category 1B carcinogen (EU-GHS/CLP regulation number 1272/2008) Thioacetamide will never be used directly in the clinic. However, the common structure it shares with other thioamides indicates that it would likely have the same effect on TH levels and activity. Clinical chemistry and histopathology revealed that the Thioacetamide-

treated rat was suitable for use as an additional model of compound-induced hepatotoxicity (Fig. 4.5) and would supplement the findings obtained from the PredTox compounds.

Western blot analysis demonstrated that D3 protein was reduced following treatment with Thioacetamide and all of the PredTox compounds (Fig. 4.6), thereby, suggesting a common mechanism in the response of the liver to compound-induced hepatotoxicity. Furthermore, only those PredTox compounds with a severity rating of ++ or higher (Chapter 3, Table 3.2), demonstrated a statistically significant reduction in D3 levels, and the extent of protein reduction was increased with increasing dose and time of exposure (Fig. 4.7). This suggests that D3 levels were reduced in accordance with the extent of liver injury.

Changes in D3 activity have been found to correlate strongly with changes in expression of *Dio3* mRNA (Mori et al., 1995; St Germain et al., 1994). However, as Fig. 4.8 shows, the change in protein production observed here was independent of changes in mRNA level. In fact, the levels of *Dio3* mRNA were increased following high dose treatment with three of the compounds (Fig. 4.8 A-C). Such increases in *Dio3* mRNA have been reported following enhanced cellular proliferation (Kester et al., 2009; Peeters et al., 2003; Wassen et al., 2002). Cellular proliferation is particularly high in the developing foetus (Bates et al., 1999) and in the adult at times of cellular stress, for example during critical illness (Peeters et al., 2003). As already stated, the liver injury induced by Thioacetamide and the PredTox compounds was acute and the histopathology indicated signs of regeneration (Fig. 4.5, Table 3.2 (Chapter 3) and (Matheis et al., 2011a)). Therefore, increased cellular proliferation was likely, and may account for the observed increase in *Dio3* mRNA expression following high dose treatment with FP004BA, FP007SE and Thioacetamide. However, despite this increase in *Dio3* mRNA there remained a significant reduction in D3 protein (Fig. 4.6), indicating that very little of the message was being converted to protein and thus, the changes in D3 were not regulated at the transcriptional level.

The mRNA levels of *Dio2* and *Dio1* were also measured using qRT-PCR (Fig. 4.8). *Dio2* mRNA levels were very low following treatment with all of the compounds, as indicated by high CT values. This correlates well with the literature, which indicates very limited *Dio2* mRNA expression in the liver (Bates et al., 1999; Bianco et al., 2002; Croteau et al., 1996). In contrast, levels of *Dio1* mRNA were detectable. The down-regulation of *Dio1* mRNA can act as a marker of hypothyroidism (Paquette et al., 2011) and, as already discussed, treatment with Thioacetamide is likely to induce a hypothyroid state due to its pharmacological structure as a thioamide. Thioacetamide-treatment did indeed cause a reduction in *Dio1* mRNA levels, as did

treatment with two of the PredTox compounds (FP007SE and FP004BA), suggesting a common hypothyroid state (Fig. 4.8). There are examples in the literature of a link between hypothyroidism and reduced activity of D3 in the rat liver (Escobar-Morreale et al., 1997; Kaplan and Yaskoski, 1980; Mori et al., 1995). This provides evidence that the compound-induced hepatotoxicity observed following treatment with Thioacetamide and the PredTox compounds caused not only a reduction in D3 levels, but also a hypothyroid liver. Interestingly, treatment with FP014SC caused quite a different expression pattern of the *Dio* mRNAs, particularly *Dio1* and *Dio3* (Fig. 4.8 D). The reason for this is unclear, particularly as cellular regeneration was evident and reported in the summary reports (Suter et al., 2011). Perhaps because FP014SC was the most severe of the hepatotoxins investigated, alternative regulatory pathways and mechanisms were also involved and these were affecting mRNA expression.

Since the changes in D3 were independent of *Dio3* mRNA transcription, the efficiency of *Dio3* mRNA translation was investigated. The polysome profiling, described in Chapter 3, section 3.4.5 had already revealed that *Dio3* mRNA moved from the heavy polysomes towards the light polysomes and monosomes following treatment with FP014SC. This movement was verified using both qRT-PCR (Fig. 4.4) and Northern blotting techniques (Fig. 4.9). Furthermore, using Northern blotting and micro dot blotting, a similar movement of *Dio3* mRNA from the heavy polysomes towards the monosomes was observed following treatment with Thioacetamide and two additional PredTox compounds (FP007SE and FP004BA) (Fig. 4.9). This was indicative of a conserved reduction in translational efficiency following treatment with a range of hepatotoxic compounds. Although a role for increased protein degradation cannot be ruled out, the data presented here across multiple models of hepatotoxicity showing reduced ribosomal association of *Dio3* mRNA, provides strong evidence for translational repression being the predominant mechanism leading to the reduction in D3 protein. In cases where *Dio3* transcription was significantly up-regulated (FP007SE and FP004BA, Fig. 4.8) protein degradation may have contributed to the reduced D3 protein.

It is well established that another of the deiodinases, *Dio2,* is regulated at levels distinct from transcription and that these alter the levels of D2 expression independently of changes at the mRNA level (Arrojo and Bianco, 2011; Bianco and Kim, 2006; Leonard et al., 1990; Steinsapir et al., 2000; Steinsapir et al., 1998). The change in D2 is often greater than the change in *Dio2* mRNA; for example, in brown adipose tissue following cold exposure (Curcio-Morelli et al., 2003) and the brain following experimentally-induced hypo- and hyper-thyroidism (Fekete et al., 2007). This is essential to maintain homeostasis of the THs. Certainly, in cases of ER stress, D2 activity is reduced independently of transcriptional changes and this leads to a rapid, but

significant decrease in the levels of T3 (Arrojo and Bianco, 2011). However, within the rat and human liver *Dio2* and D2 are only very weakly expressed (Fig. 4.8 and (Bianco et al., 2002)). Consequently, an alternative method of regulation is required. It is therefore hypothesised that, following hepatotoxicity, D3 is recruited to maintain TH homeostasis in the liver. D3 functions primarily by inactivating T3 and T4 through conversion of each to its inactive metabolite, reverse T3 and 3,3'-diiodothyronine (rT3 and T2), respectively (Bianco et al., 2002). As an inactivating enzyme, D3 primarily protects tissues from an excess of TH. If this mechanism is disrupted in some way, severe hypothyroidism or hyperthyroidism can occur (Huang et al., 2000; Mori et al., 1995; Paquette et al., 2011).

Due to the control D3 has over the levels of THs, T3 and T4 were measured in the livers of animals treated with Thioacetamide, FP007SE, FP004BA or FP014SC. The levels of T3 and T4 were both reduced with high dose treatment (Fig. 4.10). Treatment with Thioacetamide caused a larger change in T3 than T4, a finding replicated in the literature (Bianco et al., 2002). However, 48 h after treatment, levels of T3 were closer to the control levels than T4, indicating that T4 had a longer lasting effect. Support for this came from the measurement of TH levels in the livers of the PredTox animals. Following high dose treatment with FP004BA or FP014SC for 15 days the change in levels of T4 were significant and larger than the change in levels of T3, which was perhaps reflective of the two week study design implemented with the PredTox compounds.

Although the levels of T3 and T4 within tissues are largely independent of those seen in the plasma and the expression of the deiodinases is generally under localised regulation (Bianco, 2011), the activity rate of the three deiodinases can directly affect the levels of circulating T3 and T4 (Dentice and Salvatore, 2011). Limited sample availability from the PredTox consortium meant that TH levels in the plasma of these animals could not be measured; however, measurements were taken using the plasma from the Thioacetamide-treated rats. The change in the levels of THs in the plasma were very similar to the changes observed in the liver samples (Fig. 4.11), whereby the initial reduction in T3 was larger than the reduction in T4, but after 48 h T4 levels showed less evidence of returning to normal. One explanation for this is that T4 has a longer half life in the plasma than T3 and therefore, the concentration of this enzyme within the systemic circulation usually remains relatively stable (Bianco et al., 2002).

An interaction between the levels of TH in the liver and the plasma enables the feedback loop between the systemic organs and the thyroid gland to be maintained and has been experimentally validated in the case of D2 (Arrojo and Bianco, 2011). D3 is located within the

plasma membrane, with the majority of it being extracellular (Baqui et al., 2003). This gives it ready access to, and control over, the levels of circulating THs. It is possible that, because the liver is in rapid equilibrium with the plasma, D3 detects a change in THs and acts rapidly to prevent the further production of inactive metabolites. This is achieved by rapidly reducing the levels of D3 protein, meaning less rT3 and T2 are produced and the levels of T3 and T4 are restored to normal. This process is summarised in Fig. 4.14 and is likely to be vital for maintaining the hypothalamic-pituitary-thyroid axis, allowing all control to be carried out at the local level, in concordance with the current literature (Gereben et al., 2008).

The work presented in this chapter demonstrates that the TH pathway is perturbed by compound-induced hepatotoxicity. It is hypothesised that part of the reason for this perturbation is the inflammatory and regeneration response within the liver following cell damage. The requirement for increased energy for cellular proliferation is achieved through a rapid decrease in *Dio3* mRNA translation and consequent reduction in the level of D3 protein. By targeting *Dio3* translationally the levels of THs can rapidly return to normal and the TR/RXR pathway can be efficiently maintained. With clinical signs of regeneration (histopathology and ALT/AST levels) the levels of D3 were further reduced (Fig. 4.7). It is proposed that this enables the liver to expend substantial energy into tissue repair, maintaining overall homeostasis of the hypothalamic-pituitary-thyroid axis.

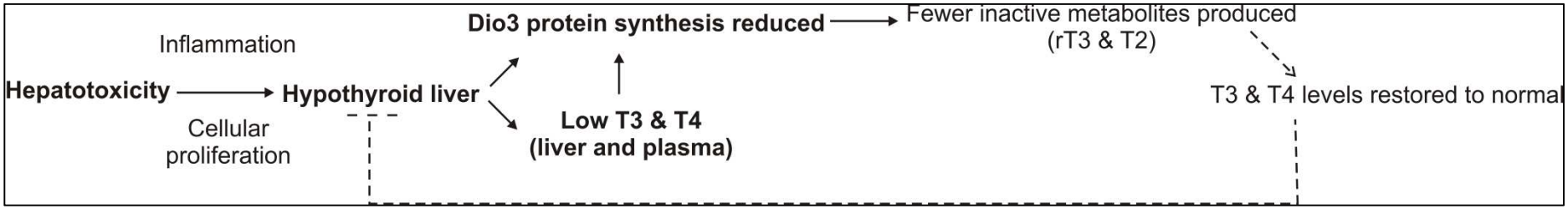

Fig. 4.14. Proposed mechanism of action following compound-induced hepatotoxicity. During hepatotoxicity the liver is in a hypothyroid state and both the plasma and liver have reduced levels of T3 and T4. Consequently, the expression of Dio3 protein is reduced so that fewer of the inactive metabolites of T3 and T4 are produced and levels of both can return to normal, both locally (liver) and systemically (via plasma signals). Steps in bold type are those experimentally demonstrated in the course of this study. Standard type is used for the hypothesised mechanism of action and closure of the feedback loop.

The generation of a suitable *in vitro* model for exploring the proposed mechanism in more detail would have been of great value. Unfortunately, the rat liver cell lines available did not endogenously express D3 (Fig. 4.12) and attempts to induce expression failed (Fig. 4.13), even when using methods that were successful in the literature (Esfandiari et al., 1994; Hernandez et al., 1998). The difficulties in inducing expression of *Dio3*/D3 in cells may have been cell-type specific. Esfandiari *et al* report that there is a wide difference in potency between cell types (Esfandiari et al., 1994). There are no published papers on the induction of *Dio3* in liver cells; therefore, the methods attempted here were those that, whilst successful in previous work, had been optimised for entirely different cell types. No further work was undertaken on attempting to induce the expression of *Dio3*/D3 because the more interventions that were made prior to treating the cells with the compounds of actual interest, the more artificial the situation and the greater the possibility of secondary molecular effects. For example, EGF can directly cause cellular proliferation (Llorens et al., 2013), which might potentially mask the cellular proliferation observed during compound-induced hepatotoxicity. In terms of future work, the use of primary hepatocytes could be considered. These might function as a better model for what is happening in a dynamic, *in vivo* situation.

4.7 CONCLUSION

The reduction in D3 expression levels during hepatotoxicity correlated with a decrease in *Dio3* mRNA translation, but remained independent of mRNA levels. It is hypothesised that this is an example of dynamic translational control, enabling the liver to respond rapidly to compound-induced damage. The magnitude of the decrease in D3 was directly proportional to the extent of liver damage. It is likely that with more damage, there will be a higher energy demand placed on the liver for active repair processes to be initiated. TH homeostasis has already been shown to play a role in a range of pathophysiological conditions and the data presented here suggests that the TH pathway is also perturbed during compound-induced hepatotoxicity, possibly as a result of increased energy usage during the liver's response to cellular injury. By rapidly responding to the injury caused by Thioacetamide and the PredTox compounds (through the dynamic reduction of D3 levels and restoration of TH homeostasis), the liver prevents damage spreading to the entire hypothalamus-pituitary-thyroid axis. What began as an adverse localised event remains confined to the liver and further protective mechanisms are not required.

Despite it being over 15 years since *Dio3* was first cloned (Croteau et al., 1995), the regulation of the gene is complex and not yet fully understood. Many translational changes are regulated by miRNAs (Bartel, 2004), therefore, Chapter 5 investigates whether *Dio3* is an example of a mRNA whose translational regulation is miRNA-mediated and whether miRNAs in general are involved in compound-induced hepatotoxicity.

CHAPTER 5: miRNA PROFILING OF LIVER SAMPLES FOLLOWING COMPOUND-INDUCED HEPATOTOXICITY

5.1 SUMMARY

Chapter 4 showed that the mRNA *Dio3* was translationally repressed across two model systems of compound-induced hepatotoxicity (PredTox and Thioacetamide), and that this repression led to a large reduction in D3 protein. miRNAs have been identified as translational regulators, therefore, the work presented in the first part of this chapter investigated whether the translational repression of *Dio3* might be miRNA-mediated. None of the miRNAs predicted to target *Dio3* mRNA showed a significant corresponding increase in expression, suggesting that they did not regulate *Dio3* in these models. Thus, analysis was extended to explore global miRNA expression profiles of the PredTox, Thioacetamide and Griseofulvin models of hepatotoxicity. This demonstrated that, whilst they may not have been involved in mediating *Dio3* expression, miRNAs did appear to mediate large networks important in the cellular response to compound-induced liver injury. By correlating miRNA and translational profiling data sets from the same models, it was possible to identify specific functionally-relevant miRNA-mRNA interactions within individual models.

5.2 INTRODUCTION

Having established that *Dio3* demonstrated translational regulation in cases of compound-induced hepatotoxicity, the mechanism of this regulation was considered in more detail. Between 30% and 60% of all human mRNAs are thought to be subject to miRNA-mediated control (Carthew, 2006; Filipowicz et al., 2008; Huntzinger and Izaurralde, 2011). miRNAs post-transcriptionally regulate mRNA expression by base pairing to a target mRNA and causing reduced protein synthesis, via either target degradation or translational repression. As the change in *Dio3* translational activity correlated with a reduction in overall protein levels, it was hypothesised that *Dio3* mRNA might undergo miRNA-mediated regulation.

5.2.1 miRNAs

miRNAs are a family of endogenous small non-coding RNAs, first characterised in *C. elegans* in 1993 (Lee et al., 1993; Wightman et al., 1993). Although known not to directly encode proteins themselves, interest has grown in these small RNA species due to the control they exert over protein coding genes and, as a result, their role in all areas of cellular activity; including cancer differentiation, proliferation, apoptosis and tumourigenesis (Ambros, 2004; Iorio and Croce, 2009). The high conservation of miRNA sequences between species (Wang, 2013) is further

motive for the vast interest in, and large number of publications on, the structure, role and function of these RNA species. The importance of miRNAs has been highlighted by the fact that in certain cases of cellular stress there is a co-ordinated response between transcription factors, miRNAs and mRNA targets, which has been shown to precede a phenotypic outcome (Ferland-McCollough et al., 2012).

The biosynthesis of miRNAs and the proposed mechanisms of miRNA-mediated regulation are discussed in Chapter 1, sections 1.3.2.2.1 and 1.3.2.2.2.

5.2.2 Target prediction

A number of computer algorithms have been developed to help identify potential miRNA-mRNA interactions. These include, but are not limited to, Target Scan (Lewis et al., 2005), miRDB (Wang, 2008; Wang and El Naqa, 2008) and miRanda (Betel et al., 2008). There are additional databases that store validated interactions and cross reference other available algorithms to provide more extensive coverage. For example, both validated miRNA targets and targets predicted by up to 8 different algorithms can be downloaded from the miRWalk database (Dweep et al., 2011). The complexities of miRNA-mediated regulation (described in Chapter 1, section 1.3.2.2.2), make identification of putative targets a challenging process and only a limited number of target sites have been experimentally verified (Orom and Lund, 2010). In addition, many computer algorithms make assumptions that are not always true; for example, limiting the search for sequence complementarity to the 3' UTR region of the mRNA (Ambros, 2004). As discussed in Chapter 1, section 1.3.2.2.2 some miRNAs interact with their target mRNA by binding to the 5' region (Da Sacco and Masotti, 2012). Therefore, identifying all genuine interactions is a challenging process, best tackled through a combinatorial approach of miRNA profiling and bioinformatic target prediction, alongside mRNA and proteomic analysis (Gunaratne et al., 2010; Lim et al., 2005).

5.2.3 miRNAs and hepatotoxicity

It has already been demonstrated that miRNAs are involved in toxicology (Lema and Cunningham, 2010) and liver disease (Chen, 2009). They are recruited following toxic exposure to the liver (Koufaris et al., 2012; Pogribny et al., 2007; Zhang and Pan, 2009), and have been shown to mediate apoptotic and necrotic cell death following liver damage (Guicciardi et al., 2013). This suggests that miRNAs have a physiologically relevant, functional role in the response to compound-induced hepatotoxicity.

Thus, in addition to identifying putative miRNAs targeting *Dio3* mRNA, global miRNA profiling was performed on all of the models of compound-induced hepatotoxicity used throughout this thesis. Of particular interest were those miRNAs demonstrating a change across the different models or species and those that targeted any of the mRNAs previously shown to be translationally regulated (Chapter 3). The identification and validation of miRNA-mRNA interactions would indicate physiologically relevant responses to compound-induced hepatotoxicity.

5.3 AIM

To identify and analyse the expression of putative miRNAs that might regulate the translational repression of *Dio3* mRNA and to profile global miRNA expression in independent models of compound-induced hepatotoxicity in order to investigate the wider role of miRNAs in liver toxicity.

5.4 MATERIALS AND METHODS

5.4.1 Animal models

The animal models used for the work described in this chapter were the Griseofulvin-treated mice, the Thioacetamide-treated rats and the PredTox compound-treated rats.

Animals were maintained and treated as described in Chapter 2, section 2.1.1, 2.1.2 and 2.1.3.

5.4.2 RNA extraction and quantification

RNA was extracted and quantified as described in Chapter 2, section 2.3.1, 2.3.3 and 2.3.4.

5.4.3 Target site prediction

The databases TargetScan (http://www.targetscan.org/) and miRDB (http://mirdb.org/miRDB/) were used to identify putative binding sites within *Dio3* mRNA and putative mRNA targets of all the differentially regulated miRNAs following treatment with FP014SC. TargetScan works by identifying conserved 7mer and 8mer binding sites which are complementary to the seed region of a particular miRNA (Lewis et al., 2005). It is one of the most widely cited computer algorithms used to identify putative targets. miRDB was used primarily because it was one of the few available algorithms to offer coverage of the rat when this work was first performed. miRDB uses a support vector machine to identify a target prediction score (Wang, 2008; Wang and El Naqa, 2008). The miRDB algorithm utilises a large number of publically available high-throughput datasets to generate the prediction score; the higher the score, the more likely the interaction is genuine.

A further target prediction algorithm, PITA (http://genie.weizmann.ac.il/pubs/mir07/mir07_dyn_data.html), was applied alongside TargetScan to identify putative mRNA targets of all the differentially expressed miRNAs following treatment with Griseofulvin. PITA is an algorithm that maps miRNA-mRNA target interactions according to the accessibility of the target site (Kertesz et al., 2007), generating a ΔΔG score. The ΔΔG score is an energetic measure of the likely interaction; the more negative the score the stronger the binding between miRNA and target is likely to be.

5.4.4 Quantitative RT-PCR

RNA samples that were of sufficient quality as determined using the Bioanalyser (RIN score ≥ 8) were used in combination with specific Taqman assays (Life Technologies, Paisley, UK) to measure changes in expression of individual miRNAs. The chemistry behind the Taqman

assays is depicted in Fig. 5.1. Protocols were performed according to the manufacturer's instructions.

5.4.4.1 Reverse transcription

Briefly, 500 ng of RNA was reverse transcribed in a reaction comprising of 1.5 µl 10X buffer, 0.15 µl dNTPs, 1 µl reverse transcriptase, 0.19 µl RNase inhibitor and 2 µl miRNA-specific stem-loop primer. Reactions were multiplexed as required, with up to three different miRNAs added to each reverse transcription reaction. Negative controls in which the reverse transcriptase was replaced with 1 µl ultra pure (18 MΩ water) were set up alongside. Any amplification from these negative controls would indicate genomic DNA contamination as no reverse transcription should take place. Reactions were mixed and incubated at 16°C for 30 min, 42°C for 30 min and 85°C for 5 min (denaturation), followed by a hold at 4°C for at least 2 min. cDNA was stored at -20°C until required.

5.4.4.2 PCR

2 µl of cDNA was added to a PCR master mix containing 10 µl 2X Taqman Universal PCR Master Mix with No AmpErase UNG and 1 µl of each relevant miRNA primer in a 96-well optical MicroAmp® Reaction Plate (Life Technologies, Paisley, UK). The Taqman Universal PCR Master Mix is a proprietary all-in-one reagent comprised of a Taqman probe, a blend of dNTPS with dUTP, AmpliTaq Gold® DNA polymerase and a passive reference dye (ROX™), to minimise non-specific fluctuations in fluorescence. Negative controls contained 1 µl of the negative control reverse transcription reactions (-RT), and non-template controls (NTCs) contained 1 µ water in the place of cDNA. Each 20 µl reaction was prepared in triplicate. Plates were centrifuged (453g, RT, 5 min) and loaded into an Applied Biosystems® 7500 Fast Real-Time PCR system (Life Technologies, Paisley, UK). The PCR protocol began with activation of the Taq polymerase (95°C for 10 min), followed by 40 cycles of denaturing (95°C, 15 s) and annealing/extending (60°C, 1 min).

5.4.4.3 Data analysis

Provided there was no amplification in the –RT and NTC controls, the raw cycle threshold (CT) values were extracted and the $2^{-\Delta\Delta CT}$ method (Chapter 2, Fig. 2.6) was used to determine whether there were any changes in relative expression between samples. U6 snRNA or snoRNA-202 were used as endogenous controls. Statistically significant differences were calculated using a two-tailed Student's T-Test or an ANOVA with Tukey's multiple comparison post hoc test.

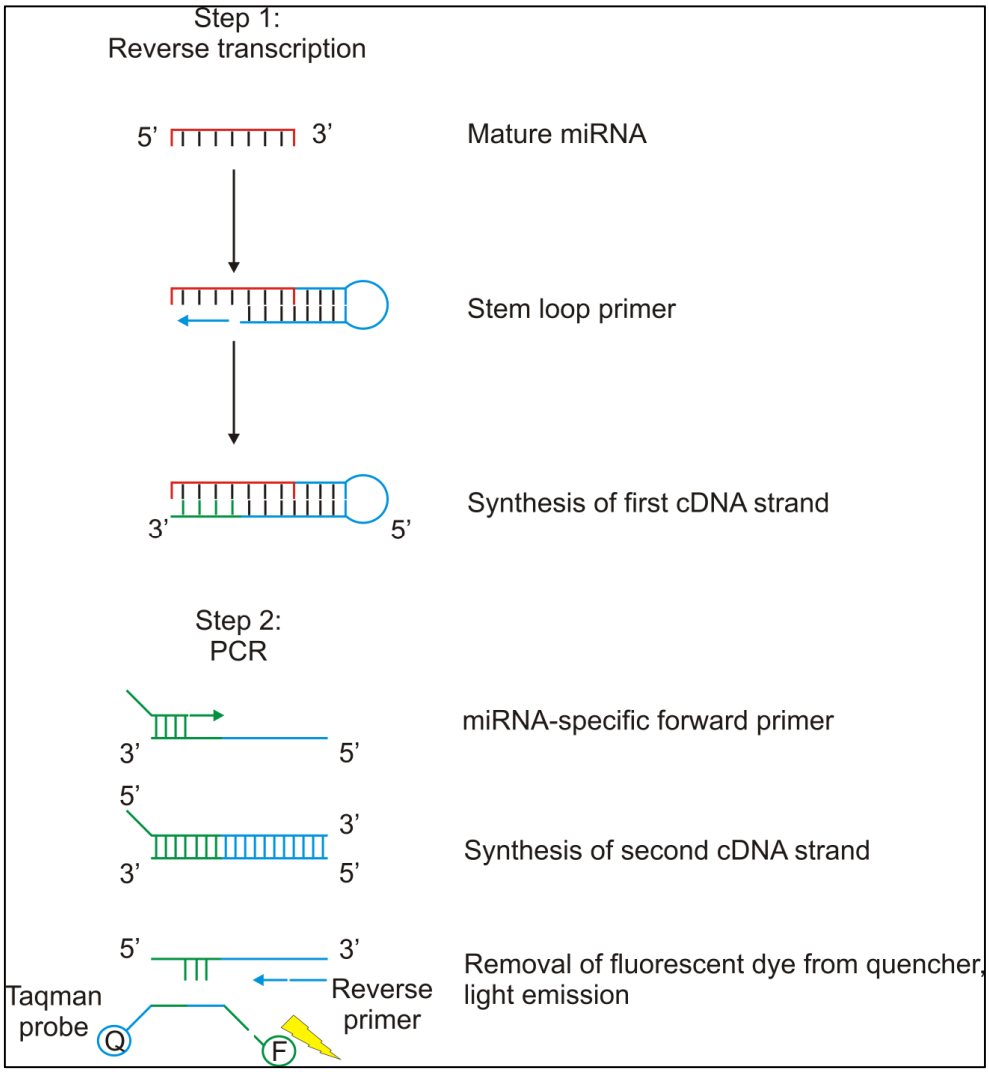

Fig. 5.1. Schematic representation of the two stages of Taqman miRNA qRT-PCR profiling. Step 1: Reverse transcription proceeds through the recruitment of stem-loop miRNA primers specific to the 3' end of the miRNA. Step 2: During PCR, a miRNA-specific forward primer and a reverse primer are recruited. The Taqman probe is hydrolysed and fluorescent dye (FAM) is released from the quencher. This enables light to be emitted, generating the signal used to calculate the cycle threshold (CT) for each reaction.

5.4.5 miRNA profiling using microarrays

5.4.5.1 Labelling

RNA samples that were of sufficient quality as determined using the Bioanalyser (RIN score ≥ 8) were labelled using an NCode™ Rapid miRNA labelling system kit (Life Technologies, Paisley, UK) according to the manufacturer's instructions. Briefly, 1.5 µg of each RNA sample (in 5 µl ultra pure (18 MΩ) water) was poly A tailed in a reaction comprising of 0.75 µl 10X reaction buffer, 0.75 µl 25 mM $MnCl_2$, 0.5 µl ATP (diluted 1 in 500 with ultra pure (18 MΩ) water), and 0.5 µl poly A polymerase. Following incubation at 37°C for 15 min, the tailed RNA was ligated to a fluorophore (alexa-555 or alexa-647) by addition of 2 µl alexa-555/647 and 1 µl T4 DNA ligase. The recommended incubation for ligation was at RT for 30 min, however, better results were obtained by performing this incubation at 16°C. The reaction was terminated by the addition of 1.25 µl stop solution. All labelling reactions were performed in duplicate, incorporating a dye swap technique for n ≥ 3 pairs of samples.

5.4.5.2 Hybridisation and scanning

Control (alexa-555 labelled) and test (alexa-647 labelled) RNA samples were pooled and 26 µl 2X Enhanced hybridisation buffer and 2.5 µl BSA were added. Samples were denatured at 65°C for 10 min prior to loading onto a miRNA microarray, containing miRCURY LNA™ probes (Exiqon, Vedbaek, Denmark). Microarray design and printing is described in Chapter 2, section 2.6. Hybridisation was performed at 52°C overnight (for a minimum of 16 h).

Following hybridisation slides were washed in solutions of increasing stringency (wash 1: 2X SSC, 0.2% SDS, wash 2: 2X SSC, wash 3: 0.2X SSC) for 2 min each, dried by centrifugation (200g, RT, 4 min) and scanned on a 4200A Axon scanner (Molecular Devices, Sunnyvale, CA).

5.4.5.3 Data analysis

The scanned microarray images were analysed with GenePix pro 6.0 to generate raw data files, which were normalised using Lowess and tested for statistical significance using a reverse labelled t-Test as previously described (Zhang and Gant, 2004). miRNAs that had a p value < 0.05 and a fold change > 1.5 were considered to be both statistically and biologically significant.

5.4.5.4 Regulatory pathway analysis

Lists of validated target mRNAs were generated using the miRWalk database. These lists were filtered to remove replicates and analysed using Ingenuity IPA software (Ingenuity® Systems, www.ingenuity.com) to identify miRNA-mediated pathways involved in compound-induced hepatotoxicity.

5.4.5.5 Identification of functionally relevant miRNA-mRNA interactions

TargetScan and miRDB were used to identify putative target mRNAs for all miRNAs that demonstrated differential expression following treatment with FP014SC for 15 days. These targets were then mapped to the list of mRNAs found in Chapter 3 to be altered at the translational and/or transcriptional level following the same treatment (section 3.5.4.1) to identify putative functionally relevant miRNA-mRNA interactions. Since the miRNA target prediction algorithms focus on the 3' UTR binding sites, and miRNAs predominantly repress translation when bound to the 3' UTR of their target mRNAs, results were limited to miRNAs and mRNAs that showed opposing changes in expression.

The same mapping process was used to identify miRNA-mRNA interactions following treatment with Griseofulvin for 22 days. In this instance, PITA and TargetScan were used to identify putative mRNA targets for all of the differentially expressed miRNAs.

5.4.6 Cell culture

Hepa 1-6 cells were grown and maintained as described in Chapter 2, section 2.2. The cells were treated with Griseofulvin at 2 doses (5 µM and 10 µM) as described in Chapter 3, section 3.4.2.3.

5.5 RESULTS

5.5.1 Identification of miRNAs predicted to target *Dio3* mRNA

TargetScan and miRDB were used to identify miRNAs predicted to target *Dio3* mRNA. Two of the miRNAs identified for further investigation (miR-214 and miR-761) had conserved binding sites within TargetScan and were identified by both algorithms. Two further miRNAs (miR-336 and miR-192*) had a high target prediction score in miRDB and were already demonstrated to have a role in liver cancer and/or cellular proliferation (Song et al., 2008; Sukata et al., 2011). The predicted binding sites for each of these miRNAs are shown in Fig. 5.2.

5.5.2 Changes in levels of miRNAs predicted to target *Dio3* mRNA following treatment with FP014SC or Thioacetamide

It was hypothesised that any miRNA regulating the translational repression of *Dio3* mRNA would show an inverse increase in expression. FP014SC treatment induced the largest change in D3 protein, with levels reduced to 14% of those seen in the vehicle-treated controls. Whilst the change in D3 following Thioacetamide treatment was not as pronounced (levels were reduced to 40% of the equivalent controls), it was significant and reproducible, and furthermore, this model system was more adaptable to manipulation. Thus, qRT-PCR was performed following high dose treatment on samples taken from animals treated with the highest dose of FP014SC or Thioacetamide. miR-214 showed a small increase in the two models, with a greater up-regulation at the earlier time points, however, this change did not reach statistical significance (Fig. 5.3 A). In general miR-336 and miR-192* were down-regulated in both models; with miR-336 reaching significance 48 h after treatment with Thioacetamide, and miR-192* showing a time-dependent reduction, achieving significance after 15 days treatment with FP014SC (Fig. 5.3 B & C). Finally, the expression of miR-761 was variable across the two models, but no statistical significance was reached and the CT values were between 33 and 35 and, thus, on the upper limit of detection (Guthrie et al., 2008) (Fig. 5.3 D).

***Dio3* (537-543)**	5' … G C U C A C G U G G U G C U C **C U G C U G A** U …
	I I I I I I
rno-miR-214	3' … G A C G G A C A G A C A C G **G A C G A C** A …

***Dio3* (537-543)**	5' … G C U C A C G U G G U G C U C **C U G C U G A** U …
	I I I I I I
rno-miR-761	3' … A C A C A G U C A A A G U G G **G A C G A C** A …

***Dio3* (484-490)**	5’ … G A G G G G C T C A A G A T A **A A G G G T G** G …
	I I I I I I I
rno-miR-336	3’ … U C U G A U C U A U A C C **U U C C C A C** U …

***Dio3* (221-227)**	5’ … A T T G C T G T G G C T C G A **A C T G G C A** A …
	I I I I I I I
rno-miR-192*	3‘ … G A C A C U G G A U A C C U **U G A C C G U** C …

Fig. 5.2. Predicted binding sites for miRNAs within the *Dio3* mRNA 3’ UTR. Targetscan and miRDB were used to identify miRNAs predicted to target *Dio3* mRNA. The predicted binding sites for each of the four miRNAs selected for further investigation are highlighted in red.

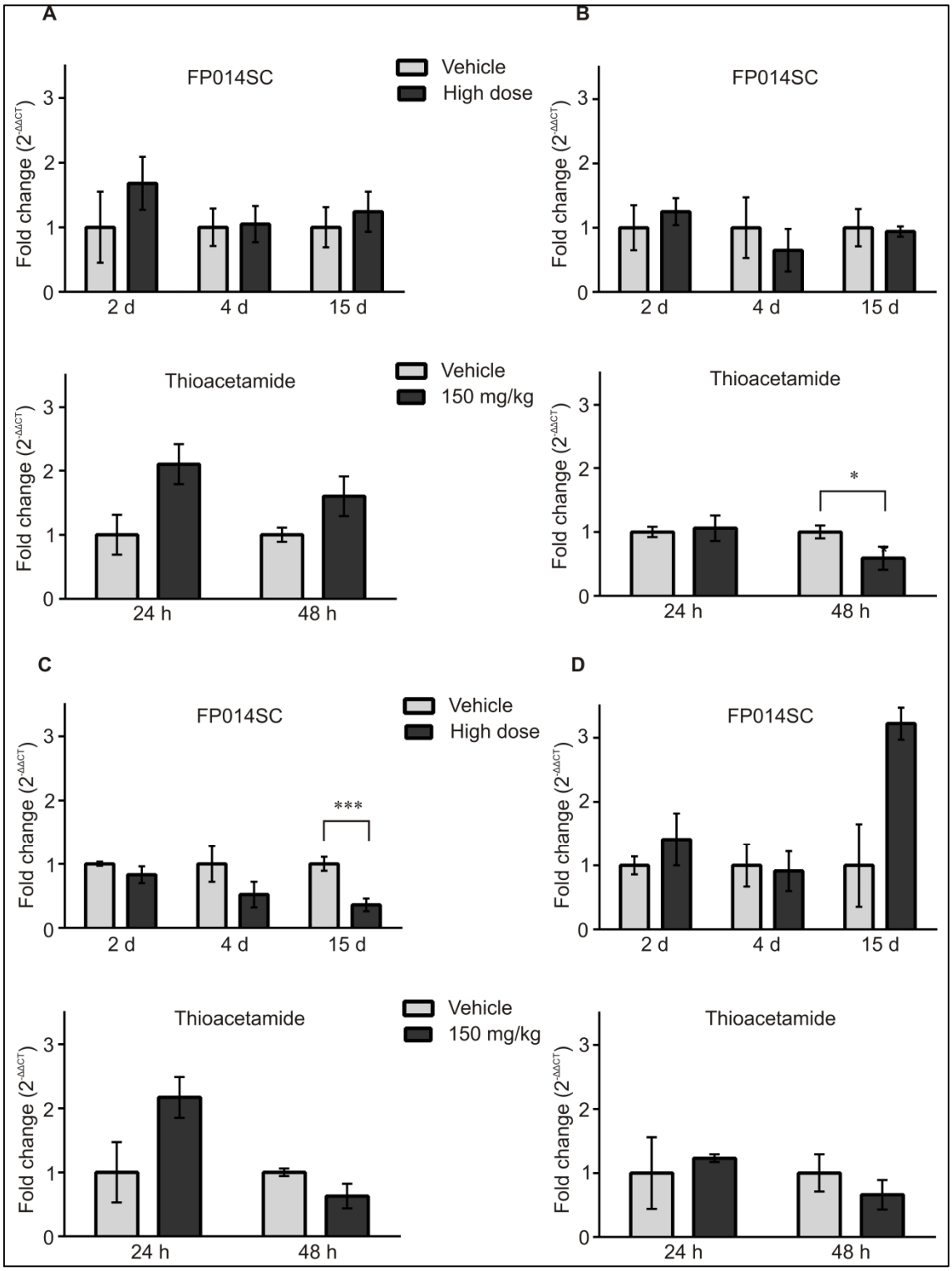

Fig. 5.3. qRT-PCR revealed some changes in the expression of miRNAs predicted to target *Dio3* mRNA. (**A**) miR-214, (**B**) miR-336, (**C**) miR-192* and (**D**) miR-761. qRT-PCR data were normalised to U6 snRNA and represent mean ± SEM. * $p \leq 0.05$, *** $p \leq 0.001$ (T-test). FP014SC-treated rats received high dose FP014SC or vehicle-only treatment for up to 15 days (n≥3 for all doses/time points). Thioacetamide-treated rats received 150 mg/kg Thioacetamide or vehicle-only (0.9% saline) treatment and were sacrificed after 24 h or 48 h (n=3 for all treatments/doses).

5.5.3 miRNA profiling

Global hepatic miRNA levels were measured across the different model systems using microarray profiling.

5.5.3.1 PredTox model

Following high dose treatment for 15 days, 68 miRNAs were significantly differentially expressed ($p \leq 0.05$, fold change ≥ 1.5) in one or more of the studies (Table 5.1). There were no large significant miRNA changes across all five studies. However, miR-292-5p_MM1 demonstrated a significant increase in expression in 3 of the studies (FP005ME, FP013NO and FP014SC).

5.5.3.2 Thioacetamide model

Following treatment with Thioacetamide, 76 miRNAs were significantly differentially expressed ($p \leq 0.05$, fold change ≥ 1.5) (Table 5.2) at one or more dose or time point. There were a number of miRNAs that demonstrated a dose-response, one example being miR-92b; 24 h after dosing this miRNA was significantly up-regulated at each dose and this change increased with higher dose, until it reached a plateau at the highest dose. 8 miRNAs were differentially expressed at both time points (miR-100, miR-216a, miR-3546, miR-3573-3p, miR-3596c, miR-484, miR-664-1* and miR-664-2*). Of these, miR-216a was of particular interest because it showed a dose-response both 24 and 48 h after treatment with Thioacetamide. The maximum fold change was slightly reduced across the doses at the 48 h time point compared to the 24 h.

5.5.3.3 Griseofulvin model

Following treatment with Griseofulvin for 5 days or 22 days, 54 miRNAs were significantly differentially expressed ($p \leq 0.05$, fold change ≥ 1.5) (Table 5.3) at one or both of the time points. Of these miRNAs, 10 showed significant differential expression in a time-related manner; 5 (miR-195, miR-381, miR-27a, miR-7a and miR-193*) were significantly up-regulated over time, and 5 (miR-214, miR-27b*, miR107, miR-146a and miR-215) were significantly down-regulated over time.

Table 5.1. Significant miRNA changes in the livers of rats treated with the PredTox compounds.

Name	ID	PredTox study name					Fold change
		FP004BA	FP005ME	FP007SE	FP013NO	FP014SC	
rno-miR-292-5p_MM1	11086	0.25	**0.78**		**0.98**	**2.08**	4.69
rno-miR-330*	11228	0.08	**0.55**		0.18	0.13	1.00
rno-miR-483_MM1	13180	0.30	0.40	**0.42**	-0.12	**0.91**	0.47
rno-miR-299	11038	**0.29**	**0.40**	-0.05	0.21	**1.00**	
rno-miR-500	11132	0.13	0.36	**0.42**	-0.11	**0.88**	
rno-miR-93	17386	0.21	-0.23	0.21	**0.37**	**0.95**	
rno-miR-17/17-5p	17605	**0.28**	0.27	0.17	0.17	**-0.53**	
rno-miR-290	17950	0.00	-0.09	0.20	**0.43**	**1.78**	
rno-miR-92b	17479	0.26	-0.14	**0.55**	0.06	**0.85**	
rno-miR-21_MM1	17400	0.12	0.16	**1.47**	-0.01	-0.36	
rno-miR-188	19589		0.66		**0.65**		
rno-miR-483	13184	0.31	0.21	0.09	**-0.37**	**1.05**	
rno-miR-532-5p	17624		0.64		0.45		
rno-miR-181a	10971		0.26	**0.57**			
rno-miR-129*	11200	0.12	**0.30**	**-0.43**	0.16	**0.59**	
rno-miR-92a	11179	0.25	0.14		-0.35	0.69	
rno-miR-31_MM1	17695	**-0.16**	0.06	**0.63**	-0.10	0.28	
rno-miR-26a	11030	**0.42**	0.22	0.08	0.65	**-0.93**	
rno-miR-9_MM2	13526	0.09	0.25		**0.42**	**-0.57**	
rno-miR-341	11229	0.20	0.35		**-0.94**	0.22	
rno-miR-193*	17878	-0.21	**-0.64**	**0.76**	0.56	**1.85**	
rno-miR-331	11064	-0.15	**1.06**	0.44	-0.13	0.13	
rno-miR-92b_MM1	13514		0.45		**0.78**	-0.09	
rno-miR-410	17311		**0.75**		**0.49**	**-0.24**	
rno-miR-485	11119					**0.57**	
rno-miR-107	10923	0.19	0.49	**-0.31**	0.49	**-0.43**	
rno-miR-292-3p	11215	0.16	-0.12	0.15	**-0.32**	**0.54**	
rno-miR-378*	11092		0.46		**0.37**	-0.48	
rno-miR-29b	11040	**0.21**	-0.42	0.56	**0.47**	-0.60	
rno-miR-350	11234	0.00	0.23	-0.45	-0.06	**0.33**	
rno-miR-100	19581	0.17	**-0.27**	0.26	**0.23**	-0.46	
rno-miR-543*	14292	0.02	**0.55**		**-1.05**	0.33	
rno-miR-101a_MM1	11198	0.15	0.17	**-0.28**	0.55	**-1.02**	
rno-miR-20a*	11261	**-0.80**	0.30	0.22	0.17	**-0.45**	
rno-miR-296*	19594	-0.01	0.07	-0.20	0.09	**2.23**	
rno-miR-365	17839	-0.07	-0.18	-0.02	**0.27**	**1.82**	
rno-miR-134	10234	**-0.43**	-0.24	**0.51**	-0.01	**0.97**	
rno-miR-20b-3p	14297		-0.07		**0.81**		
rno-miR-205	11006				-0.29	**0.86**	
rno-miR-187	17643	-0.12	0.21	0.07	**0.43**	**-0.58**	

Table 5.1. continued

Name	ID	PredTox study name				
		FP004BA	FP005ME	FP007SE	FP013NO	FP014SC
rno-miR-142-3p	10947		-0.07		**0.63**	-0.67
rno-miR-29c	11041	-0.05	-0.36	0.25	**0.68**	-0.64
rno-miR-124	14328	0.06	**-0.59**	-0.33	0.22	0.15
rno-miR-21	5740	-0.15	-0.34	**1.33**	**0.97**	-0.24
rno-miR-200c	17427	-0.19	-0.08	0.05	-0.04	**0.80**
rno-miR-31	11052	-0.13	-0.21	**0.58**	-0.21	0.35
rno-miR-199a-5p_MM1	11205		0.74		-0.11	**-0.41**
rno-miR-22	11020	-0.29	-0.19	0.40	**0.78**	-0.63
rno-let-7f	17752	-0.30	-0.26	0.45	0.63	**-0.47**
rno-miR-30b-5p	17565		-0.10	-0.44	**0.31**	
rno-miR-132	10937		0.18	-0.25	**-0.43**	0.12
rno-miR-194	10988	-0.14	**-0.57**	-0.20	0.24	0.20
rno-miR-291a-3p	17609	0.22	-0.21	**-0.46**	**0.45**	**-0.49**
rno-miR-9*_MM2	17314	**-0.45**	-0.10	-0.47	0.17	0.15
rno-miR-30a	11048	-0.40	**-0.56**	0.17	0.32	-0.44
rno-miR-199a-3p	10995	-0.16	-0.10	**0.35**	**-0.48**	-0.08
rno-miR-27b	13175	-0.15	-0.07	0.18	-0.13	**-0.48**
rno-miR-211	19601	-0.51	**0.07**		-0.28	-0.01
rno-miR-122	19583	-0.13	**-0.65**	0.01	0.56	**-0.61**
rno-miR-429	17478		**-0.75**		-0.16	
rno-miR-217	19016	**-1.08**		-0.21	0.08	0.03
rno-miR-196b_MM2	17432	-0.02	**-0.44**	-0.12	0.01	-0.08
rno-miR-215	11210	-0.17	-0.12	**-0.42**	-0.05	0.00
rno-miR-346	11269	-0.12	0.38	**-0.56**	-0.14	**-0.36**
rno-miR-192	17732	-0.20	-0.25	**-0.41**	0.46	**-0.49**
rno-miR-182	10975	0.12		**-0.41**	-0.44	-0.23
rno-miR-497	11129		-0.17	-0.14	0.01	**-0.69**
rno-miR-27a	19593	-0.20	**-0.37**	-0.03	-0.16	-0.65

All miRNAs demonstrating a significant ($p \leq 0.05$) fold change of > 1.5 in one or more of the PredTox studies are shown. Bold type denotes statistical significance. Rats received high dose compound (n=5) or vehicle-only treatment (n=5) for 15 days. Blank cells denote cases where no value was obtained for that miRNA with that treatment.

Table 5.2. Significant miRNA changes in the livers of rats treated with Thioacetamide.

Name	ID	Time point	50 mg/kg	100 mg/kg	150 mg/kg
rno-miR-92b	145897	24 h	**0.63**	**1.13**	**1.09**
rno-miR-3584-3p	148583	24 h	**0.70**	**0.72**	**0.55**
rno-miR-664-1*	148397	24 h	0.63	**0.89**	0.44
rno-miR-223	11024	24 h	**0.64**	**0.68**	0.39
rno-miR-216a	42553	24 h	0.25	**0.68**	**0.75**
rno-miR-3596c	148139	24 h	0.17	0.40	**0.82**
rno-miR-543	42665	24 h	0.38	0.35	**0.61**
rno-miR-21	147506	24 h	0.16	**0.64**	0.53
rno-miR-3546	148257	24 h	0.27	**0.70**	0.33
rno-miR-760-5p	42741	24 h	**0.55**	**0.46**	0.20
rno-miR-484	145753	24 h	0.09	0.94	**0.93**
rno-miR-3573-3p	148348	24 h	-0.34	**1.15**	0.92
rno-miR-664-2*	148260	24 h	0.03	1.01	0.69
rno-miR-201	148472	24 h	0.10	**0.69**	0.40
rno-miR-483	42500	24 h	-0.21	0.43	**0.62**
rno-miR-341	11229	24 h	-0.09	**0.56**	-0.19
rno-miR-409-3p	11240	24 h	**0.31**	0.08	**-0.58**
rno-miR-30e	28191	24 h	0.18	**-0.44**	**-0.27**
rno-miR-217*	148294	24 h	**-0.79**	-0.13	0.23
rno-miR-30c-1*	42702	24 h	0.17	**-0.54**	-0.34
rno-miR-23b	145841	24 h	0.20	**-0.69**	-0.25
rno-miR-505*	42490	24 h	0.08	**-0.66**	-0.28
rno-miR-543*	42470	24 h	0.14	**-0.95**	-0.27
rno-miR-3588	148350	24 h	**-0.47**	-0.04	-0.09
rno-miR-34a*	148595	24 h	0.06	**-0.49**	-0.21
rno-miR-181c*	145759	24 h	0.05	-0.29	**-0.44**
rno-miR-3597-5p	148131	24 h	0.00	0.02	**-0.71**
rno-miR-3563-5p	148404	24 h	-0.12	**-0.44**	-0.20
rno-miR-761	32608	24 h	-0.07	-0.21	**-0.49**
rno-miR-185	42902	24 h	-0.29	-0.09	**-0.49**
rno-let-7f	17752	24 h	-0.07	**-0.54**	**-0.44**
rno-miR-379*	42889	24 h	-0.42	**-0.44**	-0.24
rno-let-7f-1*	145840	24 h	**-0.44**	-0.33	**-0.35**
rno-miR-501	148491	24 h	-0.03	-0.68	**-0.46**
rno-miR-3556b	148157	24 h	**-0.39**	**-0.71**	-0.22
rno-miR-196c	42632	24 h	**-0.43**	-0.34	**-0.62**
rno-miR-100	145943	24 h	-0.45	-0.30	**-0.69**
rno-miR-3570	148540	24 h	-0.23	-0.65	**-0.65**
rno-miR-214	11014	24 h	**-0.53**	**-0.70**	**-0.43**
rno-miR-380*	11238	24 h	-0.56	**-0.85**	
rno-miR-3596b	148182	24 h	-0.56	**-0.70**	**-0.89**

Fold change
2.22
1.00
0.40

Table 5.2. continued

Name	ID	Time point	50 mg/kg	100 mg/kg	150 mg/kg
rno-miR-92a-2*	148576	24 h	-0.69	-0.58	**-1.03**
rno-miR-7a-2*	148614	24 h	-0.64	**-0.76**	**-0.95**
rno-let-7d	145968	24 h	-1.07	**-1.31**	**-1.25**
rno-miR-494	147514	48 h	0.33	0.96	**0.53**
rno-miR-664-2*	148260	48 h	0.28	0.90	**0.62**
rno-miR-344b-2-3p	148099	48 h	**0.55**	0.43	0.69
rno-miR-431	145705	48 h	0.41	**0.73**	0.40
rno-miR-219-2-3p	42834	48 h	0.10	**0.64**	**0.64**
rno-miR-3582	148246	48 h	0.43	0.40	**0.56**
rno-miR-3546	148257	48 h	**0.33**	0.30	**0.71**
rno-miR-211*	148176	48 h	0.15	**0.64**	**0.53**
rno-miR-664-1*	148397	48 h	0.18	**0.46**	**0.60**
rno-miR-3567	148173	48 h	**0.56**	0.30	**0.35**
rno-miR-433	42853	48 h	**0.54**	0.38	0.26
rno-miR-3573-3p	148348	48 h	**0.84**	**0.42**	0.14
rno-miR-181a-1*	11013	48 h	**1.15**	0.17	0.04
rno-miR-216a	42553	48 h	0.07	**0.57**	**0.63**
rno-miR-383	145825	48 h	0.18	0.13	**0.62**
rno-miR-484	145753	48 h	-0.03	**0.57**	**0.31**
rno-miR-3547	148456	48 h	0.07	0.17	**0.60**
rno-miR-3554	148240	48 h	0.13	**0.57**	0.11
rno-miR-25*	42481	48 h	0.03	0.10	**0.57**
rno-miR-217	19016	48 h	**0.60**	-0.11	0.15
rno-miR-320	27533	48 h	-0.10	0.15	**0.55**
rno-miR-3596c	148139	48 h	**0.82**	-0.27	0.01
rno-miR-331*	148385	48 h	0.50	-0.12	**-0.79**
rno-miR-93	30687	48 h	-0.41	0.18	**-0.66**
rno-miR-96*	42971	48 h	0.01	**-0.54**	0.03
rno-miR-3578	148116	48 h	**-0.43**	-0.15	-0.06
rno-miR-668	145701	48 h	-0.27	-0.04	**-0.48**
rno-miR-125b*	42845	48 h	0.08	**-0.41**	**-0.53**
rno-miR-200a	11000	48 h	-0.19	-0.26	**-0.46**
rno-miR-323*	42457	48 h	-0.15	**-0.46**	-0.32
rno-miR-100	145943	48 h	0.05	-0.39	**-0.66**
rno-miR-434*	11247	48 h	-0.41	-0.09	**-0.56**
rno-miR-544	42799	48 h	-0.14	-0.31	**-0.71**
rno-miR-221	11022	48 h	**-0.45**	**-0.44**	**-0.59**
rno-miR-191*	42748	48 h	-0.22	**-0.61**	**-0.72**
rno-miR-363*	27544	48 h	-0.48	-0.37	**-0.76**
rno-miR-493	14270	48 h	**-0.39**	**-0.81**	-0.54

Table 5.2. continued

Name	ID	Time point	50 mg/kg	100 mg/kg	150 mg/kg
rno-miR-19b-2*	148031	48 h	-0.56	-0.53	**-0.69**
rno-miR-122	148670	48 h	-0.47	-0.76	**-0.78**
rno-miR-17-2-3p	148213	48 h	0.00	**-1.09**	**-1.18**

All miRNAs demonstrating a significant ($p \leq 0.05$) fold change of > 1.5 following treatment with Thioacetamide at one or more doses/time points are shown. Bold type denotes statistical significance. Rats received 50 mg/kg, 100 mg/kg or 150 mg/kg Thioacetamide or vehicle only (0.9% saline) treatment and were sacrificed after 24 h or 48 h (n=3 for all treatments/doses).

Table 5.3. Significant miRNA changes in the liver of mice treated with Griseofulvin.

Name	ID	5 d	22 d
mmu-miR-195	13148	**0.78**	**0.92**
mmu-miR-302b*	17437	**0.94**	**0.69**
mmu-miR-194	17820	**0.78**	**0.75**
mmu-miR-302a	11222	**0.85**	0.56
mmu-miR-302c	11044	**0.70**	**0.49**
mmu-miR-692	17639	**0.48**	**0.60**
mmu-miR-302b	17609	**0.62**	**0.44**
mmu-miR-193*	17878	**0.51**	**0.54**
mmu-miR-183*	17953	**0.65**	0.35
mmu-miR-27b	13175	0.19	**0.79**
mmu-miR-381	14306	**0.32**	**0.62**
mmu-miR-93*	11171		**0.58**
mmu-miR-27a	19593	**-0.13**	**1.10**
mmu-miR-21	5740	-0.20	1.03
mmu-let-7f	17752	-0.31	**1.11**
mmu-let-7d	17750	-0.32	**1.00**
mmu-miR-98	17275	-0.22	**0.81**
mmu-miR-135a	17414	-0.22	**0.79**
mmu-miR-15a	10965	-0.12	**0.67**
mmu-miR-23b	11027	-0.15	**0.68**
mmu-miR-431*	17346	-0.21	**0.74**
mmu-miR-671-5p	14456	-0.12	**0.64**
mmu-miR-744	17864	-0.11	**0.61**
mmu-miR-23a	11026	-0.20	**0.68**
mmu-miR-200c*	13373	-0.08	**0.54**
mmu-miR-106a	19599	-0.16	**0.62**
mmu-let-7g	17342	-0.30	**0.75**
mmu-miR-1196	13263	-0.15	**0.56**
mmu-miR-122	19583	**-0.62**	0.98
mmu-miR-16	10967	-0.41	**0.63**
mmu-let-7a	17748	**-0.64**	**0.40**
mmu-miR-488	17897	0.13	**-0.43**
mmu-miR-24-2*	17602	**-0.54**	0.23
mmu-miR-144	10170	**-0.60**	0.08
mmu-miR-9	7190	0.32	**-0.89**
mmu-miR-335-3p	17929	-0.18	**-0.42**
mmu-miR-470	17607	**-0.54**	-0.07
mmu-miR-214	13528	**-0.18**	**-0.46**
mmu-miR-30d	19596	-0.17	**-0.47**
mmu-miR-1968	13257	**-0.59**	-0.08
mmu-miR-1944	17848	-0.12	**-0.65**

Fold change
2.16
1.00
0.24

Table 5.3. continued

Name	ID	5 d	22 d
mmu-let-7f*	17816	-0.26	**-0.57**
mmu-miR-27b*	17956	**-0.33**	**-0.53**
mmu-miR-107	17383	**-0.26**	**-0.73**
mmu-miR-146a	17409	**-0.36**	**-0.66**
mmu-miR-291b-3p	14275		**-0.52**
mmu-miR-218-2*	17542		**-0.61**
mmu-miR-382*	17587	-0.06	**-1.20**
mmu-miR-141*	17842	0.04	**-1.73**
mmu-miR-101a	17725	**-0.86**	-0.90
mmu-miR-30a*	17853		**-0.93**
mmu-miR-215	11210	**-0.80**	**-1.33**
mmu-miR-301a	9642		**-1.53**
mmu-miR-495	11274		**-2.03**

All miRNAs demonstrating a significant fold change of > 1.5 following treatment with Griseofulvin at one or both time points. Bold type denotes statistical significance. Mice were placed on a diet of 1% Griseofulvin in 2% arachis oil or 2% arachis oil for up to 22 days (n≥4 for all treatments/time points). Blank cells denote cases where no value was obtained for that miRNA at that time point.

5.5.4 Validation of microarray changes using qRT-PCR

Microarray profiling revealed that there were no common miRNA changes across all of the different models. However, miR-292-5p_MM1 was significantly up-regulated following treatment with three of the PredTox compounds, with FP014SC inducing the largest change (Table 5.1). This change could not be confirmed using qRT-PCR analysis (Fig. 5.4). An additional miRNA of interest was miR-92b, which was significantly up-regulated following treatment with two of the PredTox compounds (FP014SC and FP007SE) (Table 5.1) and increased in expression, in a dose-dependent manner, 24 h after treatment with Thioacetamide (Table 5.2). qRT-PCR confirmed this result, showing a significant increase in expression of miR-92b following high dose treatment with FP014SC (3.3-fold increase), FP007SE (2.6-fold increase) or Thioacetamide (6.5-fold increase) (Fig. 5.5 A-C). In contrast to the microarray results, the qRT-PCR data suggested that the change in miR-92b expression was greatest 48 h after Thioacetamide treatment, and 24 h after treatment, statistical significance was not achieved (Fig. 5.5 C). The microarray results indicated that another of the PredTox compounds, FP013NO, did not cause a change in expression of miR-92b (Table 5.1). However, whilst statistical significance was not obtained (p = 0.21) there was a trend for an increase in the expression of this miRNA (reaching 1.9-fold) when qRT-PCR analysis was performed (Fig. 5.5 D). It was interesting to see a conserved change in expression of miR-92b following treatment of rats with different hepatotoxic compounds, so qRT-PCR was also performed on the Griseofulvin-treated samples to determine whether this change was also observed across the species barrier. Treatment of mice with Griseofulvin for 22 days induced a significant, 3.1-fold increase in miR-92b (Fig. 5.5 E).

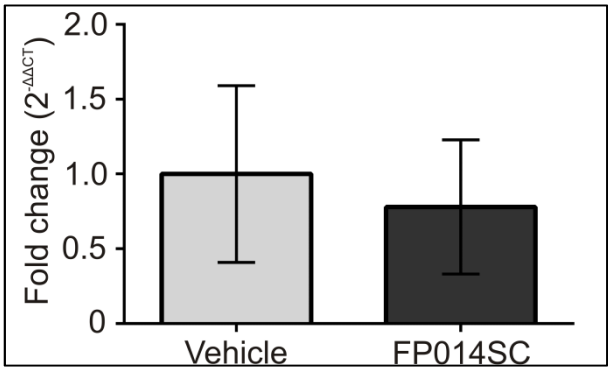

Fig. 5.4. qRT-PCR did not validate the up-regulation of miR-292-5p following treatment with FP014SC. qRT-PCR data were normalised to U6 snRNA and represent mean ± SEM. p = 0.63 (T-test). Rats received high dose FP014SC or vehicle-only treatment for 15 days (n=5).

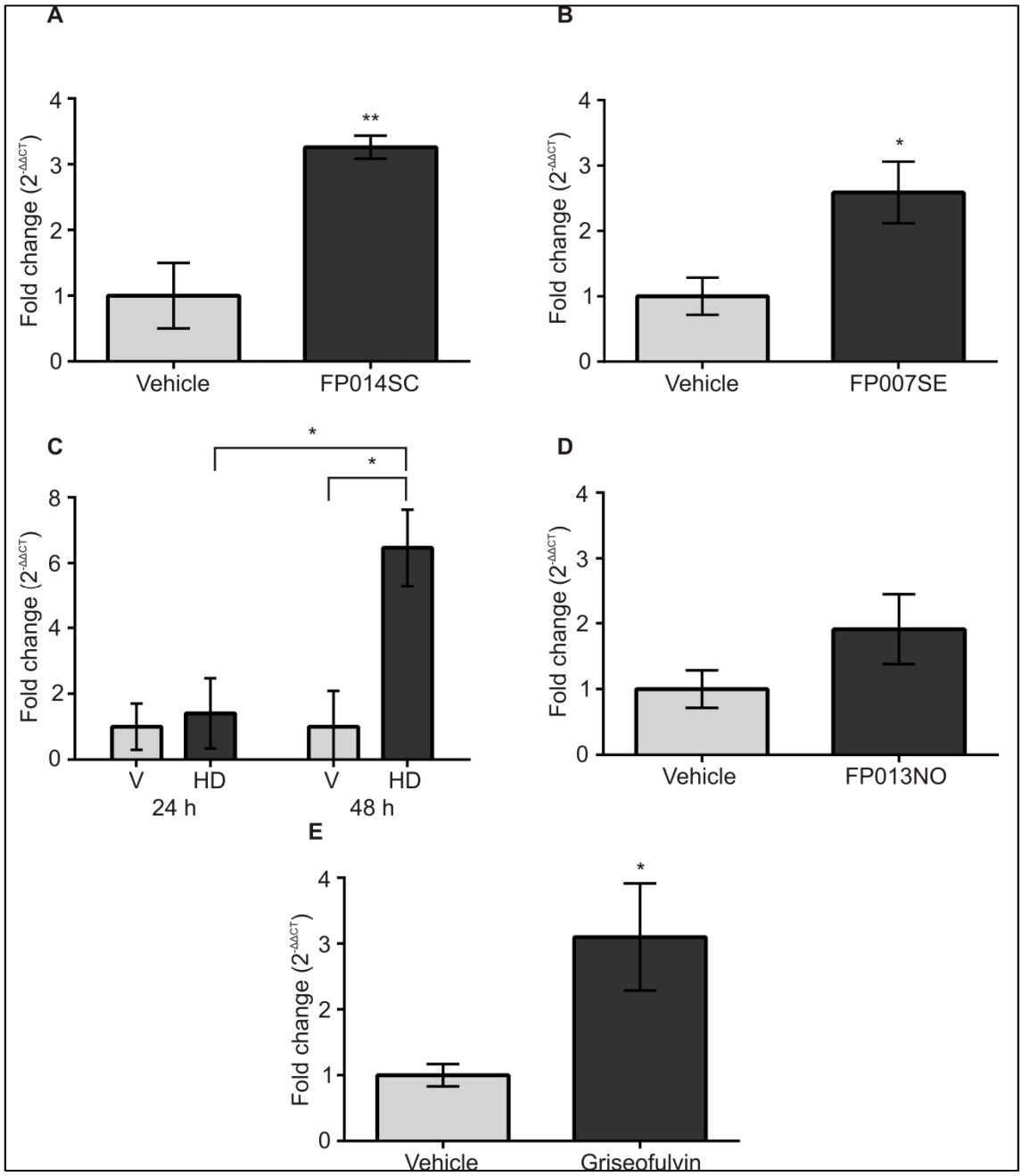

Fig. 5.5. miR-92b levels were increased following compound-induced hepatotoxicity. (**A**) Thioacetamide, (**B**) FP014SC, (**C**) FP007SE, (**D**) FP013NO and (**E**) Griseofulvin. qRT-PCR data were normalised to U6 snRNA (Thioacetamide- and PredTox-treated) or snoRNA-202 (Griseofulvin-treated) and represent mean ± SEM. * $p \leq 0.05$, ** $p \leq 0.01$ (T-test/ANOVA + Tukey's post hoc test). PredTox compound-treated rats received high dose compound or vehicle-only treatment for 15 days (n≥3). Thioacetamide-treated rats received 150 mg/kg Thioacetamide or vehicle only (0.9% saline) treatment and were sacrificed after 24 h or 48 h (n=3). Griseofulvin-treated mice were placed on a diet of 1% Griseofulvin in 2% arachis oil or 2% arachis oil for 22 days (n=4).

5.5.5 Identification of common miRNA-mediated networks

To identify whether there were common regulatory networks between the different models, indicative of the deregulated miRNAs working together as a functional group, each list of differentially expressed miRNAs was uploaded to the miRWalk database. A list of validated mRNA targets was downloaded for each model and these mRNA lists were uploaded to IPA for pathway analysis. Whilst the number of mapped targets differed between the models; PredTox (457), Thioacetamide (341), Griseofulvin (911), the Hepatic Fibrosis / Hepatic Stellate Cell Activation pathway (Fig. 5.6) was identified as the most significantly enriched canonical pathway for each model. Furthermore, liver proliferation was one of the top toxicological-associated features identified with each set of data.

Despite the fact that the specific miRNAs that demonstrated differential expression varied between the model systems, the lists of downloaded validated targets were similar. There were 65 validated mRNA targets associated with the Hepatic Fibrosis / Hepatic Stellate Cell Activation pathway, of which 32 were common to all models (Fig. 5.7 and Appendix VII). The larger number of associated mRNAs from the Griseofulvin model is representative of the larger total number of validated targets identified.

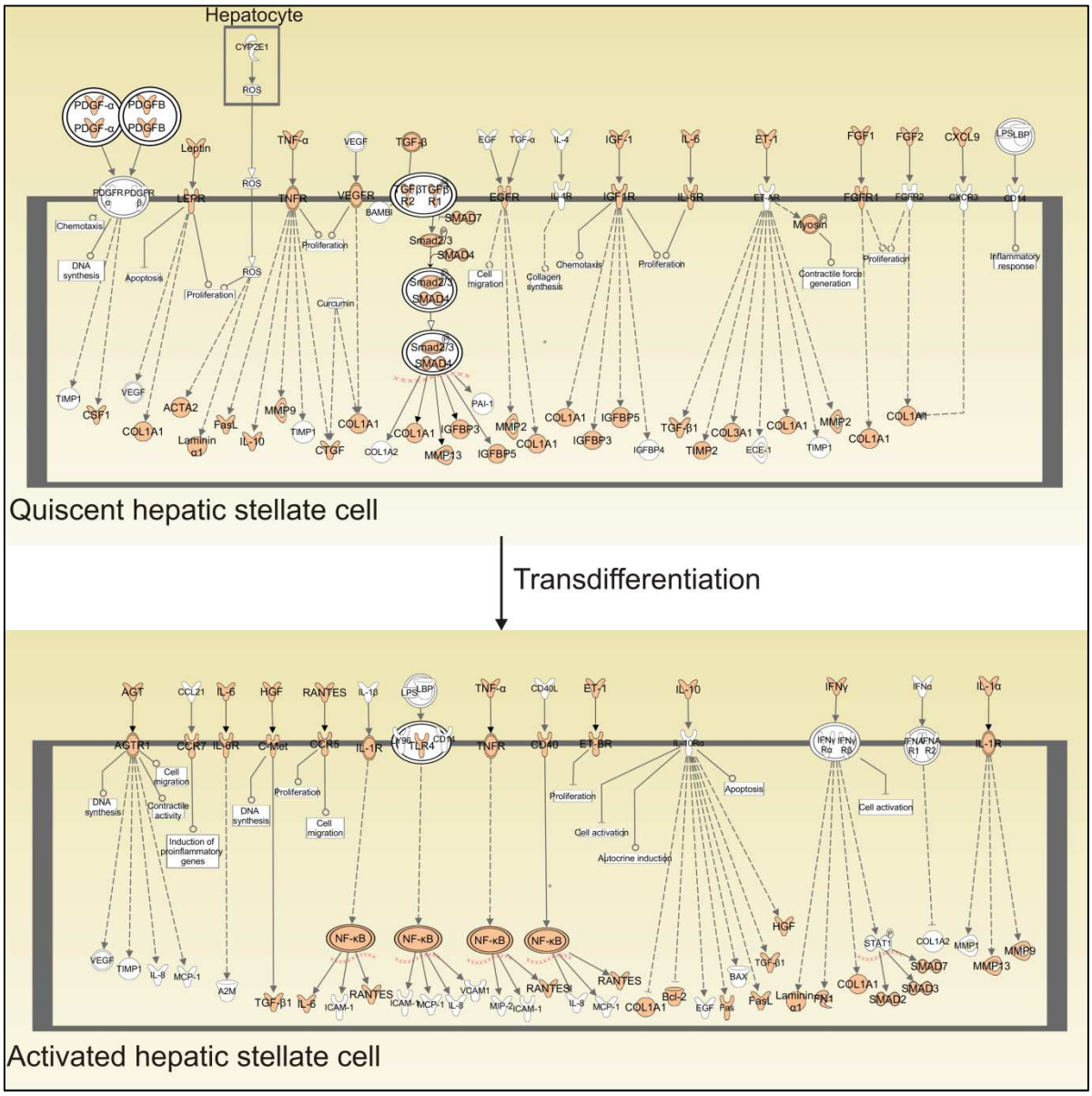

Fig. 5.6. The Hepatic Fibrosis / Hepatic Stellate Cell Activation canonical pathway. Validated target mRNA are shown in orange. Solid and dashed lines indicate interactions between molecules (solid represent direct interactions, and dashed indirect interactions).

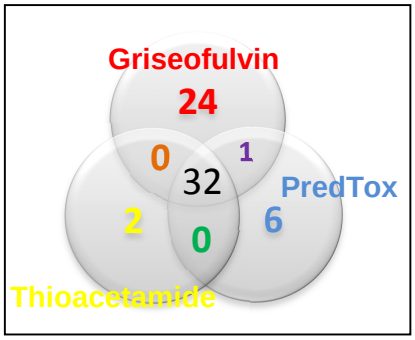

Fig. 5.7. Nearly half of the identified mRNA targets that were associated with the Hepatic Fibrosis / Hepatic Stellate Cell Activation pathway were common to all models of compound-induced hepatotoxicity.

5.5.6 Changes in miRNA expression were mapped to those mRNAs demonstrating a change in translational and/or transcriptional efficiency

5.5.6.1 FP014SC

Mapping of putative target mRNAs for all miRNAs that demonstrated differential expression following treatment with FP014SC for 15 days to the list of mRNAs found in Chapter 3 to be altered at the translational and/or transcriptional level following the same treatment (section 3.5.3.1) enabled functionally relevant miRNA-mRNA interactions to be identified. 67 miRNA-mRNA interactions were identified (Table 5.4), amongst them an interaction between *Dio3* and miR-336. As previously described in section 5.5.2 and shown in Fig. 5.3 B, the change in expression of miR-336 was not validated by qRT-PCR.

5.5.6.2 Griseofulvin

The same mapping process was used to identify functionally relevant miRNA-mRNA interactions following treatment with Griseofulvin for 22 days. 30 putative interactions were identified by both algorithms (PITA ΔΔG score ≤ -8) (Table 5.5), amongst them an interaction between *Smarce1* mRNA and miR-135a. *Smarce1* was identified in Chapter 3 as an example of a mRNA that demonstrated translation repression, resulting in a reduction in SMCE1 protein levels, following treatment with Griseofulvin for 22 days (Chapter 3, Fig. 3.9 and 3.10). Treatment with Griseofulvin caused a 1.7-fold up-regulation of miR-135a (Table 5.3). Further investigation revealed that *Smarce1* was also a putative target mRNA of miR-135b. As shown in Fig. 5.8, the sequences of miR-135a and miR-135b differ by only a single nucleotide and this difference is not located within the core seed region. Thus, both miRNAs are likely to exert similar effects on their target mRNAs. qRT-PCR analysis confirmed that Griseofulvin treatment induced a significant increase in the levels of both miR-135a and miR-135b (Fig. 5.9).

Table 5.4. Putative miRNA-mRNA interactions following treatment with FP014SC.

Name	Ave T_C change	T_C	Slope	T_L	miRNA name (miRDB)	miRNA FC	miRNA name (TargetScan)	miRNA FC
Zfp367	0.91	↔	-0.16	↓	rno-miR-93 rno-miR-130b	1.93 1.50		
Ube2i	0.82	↔	-0.21	↓	rno-miR-200c	1.73		
Smarcd2	0.94	↔	-0.17	↓	rno-miR-130b	1.50		
Slc9a2	0.94	↔	-0.33	↓	rno-miR-93 rno-miR-130b	1.93 1.50	rno-miR-93	1.93
Rab11fip4	0.90	↔	-0.16	↓	rno-miR-483 rno-let-7e	2.06 1.50	 rno-miR-485 rno-miR-145	 1.49 1.48
Pacs1	0.76	↔	-0.44	↓	rno-miR-485	1.49		
Npas2	0.92	↔	-0.22	↓	rno-miR-93	1.93	rno-miR-93 rno-miR-216a	1.93 1.97
Gfi1	0.95	↔	-0.16	↓	rno-miR-145	1.48		
Fkbp4	1.24	↔	-0.27	↓	rno-miR-361	1.76		
Dio3	0.59	↓	-0.35	↓	rno-miR-336	1.55		
Cyp11b2	0.76	↔	-0.16	↓	rno-miR-216a rno-miR-874	1.97 2.16		
Brp16	0.95	↔	-0.22	↓	rno-miR-485	1.49		
Banf1	0.80	↔	-0.21	↓	rno-miR-134	1.96		
Arl2bp	0.87	↔	-0.31	↓	rno-miR-485	1.49	rno-miR-485	1.49
Adamtsl3	0.72	↓	-0.18	↓	rno-miR-205	1.81	 rno-miR-485	 1.49
Zic4	0.90	↔	-0.16	↓			rno-miR-500	1.83
Sall1	1.07	↔	-0.25	↓			rno-miR-365	3.52
Ptgdr	1.78	↑	-0.16	↓			rno-miR-365	3.52
Plcd3	0.94	↔	-0.39	↓			rno-miR-485	1.49
Nsmaf	1.19	↔	-0.18	↓			rno-miR-299	2.00
Inppl1	0.75	↔	-0.28	↓			rno-miR-205	1.81
Hoxc8	1.01	↔	-0.16	↓			rno-miR-92a	1.48
Fstl1	0.66	↓	-0.39	↓			rno-miR-378	1.92
Bpnt1	0.74	↓	-0.21	↓			rno-miR-874	2.16
Arrdc2	0.76	↔	-0.43	↓			rno-miR-378	1.92
Ssh2	0.98	↔	0.17	↑	rno-miR-26a rno-miR-17-5p	0.53 0.68	rno-miR-26a	0.53
Slc29a4	1.11	↔	0.21	↑	rno-miR-128	0.74		
Sesn1	0.95	↔	0.21	↑	rno-miR-497	0.62		
Pgrmc1	1.03	↔	0.33	↑	rno-miR-1 rno-let-7f	0.70 0.72	rno-miR-1	0.70
Peli2	1.09	↔	0.21	↑	rno-miR-26a rno-miR-27b	0.53 0.72	rno-miR-26a rno-miR-128	0.53 0.74
Pck1	0.99	↔	0.33	↑	rno-miR-26a	0.53		
Nbl1	0.79	↔	0.22	↑	rno-miR-17-5p	0.68	rno-miR-17	0.68

Table 5.4. continued

Name	Ave T_C change	T_C	Slope	T_L	miRNA name (miRDB)	miRNA FC	miRNA name (TargetScan)	miRNA FC
Hook1	1.15	↔	0.25	↑	rno-miR-26a	0.53	rno-miR-26a	0.53
Fzd6	1.08	↔	0.15	↑	rno-miR-128	0.74	rno-miR-291a-3p	0.71
Fts	1.17	↔	0.41	↑	rno-miR-101b	0.49		
Dusp1	0.70	↓	0.37	↑	rno-miR-101b	0.49		
Ccng1	1.01	↔	0.17	↑	rno-miR-128 rno-miR-122 rno-miR-27b	0.74 0.66 0.72	rno-miR-128 rno-miR-122	0.74 0.66
Brd8	0.99	↔	0.23	↑	rno-miR-101b	0.49	rno-miR-101b	0.49
Arhgap8	1.08	↔	0.24	↑	rno-miR-187	0.67		
Adarb1	1.05	↔	0.20	↑	rno-miR-17-5p rno-miR-291a-3p	0.68 0.71		
Rgs16	0.98	↔	0.24	↑			rno-let-7f	0.72
Ptbp1	1.16	↔	0.25	↑			rno-miR-17	0.68
Pip5k1c	1.10	↔	0.19	↑			rno-miR-101b	0.49
Pank1	0.86	↔	0.23	↑			rno-miR-128	0.74
Nin	1.06	↔	0.46	↑			rno-miR-17	0.68
Kif21b	1.04	↔	0.27	↑			rno-miR-26a	0.53
Kif1c	1.05	↔	0.17	↑			rno-miR-497	0.62
Enah	1.22	↔	0.17	↑			rno-miR-497 rno-miR-128 rno-miR-101b	0.62 0.74 0.49
Arhgap1	0.54	↓	0.40	↑			rno-miR-128	0.74

Rats received high dose FP014SC or vehicle-only treatment for 15 days (n≥3). Results were refined through the use of two independent algorithm programmes (miRDB and Target Scan). T_C – transcription, T_L – translation FC – fold change.

Table 5.5. Putative miRNA-mRNA interactions following treatment with Griseofulvin.

Name	Ave T_C change	T_C	Slope	T_L	miRNA name	miRNA FC
4432412L15Rik	0.73	↓	-0.16	↓	mmu-let-7d	2
5830472M02Rik (Ttpal)	0.87	↔	-0.19	↓	mmu-miR-106a	1.54
Fgfr1	0.79	↔	-0.22	↓	mmu-miR-671-5p	1.56
Jun	2.01	↑	0.34	↑	mmu-miR-1196	1.46
Klf12	0.76	↔	0.19	↑	mmu-miR-106a	1.54
Myt1l	0.96	↔	-0.18	↓	mmu-miR-106a mmu-miR-15a mmu-miR-16 mmu-miR-195 mmu-miR-302b	1.54 1.59 1.55 1.89 1.8
Pcdh9	0.27	↓	-	↔	mmu-miR-15a mmu-miR-16 mmu-miR-195	1.59 1.55 1.89
Phc2	1.08	↔	-0.23	↓	mmu-miR-671-5p	1.56
Ptprd	1.13	↔	-0.16	↓	mmu-let-7d mmu-let-7f mmu-let-7g mmu-miR-106a mmu-miR-15a mmu-miR-671-5p mmu-miR-98	2 2.16 1.68 1.54 1.59 1.56 1.76
Rasl10b	0.98	↔	-0.16	↓	mmu-let-7d mmu-let-7f mmu-let-7g mmu-miR-98	2 2.16 1.68 1.76
Smarce1	0.74	↓	-0.11	↓	mmu-miR-135a	1.73
Klf12	0.76	↔	0.19	↑	mmu-miR-335-3p mmu-miR-291b-3p	0.75 0.7
Mapk1	0.52	↓	0.31	↑	mmu-miR-291b-3p	0.7
Myt1l	0.96	↔	-0.18	↓	mmu-miR-301a	0.35

Mice were placed on a diet of 1% Griseofulvin in 2% arachis oil or 2% arachis oil for 22 days (n≥4). Results were refined through the use of two independent algorithm programmes (Target Scan and PITA). T_C – transcription, T_L – translation FC – fold change.

***Smarce1* (306-313)**	5'	…	A	C	G	U	G	G	U	G	C	U	C	A	C	C	A	A	A	G	C	C	A	U	A	…
																		I	I	I	I	I	I	I		
mmu-miR-135a	3'		A	G	U	G	U	A	U	C	C	U	U	A	U	U	U	U	U	C	G	G	U	A	U	
mmu-miR-135b	3'		A	G	U	G	U	A	U	C	C	U	U	A	C	U	U	U	U	C	G	G	U	A	U	

Fig. 5.8. Predicted binding interaction between *Smarce1* mRNA and miR-135a and miR-135b. The predicted binding site between *Smarce1* mRNA and miR-135a and miR-135b is highlighted in red.

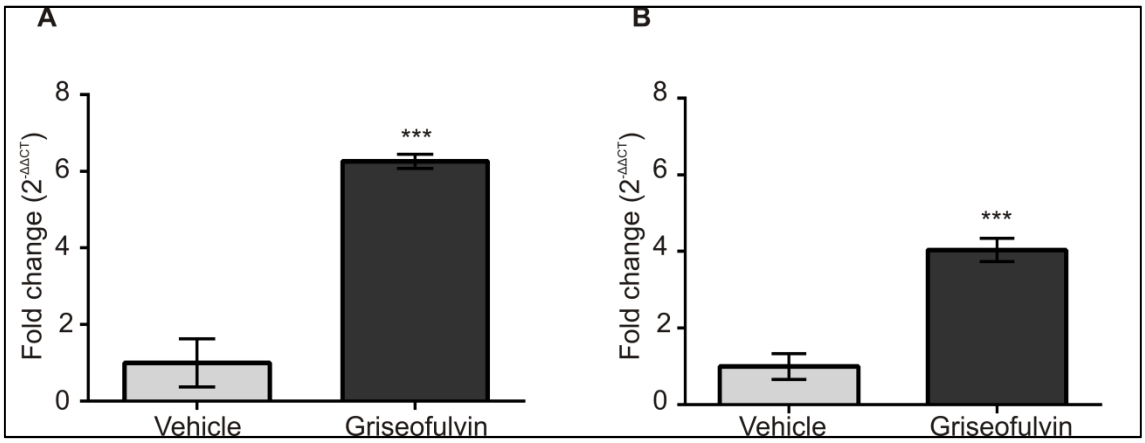

Fig. 5.9. miR-135a and miR-135b were significantly increased following treatment with Griseofulvin. (**A**) miR-135a and (**B**) miR-135b. qRT-PCR data were normalised to snoRNA-202 and represent mean ± SEM. *** $p \leq 0.001$ (T-test). Mice were placed on a diet of 1% Griseofulvin in 2% arachis oil or 2% arachis oil for 22 days (n≥4).

5.5.9 Levels of miR-135a and miR-135b were not reduced in an in vitro model system

Levels of SMCE1 protein showed reduced expression in Hepa 1-6 cells treated with Griseofulvin for 72 h (Chapter 3, section 3.5.3.4). qRT-PCR revealed that there was no significant change in expression of either miRNA following Griseofulvin treatment (Fig. 5.10).

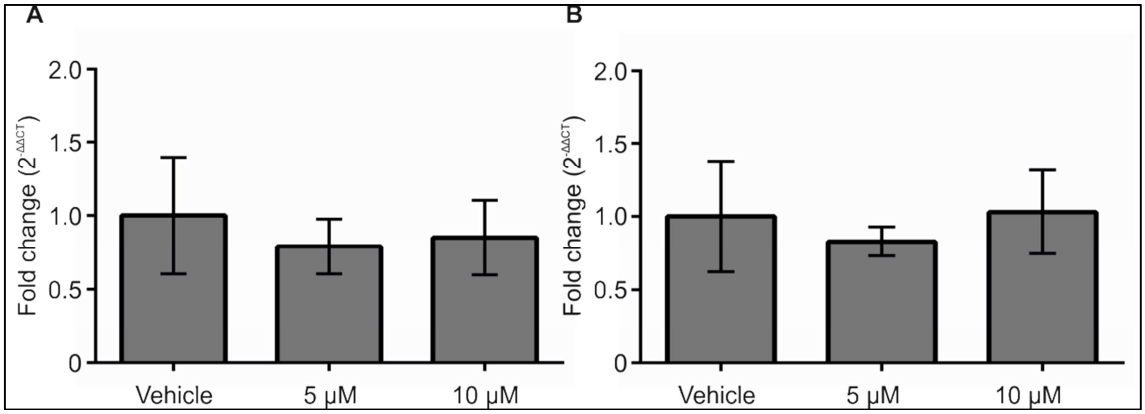

Fig. 5.10. An *in vitro* model system did not show any change in expression of miR-135a or miR-135b following treatment with Griseofulvin. (**A**) miR-135a and (**B**) miR-135b. qRT-PCR data were normalised to U6 snRNA and represent mean ± SEM. Hepa 1-6 cells were treated with 5 µM and 10 µM Griseofulvin for 72 h, control samples were cells treated with 0.1% DMSO (n=3).

5.6 DISCUSSION

Chapter 4 demonstrated that *Dio3* mRNA was translationally repressed in the PredTox and Thioacetamide models of hepatotoxicity. There is substantial evidence in the literature that miRNAs function to regulate translation (Carthew and Sontheimer, 2009; Filipowicz et al., 2008; Huntzinger and Izaurralde, 2011), although the exact mechanism remains unclear (Omer et al., 2009). None of the miRNAs predicted to target *Dio3* mRNA showed a significant corresponding increase in expression, and thus they were unlikely to be regulating its expression. However, global miRNA expression profiling demonstrated that miRNAs did appear to mediate regulatory networks important in the cellular response to compound-induced liver injury.

Four miRNAs, predicted to target the 3' UTR of *Dio3* mRNA by TargetScan and/or miRDB, were identified; miR-214, miR-336, miR-192* and miR-761. It was hypothesised that if any of these miRNAs were regulating the translational repression of *Dio3* mRNA they would show an inverse increase in expression. None of the four miRNAs were significantly up-regulated following high-dose treatment with FP014SC or Thioacetamide (Fig. 5.3). FP014SC induced the largest reduction in D3 protein, whilst Thioacetamide induced a more moderate reduction (Chapter 4, Fig. 4.6). Using compounds that differed in the extent of their translational repression enabled any potential differences in the mechanism of D3 regulation to be identified. The reduction in D3 was more pronounced at the highest dose (Chapter 4, Fig. 4.7); therefore, miRNA analysis was restricted to samples treated with high dose FP014SC or 150 mg/kg Thioacetamide. Early time points were analysed in case the miRNAs were altering rapidly, inducing a change in translation, and then returning to near normal levels. However, no significant changes were seen following 2 day or 4 day FP014SC treatment or 24 h after Thioacetamide treatment (Fig. 5.3). Time-course analysis did, however, reveal that miR-192* might be an interesting candidate for further study. Following treatment with FP014SC, miR-192* was down-regulated in a time-dependent manner, reaching statistical significance by 15 days (Fig. 5.3 C). miR-192* derives from the miR-192 stem-loop, but was regarded as the alternative (miRNA*) strand. The consensus used to be that the * strand was degraded and thus rarely involved in downstream regulation (Carthew and Sontheimer, 2009). However, it is now known that in certain cases, both strands are maintained and act synergistically, usually via differing target mRNAs, to exert a physiological effect (Shan et al., 2013; Yang et al., 2013). Whilst not yet experimentally demonstrated, this may be the case for miR-192*. To avoid potential confusion all miRNAs have been recently renamed depending on which arm of the precursor molecule (5' or 3') they were derived from. miR-192* is now better known as miR-

192-3p, meaning it came from the 3' arm of the precursor molecule. Whilst publications on miR-192* are limited, there is literature on miR-192, revealing a role in cancer (Chiang et al., 2012a; Chiang et al., 2012b; Khella et al., 2013) and, perhaps, more intriguingly a potential role for this miRNA as a biomarker in drug-induced liver damage (Starkey Lewis et al., 2011; Wang et al., 2009).

Although these results suggest that the translation of *Dio3* mRNA was not under miRNA-mediated control, a role for these species should not be ruled out completely. Whilst most mRNA regulation is inhibitory in nature (Gebauer and Hentze, 2004), work has been published demonstrating that increased miRNA expression can correlate with the relief from repression of target mRNAs, usually in cases of cellular stress (Orom et al., 2008; Tsai et al., 2009). In such cases, the miRNA exerts its effect through binding to a site within the 5' UTR of its target mRNA, activating translation (Da Sacco and Masotti, 2012). It is therefore possible that if a miRNA that normally activates the translation of *Dio3* mRNA is down-regulated during hepatotoxicity, this would cause repressed translation and consequently less protein. This type of miRNA-mRNA interaction would not be identified by target prediction algorithms, which tend to focus on miRNA binding sites within the 3' UTRs of target mRNAs (Watanabe et al., 2007). Thus, the possibility remains that an as yet unidentified miRNA:*Dio3* mRNA interaction might exist. Furthermore, it is also possible that novel, functionally-relevant interactions will be uncovered, as more miRNAs are identified and target prediction algorithms are improved. Due to the dynamic, rapidly developing nature of miRNA work, the dataset presented in this thesis should be revisited as the field expands. The probe set used for a lot of the microarray analysis described here was one of the earliest produced and only mapped to approximately 1500 miRNAs, 360 of which had known analogues in the rat. The newest release from Sanger (version 20, June 2013) contains sequences for 728 mature miRNA species in the rat. This demonstrates how rapidly the field is changing and developing and further highlights the need to revisit older data sets.

However, it must also be considered that, in the case of compound-induced hepatotoxicity the translational repression of *Dio3* may be mediated via an alternative mechanism. Although miRNAs are important and have generated vast interest in recent years, they do not account for all translational regulation. Even if 50% - 60% of mammalian protein-coding genes are regulated by miRNAs, which is the most generous estimate (Friedman et al., 2009; Krol et al., 2010), a further 40% - 50% of mRNAs must therefore be regulated by alternative mechanisms. One such mechanism is through the association of RNA binding proteins, which bind selectively to the 3' UTR of a target mRNA, and also exert inhibitory effects (Jackson et al., 2010). *Dio3* is

imprinted and preferentially expressed from the paternal allele (Hernandez et al., 2002). In the mouse and human, a non-coding gene transcribed in the antisense orientation, *Dio3os*, has been identified (Hernandez et al., 2004). This is an example of a long noncoding RNA (lncRNA). lncRNAs are some of the most common, yet poorly understood RNA species (Derrien et al., 2012). They were first identified in 2005 by the FANTOM consortium (Carninci et al., 2005; Maeda et al., 2006), however, their regulatory role and functionality within the genome remains largely unexplored (Derrien et al., 2012). Although early work suggested low sequence conservation and limited disease association (Ponting et al., 2009), more recent studies have revealed an intriguing role for these family members in regulating translation (Johnsson et al., 2013). For example, antisense Uchl1, a lncRNA located in the brain, binds to a protein coding mRNA within a partially overlapping region on the sense strand and increases protein synthesis at the post-transcriptional stage (Carrieri et al., 2012). *Dio3* and *Dio3os* are also partially overlapping and demonstrate inverse correlation in expression (Hernandez et al., 2004). Furthermore, the stability of thyroid hormone receptors can be moderated by naturally occurring antisense RNAs (Hastings et al., 2000) and lncRNAs have been shown to directly regulate ribosomal association of their coding equivalent mRNAs (Carrieri et al., 2012). Therefore, it is possible that, following compound-induced damage to the liver, *Dio3* is post-transcriptionally regulated by *Dio3os*, leading to less efficient translation and a reduction in D3 protein levels. This hypothesis is further supported by recent work that has identified a homolog to the *Dio3os* gene in the rat (Dietz et al., 2012). Now that work has commenced on identifying the structure and function of this gene in the rat, there is the opportunity to further develop the work on *Dio3* to investigate regulatory mechanisms distinct from miRNAs.

Although the evidence presented here does not support miRNA-mediated translational repression of *Dio3* mRNA, there was still the possibility that miRNAs might be involved in alternative physiological responses to compound-induced hepatotoxicity. miRNAs have already been demonstrated to play a fundamental role in liver physiology and pathophysiology, particularly in the response to, and recovery from, injury and illness (Starkey Lewis et al., 2011; Wang et al., 2009; Wang et al., 2012c). Furthermore, their levels have been shown to change following exposure of the liver to a range of hepatocarcinogens (Koufaris et al., 2012). Thus, global miRNA microarray expression profiling was performed on the liver samples from each of the models used (PredTox compound-treated rats, Thioacetamide-treated rats and Griseofulvin-treated mice) with a view to identifying common miRNA expression profiles and miRNA-mediated networks across the different compounds and species.

miRNAs were differentially expressed in each of the models. Following high dose treatment with one or more of the PredTox compounds for 15 days, 68 miRNAs showed altered expression (Table 5.1). The number and magnitude of miRNA changes between the different PredTox compounds varied with differing severity. Grading of the PredTox compounds according to the severity of liver damage is shown in Chapter 3, Table 3.2. FP014SC caused the most pronounced hepatotoxic effects, with a severity rating of +++; miRNA microarray analysis revealed that this compound also induced the largest number of miRNA changes, compared to the other PredTox compounds. miR-292-5p_MM1 was the miRNA of most potential interest because it was significantly increased following treatment with 3 of the compounds and showed the largest change in expression of all tested miRNAs across all of the PredTox compounds (4.7-fold up-regulation following treatment with FP014SC). qRT-PCR analysis, using a Taqman probe and primers designed against miR-292-5p, on the FP014SC samples did not validate this change (Fig. 5.4). One reason for the discrepancy in the microarray and qRT-PCR results might be due to the use of different profiling platforms. There are several challenges to be met with any miRNA-based profiling technique, not least the difficulty associated with maintaining both high specificity and sensitivity for such closely-related, short sequences. With an average length of 22 nucleotides (Bartel, 2004) the sequence of one miRNA may only differ from another miRNA by a single nucleotide (Mondol and Pasquinelli, 2012). In addition to distinguishing between closely-related family members, a suitable profiling technique also needs to accurately discern, and quantify, levels of the mature miRNA rather than the precursor molecules, depicted in Chapter 1, Fig. 1.7. Further complexities arise from the wide variance in melting temperature of miRNAs, caused by their short length and variable GC content (Pritchard et al., 2012). This particularly affects microarray profiling, where many miRNAs are simultaneously measured. The Exiqon microarrays described and used in this chapter were comprised of locked nucleic acid (LNA) probes (Castoldi et al., 2006). This is a proprietary technique developed by Exiqon whereby the 2'-O and 4'-C atoms are chemically linked by a methylene bridge, thus "locking" the ribose ring in place. Thermal stability is thus increased and, by varying the quantity of LNA present, the melting temperature can be normalised across the probes. qRT-PCR does not have to overcome the problem of variable melting temperatures as most miRNAs are measured in independent experiments. Sensitivity and specificity are still an issue, although qRT-PCR is generally a more sensitive technique than microarray profiling (Chen et al., 2009; Jensen et al., 2011).

The inability to correlate results between platforms has been described elsewhere, although the literature is conflicting. Ach *et al* found excellent correlation between Agilent microarrays

and Taqman-based qRT-PCR (Ach et al., 2008), only 7 miRNAs out of 60 did not have a correlation (R) value > 9. However, this has been disputed by others, who find low rates of correlation between platforms (Chen et al., 2009; Git et al., 2010). One proposed explanation is that lowly expressed miRNAs show more inter-platform variability, thus reducing the correlation score, particularly in studies where a large number of miRNAs are simultaneously measured. For example, Chen *et al* investigated over 500 miRNAs and hypothesised that to measure each miRNA individually would have produced a large number of false positives (Chen et al., 2009). The raw CT values for miR-292-5p were high (between 34 and 35), suggesting low expression of this miRNA in the rat liver samples, thus providing one possible reason for the discrepancy between platforms. The higher sensitivity of qRT-PCR as a technique, compared to microarray expression profiling (Fehr et al., 2000) suggests that this method would be more accurate at identifying lowly expressed miRNAs. Therefore, the change seen with microarray analysis could be an example of a false positive. However, there is an alternative explanation for the discrepancy between the two platforms used here, which relates to the naming process adopted by Exiqon. The differentially expressed probe on the microarray was miR-292-5p_MM1. The "MM1" nomenclature is unique to Exiqon, and was used to indicate a probe that corresponded to a miRNA from a different organism, which had a closely related sequence to the organism of interest, usually differing by 1 nucleotide. This was a feature of their earlier probe sets, but was discontinued due to the increased confusion caused by making such assumptions. Indeed, some miRNA family clusters; members of the let-7 group, for example, frequently differ by only a single nucleotide (Mondol and Pasquinelli, 2012), yet have different expression profiles (Boyerinas et al., 2010). Thus the miR-292-5p_MM1 probe on the Exiqon array may target a miRNA completely unrelated to miR-292-5p, leading to discrepancies between this and the Taqman qRT-PCR platforms. Unfortunately, the exact rat miRNA that the miR-292-5p_MM1 probe targets remains unknown and is one of the limitations of early miRNA work.

Following treatment with Thioacetamide 76 miRNAs were differentially expressed at one or more dose or time point (Table 5.2). One of these, miR-92b, showed a dose-dependent up-regulation 24 h after dosing. This miRNA was also significantly increased in expression following high dose treatment with two of the PredTox compounds, FP007SE and FP014SC (Table 5.1). qRT-PCR confirmed and enhanced the microarray results (Fig. 5.6 A-C); although in the case of miR-92b the increase was larger at the 48 h time point. Microarray analysis of the Thioacetamide samples indicated a non-significant increase in expression of miR-92b at the 48 h time point, therefore this small discrepancy was probably due to small sample sizes and thus

increased variation. Treatment with FP013NO also resulted in an up-regulation of miR-92b, although statistical significance was not reached (Fig. 5.5 D). Whilst seeing this change replicated across both the PredTox and Thioacetamide model systems was interesting, and appeared to indicate a conserved effect following exposure to very different compounds, both systems used the same Wistar rat strain and a similar end point of toxicity. To expand upon these findings, Griseofulvin-treated samples were also investigated. In this mouse model of hepatotoxicity, Griseofulvin treatment for 5 days or 22 days resulted in the differential expression of 54 miRNAs at one or both time points (Table 5.3). Although miR-92b was not one of these 54 miRNAs, qRT-PCR revealed a significant up-regulation following treatment with Griseofulvin for 22 days (Fig. 5.5 E). This again highlights the discrepancies that can be seen between profiling platforms. The change in miR-92b seen with Griseofulvin treatment indicated a cross-species effect. There are only a limited number of studies investigating toxic effects across different species. It has been known for some time that basal gene expression varies across different species (Gant and Zhang, 2005), which makes analysing a toxic response difficult. Importantly, where cross-strain and cross-species studies have taken place, markedly different miRNA expression profiles have usually been observed (Mor et al., 2011; Pogribny et al., 2010). It is hypothesised that this may be due to differences in miRNA processing and regulation (Koufaris and Gooderham, 2013) and in some instances species- or strain-specific miRNAs (Berezikov et al., 2006; Linsen et al., 2010). The conservation of this up-regulation in expression of miR-92b across species is, therefore, very interesting. Liu *et al* identified a critical role for miR-92b in regulating neuronal stem cell differentiation and proliferation (Liu et al., 2009). Therefore, miR-92b may be involved in regulating cellular proliferation following liver injury and has the potential to function as a general, cross-species hepatic-based biomarker of compound-induced toxicity, although further work is required to explore the regulatory mechanism in more detail.

Whilst the up-regulation of miR-92b was interesting, it was not common to all of the PredTox compounds (Table 5.2). In fact, there were no miRNA changes that were conserved across each of the models and all of the compounds. For this reason miRNA-mediated regulatory networks were also investigated. Changes in the expression profiles of miRNAs following toxic exposure can have a large effect on the whole transcriptome. Each individual miRNA targets many different mRNAs and each mRNA can be targeted by a number of miRNAs (Friedman et al., 2009; Gunaratne et al., 2010), resulting in a complex network of interactions. Thus, it may not be the individual miRNAs, but the miRNA-mediated regulatory pathways that are common across the models of hepatotoxicity. Pathway analysis was performed using the validated

targets for each differentially expressed miRNA. This process was performed independently for each model of hepatotoxicity, but the most significantly enriched pathway for each was the same; Hepatic Fibrosis / Hepatic Stellate Cell Activation (Fig. 5.6). The canonical representation of this pathway consists of two parts, a quiescent hepatic stellate cell (part 1), which can be activated by the secretion of inflammatory mediators following liver damage (part 2). Hepatic stellate cells are known to serve a protective function in the cellular response to liver injury, including activation of fibrogenesis (Schulze-Krebs et al., 2005; Wang et al., 2013a). Fibrosis is one of the predominant histopathological signs of compound-induced hepatotoxicity and has previously been identified following treatment with Thioacetamide and Griseofulvin (Knasmuller et al., 1997; Li et al., 2002). These findings were replicated in this work (Chapter 3, section 3.5.3 and Chapter 4, section 4.5.2) and, furthermore, the PredTox consortium also reported signs of liver fibrosis with high dose treatment (Suter et al., 2011). This provides strong evidence that miRNA-mediated regulation plays a vital role in compound-induced hepatotoxicity and suggests that it is the miRNA networks rather than the specific miRNA changes that are important. Whilst the lists of differentially expressed miRNAs varied between the models, the target mRNAs implemented in the Hepatic Fibrosis / Hepatic Stellate Cell Activation pathway were more similar with 49% common to all three models (Fig. 5.8 and Appendix VII).

Putative miRNA-mRNA interactions of physiological relevance were then investigated, focusing on the FP014SC and Griseofulvin models that had already undergone translational profiling as described in Chapter 3. By mapping the predicted mRNA targets of all the differentially expressed miRNAs to those experimentally identified during the translational profiling, interactions of physiological relevance could be identified. Accepting the limitations discussed previously, only those interactions where there was an inverse expression pattern between miRNA and mRNA were considered (Table 5.4 and Table 5.5). In both models, most of the putative miRNA-mRNA interactions involved a change at the translational level, suggesting that the predominant miRNA-mediated regulation was translational repression rather than mRNA degradation. This is in agreement with other *in vivo* studies (Bazzini et al., 2012; Djuranovic et al., 2012) and highlights the importance of translational profiling when investigating functionally relevant miRNA targets.

One of the more interesting putative interactions within the FP014SC model (miR-336-*Dio3* mRNA) was unlikely to be validated since qRT-PCR had already failed to confirm up-regulation of miR-336 following treatment with high dose FP014SC (Fig. 5.3 B). Therefore, miR-336 was unlikely to be regulating *Dio3* mRNA translation and so this interaction was not pursued

further. However, the putative interaction between *Smarce1* and miR-135a within the Griseofulvin model (Table 5.5) was selected for further investigation. qRT-PCR validated the up-regulation of miR-135a following treatment with Griseofulvin for 22 days (Fig. 5.9 A), and revealed that the very closely related miR-135b was also up-regulated (Fig. 5.9 B). miR-135a and miR-135b are located on different chromosomes (9 and 1 respectively), but only differ in sequence by a single nucleotide, which is not located in the core seed region (Fig. 5.8). The common change in expression supports the hypothesis that members of the same miRNA family cluster and can work in combination to exert a net physiological effect (Abbott et al., 2005; Vasudevan et al., 2007). Furthermore, it was demonstrated in Chapter 3 that repression of *Smarce1* mRNA translation resulted in reduced SMCE1 protein following Griseofulvin treatment for 22 days (Fig. 3.9 and Fig. 3.10). Ideally this interaction would have been duplicated and further validated in an *in vitro* system, and initial work was encouraging, with Griseofulvin inducing a reduction in SMCE1 protein in Hepa 1-6 cells (Chapter 3, Fig. 3.12). However, neither miR-135a nor miR-135b were up-regulated in Hepa 1-6 cells treated with Griseofulvin (Fig. 5.10). A positive interaction at the *in vitro* level would have been a good basis on which to perform future regulation validation studies, for example by utilising some of the methods described by Ferland-McCollough *et al* in their confirmation of *Gdf3* as a target of miR-483-3p (Ferland-McCollough et al., 2012), which include luciferase-based assays and transfection studies. Unfortunately not all *in vivo* effects can be accurately replicated *in vitro,* hence the continued use of animal experimentation. Replacing the established cell line Hepa 1-6 with a primary cell line may provide an *in vitro* model that is more indicative of the *in vivo* situation (Kikkawa et al., 2006).

5.7 CONCLUSION

miRNAs are a large family of translational mediators predicted to regulate up to 60% of protein coding genes. Whilst they did not appear to regulate the repression of *Dio3* mRNA identified in Chapter 4, they did appear to be involved in a wider response to compound-induced hepatotoxicity. With the exception of miR-92b, which was highlighted as a potential biomarker due to its common differential expression across the different models, the majority of the altered miRNAs were unique to each model. Thus, it appeared that in general it was the miRNA-mediated networks, rather than specific miRNAs, that were common to different models of compound-induced hepatotoxicity. By looking concurrently at miRNA and translational profiling data sets from the same model, it was possible to identify specific functionally-relevant miRNA-mRNA interactions. Provided a suitable *in vitro* system was available these interactions could then be further validated and developed. Due to disappointing initial results it was decided not to continue with developing *in vitro* models, but instead to explore the use of circulating miRNAs as biomarkers of hepatotoxicity. Therefore, the next chapter focuses on miRNA expression profiling of plasma samples. Due to limited sample availability initial profiling was limited to plasma derived from those Thioacetamide-treated rats, treated for 25 h with the mid-range dose (100 mg/kg).

CHAPTER 6: THE IDENTIFICATION OF PUTATIVE CIRCULATING miRNA BIOMARKERS OF COMPOUND-INDUCED HEPATOTOXICITY

6.1 SUMMARY

Microarray profiling of RNA extracted from the plasma of rats treated with Thioacetamide revealed that a subset of miRNAs were differentially expressed following treatment. These miRNAs appeared to mediate pathways involved in hepatic fibrosis and stellate cell activation, suggesting that they might function as predictive biomarkers following compound-induced hepatotoxicity. The changes correlated well with increases in ALT levels, which are the current gold standard method for determining the extent of liver injury. Furthermore, it is hypothesised that particular aetiologies of liver damage might cause differing expression profiles of miRNAs, thus certain miRNAs could be implemented in a panel-type expression study to distinguish between different types of hepatic injury.

6.2 INTRODUCTION

6.2.1 The need for novel biomarkers ofcompound-induced hepatotoxicity

Drug development is a time consuming and costly process; it is estimated that the average cost for a pharmaceutical company to bring a new compound to market is about $1.8 billion (Paul et al., 2010). Therefore, improving the efficiency, and thus reducing the cost, of drug development is a constant goal for pharmaceuticals. If improved biomarkers of toxicity, which were truly predictive of later stage toxicity, could be discerned during preliminary stages of the development process, expenditure could be reduced and drug effectiveness increased. The model systems discussed throughout this thesis are established models of hepatotoxicity, or in the case of the PredTox study, compounds demonstrated to have failed late on in the drug development process due to pronounced hepato- and/or nephro-toxicity. Using models of hepatotoxicity that are already well characterised, means that novel molecular biomarkers of toxicity can be identified, which can then be used when new drug candidates are identified and tested.

The current gold standard used as a circulating biomarker of hepatotoxicity is alanine transaminase (ALT) activity. The activity of ALT in the plasma increases with damage (James et al., 1975); however, whilst highly sensitive, alternative isoforms exist elsewhere in the body (Glinghammar et al., 2009; Lindblom et al., 2007), and therefore the technique lacks specificity. For this reason a novel biomarker, with equivalent sensitivity and enhanced specificity is required.

Many miRNAs have been demonstrated to exhibit tissue-specific expression patterns (Liang et al., 2007), which can be useful for determining a pathophysiological state within that tissue. Chapter 5 explored the role of hepatic miRNAs during compound-induced liver injury. However, whilst profiling of tissue samples yields potentially interesting results as well as possible markers of liver damage, accessibility is an issue. With animal studies sampling from any organ will normally require termination of the experiment, thus limiting the potential for a longitudinal study, and to take tissue biopsies in the clinic (particularly from healthy volunteers) is not a minor procedure.

6.2.2 miRNAs in the plasma

The discovery that miRNAs are present in plasma was a significant break-through. Plasma and serum are easily accessible and collected routinely in the clinic (Kirschner et al., 2013).Thus, the identification by Mitchell *et al* of highly stable miRNAs in human plasma samples was well received (Mitchell et al., 2008). The feasibility of using miRNAs as biomarkers for cancer detection was heightened by their deregulation in cancer (Zhang et al., 2007), tissue specificity (Lu et al., 2005) and proven stability in formalin-fixed, paraffin-embedded samples (Li et al., 2007). Not only were plasma miRNAs demonstrated to be present at quantifiable levels and differentially expressed in tumour compared to control samples, they also appeared to be highly resistant to the activities of endogenous RNases (Chen et al., 2008; Mitchell et al., 2008), which are found at high levels within the plasma (Tsui et al., 2002). This stability is likely due to the location of miRNAs within the plasma, where they are thought to exist in at least two physical forms; packaged into vesicles (Kosaka et al., 2010) or associated with protein complexes, such as the Argonaute 2 complex (Arroyo et al., 2011). Whilst the exact proportion of each form remains unclear, the associated stability given to the miRNA aids with downstream processing and is one factor that renders plasma-derived miRNAs attractive for use as biomarkers.

Initial studies on the expression levels of miRNAs in plasma remained focused on cancer; predominantly exploring detection, diagnosis and grading. A range of cancer types have been investigated, including B-cell lymphoma (Lawrie et al., 2008), pancreatic (Kong et al., 2011), breast (Cuk et al., 2013; Roth et al., 2010), colorectal (Huang et al., 2010; Wang et al., 2012b), squamous cell (Wong et al., 2008), lung (Hu et al., 2010) and melanoma (Kanemaru et al., 2011). These findings led others to explore the expression profile of miRNAs in the plasma and serum for other physiological states and conditions including, cardiovascular disease (Hagiwara

et al., 2013), Alzheimer's disease (Kumar et al., 2013) and even psychiatric conditions such as bipolar disorder (Rong et al., 2011).

The first study to explore whether miRNAs in the plasma could function as biomarkers of drug-induced liver injury was completed by Wang *et al* in 2009. They proposed that miRNAs in the plasma could be used to map the pathological development of hepatotoxicity, specifically in cases of human overdose (Wang et al., 2009). Using a mouse model of acetaminophen overdose they identified a subset of miRNAs, some of which were already known to be liver specific, that were more sensitive and identified earlier than standardised diagnostic tests. Much of the work performed subsequently has investigated specific miRNAs, for example miR-122 and miR-192 (Starkey Lewis et al., 2012); miR-122, miR-155 and miR-146a (Bala et al., 2012); and miR-122, miR-192 and miR-193 (Su et al., 2012). Due to its identification in a number of different studies, miR-122 was of particular interest. Whilst, not specific to drug-induced damage, as it was also elevated in plasma samples from patients with non-alcoholic fatty liver (Yamada et al., 2013) and in mouse models of inflammatory liver disease (Bala et al., 2012); increases in miR-122 expression correlated well with changes in ALT levels (Bala et al., 2012; Wang et al., 2009). Furthermore, in some instances the change in expression of miR-122 was more sensitive than (and even preceded) changes in ALT and AST levels (Starkey Lewis et al., 2012; Su et al., 2012; Wang et al., 2009; Zhang et al., 2010). This gives merit to its use as a functional biomarker of liver toxicity. Moreover, miR-122 has the potential to function as a positive control when other differentially expressed plasma miRNAs are investigated. When included as one of a panel of miRNAs, the response across all panel members may give a more specific indication of what type of hepatic injury has occurred (Su et al., 2012). This utilises the known sensitivity of miRNAs as biomarkers and increases their specificity, further enhancing their overall potential (Su et al., 2012).

6.2.3 Challenges with profiling plasma samples

One of the major challenges in performing work on plasma samples is obtaining sufficient amounts of high quality RNA. The approximate concentration of total RNA in the plasma is 300 ng/ml (Weber et al., 2010), of which only a small proportion constitutes miRNAs (Jensen et al., 2011). Due to this low abundance, an RNA carrier is often added during extraction. One of the simplest methods in use is the addition of highly pure glycogen as a co-precipitant. Glycogen improves nucleic acid extraction efficiencies(Turchinovich et al., 2011), and is often selected over alternative carrier molecules such as MS2 carrier RNA, because of its low cost and inert nature (Hengen, 1996).

The most widely used extraction techniques are kit-based methods, including the Qiagen miRNeasy kit (Cheng et al., 2013; Jensen et al., 2011; Kroh et al., 2010; Starkey Lewis et al., 2011), and the miRVana miRNA Isolation kit from Life Technologies (Su et al., 2012; Zhang et al., 2010); or a Trizol LS method (Hastings et al., 2012; Wang et al., 2013b). However, even when using such methods, which have been specifically adapted for isolating plasma RNA, the yield is often too low to accurately quantify (Kroh et al., 2010).To overcome the issue of quantification, most groups undertaking miRNA profiling of plasma samples use an equal volume of RNA, rather than an equal mass. Furthermore, a spiked-in synthetic miRNA from a different species is added to each sample after initial denaturation (Kroh et al., 2010). Due to the fact that any exogenously added miRNAs are not encapsulated in extracellular structures and, therefore, do not benefit from the same protection afforded to endogenous plasma miRNAs, it is essential that they are added after initial denaturation to prevent degradation by the large quantity of RNases found in the plasma (McAlexander et al., 2013). To be used as an accurate reference it is also essential to maintain the spike-in at a physiologically relevant concentration (Kim et al., 2012). The spike-in miRNA enables any differences in the extraction efficiencies between samples to be normalised and/or enables PCR products to be assayed for any inhibitory contamination.

Accurately assessing the quality of recovered RNA from plasma is also very difficult to do. In general, even if a sufficient yield of RNA is obtained to quantify accurately, the normal quality control methods are seldom implemented. One source of contamination that is difficult to avoid is protein. Plasma samples have a high protein concentration (Kroh et al., 2010), which can result in low purity, and elevated A_{320nm} readings (Hastings et al., 2012) on the nanodrop. Furthermore, because plasma RNA does not have the 18S and 28S ribosomal subunits common to normal RNA (Valadi et al., 2007), measurement with a Bioanalyser will not generate a RIN score and thus, there are no reports in the literature of plasma derived RNA being checked for quality in this manner prior to downstream use.

6.3 AIM

To profile miRNA expression in the plasma of rats treated with 100 mg/kg Thioacetamide. In particular to explore whether the large changes seen in other studies of compound-induced hepatotoxicity were also seen in this model system, and whether any novel, physiologically relevant, putative biomarkers could be identified.

6.4 MATERIALS AND METHODS

6.4.1 Animal model

The animal model used for the work described in this chapter was the Thioacetamide-treated rat, dosed at 100 mg/kg and sacrificed after 24 h. Animals were maintained and treated as described in Chapter 2, section 2.1.2.

6.4.2 RNA extraction and quantification

Two methods of RNA extraction were trialled in an attempt to maximise yield.

6.4.2.1 Trizol LS method

This method was adapted from that described in (Hastings et al., 2012). An equal volume of each plasma sample (125 µl) was diluted 1:1 with ultra pure (18 MΩ) water and added to 750 µl Trizol LS (Life Technologies, Paisley, UK) in 1.5 ml tubes. Tubes were vortexed for 10 s and incubated at RT for 5 min. 200 µl chloroform was added and each tube was vortexed for 10 sand incubated at RT for an additional 15 min. Tubes were centrifuged (12,000g, 4°C, 15 min) and the upper aqueous phase was transferred to a clean 1.5 ml tube. The carrier molecule GlycoBlue (Life Technologies, Paisley, UK) was added to a final concentration of 15 µg/ml. 562 µl of a 2 : 1 (375 : 187 µl) EtOH : isopropanol solution was added (0.75X volume of starting Trizol LS) and tubes were vortexed for 10 s and incubated at RT for 10 min. RNA was pelleted by centrifugation (12,000g, 4°C, 20 min) and washed twice with 80% (v/v) EtOH. All traces of EtOH were removed using a DNA SpeedVac (ThermoFisher Scientific, Loughborough, UK) on medium heat for 2 min and RNA pellets were resuspended in 100 µl ultra pure (18 MΩ) water.

To further purify the RNA, an acid-phenol : chloroform clean up was performed as described in Chapter 2, section 2.3.3.1, except that: 1) following transfer of the second upper aqueous phase (and immediately prior to precipitation) GlycoBlue was added to a final concentration of 15 µg/ml; 2) samples were precipitated in 1/10th volume of 3 M NaOAc (pH 5.2) and 2.75X volume of a 2 : 1 EtOH : isopropanol solution; 3) following washing, all traces of EtOH were removed using a DNA SpeedVac as described above; and 4) RNA pellets were resuspended in 20 µl ultra pure (18 MΩ) water.

6.4.2.2 Qiagen miRNeasyMini kit

RNA was extracted according to the manufacturer's instructions (Qiagen, Venlo, Netherlands). Briefly, 50 µl of each plasma sample was added to 5X volume of QIAzol Lysis reagent in 1.5 ml tubes, vortexed for 10 s and incubated at RT for 5 min. Chloroform (1X starting plasma volume) was added, tubes were vortexed for 10 s and incubated at RT for an additional 3 min. Tubes were centrifuged (12,000g, 4°C, 15 min) and the upper aqueous phase was transferred to a clean 1.5 ml tube. 1.5X volume 100% EtOH was added and mixed by pipetting, and the entire volume was transferred to an RNeasy Mini spin column. Columns were centrifuged (8000g, RT, 15 sec) and washed sequentially with 500 µl buffer RWT and 500 µl buffer RPE. RNA was eluted using RNase-free water; 50 µl was added to the spin column filter and incubated at RT for 1 min. Centrifugation (8000g, RT, 1 min) recovered the RNA.

6.4.2.3 Quantification and quality control

Under normal conditions, prior to any downstream analysis, extracted RNA samples from any source are quantified and QC checked using a Nanodrop-1000 spectrophotometer (ThermoFisher Scientific, Loughborough, UK) and a 2100 Bioanalyser (Agilent Technologies, Santa Clara, CA), see Chapter 2, sections 2.3.3 and 2.3.4.2. In this case the Bioanalyser analysis was performed, not to assess RNA quality by RIN score (as RNA from plasma should not contain ribosomal RNA, see section 6.2.3), but to confirm there was no RNA contamination from lysed blood cells.

6.4.2.4 RNA extraction including spike-in

RNA was extracted from each plasma sample using the Trizol LS method, exactly as described in section 6.4.2.1, except that following addition of Trizol LS (and prior to addition of chloroform) synthetic cel-miR-39 (Qiagen, Venlo, Netherlands) was added. Prior to using, it was necessary to dilute the spike-in to a concentration similar to the observed endogenous levels of RNA within plasma (Kim et al., 2012). Due to the low RNA yields from plasma samples, this typically means diluting to the femtomolar to attomolar range (Hastings et al., 2012). Qiagen recommended that the final concentration of spike-in added to each PCR was 2.7×10^5 copies/µl. Thus, a serial dilution was performed to obtain a concentration of 4.6×10^6 copies/µl and 3.5 µl was added to each extraction, resulting in a final concentration of 8.1×10^5. The final RNA was diluted 1:3 in the reverse transcription master mix, giving a working concentration of 2.7×10^5 copies/µl.

6.4.3 miRNA profiling using microarrays

6.4.3.1 Microarrays: Agilent

For improved sensitivity Agilent miRNA microarrays and labelling kits were used according to the manufacturer's instructions, with the exception of a reduced starting quantity of RNA. This probe set contained 15,000 probes and corresponded to version 16 of miRBase. Due to the low yields of RNA from plasma, most of the literature agrees that for profiling experiments equal volumes of RNA, rather than equal concentrations, should be used (Zampetaki and Mayr, 2012). Therefore, instead of labelling the (Agilent) recommended 100 ngs RNA, 2 µl of each plasma RNA sample was used.

6.4.3.1.1 Labelling

RNA was added to a Calf Intestinal Alkaline Phosphatase (CIP) reaction comprised of 0.4 µl 10X CIP buffer, 0.5 µl CIP and1.1 µl diluted labelling spike-in solution. The reaction was incubated at 37°C for 30 min to dephosphorylate the RNA. 2.8 µl 100% DMSO was added, samples were denatured at 100°C for 5 min and chilled on ice. RNA was ligated to 3 µl cyanine3-pcp, in a reaction also comprised of 1 µl 10X T4 RNA Ligase buffer and 0.5 µl T4 RNA ligase. Ligation proceeded at 16°C for 2 h. Labelled RNA was purified using Micro Bio-Spin™6 columns (Bio-Rad, Hertfordshire, UK), according to the manufacturer's instructions. Briefly, columns were drained of buffer and samples were applied and centrifuged (1000g, RT, 4 min). Purified RNA was dried down using a DNA SpeedVac (ThermoFisher Scientific, Loughborough, UK) on medium heat for 1 h.

6.4.3.1.2 Hybridisation and scanning

The resulting RNA pellets were resuspended in 17 µl RNase-free water, mixed with 22.5 µl 2X Hi-RPM Hybridisation buffer, 4.5 µl 10X blocking agent and 1 µl diluted hybridisation spike-in solution, and denatured at 100°C for 5 min. Samples were chilled on ice and loaded onto rat miRNA Microarray Release 16.0, 8x15k microarrays. Hybridisation was performed at 55°C overnight in a rotating (20 RPM) chamber (for a minimum of 20 h).

Following hybridisation, slides were washed using the Agilent wash buffer reagents (wash 1: wash buffer 1, 5 min; wash 2: pre-warmed (37°C) wash buffer 2, 5 min) and scanned with a G2505C Agilent Microarray Scanner (scan control version A.8.4.1).

6.4.3.1.3 Data analysis

Data was extracted using the Agilent Feature Extraction software (version 10.7.3.1) and analysed using Agilent GeneSpring GX software (version 12.1). A quality control report was produced by the software for each scanned image. Any report that indicated failure of the defined QC parameters was excluded from downstream analysis. To analyse statistically significant differential expression an unpaired Student's T-Test with Benjamini-Hochberg multiple testing correction was applied. miRNAs that had a *p* value≤ 0.05 and a fold change of >1.5 were considered to be both statistically and biologically significant.

6*.4.3.1.4 Regulatory pathway analysis*

Pathway analysis was performed by first using the miRwalk database to identify validated mRNA targets, and then Ingenuity IPA Software to identify functional interactions, as described in Chapter 5, section 5.4.5.4.

6.4.4. Quantitative RT-PCR

The RNA samples used for qRT-PCR contained synthetic cel-miR-39, spiked-in during the extraction process, as described in section 6.4.2.4. qRT-PCR was performed using Taqman reagents as described in Chapter 5, section 5.4.4, except due to the limited amount of RNA obtained from plasma an equal volume of RNA from each sample was used. A standard curve was prepared by reverse transcribing different dilutions of RNA and performing PCR with primers designed against cel-miR-39 on each dilution. The relative cDNA (Log_{10}[RNA input (µl)] was plotted and used to assess efficiency for each RNA sample. miR-16 was used as an endogenous control as the expression of this miRNA did not change across the samples (*p*=0.3).Statistically significant differences were calculated using a two-tailed Student's T-Test.

6.4.5 Measurement of alanine transaminase and correlation with miRNA expression

ALT activity levels for each plasma sample were measured as described in Chapter 4, section 4.4.2.2. These were correlated with the qRT-PCR measurements for those miRNAs of interest using Pearson's correlation test in GraphPad Prism software (GraphPad, La Jolla, CA).

6.4.6 miRNA profiling of liver samples from Thioacetamide-treated rats using microarrays

Global hepatic miRNA expression analysis of the rat liver samples was performed as described in Chapter 5, section 5.4.5.

6.5 RESULTS

6.5.1 RNA extraction from plasma samples

6.5.1.1 Using a Trizol LS extraction method resulted in the greatest RNA yield from the plasma of rats treated with Thioacetamide

Extracting RNA from the plasma was not a straightforward process. The low quantities of circulating nucleic acids make quantification difficult. Using a Trizol LS method resulted in a 6- to 24-fold increase in RNA yield when compared to the miRNeasy kit (Table 6.1). Attempts to increase the yield obtained from the miRNeasy kit by increasing the starting amount of plasma from 50 µl to 100 µl were unsuccessful, actually reducing the yield further (data not shown).

The normal methods for quality control assessment following RNA extraction are not suitable for use with plasma-derived RNA. The high protein carryover resulted in low nanodrop ratios, and the lack of ribosomal RNA meant a RIN score could not be accurately determined (Table 6.1). However, the absence of ribosomal RNA in all samples indicated that there was no contamination from blood cells.

Since the Trizol LS method consistently resulted in higher yields of extracted plasma RNA, with generally less protein contamination than the Qiagen miRNeasy kit, it was this method that was selected as most suitable for all future plasma extractions.

6.5.1.2 Inclusion of a synthetic spike-in did not reduce RNA yields and demonstrated that, at the quantity used, samples were free from inhibitory contaminants

Synthetic *Caenorhabditis elegans* (Cel) miR-39 was spiked into each RNA sample to check that any PCR reactions were not contaminated with inhibitors. Serial dilutions of RNA were reverse transcribed and PCR was performed. When the relative cDNA (Log_{10}[RNA input (µl)]) was plotted against CT value the amplification efficiency for each plasma sample had a linear correlation coefficient (R^2) of ≥ 0.95 and a PCR efficiency of between 100% and 128% (Fig. 6.1). Where the PCR efficiency was particularly high (Fig. 6.1 A and B) it was possible that there was some contamination, at the larger starting volumes (2 µl – 0.5 µl). As such, the standard curves were used to determine a suitable starting volume of RNA, at which no PCR inhibition was evident. Thus, a standard starting volume of 0.25 µl RNA was selected for further qRT-PCR work. The sensitivity of the technique ensured that using such a small starting quantity would not be detrimental.

Table 6.1. Nanodrop and Bioanalyser results following RNA extraction from plasma.

Extraction method	Sample	Nanodrop			Bioanalyser
		Concentration (ng/µl)	260/280	260/230	RIN score
Trizol LS	Plasma 1	26.91	1.54	1.02	2.60
	Plasma 2	29.49	1.61	1.11	2.70
	Plasma 3	26.28	1.58	1.04	1.70
	Plasma 4	28.23	1.56	1.03	2.60
	Plasma 5	32.89	1.60	1.13	2.60
	Plasma 6	41.85	1.61	1.34	2.60
miRNeasy kit	Plasma 1	3.14	1.04	0.42	N/A
	Plasma 2	2.62	1.41	0.59	N/A
	Plasma 3	3.17	1.10	0.48	N/A
	Plasma 4	1.72	1.12	0.39	N/A
	Plasma 5	4.21	1.91	0.68	N/A
	Plasma 6	2.53	1.22	0.15	N/A
Tri reagent (Sigma)	Liver RNA	1592.93	2.07	2.00	9.60

6 independent plasma samples were measured. Results obtained from a Tri reagent liver RNA extraction are shown for comparison purposes. Recommended values for a normal RNA extraction are: 260/280 >1.8, 260/230 >1.5, RIN ≥ 7. These criteria are not valid for the quality assessment of RNA extracted from the plasma.

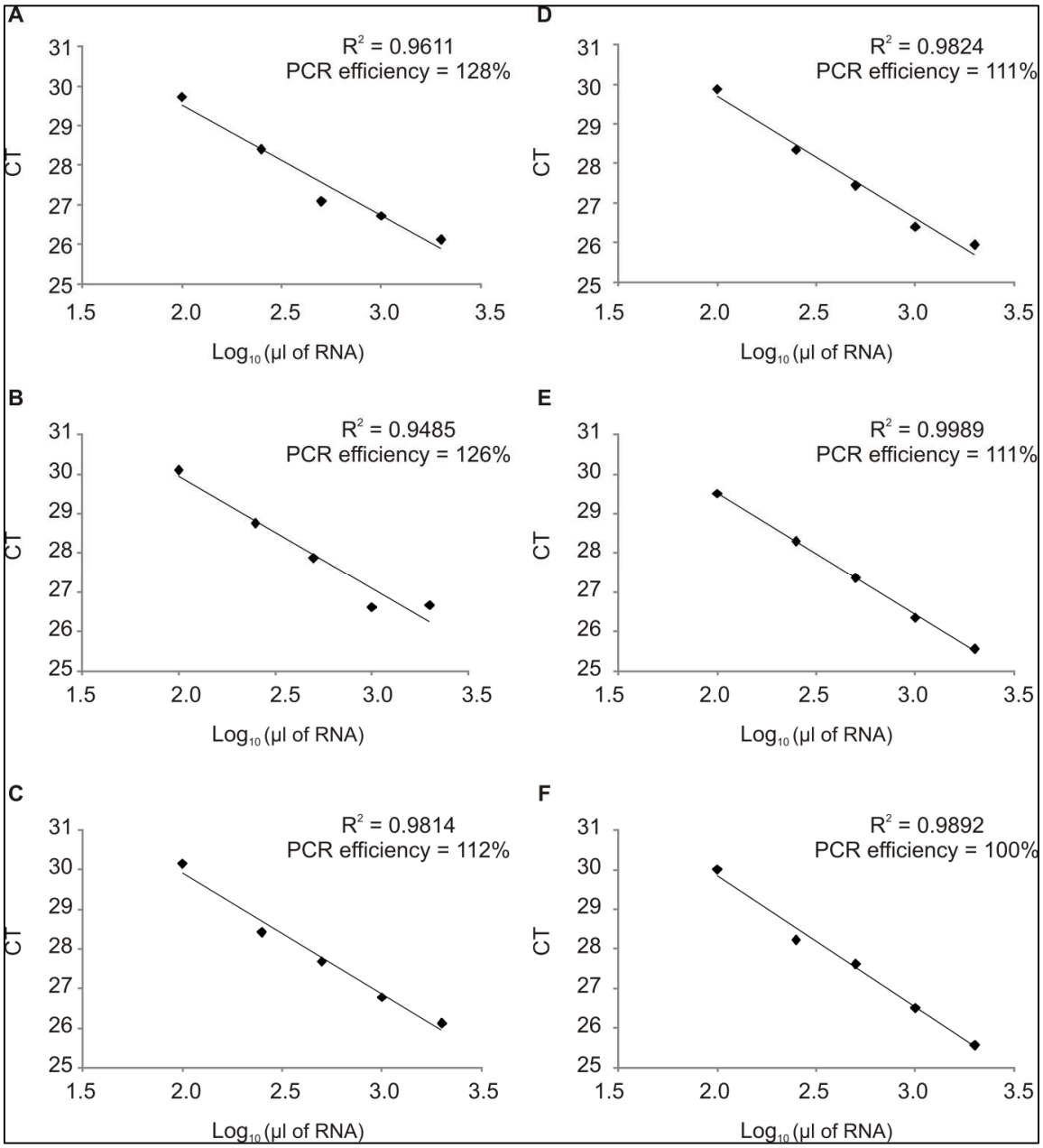

Fig. 6.1. Standard curves of cel-miR-39 provide evidence of efficient PCR. Serial dilutions of plasma RNA that included a synthetic cel-miR-39 spike-in were analysed by qPCR. Raw CT values were plotted against the $\log_{10}$(volume of RNA). The percentage efficiency and linear correlation coefficient are marked on each graph. **A**-**C** were from vehicle-treated rats that received 0.9% saline, whilst **D**-**F** were from rats treated with 100 mg/kg Thioacetamide in 0.9% saline.

6.5.2 Microarray analysis revealed that miRNAs were detected in the plasma of rats treated with Thioacetamide

There is little published work on the microarray profiling of circulating miRNAs. This is probably due to the low yields of RNA extracted from plasma being more easily profiled by qRT-PCR, which is a more sensitive technique (Pritchard et al., 2012). Microarrays were used here in an attempt to identify any novel circulating miRNA species. Our group had previously used an Exiqon microarray platform to successfully profile miRNAs from human sperm, which is another biological fluid with a limited amount of RNA (Marczylo et al., 2012). This demonstrated that miRNAs could be profiled from limited starting material using microarrays. The Agilent microarray platform was selected as it has been shown to have increased accuracy over the Exiqon platform (used for the miRNA profiling of the liver samples, Chapter 5) (Sah et al., 2010). Furthermore, the Agilent platform had already been used to successfully profile plasma miRNAs (Wang et al., 2009).

Fig. 6.2 A shows an example of a microarray hybridised with rat plasma RNA. An example of a microarray hybridised with a rat liver cell line is shown in Fig. 6.2 B for comparison. Although fewer miRNAs were detected in the plasma; a sufficient number of probes were detected for the software to generate a results file and, when looking at replicate samples, many of the miRNAs were reproducible between arrays, indicating that it was not a case of non-specific hybridisation.

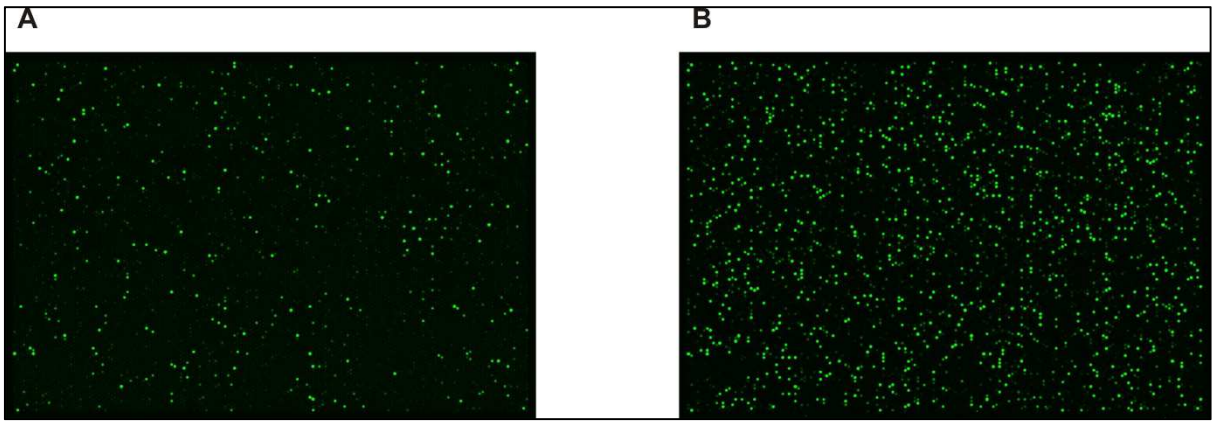

Fig. 6.2. Microarray profiling of miRNAs from rat plasma samples and a rat liver cell line resulted in hybridisation. (**A**) plasma miRNAs and (**B**) rat liver cell line miRNAs. Thioacetamide-treated rats received a single dose of 100 mg/kg Thioacetamide or vehicle-only (0.9% saline) treatment and were sacrificed after 24 h (n=3). Blood was collected from the descending vena cava and centrifuged to separate the plasma.

6.5.3 miRNA expression analysis

Following treatment with Thioacetamide, 11 plasma miRNAs with a fold change ≥ 2.5 were identified as significantly differentially expressed (Table 6.2). These altered miRNAs were uploaded to Ingenuity IPA software (Ingenuity® Systems, www.ingenuity.com) and connections between them were investigated (Fig. 6.3). This revealed that the majority of the deregulated miRNAs targeted common mRNAs, providing support for microarrays as a useful tool for identifying circulating miRNAs with physiological relevance.

Table 6.2. Significant miRNA changes in the plasma of rats treated with Thioacetamide.

miRNA name	Fold change (log_2)	*P* value	Expression
rno-miR-122-5p	7.715	0.001	↑
rno-miR-133b-3p	-8.883	0.001	↓
rno-miR-140-5p	-9.581	0.000	↓
rno-miR-144-3p	-9.005	0.000	↓
rno-miR-185-5p	-9.251	0.000	↓
rno-miR-18a-5p	-9.616	0.001	↓
rno-miR-215	-9.300	0.000	↓
rno-miR-27b-3p	1.736	0.001	↑
rno-miR-301a-3p	-9.246	0.000	↓
rno-miR-328a-5p	1.612	0.000	↑
rno-miR-425-5p	-8.943	0.000	↓

Fold change
210.157
1.00
0.001

Rats received 100 mg/kg Thioacetamide or vehicle-only (0.9% saline) and were sacrificed after 24 h. Statistical significance ($p \leq 0.05$) was determined using an unpaired T-Test with Benjamini-Hochberg multiple testing correction.

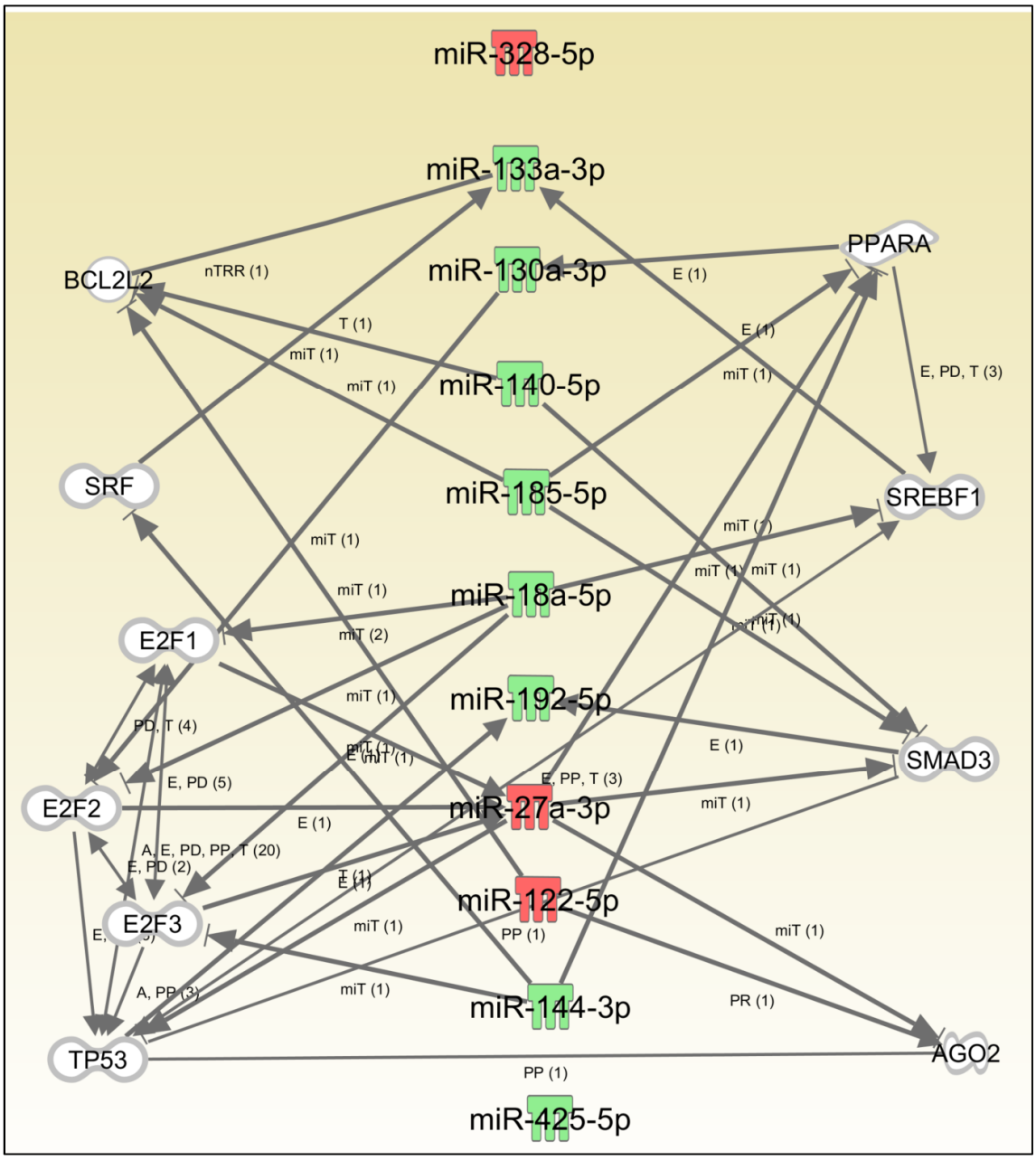

Fig. 6.3. Differentially expressed plasma miRNAs following Thioacetamide treatment target common mRNAs. The list of significantly altered miRNAs ($p \leq 0.05$, fold change ≥ 2.5) was uploaded to Ingenuity IPA software and any connections between them were mapped. miRNAs up-regulated following treatment are shown in red, whilst down-regulated miRNAs are shown in green. Thioacetamide-treated rats received a single dose of 100 mg/kg Thioacetamide or vehicle-only (0.9% saline) treatment and were sacrificed after 24 h (n=3). (Arrows denote targeting relationships between molecules; straight lines denote non-targeting relationships between molecules).

Due to the nature of the work described in this chapter the number of statistically significant differentially expressed miRNAs was too small for a more comprehensive pathway analysis. Whilst inclusion of a multiple testing correction reduces the likelihood of false positives when datasets with a large number of potentially deregulated targets are simultaneously compared, for example with microarrays performed on tissue samples (Zhang, 2011), it can also lead to the exclusion of true positives when considering datasets with reduced numbers of targets (as is seen when profiling plasma RNA with microarrays). Thus, accepting a higher false positive rate can be advantageous when analysing smaller datasets with a smaller number of targets. Therefore, the plasma miRNA dataset was reanalysed using less stringent settings, with the exclusion of multiple testing corrections. This increased the significant ($p \leq 0.05$) list of differentially expressed miRNAs from 11 to 27 (for full list see Table 6.3) and enabled a more comprehensive pathway analysis. Validated target mRNAs of the deregulated miRNAs were downloaded from the miRWalk database. Of the 27 differentially expressed miRNAs uploaded to miRWalk, all had at least 1 validated target and once duplicates were removed and the list had been uploaded to IPA, 264 mRNAs were successfully mapped by the software. As in the liver (Chapter 5, Fig. 5.6), the most significantly enriched pathway was Hepatic Fibrosis / Hepatic Stellate Cell Activation. The two main components to this pathway, together with miRNA interactions are shown in Fig. 6.4 and Fig. 6.5.

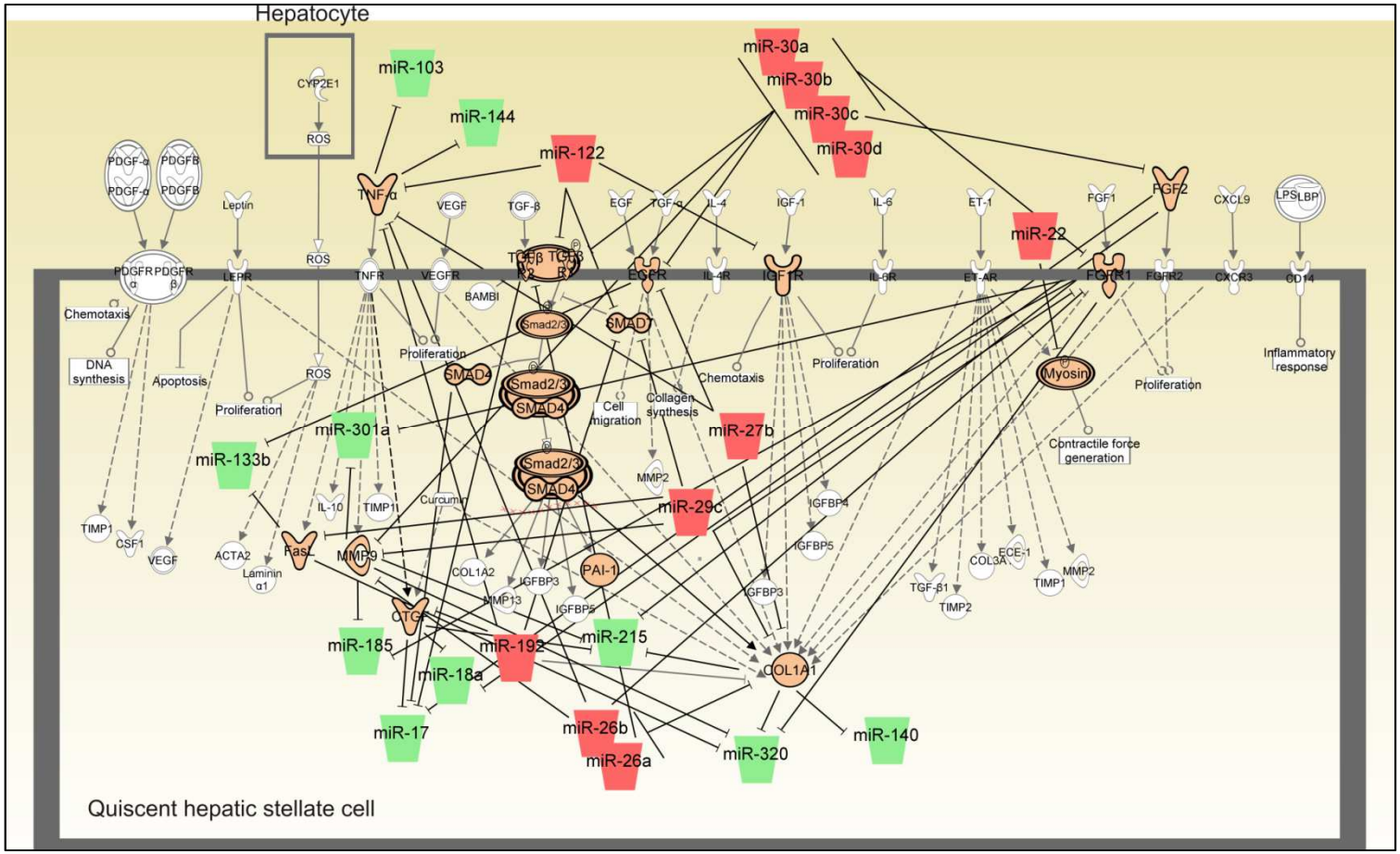

Fig. 6.4. Part 1 of the Hepatic Fibrosis / Hepatic Stellate Cell Activation canonical pathway. Validated target mRNA are shown in orange, miRNAs that are deregulated in the plasma of Thioacetamide-treated rats are coloured according to their change in expression (up-regulated are shown in red, down-regulated in green). Solid and dashed lines indicate interactions between molecules (solid represent direct interactions, and dashed indirect interactions).

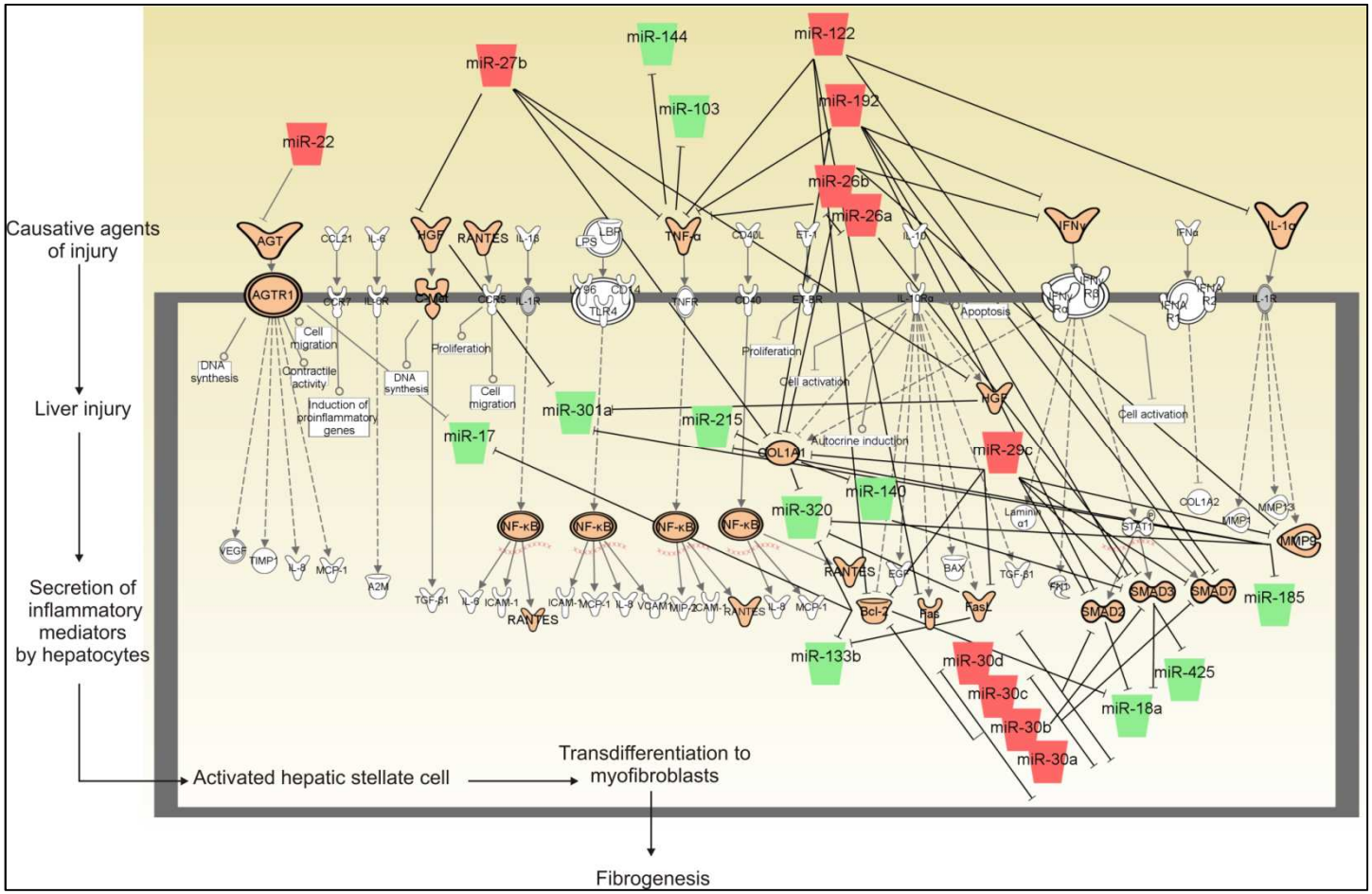

Fig. 6.5. Part 2 of the Hepatic Fibrosis / Hepatic Stellate Cell Activation canonical pathway. Following damage the normally quiescent hepatic stellate cell is activated and forms myofibroblasts. These function to resolve liver injury through regulatory mechanisms and secretory activities. Validated target mRNA are shown in orange, miRNAs that are deregulated in the plasma of Thioacetamide-treated rats are coloured according to their change in expression (up-regulated are shown in red, down-regulated in green). Solid and dashed lines indicate interactions between molecules (solid represent direct interactions, and dashed indirect interactions).

6.5.4 Validation of microarray changes using qRT-PCR

qRT-PCR was used to measure changes in specific miRNA expression levels following treatment with 100 mg/kg Thioacetamide.

6.5.4.1 miR-122

The most significantly up-regulated miRNA identified by microarray analysis was miR-122, with a 210-fold increase in the plasma following Thioacetamide treatment (Table 6.2). qRT-PCR validated this change, with a similarly large 235-fold increase in expression (Fig. 6.6 A).

6.5.4.2 miR-30d

Using the less stringent analysis settings for microarray analysis the whole miR-30 family of miRNAs, encompassing miR-30a, miR-30b, miR-30c and miR-30d, were up-regulated in the plasma following Thioacetamide treatment (Table 6.3). miR-30d demonstrated the largest increase in expression of the family members with a 6-fold increase in expression. qRT-PCR validated this change, with a 12-fold increase in expression following treatment (Fig. 6.6 B).

*6.5.4.3 miR-192**

miR-192* was identified as a miRNA of interest in Chapter 5, demonstrating a significant, time-dependent down-regulation following FP014SC treatment and an almost significant up-regulation (p=0.07) 24 h after Thioacetamide treatment (Fig. 5.4 C). qRT-PCR revealed that this miRNA was up-regulated in the plasma following Thioacetamide treatment, with a significant 39-fold increase in expression (Fig. 6.6 C).

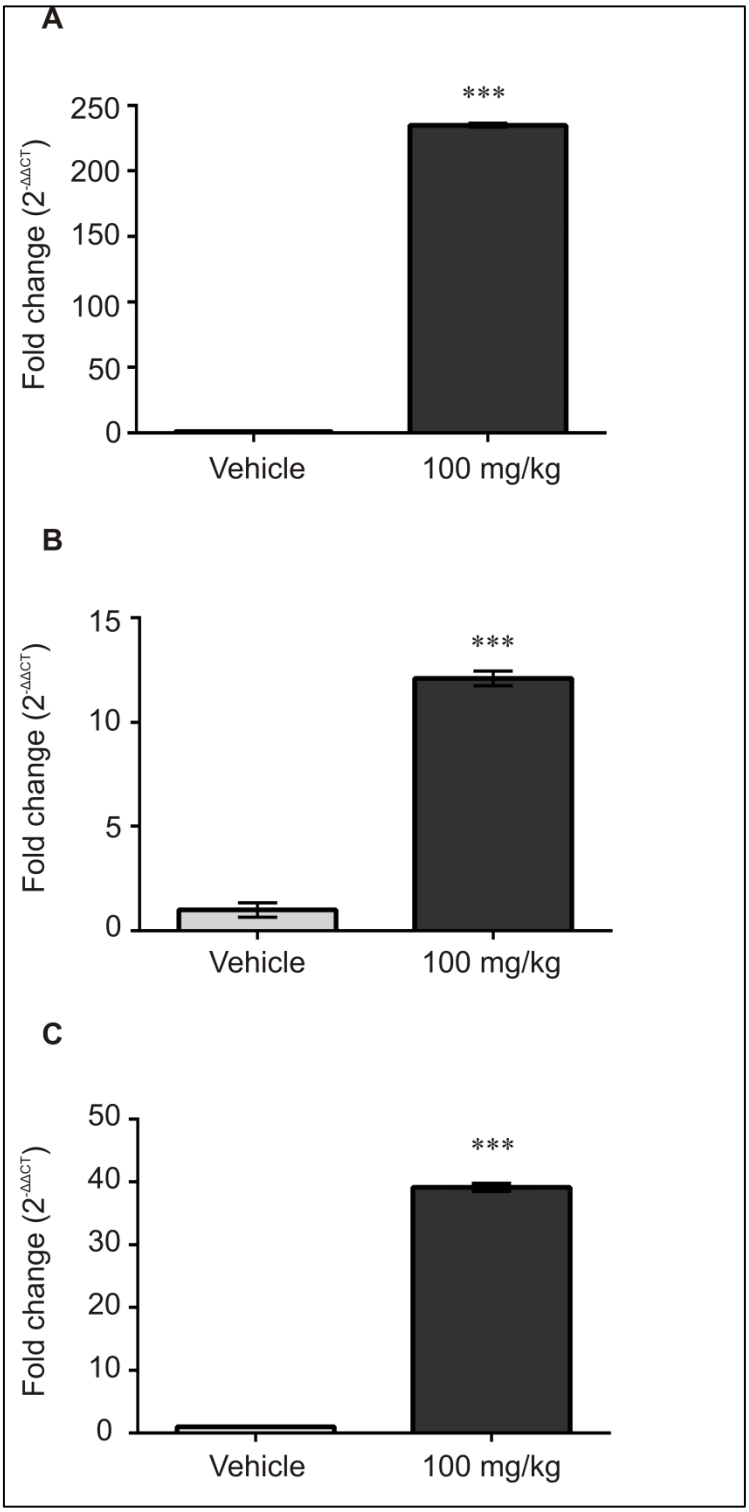

Fig. 6.6. qRT-PCR analysis validated the microarray results. (**A**) miR-122, (**B**) miR-30d and (**C**) miR-192*. qRT-PCR data were normalised to miR-16 and represent mean ± SEM. *** $p \leq 0.001$ (T-Test). Thioacetamide-treated rats received a single dose of 100 mg/kg Thioacetamide or vehicle-only (0.9% saline) treatment and were sacrificed after 24 h (n=3).

6.5.4 miRNA changes correlated with increased ALT levels

The gold standard biochemical markers for evaluation of liver integrity both in the clinic and in animal models are ALT and AST (Ozer et al., 2008). Due to their widespread use and sensitivity any novel biomarker would need to show good correlation with ALT or AST measurements. Most groups opt to correlate miRNA expression changes with ALT activity, as this is more liver-specific than AST. AST can also be released from damaged myocytes. (Ozer et al., 2008), thus, of the two, ALT is considered the more sensitive marker of liver inflammation. A Pearson's correlation test was performed to compare the relative abundance of each miRNA of interest with ALT activity. The increase in expression of all three miRNAs of interest significantly correlated with peak plasma ALT activity (Fig. 6.7).

6.5.6 miRNAs differentially expressed in the plasma did not overlap with those differentially expressed in the liver

Comparison of the global liver and plasma miRNA profiles from the same rats 24 h after Thioacetamide treatment revealed that there was no overlap between the differentially expressed miRNAs. None of the miRNAs altered in the plasma were also altered in the liver or vice versa (Table 6.3). The changes in the plasma were generally of a greater magnitude than those observed in the liver.

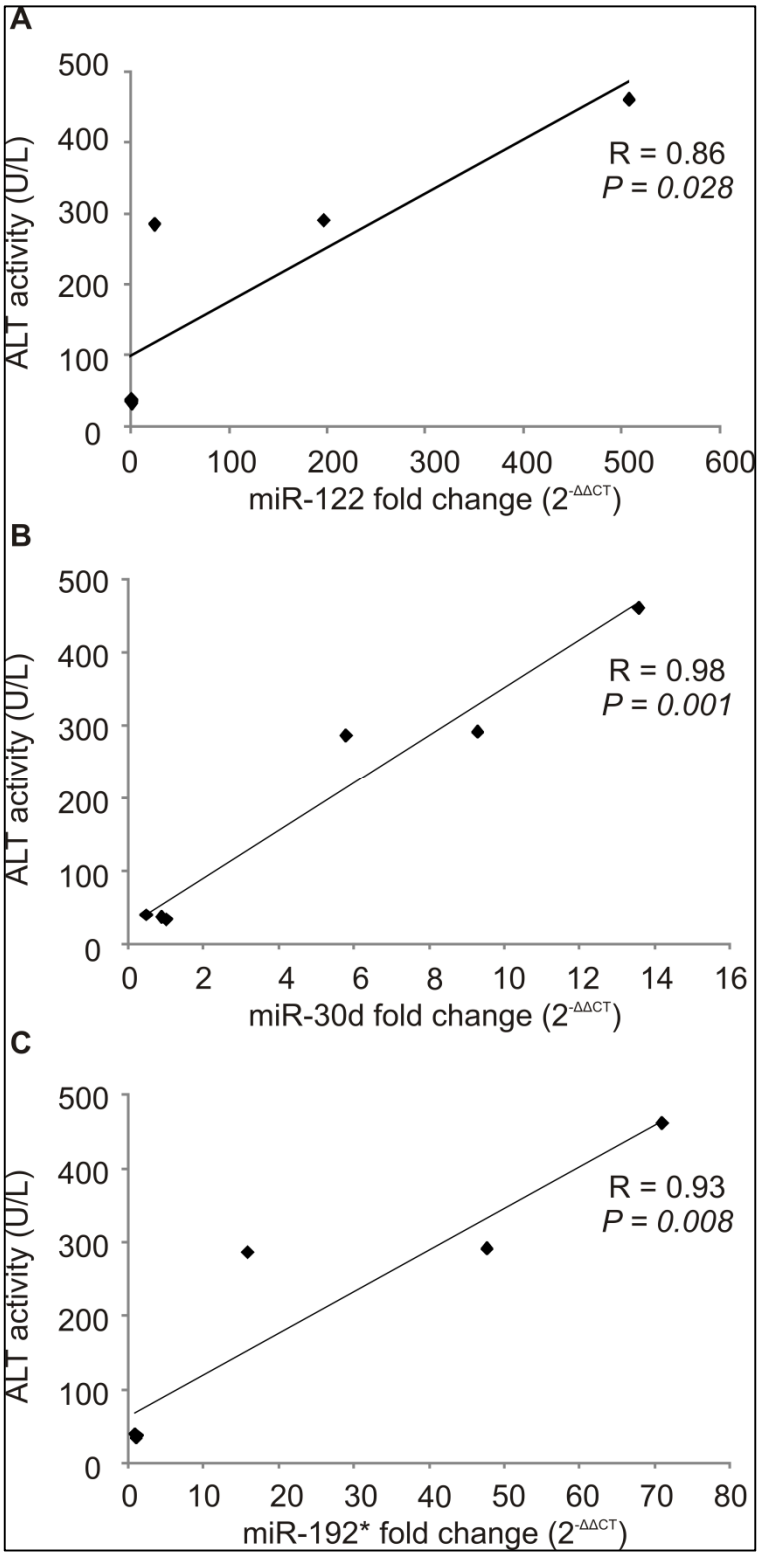

Fig. 6.7. Plasma miRNA levels significantly correlated with ALT activity following Thioacetamide treatment. The fold change in expression of (**A**) miR-122, (**B**) miR-30d and (**C**) miR-192* was plotted against ALT activity. Thioacetamide-treated rats received a single dose of 100 mg/kg Thioacetamide or vehicle-only (0.9% saline) treatment and were sacrificed after 24 h (n=3).

Table 6.3. Significant miRNA changes in the liver and the plasma of rats treated with Thioacetamide.

Liver

miRNA name	Fold change (log_2)	*p* value	Expression
rno-let-7d	-1.307	0.029	↓
rno-let-7f	-0.539	0.037	↓
rno-miR-201	0.686	0.037	↑
rno-miR-21	0.639	0.008	↑
rno-miR-214	-0.703	0.028	↓
rno-miR-216a	0.682	0.029	↑
rno-miR-223	0.675	0.024	↑
rno-miR-23b	-0.691	0.020	↓
rno-miR-30c-1*	-0.542	0.026	↓
rno-miR-30e	-0.438	0.027	↓
rno-miR-341	0.557	0.004	↑
rno-miR-34a*	-0.489	0.022	↓
rno-miR-3546	0.703	0.004	↑
rno-miR-3556b	-0.712	0.001	↓
rno-miR-3563-5p	-0.437	0.000	↓
rno-miR-3573-3p	1.152	0.002	↑
rno-miR-3584-3p	0.724	0.001	↑
rno-miR-3596b	-0.700	0.025	↓
rno-miR-379*	-0.438	0.042	↓
rno-miR-380*	-0.852	0.037	↓
rno-miR-505*	-0.660	0.040	↓
rno-miR-543*	-0.953	0.028	↓

Plasma

miRNA name	Fold change (log_2)	*p* value	Expression
rno-miR-103-3p	-1.482	0.002	↓
rno-miR-122-5p	7.715	0.001	↑
rno-miR-133b-3p	-8.883	0.001	↓
rno-miR-140-5p	-9.581	0.000	↓
rno-miR-144-3p	-9.005	0.000	↓
rno-miR-17-5p	-1.141	0.033	↓
rno-miR-185-5p	-9.251	0.000	↓
rno-miR-188-5p	3.631	0.001	↑
rno-miR-18a-5p	-9.616	0.001	↓
rno-miR-192-5p	4.614	0.007	↑
rno-miR-211-3p	2.299	0.035	↑
rno-miR-215	-9.300	0.000	↓
rno-miR-22-3p	5.796	0.015	↑
rno-miR-26a-5p	1.879	0.006	↑
rno-miR-26b-5p	1.188	0.023	↑
rno-miR-27b-3p	1.736	0.001	↑
rno-miR-29c-3p	1.767	0.010	↑
rno-miR-301a-3p	-9.246	0.000	↓
rno-miR-30a-5p	1.998	0.009	↑
rno-miR-30b-5p	2.321	0.007	↑
rno-miR-30c-5p	0.803	0.035	↑
rno-miR-30d-5p	2.582	0.012	↑

Fold change
210.157
1.00
0.001

Table 6.3.continued

Liver

miRNA name	Fold change (log_2)	*p* value	Expression
rno-miR-664-1*	0.894	0.010	↑
rno-miR-664-2*	1.006	0.050	↑
rno-miR-7a-2*	-0.759	0.007	↓
rno-miR-92b	1.130	0.001	↑

Plasma

miRNA name	Fold change (log_2)	*p* value	Expression
rno-miR-320-3p	**-0.488**	**0.006**	**↓**
rno-miR-328a-5p	1.612	0.000	↑
rno-miR-3596a	-8.777	0.001	↓
rno-miR-425-5p	-8.943	0.000	↓
rno-miR-652-5p	1.899	0.003	↑

Rats received 100 mg/kg Thioacetamide or vehicle-only (0.9% saline) and were sacrificed after 24 h. Statistical significance ($p \leq 0.05$) was determined using an unpaired T-Test.

6.6 DISCUSSION

Chapter 5 demonstrated that miRNAs are differentially expressed in the liver following treatment with a range of hepatotoxic compounds. With the recent identification of miRNAs in plasma (Mitchell et al., 2008) and serum (Chen et al., 2008) much work has been undertaken to explore the feasibility of using these small RNA species as early biomarkers of a variety of physiological conditions. The work presented in this chapter supports the use of circulating miRNAs as novel miRNA biomarkers of compound-induced hepatotoxicity.

There is no common consensus in the literature as to whether to extract circulating miRNAs from the serum or the plasma. The first study to isolate miRNAs from blood suggested that there were few differences between the two circulating fluids (Mitchell et al., 2008). However, more recent work indicated that out of 282 miRNAs identified endogenously in the circulation, 6% showed differential expression between the serum and plasma (Cheng et al., 2013). The authors did not express a preference for one over the other, but concluded that it is important to consider both options. Alternative work has suggested that serum samples result in reduced RNA yields compared to plasma samples (Heneghan et al., 2010). Due to the already low recovery of RNA from the samples used in this chapter (Table 6.1), analysis was restricted to the plasma. None of the miRNAs selected for further validation in this chapter featured on Cheng *et al*'s list of differentially expressed miRNAs (Cheng et al., 2013), indicating that the changes in expression were not due to plasma processing and that a conserved effect would likely be observed in the serum. This is important because a putative biomarker should ideally be readily identifiable in both blood-based fluids (i.e. whichever is available for testing).

Two plasma RNA extraction methods were attempted; a Trizol LS method (Hastings et al., 2012), with minor adaptations; and a miRNeasy kit (Qiagen). The Trizol LS method proved to be superior to the miRNeasy kit, resulting in up to 24-fold higher RNA yields (Table 6.1). The yields obtained were similar to those reported in the literature (Zhang et al., 2010). Furthermore, in keeping with the literature, attempts to increase the RNA yield by increasing the starting quantity of plasma proved unsuccessful (section 6.5.1.1) (Kim et al., 2012; McAlexander et al., 2013). This was probably due to an increased presence of inhibitory contaminants (Kim et al., 2012; McAlexander et al., 2013).

Conventional methods for determining RNA quality (nanodrop and Bioanalyser) were unsuitable for use with the RNA derived from plasma due to the fact that plasma is protein-rich (Kroh et al., 2010; Zampetaki and Mayr, 2012) and, thus, some carryover is inevitable. This results in elevated A_{320nm} readings (Hastings et al., 2012). Furthermore, the low RNA yields

cause increased phenol carryover (Rio et al., 2010), which leads to low 260/280 and 260/230 ratios, and the absence of the rRNAs, 18S and 28S (Valadi et al., 2007), prevents determination of a RIN score on the Bioanalyser. It was important for downstream analysis that the RNA was free from contaminants that might inhibit reverse transcription, PCR or labelling reactions. To avoid contamination with heparin, which is a potent inhibitor of reverse transcription reactions (Johnson et al., 2003), potassium/EDTA tubes were used for blood collection, as recommended by (Zampetaki and Mayr, 2012). There was still the possibility that other contaminants might be present, therefore, as recommended in the literature, a spike-in miRNA (synthetic cel-miR-39) was added during the extraction process (Hastings et al., 2012; Kroh et al., 2010). This synthetic cel-miR-39 was measured by qRT-PCR across a 20-fold dynamic range (from 2 µl to 0.1 µl) and demonstrated efficient amplification in all samples at the lower volumes (Fig. 6.1), suggesting that there would be no interference by inhibitory contaminants when these volumes were input into downstream qRT-PCR.

The majority of the work published to date has used qRT-PCR to profile circulating miRNAs (Bala et al., 2012; Chen et al., 2008; Cheng et al., 2013; Starkey Lewis et al., 2011; Yang et al., 2012), due to the high sensitivity of this technique (Jensen et al., 2011; Pritchard et al., 2012). One of these studies did attempt a comparison of different profiling technologies(Jensen et al., 2011), including a microarray-based approach (the GeneChip 2.0 Array from Affymetrix combined with Genisphere's 3DNA FlashTag labelling kit). However, they concluded that this particular platform lacked sufficient sensitivity for profiling plasma miRNAs (Jensen et al., 2011). Although the combination of this labelling kit and microarray platform proved unsuccessful, the Agilent miRNA microarray platform was used successfully by Wang *et al* to identify 43 differentially expressed miRNAs following Acetaminophen overdose in a mouse model of drug-induced hepatotoxicity (Wang et al., 2009). The benefit of microarray-based profiling is the simultaneous measurement of a large number of miRNAs at a time. Thus, to identify novel plasma miRNA biomarkers of Thioacetamide-induced toxicity the Agilent microarray system was used.

Despite using less than the recommended starting amount of total RNA, the plasma RNA samples labelled and hybridised successfully (Fig. 6.2). Preliminary analysis revealed 11 miRNAs that were differentially expressed in the plasma of rats treated with Thioacetamide (Table 6.2). These miRNAs correlated well with the current literature; for example, the positive identification of miR-122, which is a highly expressed plasma miRNA in cases of hepatotoxicity (Bala et al., 2012; Starkey Lewis et al., 2012; Su et al., 2012). Ingenuity pathway analysis software revealed that many of the 11 differentially expressed miRNAs had common mRNA

targets (Fig. 6.3). Furthermore, a number of the putative targets were already known to be involved in liver proliferation; E2f1 and PPAR are required for proliferation of hepatocytes in response to cellular injury (Conner et al., 2000; Peters et al., 1997); knock-out mouse models of Smad3 and TP53 demonstrate excessive hepatocyte proliferation (Delker et al., 2000; Schnabl et al., 2001); and, SRF stimulates the proliferation of hepatocellular cell lines (Farra et al., 2010). It could therefore be hypothesised that the deregulated plasma miRNAs mediate a network of associated molecules responsible for maintaining the proliferative activity of the liver.

When analysing microarray data there is a balance between having enough significant changes for further analysis and including too many false positives in a dataset. This often has to be considered on an experiment-by-experiment basis. Since the background was consistently low across all of the microarrays and any interesting miRNAs identified through the microarray screening approach would be further validated using qRT-PCR, a second, less stringent bioinformatic analysis was performed. This excluded any multiple testing corrections and thus, accepted a higher number of false positives, which increased the number of significant differentially expressed miRNAs from 11 to 27 (Tables 6.2 and 6.3). This enabled a more comprehensive pathway analysis to be performed and avoided the loss of a large proportion of true positives alongside the false positives. Validated targets of the 27 altered plasma miRNAs were identified using the miRWalk database (Dweep et al., 2011) and analysed using IPA software as described by (Marczylo et al., 2012). The most significantly enriched pathway was Hepatic Fibrosis / Hepatic Stellate Cell Activation (Fig. 6.4 and Fig. 6.5). This was exactly the same pathway as was identified when an equivalent analysis was performed using the targets of the miRNAs differentially expressed in the livers of rats treated with Thioacetamide (Chapter 5, Fig. 5.7). This further supports the hypothesis that miRNAs mediate a network of associated molecules responsible for maintaining the proliferative activity of the liver, with a particular role in the transdifferentiation of hepatic stellate cells in response to liver injury.

As in previous chapters qRT-PCR was used to validate some of the more interesting miRNA changes. It is widely acknowledged that one of the most challenging aspects of profiling miRNAs from plasma samples is finding suitable endogenous controls for normalisation, particularly since the starting quantity of RNA cannot always be accurately quantified. Although each extracted RNA sample contained a spike-in (cel-miR-39), because the same quantity was added to each one it could not account for internal variations including incomplete lysis of the microvesicles encapsulating circulating miRNAs (Zampetaki and Mayr, 2012), or certain technical differences such as hemolysis during collection of plasma samples

(Kirschner et al., 2013). Thus, whilst useful for monitoring PCR efficiency (Fig. 6.1), cel-miR-39 was not suitable for use as an endogenous control. Whilst U6 has been used as an endogenous control for plasma samples (Starkey Lewis et al., 2011; Zhang et al., 2010), the consensus is that this, and other commonly used endogenous controls such as 5S, are not suitable due to degradation (Chen et al., 2008; Su et al., 2012), low expression (Wang et al., 2013b), or variability (Huang et al., 2010). It was the latter problem that prevented the use of U6 as an endogenous control for the rat plasma samples in this study.

As an alternative to normalising to a "standard" endogenous control, some groups normalise to total RNA volume (Chen et al., 2008; Su et al., 2012), or select a miRNA known to be well expressed in the plasma, but unchanged with treatment. A particularly common choice is miR-16 due to its high abundance and low variability (Bala et al., 2012; Huang et al., 2010; Kim et al., 2012; Kroh et al., 2010; Lawrie et al., 2008; McAlexander et al., 2013; Roth et al., 2010; Wong et al., 2008). However, since miR-16 is also recognised as a marker of haemolysis (Kirschner et al., 2011), care should be taken that levels are not too high and its variability across all samples should be measured to determine that expression does not change between experimental groups (Chen et al., 2008). The expression of miR-16 in the plasma was consistent between vehicle- and Thioacetamide-treated rats, thus all plasma qRT-PCR data was normalised to miR-16.

Three miRNAs were selected for qRT-PCR validation; miR-122, miR-30d and miR-192*. miR-122 demonstrated the largest increase in expression following microarray analysis, with a fold change of 210. This miRNA is the most widely expressed miRNA in the liver (Chang et al., 2004) and has already been investigated as a potential biomarker of liver disease (Bala et al., 2012; Starkey Lewis et al., 2012; Su et al., 2012; Wang et al., 2009; Yamada et al., 2013). Therefore, the large, validated change (Fig. 6.6 A) seen in miR-122 expression following Thioacetamide treatment was a useful confirmation that the miRNA profiling was successful. A change in expression of miR-122 is, however, not specific to any single type of toxic liver insult (Bala et al., 2012; Yamada et al., 2013). A panel of miRNAs altered following compound-induced hepatotoxicity might better identify the aetiology of the liver injury (Su et al., 2012). Thus, additional miRNAs were selected for validation, which might function alongside miR-122 as members of a predictive panel for use in identifying compound-induced hepatotoxicity. Further support for the use of a selection of miRNAs to determine the specific aetiology of liver injury comes from the networks depicted in Fig. 6.3 - Fig. 6.5. There was a large degree of overlap and crosstalk between the altered miRNAs. Using these networks, miR-30d was also selected for qRT-PCR validation. As part of the miR-30 family, miR-30d plays a major regulatory

role in the Hepatic Fibrosis / Hepatic Stellate Cell Activation pathway (Fig. 6.4 and Fig. 6.5). Microarray analysis revealed that miR-30d demonstrated the largest increase in expression following Thioacetamide treatment of all of the miR-30 family members (Table 6.3).The increase in expression of miR-30d was validated by qRT-PCR. miR-192* was first identified in Chapter 5. Following treatment with the PredTox compound FP014SC, miR-192* demonstrated a time-dependent reduction in expression in the liver (Chapter 5, Fig. 5.4 C). Previous work has identified miR-192 as a potential biomarker of liver damage (Starkey Lewis et al., 2011; Wang et al., 2009), but as yet no studies have investigated miR-192*. miR-192* was therefore also selected for qRT-PCR analysis. All three miRNAs selected for qRT-PCR analysis demonstrated increased expression in the plasma of rats treated with Thioacetamide (Fig. 6.6). Whilst the changes in expression of miR-30d and miR-192* were smaller than the change in miR-122, they were statistically significant and highly consistent between samples. Therefore, it was hypothesised that they could be used alongside miR-122 to further refine the type of liver injury.

As previously mentioned, the accurate assessment of the quality of RNA derived from plasma is difficult to do using the standard techniques described in Chapter 2, section 2.3.4. In the case of haemolysis, which is a further potential source of contamination unique to plasma samples, qRT-PCR can be used to determine the extent of red blood cell contamination. In haemolysed blood, up to 65% of endogenous circulating miRNAs can show differential expression when compared to non-haemolysed blood (Kirschner et al., 2013). Despite the fact that miRNAs were first detected in the circulation in 2008 (Chen et al., 2008; Mitchell et al., 2008), it took a further three years for anybody to fully consider the impact that haemolysis of blood samples during collection might have (Kirschner et al., 2011; McDonald et al., 2011). In their most recent paper Kirschner *et al* identified which miRNAs were released into the plasma upon haemolysis (Kirschner et al., 2013).Levels of miR-16 and miR-30d were elevated in cases where haemolysis had occurred, suggesting leakage from the red blood cells, however, miR-122 levels remained unchanged (Kirschner et al., 2013). All the plasma samples used in this work were visually inspected for haemolysis prior to further work. There was no obvious indication of red blood cell contamination. To support this there was a total absence of ribosomal RNA (which would leak into the blood during haemolysis), the expression of miR-16 remained consistent across all 6 samples (hence its use as an endogenous control), and the expression of miR-30d was consistent between experimental groups (vehicle- and Thioacetamide-treated). This indicated that no samples were exhibiting signs of haemolysis

and the change in miR-30d was due to the Thioacetamide treatment and not as a result of contamination caused by haemolysis.

When considering the use of circulating miRNAs as potential novel biomarkers, comparison to existing biomarkers is vital. If they are to be developed for use in the clinic or laboratory, novel biomarkers must show an advantage over existing biomarkers. One of the most frequently used clinical markers of liver injury is ALT activity. ALT activity increases with more pronounced liver damage (James et al., 1975). It is a highly sensitive marker of damage, hence its widespread use, but it lacks specificity. Whilst highly abundant in the liver (Kim et al., 2008), other isoforms exist (Glinghammar et al., 2009; Lindblom et al., 2007), for example in skeletal muscle (Nathwani et al., 2005) and, as such, ALT levels increase following vigorous exercise (Koutedakis et al., 1993; Skenderi et al., 2006). Previously published work has shown good correlation between increases in miR-122 abundance and ALT activity (Bala et al., 2012; Starkey Lewis et al., 2011; Wang et al., 2009; Zhang et al., 2010). The work presented in this chapter supports these findings and provides evidence that the levels of miR-30d and miR-192* also significantly correlate with ALT activity (Fig. 6.7). Whilst this is encouraging, further work is required to determine whether these miRNAs show increased sensitivity when compared to pre-existing clinical markers, such as ALT. Previous work has already indicated that miR-122 has increased sensitivity and shows a more rapid change in expression than ALT (Starkey Lewis et al., 2012; Su et al., 2012; Wang et al., 2009; Zhang et al., 2010). Expansion of the current study to look at earlier time points and human patient samples would enable further clarification on the utility of these miRNAs both within the clinic and in the early stages of the drug-development process.

There was no overlap between the miRNAs that were differentially expressed in the plasma and the liver, both in terms of the extent of the change and the specific miRNAs that were altered (Table 6.3). Fold changes in the plasma reached a maximum of over 700-fold, whilst those in the liver reached a maximum of 2.25-fold. Other recent studies report similar findings (Su et al., 2012; Wang et al., 2009). Su *et al* report changes of >5-fold in the plasma, but only of approximately 1.3-fold in the liver in two distinct model systems of hepatotoxicity (Su et al., 2012). Due to the many confounding factors, including normalisation difficulties, possible hemolysis and sample availability, the change in expression of a proposed miRNA should be as large as possible, to ease detection in the experimental setting and eliminate potential bias from pre-analytical variables (McDonald et al., 2011). Thus, the large changes observed in miRNA expression in the plasma of rats treated with Thioacetamide gives support to their use as novel biomarkers of compound-induced hepatotoxicity.

The cellular origin of most circulating miRNAs remains unknown (Kirschner et al., 2013; Wang et al., 2009). Under normal conditions miRNAs are not thought to passively leak from organs into the circulatory system; however, cellular injury and apoptosis can cause the secretion of miRNAs from damaged cells into the blood (Zen and Zhang, 2012). This provides one explanation for why the miRNA fold changes seen in the plasma surpass those seen in the liver, as certain miRNAs are only likely to be observed in the plasma following hepatocyte injury. With enhanced tissue damage, more cells release their contents and, thus, the proportion of a given miRNA in the circulation increases. It could be hypothesised that Thioacetamide-induced hepatotoxicity causes damage to the hepatocytes, indicated by the disruption to the Hepatic Fibrosis / Hepatic Stellate Cell Activation pathway and this results in the passive secretion of miRNAs into the circulation. However, despite the identification of the same miRNA-mediated pathway following plasma profiling there were no differentially expressed miRNAs common to both the plasma and the liver (Table 6.3). This is supported by the literature, which also reports that changes in the plasma can occur without a corresponding change within the hepatocytes (Bala et al., 2012; Su et al., 2012; Wang et al., 2009) and suggests that miRNAs may also enter the circulation via other mechanisms. It has been speculated that miRNAs within plasma microvesicles are involved in cell to cell communication (Brase et al., 2010; Turchinovich et al., 2013). This is thought to be particularly true in cases of tumour development and progression (Skog et al., 2008). Skog *et al* have demonstrated that glioblastoma cells release exosomes, which contain amongst other things miRNAs. Such miRNA-mediated cell to cell communication could also be involved in the response of the liver to compound-induced hepatotoxicity. It is therefore possible that exosome release may contribute to both the presence of certain plasma miRNAs and the difference in miRNA expression between the plasma and the liver. Recent evidence has also indicated that miRNAs can find their way into the circulation from the external environment (Etheridge et al., 2013), for example via the diet (Zhang et al., 2012) or the microbiome (Wang et al., 2012a). A dietary influence is unlikely here as the Thioacetamide- and vehicle-treated rats received the same diet. However, off targets effects of the Thioacetamide, or a reaction at the site of injection may account for some of the miRNAs found within the plasma. To date there is no literature to support this hypothesis. The current work is limited to some extent by the use of a single time point and dose. To enable a more comprehensive assessment of dynamic changes between the plasma and the liver, and possibly other tissues, further work would be required.

6.7 CONCLUSION

Through the use of modified protocols, sufficient yields of contaminant-free RNA (containing miRNAs) can be isolated from rat plasma samples and successfully profiled using both microarrays and qRT-PCR. The wealth of literature already available and the findings reported in this chapter provide evidence for the use of circulating miRNAs as novel biomarkers of hepatotoxicity. For example, miR-122 shows a large (>200-fold) statistically significant change in expression in the plasma following liver insult, or injury and is more sensitive than the currently used ALT diagnostic test. It does however lack specificity and is unable to distinguish between different forms of liver injury. The global miRNA profiling approach implemented here identified potential networks of altered plasma miRNAs, including the miR-30 family, which could be measured simultaneously to further categorise the type and extent of hepatotoxicity.

To date most of the miRNA profiling of plasma samples has been completed using human patient cases or mouse models of liver injury. However, rats are also widely used in pre-clinical testing. The identification of common miRNAs in plasma samples from rat models of hepatotoxicity, as shown in both this work and published literature (Su et al., 2012) indicates the potential for extrapolation from animal studies to the clinic, and further supports the continuation of work exploring the feasibility of using plasma miRNAs as novel biomarkers of compound-induced hepatotoxicity.

CHAPTER 7: DISCUSSION

The main aim of this thesis was to explore mRNA translation using models of compound-induced hepatotoxicity. Whilst the structure of the liver is well understood and the most frequent clinical signs of damage can now be clearly defined and categorised (Chapter 1, Table 1.1), a huge number of compounds still fail during, or after, the drug development process (Williams, 2006). In order to overcome the potentially large social, financial and time costs caused by such compound withdrawal, there is a need to better understand the molecular mechanisms behind compound-induced hepatotoxicity. This in turn should help to improve the prevention, diagnosis and treatment of compound-induced liver injury.

Different models were explored throughout the course of this work. The PredTox model was of huge value because it included compounds that unexpectedly failed during development. The fact that they had made it so far along the process implied that these failures were due to idiopathic drug reactions not readily identifiable by the compound's chemical structure or pharmacological properties, such as the formation of toxic metabolites. Two further models were selected to supplement the PredTox samples; the Griseofulvin-treated mouse and the Thioacetamide-treated rat. These are both widely-implemented models of hepatotoxcity and so some of the toxicity has already been well characterised (Chapter 1, sections 1.2.1 and 1.2.2). However, until now gene regulation at the level of translation had not been investigated within either model.

Gene expression is a complex process with many regulatory steps throughout. Transcriptional regulation has been explored in detail for many years, but translational regulation is less well studied. During translation the transcribed mRNA strand is converted, via the recruitment of ribosomal subunits, into a complete polypeptide chain. Regulation of this process has been demonstrated to be critical in cases of cellular stress, where a rapid response is required (Bottley et al., 2010), for example, in the metabolically active cells of the CNS (Moreno et al., 2012). It was therefore hypothesised that translational regulation may be of fundamental importance following compound-induced hepatotoxicity where acute cellular stress is evident.

The modified translational profiling technique developed and implemented in Chapter 3 enabled the measurement of changes in translational (and transcriptional) activity of hundreds of mRNAs simultaneously. The gradient fractionation method provided a measure of change in the overall rate of global mRNA translation, and thus protein synthesis, alongside changes in the translational (and transcriptional) activity of specific mRNAs. In cases of severe cellular stress a prominent change in the UV absorbance trace is observed (Bates et al., 2012), similar

to that seen in the original translational profiling experiments when 5' cap-dependent initiation of translation was blocked (Johannes et al., 1999). Such large redistribution of mRNAs from the polysomes to the monosomes is indicative of a global translational shut down. In the models of compound-induced hepatotoxicity used throughout this thesis, the insult was acute, but transient. Too severe a toxic injury would have resulted in mass cell death and a difficulty in discerning toxic mechanisms specific to the hepatotoxin, which was one of the main aims of the project. Thus, the treatment regimes were designed to be sub-toxic and, consequently, neither Griseofulvin nor the PredTox compound FP014SC caused a complete movement in mRNAs from the polysomes to the monosomes. Instead, more subtle changes in the translation of individual mRNAs were observed. Although some of these translational changes were accompanied by a change in transcription, there were a greater number of changes at the translational level than at the transcriptional level. This work provided validation for the use of the modified translational profiling technique and supported the hypothesis that translational regulation was important in compound-induced hepatotoxicity.

Microarrays are an extremely useful technique in the field of toxicogenomics, enabling the identification of multiple differentially expressed mRNAs and thus important functionally relevant pathways and networks. However, they are not without their problems, including technical issues, such as dye bias (Brownstein, 2006) or poor experimental design (Gant and Zhang, 2005). Furthermore, whilst often used for high-throughput genome-wide screening of mRNAs in response to damage, insult or injury (Lipshutz et al., 1995; Schena et al., 1995), microarrays do generate intimidating datasets containing hundreds of genes, which may or may not be of physiological relevance. Determining where to focus future work can be a challenge. The genes selected for further study in this thesis were identified based upon evidence of physiological relevance.

One candidate mRNA identified for more comprehensive investigation was *Dio3* (Chapter 4). Validation of the microarray result and Western blot analysis, suggested that D3 protein was reduced following treatment with a range of hepatotoxins and that this reduction in D3 was predominantly mediated at the translational level. The magnitude of the decrease in D3 was directly proportional to the extent of liver damage, possibly as a result of the higher energy demand placed on the liver for the initiation of active repair processes. This is supported by the perturbation of the TH pathways following compound-induced hepatotoxicity. Thus the rapid repression of *Dio3* mRNA may be a protective mechanism by which the liver, upon early signs of damage, responds quickly to maintain its own energy equilibrium, thereby preventing global disruption of the hypothalamic-pituitary-thyroid axis (Dudek et al., 2013).

The positive identification and validation of translational changes such as *Dio3* (rat samples) and *Smarce1* (mouse samples) mRNA led to the hypothesis that such regulation was mediated at the miRNA level. Therefore, miRNAs predicted to target these mRNAs were investigated. miRNAs are one of the most widely studied examples of translational regulators. Debate remains as to whether they function primarily to repress translation (Djuranovic et al., 2012; Meijer et al., 2013), degrade target mRNA (Beilharz et al., 2009; Guo et al., 2010) or perhaps do both in a cyclical process (Omer et al., 2009). However, under less debate is the stage at which miRNAs are recruited to their targets during translation, widely accepted as initiation (Bazzini et al., 2012). This gives further merit to the use of the translational profiling technique described in Chapter 3, for identifying physiologically relevant mRNA targets of miRNA-mediated regulation. Although some groups correlate miRNA changes with changes in total mRNA levels (Lim et al., 2005; Wang et al., 2010), it has been proposed that some important miRNA-mRNA interactions might be missed (Qin et al., 2013). The work presented in Chapter 5 supports this; as all but one of the mRNA targets of the differentially expressed miRNAs involved a change at the translational level. This also suggests that in these *in vivo* models of hepatotoxicity the predominant miRNA-mediated mechanism of regulation was translational repression rather than mRNA degradation.

Whilst no candidate miRNA regulator of *Dio3* was identified, global miRNA profiling, across each of the models revealed some interesting results. Whilst there were no miRNAs that demonstrated common differential expression, either across all of the different models or the two species, miR-92b was up-regulated following treatment with two of the PredTox compounds, as well as with Griseofulvin and Thioacetamide. miR-92b has been shown to have a critical role in regulating neuronal stem cell differentiation and proliferation (Liu et al., 2009). It may perform a similar function in the liver, mediating cellular proliferation following liver injury. The identification of this miRNA in both mouse and rat models of hepatotoxicity means that miR-92b has the potential to function as a general, cross-species hepatic-based biomarker of compound-induced toxicity, and so is certainly one worth investigating further. In general, however, the individual miRNAs altered following treatment with the different hepatotoxins were specific to each model. Nevertheless, the validated target mRNAs of these miRNAs were more similar and resulted in significant enrichment of the same canonical pathway; Hepatic Fibrosis / Hepatic Stellate Cell Activation. Fibrosis is a common feature of hepatotoxicity; it was evident following treatment with some of the PredTox compounds (Chapter 3, Table 3.2) and Thioacetamide (Chapter 4, section 4.5.2) and is a recognised feature of Griseofulvin-induced hepatotoxicity (Knasmuller et al., 1997). This indicates that whilst the different heptotoxic

compounds caused deregulation of different individual miRNAs, these miRNAs may target similar mRNAs and regulate the same canonical pathway, thus highlighting a common mechanism of underlying toxicity. Therefore, activation of the Hepatic Fibrosis / Hepatic Stellate Cell Activation pathway may serve as an early warning sign of compound-induced liver injury.

miRNA expression profiling was then extended to the plasma samples of rats treated with Thioacetamide. In 2008, stable miRNAs were identified in the plasma (Mitchell et al., 2008). Since then much work has been undertaken to explore the feasibility of using these species as biomarkers for a range of conditions, including hepatotoxicity (Bala et al., 2012; Starkey Lewis et al., 2012; Su et al., 2012; Wang et al., 2009; Yamada et al., 2013). The work presented in Chapter 6 supports the use of miRNAs as circulating biomarkers. Specific miRNAs (miR-122, miR-30d and miR-192*) were found to be highly deregulated with damage and correlated well with the most widely implemented existing marker of hepatotoxicity (ALT). It has been proposed that a panel of miRNAs, rather than a single miRNA, may function better as a marker of the specific type of liver damage. As mentioned previously, elucidating the causative factor of hepatotoxicity is seldom straightforward (Greaves, 2012) and most of the current diagnostic techniques cannot distinguish compound-induced hepatotoxicity from other forms of liver damage. Thus, the identification of a specific subset of differentially expressed circulating miRNAs may help to better determine the aetiology of the liver damage. Indeed, following treatment with Thioacetamide, the deregulated plasma miRNAs were found to also target mRNAs associated with the Hepatic Fibrosis / Hepatic Stellate Cell Activation pathway; thus supporting the use of circulating miRNAs as mechanistically relevant biomarkers of compound-induced hepatotoxicity. The fact that there were no differentially expressed miRNAs common to both the liver and the plasma, suggests that the miRNAs may not be simply leaking directly from damaged hepatocytes into the circulation, but instead entering the blood via alternative mechanisms. It has been speculated that miRNAs within plasma microvesicles are involved in cell to cell communication (Brase et al., 2010; Turchinovich et al., 2013). It is therefore possible that exosome release may contribute to both the presence of certain plasma miRNAs (possibly with a role in cell to cell communication) and the difference in miRNA expression between the plasma and the liver. Plasma is easily obtained, both from animals and in the clinical setting, and work is ongoing to develop profiling techniques, both at the miRNA and mRNA level that are sensitive enough to be used with very small starting quantities of RNA (Kudo et al., 2010). The advent of sequencing technologies is an exciting prospect, although currently limited by the required starting quantity of RNA; however, with further research this too is improving.

Finally, a note of caution on the interpretation of results from *in vivo* studies and the extrapolation of these to the human, clinical setting. Whilst toxicology studies require the use of *in vivo* as well as *in vitro* studies, not least because the whole organ, or animal, under investigation can be explored instead of a single cellular population, this work is not without its problems. Species differences are common at both the histopathological and molecular level, for example peroxisome proliferation is common in rodents following treatment with hypolipidemic drugs, but not seen in humans (Holden and Tugwood, 1999); the number of identified Cyps and their physiological activity shows great species variability (Nelson et al., 2004); and mRNAs and miRNAs demonstrate species-dependent differential expression patterns in response to toxic insult (Gant and Zhang, 2005; Koufaris and Gooderham, 2013). Certainly, in the work presented in Chapter 5, the differentially expressed hepatic miRNAs varied with both compound and species. However, further investigation of the datasets revealed that despite their differences they mediated the same canonical pathways. This highlights the value of a combinatorial approach when investigating the molecular mechanisms of compound-induced hepatotoxicity, enabling a more thorough exploration of the gene expression pathway. The work presented in this thesis has expanded the existing data available for each of the models to encompass global changes in both mRNA translation and miRNA expression. It has shown that mRNA translation, regardless of how it is regulated, plays an important role in the dynamic response of the liver to cellular stress induced by hepatotoxic compounds.

Much of the work presented in this thesis lends itself to further investigation. To summarise some of the main examples:

- *Dio3*. This mRNA was translationally repressed following treatment with hepatotoxins in the rat. Whilst a miRNA-mediated mechanism appears unlikely, exploration of the recently identified lncRNA, *Dio3-os* might prove more successful.
- miRNA-92b. This miRNA demonstrated cross-study and cross-species differential expression. Further work in investigating dose- and time-responses to a range of different hepatotoxins in mouse, rat and human models is required to fully explore the potential of this miRNA as a cross-species biomarker of compound-induced liver injury. The over-expression or knock-down of this miRNA in an *in vitro* cell culture-based model system may also provide information on specific mechanisms of toxicity.
- Primary cell lines. The development of a suitable *in vitro* model system of compound-induced hepatotoxicity would be highly advantageous for further exploring all of the suggestions listed here. The immortalised cell lines used thus far have proved to be

ineffective models, far removed from the *in vivo* situation. Whilst the argument remains that primary cell lines start to lose some of their "*in vivo*" phenotype immediately after removal, the use of human hepatocytes would overcome the difficulties in extrapolating between species. It would certainly be worthwhile profiling human primary cells following treatment with the compounds of interest. It may even be possible to introduce specific functionally relevant genetic polymorphisms (such as a Cyp mutation) to better understand and predict the likelihood and mechanism of adverse toxicity in susceptible patients.

- Plasma profiling. The work presented in this thesis on miRNA expression changes in the plasma of Thioacetamide-treated rats is a preliminary study. Initial results are encouraging, but further work is required to further validate the use of circulating miRNAs as biomarkers, including a screen based approach to measure the specificity and sensitivity of putative biomarkers. Furthermore, whilst others have shown that differentially expressed miRNAs are seen prior to elevated blood serum enzymes, the experimental design utilised here did not enable this comparison. This should also be included within a larger scale study.

APPENDIX I: MEEBO microarray QC

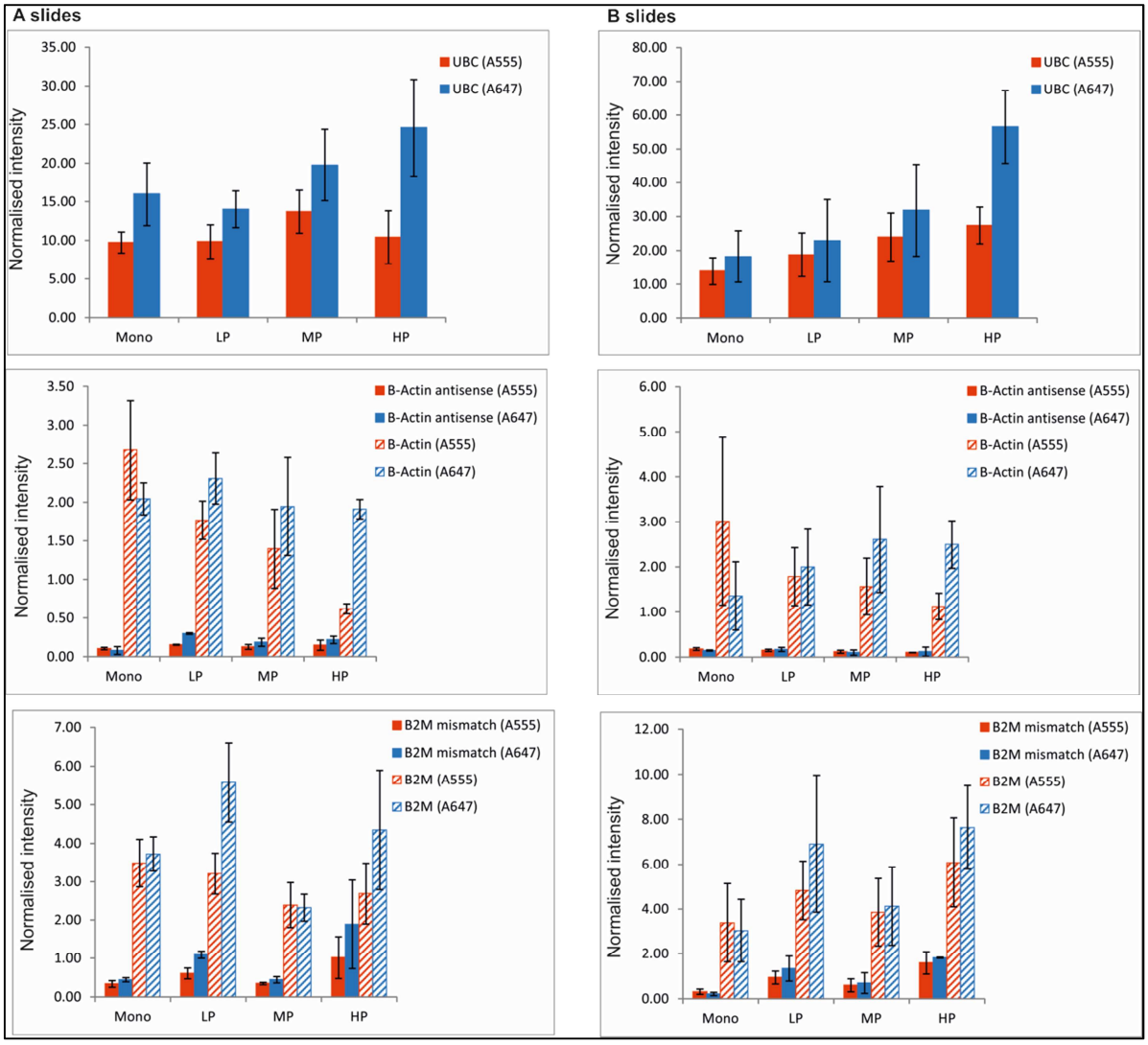

A control plate was used to check the quality of the printed MEEBO microarrays. The control plate contained probes against UBC, β-Actin, β-Actin antisense, B2M, and a B2M mismatch. Each probe was printed 64 times on each microarray. The average intensity of each probe was calculated. UBC was frequently highly expressed and demonstrated a low degree of variability across microarrays (n=3). The β-Actin antisense and B2M mismatch probes were used to demonstrate the specificity of the hybridisation. Of note is the B2M and B2M mismatch which only differed by a single nucleotide, but showed a large difference in intensity of hybridisation.

APPENDIX II: miRNA microarray QC

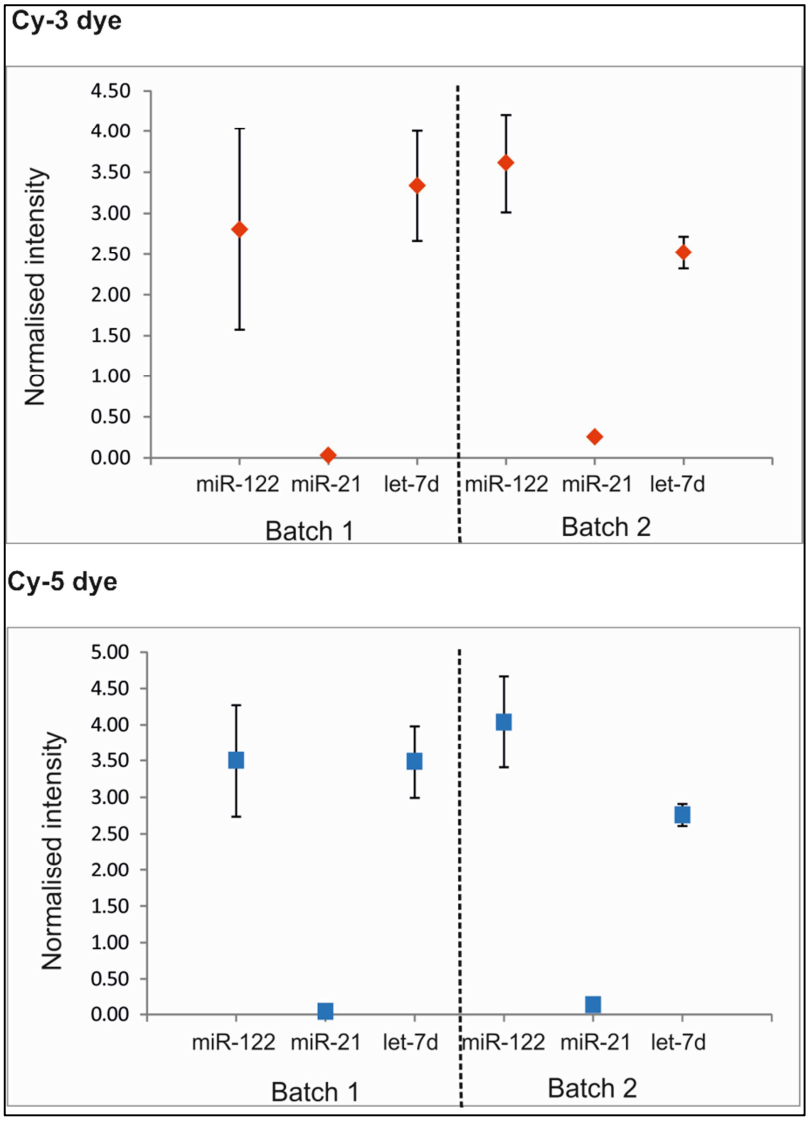

Throughout the course of this work two different batches of printed miRNA microarrays were used. Frequently highly expressed miRNAs (miR-122, miR-21 and let-7d) were used to check for variability between batches. The two batches in use demonstrated similar expression patterns of each test miRNA (n=3).

APPENDIX III: Primer sequenes.

qRT-PCR Primers

Gene	Forward/Reverse	Sequence (5' → 3')	% Efficiency	Single Melt Curve
β-Actin (Mouse)	Forward Reverse	GTGACGTTGACATCCGTAAAGA GCCGGACTCATCGTACTCC	89.18	✓
β-Actin (Rat)	Forward Reverse	CGTGAAAAGATGACCCAGATCA CACAGCCTGGATGGCTACGT	93.80	✓
Smarce1	Forward Reverse	AAAAGACCATCTTATGCCCCAC CCTGTAGTTGTTGTAGGCGAG	99.65	✓
Sesn1	Forward Reverse	TCGGCACTTTGAGGACACTAGT TCCTGGACACGAAATGTTGGA	105.58	✓
Dio1	Forward Reverse	GACACTGTTCCCAGAGAGAGTCAA TCCTGGTCATTCCGGTCTTT	102.52	✓
Dio2	Forward Reverse	CTTCTCAGCCGCTCCAAGTC TCCAGACACAGCGTAGTCCTTC	101.29	✓
Dio3	Forward Reverse	AGAGTGGCACCATCATGTACCA CCAAGTGCGCAACTCAGACA	94.91	✓

PCR Primers

Gene	Forward/Reverse	Sequence (5' → 3')
β-Actin (Mouse)*	Forward Reverse	AGAGCTATGACGTCGCATGC AGGTACCGGTCCGGAATTC
β-Actin (Rat)	Forward Reverse	ATGGTGGGTATGGGTCAGAA ACATCTGCTGGAAGGTGGAC
40S rRNA	Forward Reverse	GCATATGCTTGTCTCAAAGATTAAG TATTAGCTCTAGAATTACCACAGTTATCCA
60S rRNA	Forward Reverse	TGCCATGGTAATCCTGCTCA CCTCAGCCAAGCACATACACC
Dio3	Forward Reverse	GTGGTCGGAGAAGGTGAA AGAGGCGCTCAAAATAGG

* The mouse β-actin mRNA probe for northern blotting was generated from the EST clone BG077072. A 1kb PCR product was produced using primers designed against the pSport vector family.

Sequencing by PNACL (University of Leicester) revealed that each PCR product had high sequence identity to the relevant gene.

APPENDIX IV: Radioactive labelling protocols.

- Radioactive labelling: Klenow fragment labelling

Used for β-Actin and *Dio3.*

Labelled using Prime-a-Gene® Labelling kit (Promega, Madison, USA) according to the manufacturer's instructions.

Briefly, 25 ng DNA in 30 µl ultra pure (18 MΩ) water was denatured (95°C, 5 mins; hold at 4°C for at least 2 min) and added to a reaction comprising of 10 µl Labelling 5X buffer, 2 µl dNTPs (20 µM dATP, 20 µM dGTP and 20 µM dTTP), 2 µl BSA, 5 µl α^{32}P-dCTP (3000 ci/mmol) and 5 U DNA polymerase I large (Klenow) fragment. The reaction was incubated at RT for approximately 1 h. The labelling reaction was terminated by the addition of 5 µl 0.2 M EDTA. To remove unincorporated label, samples were applied to Illustra™ ProbeQuant™ G-50 Micro Columns (GE Healthcare, Buckinghamshire, UK). Columns were centrifuged according to the manufacturer's instructions (735g, RT, 2 min) and 1 µl eluate was added to scintillation fluid for counting. Dpm was determined using a Wallac WinSpectral™ 1414 liquid scintillation counter and $1x10^6$ dpm/ml probe was used for hybridisation.

- Radioactive labelling: End labelling

Used for 40S and 60S rRNA.

25 ng DNA in 2 µl ultra pure (18 MΩ) water was added to a reaction comprising of 1 µl 10X T4 polynucleotide kinase buffer, 2 µl T4 polynucleotide kinase (New England Biolabs, Hitchin, UK) and 5 µl γ^{32}P-ATP (3000 Ci/mmol). The reaction was incubated at 37°C for approximately 1 h. The labelling reaction was terminated by denaturation (95°C, 5 mins; hold at 4°C for at least 2 min) and the addition of 5 µl 0.2 M EDTA. To remove unincorporated label, samples were applied to Illustra™ ProbeQuant™ G-50 Micro Columns (GE Healthcare, Buckinghamshire, UK). Columns were centrifuged according to the manufacturer's instructions (735g, RT, 2 min) and 1 µl eluate was added to scintillation fluid for counting. Dpm was determined using a Wallac WinSpectral™ 1414 liquid scintillation counter and $1x10^6$ dpm/ml probe was used for hybridisation.

APPENDIX V: Example worksheet used to pool fractions for translational profiling.

Griseo d 22 mouse 12				vs			Griseo d 22 mouse 17			
Sample	**RNA (ng/µl)**	**Sample**	**RNA (ng/µl)**				**Sample**	**RNA (ng/µl)**	**Sample**	**RNA (ng/µl)**
1	310.48	7	510.2				1	360.49	7	280.11
2	272.56	8	456.13				2	223.87	8	302.03
3	419.07	9	541.89				3	439.87	9	459.91
4	704.37	10	665.68				4	497.91	10	498.82
5	315.48	11	272.96				5	236.99	11	450.04
6	234.08	12	313.1				6	181.93	12	312.17

				Cy3		**Cy5**				
				Vehicle	**Sample**	**Griseo**				
	5.9µl	Total ug		**Plate Location**	**Number**	**Plate Location**		**6.6µl**	Total ug	
1	1831.832		+76.4µl H20	B5		B5	1	2379.234		+73.6µl H20
2	1608.104	10.07	+10µl NaOAc	B6	**1**	B6	2	1477.542	10.05	+10µl NaOAc
3	2472.513		+275µl EtOH	B7		B7	3	2903.142		+275µl EtOH
4	4155.783			B8		B8	4	3286.206		
		23.6							26.4	
	6.6µl							**10µl**		
5	2082.168		+73.6µl H20	B9		B9	5	2369.9		+60µl H20
6	1544.928	10.00	+10µl NaOAc	B10	**2**	B10	6	1819.3	10.01	+10µl NaOAc
7	3367.32		+275µl EtOH	B11		B11	7	2801.1		+275µl EtOH
8	3010.458			B12		B12	8	3020.3		
		26.4							40	
	5.6µl							**5.85µl**		
9	3034.584		+77.6µl H20	C1		C1	9	2690.4735		+76.6µl H20
10	3727.808	10.04	+10µl NaOAc	C2	**3**	C2	10	2918.097	10.07	+10µl NaOAc
11	1528.576		+275µl EtOH	C3		C3	11	2632.734		+275µl EtOH
12	1753.36			C4		C4	12	1826.1945		
		22.4							23.4	

APPENDIX VI: Example worksheet used to pool fractions for qRT-PCR.

Griseo d 22 mouse 12						vs	Griseo d 22 mouse 17					
Sample	**RNA (ng/µl)**	1 in 10	**Sample**	**RNA (ng/µl)**	1 in 10		**Sample**	**RNA (ng/µl)**	***1 in 10***	**Sample**	**RNA (ng/µl)**	*1 in 10*
1	310.48	31.05	7	510.20	51.02		1	360.49	36.05	7	280.11	28.01
2	272.56	27.26	8	456.13	45.61		2	223.87	22.39	8	302.03	30.20
3	419.07	41.91	9	541.89	54.19		3	439.87	43.99	9	459.91	45.99
4	704.37	70.44	10	665.68	66.57		4	497.91	49.79	10	498.82	49.88
5	315.48	31.55	11	272.96	27.30		5	236.99	23.70	11	450.04	45.00
6	234.08	23.41	12	313.10	31.31		6	181.93	18.19	12	312.17	31.22

				Vehicle Plate Location	**Sample Number**	**Griseo Plate Location**				
	1.18µl	Total ng						**1.32µl**	Total ng	
1	36.64			B5		B5	1	47.58		
2	32.16	201.36		B6	**1**	B6	2	29.55	200.92	
3	49.45			B7		B7	3	58.06		
4	83.12		H2O (µl)	B8		B8	4	65.72		H2O (µl)
		4.72	4.28						5.28	3.72
	1.32µl							**2.00µl**		
5	41.64			B9		B9	5	47.40		
6	30.90	200.10		B10	**2**	B10	6	36.39	200.21	
7	67.35			B11		B11	7	56.02		
8	60.21		H2O (µl)	B12		B12	8	60.41		H2O (µl)
		5.28	3.72						8.00	1.00
	1.12µl							**1.17µl**		
9	60.69			C1		C1	9	53.81		
10	74.56	200.89		C2	**3**	C2	10	58.36	201.35	
11	30.57			C3		C3	11	52.65		
12	35.07		H2O (µl)	C4		C4	12	36.52		H2O (µl)
		4.48	4.52						4.68	4.32

APPENDIX VII: Validated mRNA targets associated with the Hepatic Fibrosis / Hepatic Stellate Cell Activation pathway.

Target mRNA	Grisofulvin	PredTox	Thioacetamide
Acta2	mmu-miR-146a mmu-miR-15a mmu-miR-15a* mmu-miR-335-3p	-	-
Agt	mmu-miR-21 mmu-miR-21*	rno-miR-429 rno-miR-27a* rno-miR-27a rno-miR-22* rno-miR-22 rno-miR-132	rno-miR-409-3p rno-miR-221
Agtr1a	mmu-miR-16 mmu-miR-21 mmu-miR-21*	rno-miR-92a rno-miR-350 rno-miR-21* rno-miR-21	rno-miR-21* rno-miR-21 rno-miR-221
Bcl2	mmu-let-7a mmu-let-7d mmu-let-7d* mmu-let-7f mmu-let-7f* mmu-let-7g mmu-let-7g* mmu-miR-107 mmu-miR-122 mmu-miR-15a mmu-miR-15a* mmu-miR-16 mmu-miR-195 mmu-miR-200c* mmu-miR-21 mmu-miR-21* mmu-miR-214 mmu-miR-214* mmu-miR-23a mmu-miR-27a mmu-miR-27a* mmu-miR-302b mmu-miR-302b* mmu-miR-30a* mmu-miR-30d	rno-miR-92a rno-miR-497 rno-miR-365 rno-miR-30b-5p rno-miR-30a* rno-miR-30a rno-miR-29c* rno-miR-29c rno-miR-29b rno-miR-296* rno-miR-27a* rno-miR-27a rno-miR-21* rno-miR-21 rno-miR-20a* rno-miR-200c rno-miR-199a-3p rno-miR-181a rno-miR-122 rno-miR-107 rno-let-7f	rno-miR-21* rno-miR-21 rno-miR-122 rno-let-7f rno-miR-221 rno-miR-320 rno-miR-30e* rno-miR-30e rno-miR-30c-1* rno-miR-223 rno-miR-214 rno-miR-125b* rno-let-7d* rno-let-7d
Ccl5	mmu-miR-146a mmu-miR-302a mmu-miR-302a* mmu-miR-302b mmu-miR-302b*	rno-miR-188	rno-miR-320 rno-miR-25*

APPENDIX VII continued

Target mRNA	Grisofulvin	PredTox	Thioacetamide
Ccl5	mmu-miR-302c mmu-miR-302c*		
Ccr5	mmu-miR-146a	-	-
Ccr7	mmu-miR-146a	-	-
Cd40	mmu-miR-21 mmu-miR-21*	-	-
Col1a1	mmu-let-7a mmu-let-7d mmu-let-7d* mmu-let-7f mmu-let-7f* mmu-let-7g mmu-let-7g* mmu-miR-146a mmu-miR-21 mmu-miR-21* mmu-miR-214 mmu-miR-214* mmu-miR-215 mmu-miR-27b mmu-miR-27b*	rno-miR-31 rno-miR-29c* rno-miR-29c rno-miR-29b rno-miR-27b rno-miR-26a rno-miR-215 rno-miR-21* rno-miR-21 rno-miR-192 rno-let-7f	rno-miR-21* rno-miR-21 rno-let-7f rno-miR-320 rno-miR-214 rno-let-7d* rno-let-7d
Col3a1	mmu-miR-9	rno-miR-29b	-
Csf1	mmu-miR-23a mmu-miR-23b	-	-
Ctgf	mmu-miR-122 mmu-miR-16 mmu-miR-21 mmu-miR-21* mmu-miR-215	rno-miR-92a rno-miR-215 rno-miR-21* rno-miR-21 rno-miR-192	rno-miR-21* rno-miR-21
Cxcl9	mmu-miR-146a	-	-
Cyp2e1	-	rno-miR-378*	-
Edn1	mmu-miR-15a mmu-miR-15a* mmu-miR-195	-	-
Ednrb	mmu-miR-15a mmu-miR-15a*	-	-
Egfr	mmu-let-7a mmu-let-7d mmu-let-7d* mmu-let-7f mmu-let-7f* mmu-let-7g mmu-let-7g* mmu-miR-122 mmu-miR-146a	rno-miR-429 rno-miR-30b-5p rno-miR-30a* rno-miR-30a rno-miR-296* rno-miR-27b rno-miR-27a* rno-miR-27a rno-miR-217	rno-miR-217 rno-miR-21* rno-miR-21 rno-let-7f rno-miR-221 rno-miR-30e* rno-miR-30e rno-miR-30c-1* rno-let-7d*

APPENDIX VII continued

Target mRNA	Grisofulvin	PredTox	Thioacetamide
Egfr	mmu-miR-183* mmu-miR-200c* mmu-miR-21 mmu-miR-21* mmu-miR-27a mmu-miR-27a* mmu-miR-27b mmu-miR-27b* mmu-miR-30a* mmu-miR-30d mmu-miR-495	rno-miR-21* rno-miR-21 rno-miR-20a* rno-miR-205 rno-miR-200c rno-miR-182 rno-let-7f	rno-let-7d rno-miR-25* rno-miR-216a
Fas	mmu-let-7a mmu-let-7d mmu-let-7d* mmu-let-7f mmu-let-7f* mmu-let-7g mmu-let-7g* mmu-miR-122 mmu-miR-146a mmu-miR-21 mmu-miR-21* mmu-miR-23a mmu-miR-27a mmu-miR-27a* mmu-miR-335-3p mmu-miR-671-5p	rno-miR-27a* rno-miR-27a rno-miR-21* rno-miR-21 rno-miR-132 rno-miR-122 rno-let-7f	rno-miR-21* rno-miR-21 rno-miR-122 rno-let-7f rno-miR-221 rno-let-7d* rno-let-7d rno-miR-433 rno-miR-363*
Fasl	mmu-miR-21 mmu-miR-21*	-	-
Faslg	-	rno-miR-21* rno-miR-21 rno-miR-92a rno-miR-29c* rno-miR-29c rno-miR-29b rno-miR-199a-3p	rno-miR-21* rno-miR-21 rno-miR-320
Fgf1	mmu-miR-195	-	-
Fgf2	mmu-miR-106a mmu-miR-146a mmu-miR-16 mmu-miR-21 mmu-miR-21*	rno-miR-92a rno-miR-31 rno-miR-21* rno-miR-21	rno-miR-21* rno-miR-21
Fgfr1	mmu-let-7a mmu-let-7d mmu-let-7d* mmu-let-7f	rno-miR-92a rno-miR-543* rno-miR-497 rno-miR-485	rno-miR-543* rno-miR-21* rno-miR-21 rno-miR-100

APPENDIX VII continued

Target mRNA	Grisofulvin	PredTox	Thioacetamide
Fgfr1	mmu-miR-101a mmu-miR-101a* mmu-miR-21 mmu-miR-21* mmu-miR-214 mmu-miR-214* mmu-miR-215 mmu-miR-23a mmu-miR-23b mmu-miR-27a mmu-miR-27a* mmu-miR-301a mmu-miR-30a* mmu-miR-382* mmu-miR-9 mmu-miR-98	rno-miR-331 rno-miR-30b-5p rno-miR-30a* rno-miR-30a rno-miR-29c* rno-miR-29c rno-miR-29b rno-miR-290 rno-miR-27a* rno-miR-27a rno-miR-215 rno-miR-21* rno-miR-21 rno-miR-132 rno-miR-124 rno-miR-100	rno-let-7f rno-miR-409-3p rno-miR-320 rno-miR-30e* rno-miR-30e rno-miR-223 rno-miR-214 rno-let-7d* rno-let-7d rno-miR-25* rno-miR-543 rno-miR-494 rno-miR-383 rno-miR-23b rno-miR-185
Flt1	mmu-miR-106a mmu-miR-122 mmu-miR-21 mmu-miR-21* mmu-miR-27a mmu-miR-27a* mmu-miR-27b mmu-miR-27b*	rno-let-7f	-
Fn1	mmu-let-7a mmu-let-7d mmu-let-7d* mmu-let-7f mmu-let-7f* mmu-let-7g mmu-let-7g* mmu-miR-200c*	rno-miR-200c rno-let-7f	rno-let-7f rno-let-7d* rno-let-7d
Hgf	mmu-miR-200c* mmu-miR-27b mmu-miR-27b* mmu-miR-301a mmu-miR-9	rno-miR-27b rno-miR-200c	rno-miR-379*
Icam1	-	-	rno-miR-221
Ifng	mmu-let-7a mmu-let-7d mmu-let-7d* mmu-let-7f mmu-let-7f* mmu-let-7g mmu-let-7g*	rno-miR-21* rno-miR-21 rno-miR-20a* rno-miR-192 rno-let-7f	rno-miR-21* rno-miR-21 rno-let-7f rno-miR-223 rno-let-7d* rno-let-7d

APPENDIX VII continued

Target mRNA	Grisofulvin	PredTox	Thioacetamide
Ifng	mmu-miR-146a mmu-miR-21 mmu-miR-21* mmu-miR-27a mmu-miR-27a* mmu-miR-335-3p mmu-miR-9 mmu-miR-98		
Ifngr1	-	rno-miR-378*	-
Igf1	mmu-let-7a mmu-miR-21 mmu-miR-21* mmu-miR-214 mmu-miR-214* mmu-miR-495	rno-miR-31 rno-miR-21* rno-miR-21 rno-miR-122 rno-miR-100 rno-let-7f	rno-miR-21* rno-miR-21 rno-miR-122 rno-miR-100 rno-let-7f rno-miR-223
Igf1r	mmu-let-7a mmu-let-7d mmu-let-7d* mmu-let-7f mmu-let-7f* mmu-let-7g mmu-let-7g* mmu-miR-122 mmu-miR-21 mmu-miR-21* mmu-miR-335-3p mmu-miR-431* mmu-miR-9	-	rno-let-7d* rno-let-7d rno-miR-431
Igfbp3	mmu-let-7a mmu-let-7d mmu-let-7d* mmu-let-7f mmu-let-7f* mmu-let-7g mmu-let-7g*	rno-miR-100	rno-miR-100
Igfbp5	mmu-miR-27a mmu-miR-27a*	-	-
Il10	mmu-let-7a mmu-let-7d mmu-let-7d* mmu-let-7f mmu-let-7f* mmu-let-7g mmu-let-7g* mmu-miR-106a	rno-miR-31 rno-miR-181a rno-let-7f	rno-let-7f rno-miR-223 rno-let-7d* rno-let-7d

APPENDIX VII continued

Target mRNA	Grisofulvin	PredTox	Thioacetamide
Il10	mmu-miR-146a		
Il1a	mmu-miR-122	rno-miR-378* rno-miR-122	rno-miR-122
Il1rap	-	rno-miR-29c* rno-miR-29c rno-miR-29b	-
Il1rl1	mmu-miR-141*	rno-miR-378* rno-miR-26a	rno-miR-200a
Il6	mmu-let-7a mmu-let-7d mmu-let-7d* mmu-let-7f mmu-let-7f* mmu-let-7g mmu-let-7g* mmu-miR-146a mmu-miR-671-5p	rno-miR-346 rno-miR-31 rno-miR-181a rno-miR-132 rno-let-7f	rno-let-7f rno-miR-223 rno-let-7d* rno-let-7d rno-miR-433
Il6ra	mmu-miR-21 mmu-miR-21* mmu-miR-23a	-	-
Lama1	mmu-miR-214 mmu-miR-214*	-	-
Lbp	-	rno-miR-532-5p	-
Lep	mmu-miR-335-3p	-	-
Lepr	mmu-miR-21 mmu-miR-21* mmu-miR-335-3p mmu-miR-93*	-	-
Met	mmu-let-7a mmu-miR-122 mmu-miR-135a mmu-miR-141* mmu-miR-15a mmu-miR-15a* mmu-miR-200c* mmu-miR-21 mmu-miR-21* mmu-miR-27b mmu-miR-27b* mmu-miR-302a mmu-miR-302a* mmu-miR-302b mmu-miR-302b* mmu-miR-302c mmu-miR-302c*	rno-miR-429 rno-miR-378* rno-miR-31 rno-miR-30b-5p rno-miR-30a* rno-miR-30a rno-miR-27b rno-miR-21* rno-miR-21 rno-miR-205 rno-miR-200c rno-miR-199a-3p rno-miR-122	rno-miR-21* rno-miR-21 rno-miR-122 rno-miR-221 rno-miR-30e* rno-miR-30e rno-miR-30c-1* rno-miR-200a

APPENDIX VII continued

Target mRNA	Grisofulvin	PredTox	Thioacetamide
Met	mmu-miR-30a* mmu-miR-30d mmu-miR-9		
Mmp13	mmu-miR-146a mmu-miR-27a mmu-miR-27a* mmu-miR-27b mmu-miR-27b*	-	-
Mmp2	mmu-miR-21 mmu-miR-21* mmu-miR-488 mmu-miR-488* mmu-miR-9	-	-
Mmp9	mmu-let-7a mmu-let-7d mmu-let-7d* mmu-let-7f mmu-miR-101a mmu-miR-101a* mmu-miR-21 mmu-miR-21* mmu-miR-214 mmu-miR-214* mmu-miR-215 mmu-miR-23a mmu-miR-23b mmu-miR-27a mmu-miR-27a* mmu-miR-301a mmu-miR-30a* mmu-miR-382* mmu-miR-9 mmu-miR-98	rno-miR-92a rno-miR-543* rno-miR-497 rno-miR-485 rno-miR-331 rno-miR-30b-5p rno-miR-30a* rno-miR-30a rno-miR-29c* rno-miR-29c rno-miR-29b rno-miR-290 rno-miR-27a* rno-miR-27a rno-miR-215 rno-miR-21* rno-miR-21 rno-miR-132 rno-miR-124 rno-miR-100 rno-let-7f	rno-miR-543* rno-miR-21* rno-miR-21 rno-miR-100 rno-let-7f rno-miR-409-3p rno-miR-320 rno-miR-30e* rno-miR-30e rno-miR-223 rno-miR-214 rno-let-7d* rno-let-7d rno-miR-25* rno-miR-543 rno-miR-494 rno-miR-383 rno-miR-23b rno-miR-185
Myh6	-	rno-miR-22* rno-miR-22	-
Myh7	mmu-miR-27a mmu-miR-27a*	-	-
Nfkb1	mmu-miR-146a mmu-miR-21 mmu-miR-21* mmu-miR-27b mmu-miR-27b* mmu-miR-30a* mmu-miR-9	-	-

APPENDIX VII continued

Target mRNA	Grisofulvin	PredTox	Thioacetamide
Ngfr	mmu-miR-27b mmu-miR-27b* mmu-miR-30a*	-	-
Pdgfa	mmu-miR-214 mmu-miR-214*	-	-
Pdgfb	mmu-miR-106a mmu-miR-21 mmu-miR-21* mmu-miR-23a	rno-miR-429 rno-miR-31 rno-miR-205	rno-miR-200a
Rela	mmu-miR-146a mmu-miR-15a mmu-miR-15a* mmu-miR-16 mmu-miR-21 mmu-miR-21* mmu-miR-23a mmu-miR-23b mmu-miR-27a mmu-miR-27a*	rno-miR-290 rno-miR-21* rno-miR-21	rno-miR-21* rno-miR-21 rno-miR-125b*
Smad2	mmu-miR-15a mmu-miR-15a* mmu-miR-21 mmu-miR-21* mmu-miR-23a mmu-miR-302a mmu-miR-302a* mmu-miR-30a* mmu-miR-30d	rno-miR-30b-5p rno-miR-30a* rno-miR-30a rno-miR-29c* rno-miR-29c rno-miR-29b rno-miR-217 rno-miR-21* rno-miR-21 rno-miR-192	rno-miR-217 rno-miR-21* rno-miR-21 rno-miR-30e* rno-miR-30e rno-miR-30c-1*
Smad3	mmu-let-7a mmu-let-7d mmu-let-7d* mmu-let-7f mmu-let-7f* mmu-let-7g mmu-let-7g* mmu-miR-107 mmu-miR-135a mmu-miR-146a mmu-miR-15a mmu-miR-15a* mmu-miR-16 mmu-miR-195 mmu-miR-21 mmu-miR-21*	rno-miR-31 rno-miR-30b-5p rno-miR-29c* rno-miR-29c rno-miR-29b rno-miR-26a rno-miR-217 rno-miR-21* rno-miR-21 rno-miR-192 rno-miR-107 rno-let-7f	rno-miR-217 rno-miR-21* rno-miR-21 rno-let-7f rno-let-7d* rno-let-7d rno-miR-25* rno-miR-216a rno-miR-23b rno-miR-760-5p

APPENDIX VII continued

Target mRNA	Grisofulvin	PredTox	Thioacetamide
Smad3	mmu-miR-23a mmu-miR-23b		
Smad4	mmu-let-7a mmu-let-7d mmu-let-7d* mmu-let-7f mmu-let-7f* mmu-let-7g mmu-let-7g* mmu-miR-146a mmu-miR-15a mmu-miR-15a* mmu-miR-16 mmu-miR-21 mmu-miR-21* mmu-miR-23a mmu-miR-23b	rno-miR-92a rno-miR-217 rno-miR-21* rno-miR-21 rno-miR-181a rno-let-7f	rno-miR-217 rno-miR-21* rno-miR-21 rno-let-7f rno-let-7d* rno-let-7d rno-miR-216a rno-miR-23b
Smad7	mmu-miR-122 mmu-miR-146a mmu-miR-21 mmu-miR-21*	rno-miR-31 rno-miR-29c* rno-miR-29c rno-miR-29b rno-miR-21* rno-miR-21 rno-miR-192 rno-miR-122	rno-miR-21* rno-miR-21 rno-miR-122 rno-miR-223
Tgfb1	mmu-miR-215 mmu-miR-23b mmu-miR-27b mmu-miR-27b* mmu-miR-30a*	-	-
Tgfbr1	mmu-miR-122 mmu-miR-21 mmu-miR-21* mmu-miR-30a* mmu-miR-30d	rno-miR-30b-5p rno-miR-30a* rno-miR-30a rno-miR-21* rno-miR-21 rno-miR-181a rno-miR-122	rno-miR-21* rno-miR-21 rno-miR-122 rno-miR-30e* rno-miR-30e rno-miR-30c-1*
Tgfbr2	mmu-miR-106a mmu-miR-15a mmu-miR-15a* mmu-miR-21 mmu-miR-21* mmu-miR-214 mmu-miR-214* mmu-miR-302a	rno-miR-93 rno-miR-92a rno-miR-26a rno-miR-211 rno-miR-21* rno-miR-21 rno-miR-20a* rno-miR-124	rno-miR-93 rno-miR-21* rno-miR-21 rno-miR-30e* rno-miR-30e rno-miR-214

APPENDIX VII continued

Target mRNA	Grisofulvin	PredTox	Thioacetamide
Tgfbr2	mmu-miR-302a* mmu-miR-302b mmu-miR-302b* mmu-miR-302c mmu-miR-302c* mmu-miR-93*		
Timp2	mmu-let-7g mmu-let-7g* mmu-miR-200c* mmu-miR-21 mmu-miR-21* mmu-miR-98	rno-miR-21* rno-miR-21 rno-miR-31 rno-miR-200c	rno-miR-21* rno-miR-21
Tlr4	mmu-miR-146a	-	-
Tnf	mmu-let-7a mmu-let-7d mmu-let-7d* mmu-let-7f mmu-let-7f* mmu-let-7g mmu-let-7g* mmu-miR-106a mmu-miR-122 mmu-miR-144 mmu-miR-146a mmu-miR-16 mmu-miR-183* mmu-miR-194 mmu-miR-21 mmu-miR-21* mmu-miR-23a mmu-miR-27a mmu-miR-27a* mmu-miR-27b mmu-miR-27b* mmu-miR-98	rno-miR-21* rno-miR-21 rno-miR-122 rno-miR-100 rno-let-7f rno-miR-31 rno-miR-27b rno-miR-27a* rno-miR-27a rno-miR-20a* rno-miR-199a-3p rno-miR-194 rno-miR-192 rno-miR-182 rno-miR-181a rno-miR-132	rno-miR-21* rno-miR-21 rno-miR-122 rno-miR-100 rno-let-7f rno-miR-221 rno-miR-223 rno-let-7d* rno-let-7d rno-miR-25*
Vcam1	-	-	rno-miR-221
Vegfa	-	rno-miR-31	-

REFERENCES

Abbott, A.L., E. Alvarez-Saavedra, E.A. Miska, N.C. Lau, D.P. Bartel, H.R. Horvitz, and V. Ambros. 2005. The let-7 MicroRNA family members mir-48, mir-84, and mir-241 function together to regulate developmental timing in Caenorhabditis elegans. *Developmental cell*. 9:403-414.

Ach, R.A., H. Wang, and B. Curry. 2008. Measuring microRNAs: comparisons of microarray and quantitative PCR measurements, and of different total RNA prep methods. *BMC biotechnology*. 8:69.

Akerboom, T., I. Schneider, S. vom Dahl, and H. Sies. 1991. Cholestasis and changes of portal pressure caused by chlorpromazine in the perfused rat liver. *Hepatology (Baltimore, Md.)*. 13:216-221.

Alessenko, A.V., P. Boikov, G.N. Filippova, A.V. Khrenov, A.S. Loginov, and E.D. Makarieva. 1997. Mechanisms of cycloheximide-induced apoptosis in liver cells. *FEBS letters*. 416:113-116.

Ambros, V. 2004. The functions of animal microRNAs. *Nature*. 431:350-355.

Amoako, A.A., A.K. Gebeh, E.L. Marczylo, J.M. Willets, J. Elson, T.H. Marczylo, and J.C. Konje. 2013. Impact of reference gene selection for type 2 cannabinoid receptor gene expression studies in human spermatozoa. *Andrologia*. 45:278-284.

Anderson, S.F., B.P. Schlegel, T. Nakajima, E.S. Wolpin, and J.D. Parvin. 1998. BRCA1 protein is linked to the RNA polymerase II holoenzyme complex via RNA helicase A. *Nature genetics*. 19:254-256.

Andrade, C. 2013. Drug interactions in the treatment of depression in patients receiving beta-blocker drugs. *The Journal of clinical psychiatry*. 74:e75-78.

Anfinsen, C.B. 1972. The formation and stabilization of protein structure. *The Biochemical journal*. 128:737-749.

Anfinsen, C.B. 1973. Principles that govern the folding of protein chains. *Science (New York, N.Y.)*. 181:223-230.

Antoine, D.J., D.P. Williams, A. Kipar, R.E. Jenkins, S.L. Regan, J.G. Sathish, N.R. Kitteringham, and B.K. Park. 2009. High-mobility group box-1 protein and keratin-18, circulating serum proteins informative of acetaminophen-induced necrosis and apoptosis in vivo. *Toxicological sciences : an official journal of the Society of Toxicology*. 112:521-531.

Arrojo, E.D.R., and A.C. Bianco. 2011. Type 2 deiodinase at the crossroads of thyroid hormone action. *The international journal of biochemistry & cell biology*. 43:1432-1441.

Arroyo, J.D., J.R. Chevillet, E.M. Kroh, I.K. Ruf, C.C. Pritchard, D.F. Gibson, P.S. Mitchell, C.F. Bennett, E.L. Pogosova-Agadjanyan, D.L. Stirewalt, J.F. Tait, and M. Tewari. 2011. Argonaute2 complexes carry a population of circulating microRNAs independent of vesicles in human plasma. *Proceedings of the National Academy of Sciences of the United States of America*. 108:5003-5008.

Aterman, K. 1986. The parasinusoidal cells of the liver: a historical account. *The Histochemical journal*. 18:279-305.

Baer, C., R. Claus, and C. Plass. 2013. Genome-wide epigenetic regulation of miRNAs in cancer. *Cancer research*. 73:473-477.

Bala, S., J. Petrasek, S. Mundkur, D. Catalano, I. Levin, J. Ward, H. Alao, K. Kodys, and G. Szabo. 2012. Circulating microRNAs in exosomes indicate hepatocyte injury and inflammation in alcoholic, drug-induced, and inflammatory liver diseases. *Hepatology (Baltimore, Md.)*. 56:1946-1957.

Baqui, M., D. Botero, B. Gereben, C. Curcio, J.W. Harney, D. Salvatore, K. Sorimachi, P.R. Larsen, and A.C. Bianco. 2003. Human type 3 iodothyronine selenodeiodinase is located in the plasma membrane and undergoes rapid internalization to endosomes. *J. Biol. Chem.* 278:1206-1211.

Bartel, D.P. 2004. MicroRNAs: genomics, biogenesis, mechanism, and function. *Cell*. 116:281-297.

Bates, J.G., J. Salzman, D. May, P.B. Garcia, G.J. Hogan, M. McIntosh, M.S. Schlissel, and P.O. Brown. 2012. Extensive gene-specific translational reprogramming in a model of B cell differentiation and Abl-dependent transformation. *PloS one*. 7:e37108.

Bates, J.M., D.L. St Germain, and V.A. Galton. 1999. Expression profiles of the three iodothyronine deiodinases, D1, D2, and D3, in the developing rat. *Endocrinology*. 140:844-851.

Baumann, M., J. Pontiller, and W. Ernst. 2010. Structure and basal transcription complex of RNA polymerase II core promoters in the mammalian genome: an overview. *Molecular biotechnology*. 45:241-247.

Bazzini, A.A., M.T. Lee, and A.J. Giraldez. 2012. Ribosome profiling shows that miR-430 reduces translation before causing mRNA decay in zebrafish. *Science (New York, N.Y.)*. 336:233-237.

Beilharz, T.H., D.T. Humphreys, J.L. Clancy, R. Thermann, D.I. Martin, M.W. Hentze, and T. Preiss. 2009. microRNA-mediated messenger RNA deadenylation contributes to translational repression in mammalian cells. *PloS one*. 4:e6783.

Bendele, A.M., J.F. Hulman, S. White, C. Brodhecker, and R.A. Bendele. 1993. Hepatocellular proliferation in ibuprofen-treated mice. *Toxicologic pathology*. 21:15-20.

Berezikov, E., F. Thuemmler, L.W. van Laake, I. Kondova, R. Bontrop, E. Cuppen, and R.H. Plasterk. 2006. Diversity of microRNAs in human and chimpanzee brain. *Nature genetics*. 38:1375-1377.

Betel, D., M. Wilson, A. Gabow, D.S. Marks, and C. Sander. 2008. The microRNA.org resource: targets and expression. *Nucleic acids research*. 36:D149-153.

Bianco, A.C. 2011. Minireview: cracking the metabolic code for thyroid hormone signaling. *Endocrinology*. 152:3306-3311.

Bianco, A.C., and B.W. Kim. 2006. Deiodinases: implications of the local control of thyroid hormone action. *J Clin Invest*. 116:2571-2579.

Bianco, A.C., D. Salvatore, B. Gereben, M.J. Berry, and P.R. Larsen. 2002. Biochemistry, cellular and molecular biology, and physiological roles of the iodothyronine selenodeiodinases. *Endocr. Rev.* 23:38-89.

Bird, A. 2002. DNA methylation patterns and epigenetic memory. *Genes & development*. 16:6-21.

Blagden, S.P., and A.E. Willis. 2011. The biological and therapeutic relevance of mRNA translation in cancer. *Nature reviews. Clinical oncology*. 8:280-291.

Boelen, A., J. Kwakkel, W.M. Wiersinga, and E. Fliers. 2006. Chronic local inflammation in mice results in decreased TRH and type 3 deiodinase mRNA expression in the hypothalamic paraventricular nucleus independently of diminished food intake. *J Endocrinol*. 191:707-714.

Boelen, A., W.M. Wiersinga, and E. Fliers. 2008. Fasting-induced changes in the hypothalamus-pituitary-thyroid axis. *Thyroid*. 18:123-129.

Boitier, E., A. Amberg, V. Barbie, A. Blichenberg, A. Brandenburg, H. Gmuender, A. Gruhler, D. McCarthy, K. Meyer, B. Riefke, M. Raschke, W. Schoonen, M. Sieber, L. Suter, C.E. Thomas, and N. Sajot. 2011. A comparative integrated transcript analysis and functional characterization of differential mechanisms for induction of liver hypertrophy in the rat. *Toxicology and applied pharmacology*. 252:85-96.

Bolstad, B.M., R.A. Irizarry, M. Astrand, and T.P. Speed. 2003. A comparison of normalization methods for high density oligonucleotide array data based on variance and bias. *Bioinformatics (Oxford, England)*. 19:185-193.

Borchert, G.M., W. Lanier, and B.L. Davidson. 2006. RNA polymerase III transcribes human microRNAs. *Nature structural & molecular biology*. 13:1097-1101.

Bortvin, A. 2013. PIWI-Interacting RNAs (piRNAs) - a Mouse Testis Perspective. *Biochemistry. Biokhimiia*. 78:592-602.

Bottley, A., N.M. Phillips, T.E. Webb, A.E. Willis, and K.A. Spriggs. 2010. eIF4A inhibition allows translational regulation of mRNAs encoding proteins involved in Alzheimer's disease. *PloS one*. 5.

Boyerinas, B., S.M. Park, A. Hau, A.E. Murmann, and M.E. Peter. 2010. The role of let-7 in cell differentiation and cancer. *Endocrine-related cancer*. 17:F19-36.

Bradford, M.M. 1976. A rapid and sensitive method for the quantitation of microgram quantities of protein utilizing the principle of protein-dye binding. *Analytical biochemistry*. 72:248-254.

Brase, J.C., D. Wuttig, R. Kuner, and H. Sultmann. 2010. Serum microRNAs as non-invasive biomarkers for cancer. *Molecular cancer*. 9:306.

Brazma, A., P. Hingamp, J. Quackenbush, G. Sherlock, P. Spellman, C. Stoeckert, J. Aach, W. Ansorge, C.A. Ball, H.C. Causton, T. Gaasterland, P. Glenisson, F.C. Holstege, I.F. Kim, V. Markowitz, J.C. Matese, H. Parkinson, A. Robinson, U. Sarkans, S. Schulze-Kremer, J. Stewart, R. Taylor, J. Vilo, and M. Vingron. 2001. Minimum information about a microarray experiment (MIAME)-toward standards for microarray data. *Nat Genet*. 29:365-371.

Brenner, C., R. Deplus, C. Didelot, A. Loriot, E. Vire, C. De Smet, A. Gutierrez, D. Danovi, D. Bernard, T. Boon, P.G. Pelicci, B. Amati, T. Kouzarides, Y. de Launoit, L. Di Croce, and F. Fuks. 2005. Myc represses transcription through recruitment of DNA methyltransferase corepressor. *The EMBO journal*. 24:336-346.

Brownstein, M. 2006. Sample labeling: an overview. *Methods in enzymology*. 410:222-237.

Burnett, G., and E.P. Kennedy. 1954. The enzymatic phosphorylation of proteins. *The Journal of biological chemistry*. 211:969-980.

Bushell, M., M. Stoneley, Y.W. Kong, T.L. Hamilton, K.A. Spriggs, H.C. Dobbyn, X. Qin, P. Sarnow, and A.E. Willis. 2006. Polypyrimidine tract binding protein regulates IRES-mediated gene expression during apoptosis. *Molecular cell*. 23:401-412.

Bustin, S.A., V. Benes, J.A. Garson, J. Hellemans, J. Huggett, M. Kubista, R. Mueller, T. Nolan, M.W. Pfaffl, G.L. Shipley, J. Vandesompele, and C.T. Wittwer. 2009. The MIQE guidelines: minimum information for publication of quantitative real-time PCR experiments. *Clinical chemistry*. 55:611-622.

Butler, J.E., and J.T. Kadonaga. 2001. Enhancer-promoter specificity mediated by DPE or TATA core promoter motifs. *Genes & development*. 15:2515-2519.

Butler, J.E., and J.T. Kadonaga. 2002. The RNA polymerase II core promoter: a key component in the regulation of gene expression. *Genes & development*. 16:2583-2592.

Carninci, P., T. Kasukawa, S. Katayama, J. Gough, M.C. Frith, N. Maeda, R. Oyama, T. Ravasi, B. Lenhard, C. Wells, R. Kodzius, K. Shimokawa, V.B. Bajic, S.E. Brenner, S. Batalov, A.R. Forrest, M. Zavolan, M.J. Davis, L.G. Wilming, V. Aidinis, J.E. Allen, A. Ambesi-Impiombato, R. Apweiler, R.N. Aturaliya, T.L. Bailey, M. Bansal, L. Baxter, K.W. Beisel, T. Bersano, H. Bono, A.M. Chalk, K.P. Chiu, V. Choudhary, A. Christoffels, D.R. Clutterbuck, M.L. Crowe, E. Dalla, B.P. Dalrymple, B. de Bono, G. Della Gatta, D. di Bernardo, T. Down, P. Engstrom, M. Fagiolini, G. Faulkner, C.F. Fletcher, T. Fukushima, M. Furuno, S. Futaki, M. Gariboldi, P. Georgii-Hemming, T.R. Gingeras, T. Gojobori, R.E. Green, S. Gustincich, M. Harbers, Y. Hayashi, T.K. Hensch, N. Hirokawa, D. Hill, L. Huminiecki, M. Iacono, K. Ikeo, A. Iwama, T. Ishikawa, M. Jakt, A. Kanapin, M. Katoh, Y. Kawasawa, J. Kelso, H. Kitamura, H. Kitano, G. Kollias, S.P. Krishnan, A. Kruger, S.K. Kummerfeld, I.V. Kurochkin, L.F. Lareau, D. Lazarevic, L. Lipovich, J. Liu, S. Liuni, S. McWilliam, M. Madan Babu, M. Madera, L. Marchionni, H. Matsuda, S. Matsuzawa, H. Miki, F. Mignone, S. Miyake, K. Morris, S. Mottagui-Tabar, N. Mulder, N. Nakano, H. Nakauchi, P. Ng, R. Nilsson, S. Nishiguchi, S. Nishikawa, et al. 2005. The transcriptional landscape of the mammalian genome. *Science (New York, N.Y.)*. 309:1559-1563.

Carninci, P., A. Sandelin, B. Lenhard, S. Katayama, K. Shimokawa, J. Ponjavic, C.A. Semple, M.S. Taylor, P.G. Engstrom, M.C. Frith, A.R. Forrest, W.B. Alkema, S.L. Tan, C. Plessy, R. Kodzius, T. Ravasi, T. Kasukawa, S. Fukuda, M. Kanamori-Katayama, Y. Kitazume, H. Kawaji, C. Kai, M. Nakamura, H. Konno, K. Nakano, S. Mottagui-Tabar, P. Arner, A. Chesi, S. Gustincich, F. Persichetti, H. Suzuki, S.M. Grimmond, C.A. Wells, V. Orlando, C. Wahlestedt, E.T. Liu, M. Harbers, J. Kawai, V.B. Bajic, D.A. Hume, and Y. Hayashizaki. 2006. Genome-wide analysis of mammalian promoter architecture and evolution. *Nature genetics*. 38:626-635.

Carpenter, S., D. Aiello, M.K. Atianand, E.P. Ricci, P. Gandhi, L.L. Hall, M. Byron, B. Monks, M. Henry-Bezy, J.B. Lawrence, L.A. O'Neill, M.J. Moore, D.R. Caffrey, and K.A. Fitzgerald. 2013. A long noncoding RNA mediates both activation and repression of immune response genes. *Science (New York, N.Y.)*. 341:789-792.

Carrieri, C., L. Cimatti, M. Biagioli, A. Beugnet, S. Zucchelli, S. Fedele, E. Pesce, I. Ferrer, L. Collavin, C. Santoro, A.R. Forrest, P. Carninci, S. Biffo, E. Stupka, and S. Gustincich. 2012. Long non-coding antisense RNA controls Uchl1 translation through an embedded SINEB2 repeat. *Nature*. 491:454-457.

Carthew, R.W. 2006. Gene regulation by microRNAs. *Current opinion in genetics & development*. 16:203-208.

Carthew, R.W., and E.J. Sontheimer. 2009. Origins and Mechanisms of miRNAs and siRNAs. *Cell*. 136:642-655.

Cascales, M., A. Alvarez, P. Gasco, L. Fernandez-Simon, N. Sanz, and L. Bosca. 1994. Cocaine-induced liver injury in mice elicits specific changes in DNA ploidy and induces programmed death of hepatocytes. *Hepatology (Baltimore, Md.)*. 20:992-1001.

Castaneda, F., and R.K. Kinne. 1999. Effects of doxorubicin, mitomycin C, and ethanol on Hep-G2 cells in vitro. *Journal of cancer research and clinical oncology*. 125:1-8.

Castoldi, M., S. Schmidt, V. Benes, M. Noerholm, A.E. Kulozik, M.W. Hentze, and M.U. Muckenthaler. 2006. A sensitive array for microRNA expression profiling (miChip) based on locked nucleic acids (LNA). *RNA (New York, N.Y.)*. 12:913-920.

Cedar, H., and Y. Bergman. 2009. Linking DNA methylation and histone modification: patterns and paradigms. *Nature reviews. Genetics*. 10:295-304.

Chang, J., E. Nicolas, D. Marks, C. Sander, A. Lerro, M.A. Buendia, C. Xu, W.S. Mason, T. Moloshok, R. Bort, K.S. Zaret, and J.M. Taylor. 2004. miR-122, a mammalian liver-specific microRNA, is processed from hcr mRNA and may downregulate the high affinity cationic amino acid transporter CAT-1. *RNA biology*. 1:106-113.

Charalambous, M., and A. Hernandez. 2013. Genomic imprinting of the type 3 thyroid hormone deiodinase gene: regulation and developmental implications. *Biochimica et biophysica acta*. 1830:3946-3955.

Chen, X., Y. Ba, L. Ma, X. Cai, Y. Yin, K. Wang, J. Guo, Y. Zhang, J. Chen, X. Guo, Q. Li, X. Li, W. Wang, J. Wang, X. Jiang, Y. Xiang, C. Xu, P. Zheng, J. Zhang, R. Li, H. Zhang, X. Shang, T. Gong, G. Ning, K. Zen, and C.Y. Zhang. 2008. Characterization of microRNAs in serum: a novel class of biomarkers for diagnosis of cancer and other diseases. *Cell research*. 18:997-1006.

Chen, X.M. 2009. MicroRNA signatures in liver diseases. *World journal of gastroenterology : WJG*. 15:1665-1672.

Chen, Y., J.A. Gelfond, L.M. McManus, and P.K. Shireman. 2009. Reproducibility of quantitative RT-PCR array in miRNA expression profiling and comparison with microarray analysis. *BMC genomics*. 10:407.

Cheng, H.H., H.S. Yi, Y. Kim, E.M. Kroh, J.W. Chien, K.D. Eaton, M.T. Goodman, J.F. Tait, M. Tewari, and C.C. Pritchard. 2013. Plasma Processing Conditions Substantially Influence Circulating microRNA Biomarker Levels. *PloS one*. 8:e64795.

Chiang, Y., Y. Song, Z. Wang, Z. Liu, P. Gao, J. Liang, J. Zhu, C. Xing, and H. Xu. 2012a. microRNA-192, -194 and -215 are frequently downregulated in colorectal cancer. *Experimental and therapeutic medicine*. 3:560-566.

Chiang, Y., X. Zhou, Z. Wang, Y. Song, Z. Liu, F. Zhao, J. Zhu, and H. Xu. 2012b. Expression levels of microRNA-192 and -215 in gastric carcinoma. *Pathology oncology research : POR*. 18:585-591.

Chilakapati, J., K. Shankar, M.C. Korrapati, R.A. Hill, and H.M. Mehendale. 2005. Saturation toxicokinetics of thioacetamide: role in initiation of liver injury. *Drug metabolism and disposition: the biological fate of chemicals*. 33:1877-1885.

Cho, P.F., F. Poulin, Y.A. Cho-Park, I.B. Cho-Park, J.D. Chicoine, P. Lasko, and N. Sonenberg. 2005. A new paradigm for translational control: inhibition via 5'-3' mRNA tethering by Bicoid and the eIF4E cognate 4EHP. *Cell*. 121:411-423.

Christmann, M., and B. Kaina. 2013. Transcriptional regulation of human DNA repair genes following genotoxic stress: trigger mechanisms, inducible responses and genotoxic adaptation. *Nucleic acids research*. 41:8403-8420.

Chun, L.J., M.J. Tong, R.W. Busuttil, and J.R. Hiatt. 2009. Acetaminophen hepatotoxicity and acute liver failure. *Journal of clinical gastroenterology*. 43:342-349.

Chung, W.K., C. Kitner, and B.J. Maron. 2011. Novel frameshift mutation in Troponin C (TNNC1) associated with hypertrophic cardiomyopathy and sudden death. *Cardiology in the young*. 21:345-348.

Cohen, J.I., and L.E. Nagy. 2011. Pathogenesis of alcoholic liver disease: interactions between parenchymal and non-parenchymal cells. *Journal of digestive diseases*. 12:3-9.

Cohen, P. 2001. The role of protein phosphorylation in human health and disease. The Sir Hans Krebs Medal Lecture. *European journal of biochemistry / FEBS*. 268:5001-5010.

Compe, E., and J.M. Egly. 2012. TFIIH: when transcription met DNA repair. *Nature reviews. Molecular cell biology*. 13:343-354.

Conner, E.A., E.R. Lemmer, M. Omori, P.J. Wirth, V.M. Factor, and S.S. Thorgeirsson. 2000. Dual functions of E2F-1 in a transgenic mouse model of liver carcinogenesis. *Oncogene*. 19:5054-5062.

Crampton, R.F., T.J. Gray, P. Grasso, and D.V. Parke. 1977. Long-term studies on chemically induced liver enlargement in the rat. II. Transient induction of microsomal enzymes leading to liver damage and nodular hyperplasia produced by safrole and Ponceau MX. *Toxicology*. 7:307-326.

Crawford, J.M. 2012. Histologic findings in alcoholic liver disease. *Clinics in liver disease*. 16:699-716.

Croteau, W., J.C. Davey, V.A. Galton, and D.L. St Germain. 1996. Cloning of the mammalian type II iodothyronine deiodinase. A selenoprotein differentially expressed and regulated in human and rat brain and other tissues. *The Journal of clinical investigation*. 98:405-417.

Croteau, W., S.L. Whittemore, M.J. Schneider, and D.L. St Germain. 1995. Cloning and expression of a cDNA for a mammalian type III iodothyronine deiodinase. *J. Biol. Chem.* 270:16569-16575.

Cuk, K., M. Zucknick, J. Heil, D. Madhavan, S. Schott, A. Turchinovich, D. Arlt, M. Rath, C. Sohn, A. Benner, H. Junkermann, A. Schneeweiss, and B. Burwinkel. 2013. Circulating microRNAs in plasma as early detection markers for breast cancer. *International journal of cancer. Journal international du cancer*. 132:1602-1612.

Cunningham, M.L. 2002. A mouse is not a rat is not a human: species differences exist. *Toxicological sciences : an official journal of the Society of Toxicology*. 70:157-158.

Curcio-Morelli, C., A.M. Zavacki, M. Christofollete, B. Gereben, B.C. de Freitas, J.W. Harney, Z. Li, G. Wu, and A.C. Bianco. 2003. Deubiquitination of type 2 iodothyronine deiodinase by von Hippel-Lindau protein-interacting deubiquitinating enzymes regulates thyroid hormone activation. *J. Clin. Invest.* 112:189-196.

Da Sacco, L., and A. Masotti. 2012. Recent Insights and Novel Bioinformatics Tools to Understand the Role of MicroRNAs Binding to 5' Untranslated Region. *International journal of molecular sciences*. 14:480-495.

Danielson, P.B. 2002. The cytochrome P450 superfamily: biochemistry, evolution and drug metabolism in humans. *Current drug metabolism*. 3:561-597.

Darras, V.M., L.M. Huybrechts, L. Berghman, E.R. Kuhn, and E. Decuypere. 1990. Ontogeny of the effect of purified chicken growth hormone on the liver 5' monodeiodination activity in the chicken: reversal of the activity after hatching. *Gen. Comp. Endocrinol.* 77:212-220.

Davidson, D.G., and W.N. Eastham. 1966. Acute liver necrosis following overdose of paracetamol. *British medical journal*. 2:497-499.

Davidson, L.A., N. Wang, I. Ivanov, J. Goldsby, J.R. Lupton, and R.S. Chapkin. 2009. Identification of actively translated mRNA transcripts in a rat model of early-stage colon carcinogenesis. *Cancer prevention research (Philadelphia, Pa.)*. 2:984-994.

Davies, R., A. Schuurman, C.R. Barker, B. Clothier, T. Chernova, F.M. Higginson, D.J. Judah, D. Dinsdale, R.E. Edwards, P. Greaves, T.W. Gant, and A.G. Smith. 2005. Hepatic gene expression in protoporphyic Fech mice is associated with cholestatic injury but not a marked depletion of the heme regulatory pool. *The American journal of pathology*. 166:1041-1053.

Davis, D.C., W.Z. Potter, D.J. Jollow, and J.R. Mitchell. 1974. Species differences in hepatic glutathione depletion, covalent binding and hepatic necrosis after acetaminophen. *Life sciences*. 14:2099-2109.

De Matteis, F., and C. Rimington. 1963. Disturbance of porphyrin metabolism caused by griseofulvin in mice. *The British journal of dermatology*. 75:91-104.

Decristofaro, M.F., B.L. Betz, C.J. Rorie, D.N. Reisman, W. Wang, and B.E. Weissman. 2001. Characterization of SWI/SNF protein expression in human breast cancer cell lines and other malignancies. *Journal of cellular physiology*. 186:136-145.

del Prete, M.J., R. Vernal, H. Dolznig, E.W. Mullner, and J.A. Garcia-Sanz. 2007. Isolation of polysome-bound mRNA from solid tissues amenable for RT-PCR and profiling experiments. *RNA (New York, N.Y.)*. 13:414-421.

Delker, D.A., B.L. Yano, and B.B. Gollapudi. 2000. Evaluation of cytotoxicity, cell proliferation, and genotoxicity induced by p-cresidine in hetero- and nullizygous transgenic p53 mice. *Toxicological sciences : an official journal of the Society of Toxicology*. 55:361-369.

Dentice, M., R. Ambrosio, and D. Salvatore. 2009. Role of type 3 deiodinase in cancer. *Expert opinion on therapeutic targets*. 13:1363-1373.

Dentice, M., and D. Salvatore. 2011. Deiodinases: the balance of thyroid hormone: local impact of thyroid hormone inactivation. *J. Endocrinol.* 209:273-282.

Derrien, T., R. Johnson, G. Bussotti, A. Tanzer, S. Djebali, H. Tilgner, G. Guernec, D. Martin, A. Merkel, D.G. Knowles, J. Lagarde, L. Veeravalli, X. Ruan, Y. Ruan, T. Lassmann, P. Carninci, J.B. Brown, L. Lipovich, J.M. Gonzalez, M. Thomas, C.A. Davis, R. Shiekhattar, T.R. Gingeras, T.J. Hubbard, C. Notredame, J. Harrow, and R. Guigo. 2012. The GENCODE v7 catalog of human long noncoding RNAs: analysis of their gene structure, evolution, and expression. *Genome research*. 22:1775-1789.

Dever, T.E., and R. Green. 2012. The elongation, termination, and recycling phases of translation in eukaryotes. *Cold Spring Harbor perspectives in biology*. 4:a013706.

Dietz, W.H., K. Masterson, L.J. Sittig, E.E. Redei, and L.B. Herzing. 2012. Imprinting and expression of Dio3os mirrors Dio3 in rat. *Frontiers in genetics*. 3:279.

Djebali, S., C.A. Davis, A. Merkel, A. Dobin, T. Lassmann, A. Mortazavi, A. Tanzer, J. Lagarde, W. Lin, F. Schlesinger, C. Xue, G.K. Marinov, J. Khatun, B.A. Williams, C. Zaleski, J. Rozowsky, M. Roder, F. Kokocinski, R.F. Abdelhamid, T. Alioto, I. Antoshechkin, M.T. Baer, N.S. Bar, P. Batut, K. Bell, I. Bell, S. Chakrabortty, X. Chen, J. Chrast, J. Curado, T.

Derrien, J. Drenkow, E. Dumais, J. Dumais, R. Duttagupta, E. Falconnet, M. Fastuca, K. Fejes-Toth, P. Ferreira, S. Foissac, M.J. Fullwood, H. Gao, D. Gonzalez, A. Gordon, H. Gunawardena, C. Howald, S. Jha, R. Johnson, P. Kapranov, B. King, C. Kingswood, O.J. Luo, E. Park, K. Persaud, J.B. Preall, P. Ribeca, B. Risk, D. Robyr, M. Sammeth, L. Schaffer, L.H. See, A. Shahab, J. Skancke, A.M. Suzuki, H. Takahashi, H. Tilgner, D. Trout, N. Walters, H. Wang, J. Wrobel, Y. Yu, X. Ruan, Y. Hayashizaki, J. Harrow, M. Gerstein, T. Hubbard, A. Reymond, S.E. Antonarakis, G. Hannon, M.C. Giddings, Y. Ruan, B. Wold, P. Carninci, R. Guigo, and T.R. Gingeras. 2012. Landscape of transcription in human cells. *Nature*. 489:101-108.

Djuranovic, S., A. Nahvi, and R. Green. 2012. miRNA-mediated gene silencing by translational repression followed by mRNA deadenylation and decay. *Science (New York, N.Y.)*. 336:237-240.

Dudek, K.M., L. Suter, V.M. Darras, E.L. Marczylo, and T.W. Gant. 2013. Decreased translation of Dio3 mRNA is associated with drug-induced hepatotoxicity. *The Biochemical journal*. 453:71-82.

Duffield, J.S., S.J. Forbes, C.M. Constandinou, S. Clay, M. Partolina, S. Vuthoori, S. Wu, R. Lang, and J.P. Iredale. 2005. Selective depletion of macrophages reveals distinct, opposing roles during liver injury and repair. *The Journal of clinical investigation*. 115:56-65.

Dunham, I., A. Kundaje, S.F. Aldred, P.J. Collins, C.A. Davis, F. Doyle, C.B. Epstein, S. Frietze, J. Harrow, R. Kaul, J. Khatun, B.R. Lajoie, S.G. Landt, B.K. Lee, F. Pauli, K.R. Rosenbloom, P. Sabo, A. Safi, A. Sanyal, N. Shoresh, J.M. Simon, L. Song, N.D. Trinklein, R.C. Altshuler, E. Birney, J.B. Brown, C. Cheng, S. Djebali, X. Dong, J. Ernst, T.S. Furey, M. Gerstein, B. Giardine, M. Greven, R.C. Hardison, R.S. Harris, J. Herrero, M.M. Hoffman, S. Iyer, M. Kelllis, P. Kheradpour, T. Lassmann, Q. Li, X. Lin, G.K. Marinov, A. Merkel, A. Mortazavi, S.C. Parker, T.E. Reddy, J. Rozowsky, F. Schlesinger, R.E. Thurman, J. Wang, L.D. Ward, T.W. Whitfield, S.P. Wilder, W. Wu, H.S. Xi, K.Y. Yip, J. Zhuang, B.E. Bernstein, E.D. Green, C. Gunter, M. Snyder, M.J. Pazin, R.F. Lowdon, L.A. Dillon, L.B. Adams, C.J. Kelly, J. Zhang, J.R. Wexler, P.J. Good, E.A. Feingold, G.E. Crawford, J. Dekker, L. Elinitski, P.J. Farnham, M.C. Giddings, T.R. Gingeras, R. Guigo, T.J. Hubbard, M. Kellis, W.J. Kent, J.D. Lieb, E.H. Margulies, R.M. Myers, J.A. Starnatoyannopoulos, S.A. Tennebaum, Z. Weng, K.P. White, B. Wold, Y. Yu, J. Wrobel, B.A. Risk, H.P. Gunawardena, H.C. Kuiper, C.W. Maier, L. Xie, X. Chen, T.S. Mikkelsen, et al. 2012. An integrated encyclopedia of DNA elements in the human genome. *Nature*. 489:57-74.

Dweep, H., C. Sticht, P. Pandey, and N. Gretz. 2011. miRWalk--database: prediction of possible miRNA binding sites by "walking" the genes of three genomes. *Journal of biomedical informatics*. 44:839-847.

Eckmann, C.R., C. Rammelt, and E. Wahle. 2011. Control of poly(A) tail length. *Wiley interdisciplinary reviews. RNA*. 2:348-361.

El Gazzar, M., and C.E. McCall. 2010. MicroRNAs distinguish translational from transcriptional silencing during endotoxin tolerance. *The Journal of biological chemistry*. 285:20940-20951.

Ersoz, G., Z. Karasu, U.S. Akarca, F. Gunsar, G. Yuce, and Y. Batur. 2001. Nitroimidazole-induced chronic hepatitis. *European journal of gastroenterology & hepatology*. 13:963-966.

Escobar-Morreale, H.F., M.J. Obregon, A. Hernandez, F. Escobar del Rey, and G. Morreale de Escobar. 1997. Regulation of iodothyronine deiodinase activity as studied in thyroidectomized rats infused with thyroxine or triiodothyronine. *Endocrinology*. 138:2559-2568.

Esfandiari, A., F. Courtin, A.M. Lennon, J.M. Gavaret, and M. Pierre. 1992. Induction of type III deiodinase activity in astroglial cells by thyroid hormones. *Endocrinology*. 131:1682-1688.

Esfandiari, A., C. Gagelin, J.M. Gavaret, S. Pavelka, A.M. Lennon, M. Pierre, and F. Courtin. 1994. Induction of type III-deiodinase activity in astroglial cells by retinoids. *Glia*. 11:255-261.

Etheridge, A., C.P. Gomes, R.W. Pereira, D. Galas, and K. Wang. 2013. The complexity, function and applications of RNA in circulation. *Frontiers in genetics*. 4:115.

Fannin, R.D., M. Russo, T.M. O'Connell, K. Gerrish, J.H. Winnike, J. Macdonald, J. Newton, S. Malik, S.O. Sieber, J. Parker, R. Shah, T. Zhou, P.B. Watkins, and R.S. Paules. 2010. Acetaminophen dosing of humans results in blood transcriptome and metabolome changes consistent with impaired oxidative phosphorylation. *Hepatology (Baltimore, Md.)*. 51:227-236.

Fare, T.L., E.M. Coffey, H. Dai, Y.D. He, D.A. Kessler, K.A. Kilian, J.E. Koch, E. LeProust, M.J. Marton, M.R. Meyer, R.B. Stoughton, G.Y. Tokiwa, and Y. Wang. 2003. Effects of atmospheric ozone on microarray data quality. *Analytical chemistry*. 75:4672-4675.

Farra, R., B. Dapas, G. Pozzato, C. Giansante, O. Heidenreich, L. Uxa, C. Zennaro, G. Guarnieri, and G. Grassi. 2010. Serum response factor depletion affects the proliferation of the hepatocellular carcinoma cells HepG2 and JHH6. *Biochimie*. 92:455-463.

Fehr, J.E., G.W. Trotter, J.T. Oxford, and D.A. Hart. 2000. Comparison of Northern blot hybridization and a reverse transcriptase-polymerase chain reaction technique for measurement of mRNA expression of metalloproteinases and matrix components in articular cartilage and synovial membrane from horses with osteoarthritis. *American journal of veterinary research*. 61:900-905.

Fekete, C., B.C. Freitas, A. Zeold, G. Wittmann, A. Kadar, Z. Liposits, M.A. Christoffolete, P. Singru, R.M. Lechan, A.C. Bianco, and B. Gereben. 2007. Expression patterns of WSB-1 and USP-33 underlie cell-specific posttranslational control of type 2 deiodinase in the rat brain. *Endocrinology*. 148:4865-4874.

Feldstein, A.E., A. Canbay, M.E. Guicciardi, H. Higuchi, S.F. Bronk, and G.J. Gores. 2003. Diet associated hepatic steatosis sensitizes to Fas mediated liver injury in mice. *Journal of hepatology*. 39:978-983.

Feng, B., S. Wu, S. Lv, F. Liu, H. Chen, X. Yan, Y. Li, F. Dong, and L. Wei. 2007. Metabolic profiling analysis of a D-galactosamine/lipopolysaccharide-induced mouse model of fulminant hepatic failure. *Journal of proteome research*. 6:2161-2167.

Ferland-McCollough, D., D.S. Fernandez-Twinn, I.G. Cannell, H. David, M. Warner, A.A. Vaag, J. Bork-Jensen, C. Brons, T.W. Gant, A.E. Willis, K. Siddle, M. Bushell, and S.E. Ozanne. 2012. Programming of adipose tissue miR-483-3p and GDF-3 expression by maternal diet in type 2 diabetes. *Cell death and differentiation*. 19:1003-1012.

Ferri, N., P. Siegl, A. Corsini, J. Herrmann, A. Lerman, and R. Benghozi. 2013. Drug attrition during pre-clinical and clinical development: understanding and managing drug-induced cardiotoxicity. *Pharmacology & therapeutics*. 138:470-484.

Fiedler, J., and T. Thum. 2013. MicroRNAs in myocardial infarction. *Arteriosclerosis, thrombosis, and vascular biology*. 33:201-205.

Filipowicz, W., S.N. Bhattacharyya, and N. Sonenberg. 2008. Mechanisms of post-transcriptional regulation by microRNAs: are the answers in sight? *Nature reviews. Genetics*. 9:102-114.

Fire, A., S. Xu, M.K. Montgomery, S.A. Kostas, S.E. Driver, and C.C. Mello. 1998. Potent and specific genetic interference by double-stranded RNA in Caenorhabditis elegans. *Nature*. 391:806-811.

Flisiak, R. 1997. Role of Ito cells in the liver function. *Polish journal of pathology : official journal of the Polish Society of Pathologists*. 48:139-145.

Fortier, A.M., K. Riopel, M. Desaulniers, and M. Cadrin. 2010. Novel insights into changes in biochemical properties of keratins 8 and 18 in griseofulvin-induced toxic liver injury. *Experimental and molecular pathology*. 89:117-125.

Fox, D.W., M.C. Hart, P.S. Bergeson, P.B. Jarrett, A.E. Stillman, and R.J. Huxtable. 1978. Pyrrolizidine (Senecio) intoxication mimicking Reye syndrome. *The Journal of pediatrics*. 93:980-982.

Frericks, M., and C. Esser. 2008. A toolbox of novel murine house-keeping genes identified by meta-analysis of large scale gene expression profiles. *Biochimica et biophysica acta*. 1779:830-837.

Friedman, R.C., K.K. Farh, C.B. Burge, and D.P. Bartel. 2009. Most mammalian mRNAs are conserved targets of microRNAs. *Genome research*. 19:92-105.

Friedman, S.L. 2000. Molecular regulation of hepatic fibrosis, an integrated cellular response to tissue injury. *The Journal of biological chemistry*. 275:2247-2250.

Friedman, S.L. 2005. Mac the knife? Macrophages- the double-edged sword of hepatic fibrosis. *The Journal of clinical investigation*. 115:29-32.

Fritz, K.S., J.J. Galligan, M.D. Hirschey, E. Verdin, and D.R. Petersen. 2012. Mitochondrial acetylome analysis in a mouse model of alcohol-induced liver injury utilizing SIRT3 knockout mice. *Journal of proteome research*. 11:1633-1643.

Fromenty, B., A. Berson, and D. Pessayre. 1997. Microvesicular steatosis and steatohepatitis: role of mitochondrial dysfunction and lipid peroxidation. *Journal of hepatology*. 26 Suppl 1:13-22.

Fu, S., J. Fan, J. Blanco, A. Gimenez-Cassina, N.N. Danial, S.M. Watkins, and G.S. Hotamisligil. 2012. Polysome profiling in liver identifies dynamic regulation of endoplasmic reticulum translatome by obesity and fasting. *PLoS genetics*. 8:e1002902.

Fuks, F., W.A. Burgers, N. Godin, M. Kasai, and T. Kouzarides. 2001. Dnmt3a binds deacetylases and is recruited by a sequence-specific repressor to silence transcription. *The EMBO journal*. 20:2536-2544.

Fumarola, A., A. Di Fiore, M. Dainelli, G. Grani, G. Carbotta, and A. Calvanese. 2011. Therapy of hyperthyroidism in pregnancy and breastfeeding. *Obstetrical & gynecological survey*. 66:378-385.

Funk, C., M. Pantze, L. Jehle, C. Ponelle, G. Scheuermann, M. Lazendic, and R. Gasser. 2001. Troglitazone-induced intrahepatic cholestasis by an interference with the hepatobiliary export of bile acids in male and female rats. Correlation with the gender difference in troglitazone sulfate formation and the inhibition of the canalicular bile salt export pump (Bsep) by troglitazone and troglitazone sulfate. *Toxicology*. 167:83-98.

Furuichi, Y., A. LaFiandra, and A.J. Shatkin. 1977. 5'-Terminal structure and mRNA stability. *Nature*. 266:235-239.

Galban, S., J. Fan, J.L. Martindale, C. Cheadle, B. Hoffman, M.P. Woods, G. Temeles, J. Brieger, J. Decker, and M. Gorospe. 2003. von Hippel-Lindau protein-mediated repression of tumor necrosis factor alpha translation revealed through use of cDNA arrays. *Molecular and cellular biology*. 23:2316-2328.

Gallie, D.R. 1991. The cap and poly(A) tail function synergistically to regulate mRNA translational efficiency. *Genes & development*. 5:2108-2116.

Galton, V.A., E. Martinez, A. Hernandez, E.A. St Germain, J.M. Bates, and D.L. St Germain. 1999. Pregnant rat uterus expresses high levels of the type 3 iodothyronine deiodinase. *J. Clin. Invest.* 103:979-987.

Gant, T.W., P.R. Baus, B. Clothier, J. Riley, R. Davies, D.J. Judah, R.E. Edwards, E. George, P. Greaves, and A.G. Smith. 2003. Gene expression profiles associated with inflammation, fibrosis, and cholestasis in mouse liver after griseofulvin. *EHP toxicogenomics : journal of the National Institute of Environmental Health Sciences*. 111:37-43.

Gant, T.W., and S.D. Zhang. 2005. In pursuit of effective toxicogenomics. *Mutation research*. 575:4-16.

Gebauer, F., and M.W. Hentze. 2004. Molecular mechanisms of translational control. *Nature reviews. Molecular cell biology*. 5:827-835.

Gebeh, A.K., E.L. Marczylo, A.A. Amoako, J.M. Willets, and J.C. Konje. 2012. Variation in stability of endogenous reference genes in fallopian tubes and endometrium from healthy and ectopic pregnant women. *International journal of molecular sciences*. 13:2810-2826.

George, J., K.R. Rao, R. Stern, and G. Chandrakasan. 2001. Dimethylnitrosamine-induced liver injury in rats: the early deposition of collagen. *Toxicology*. 156:129-138.

Gerashchenko, M.V., A.V. Lobanov, and V.N. Gladyshev. 2012. Genome-wide ribosome profiling reveals complex translational regulation in response to oxidative stress. *Proceedings of the National Academy of Sciences of the United States of America*. 109:17394-17399.

Gereben, B., A. Zeold, M. Dentice, D. Salvatore, and A.C. Bianco. 2008. Activation and inactivation of thyroid hormone by deiodinases: local action with general consequences. *Cell. Mol. Life Sci.* 65:570-590.

Gesteland, R.F., and J.F. Atkins. 1996. Recoding: dynamic reprogramming of translation. *Annual review of biochemistry*. 65:741-768.

Ghafouri-Fard, S. 2012. siRNA and cancer immunotherapy. *Immunotherapy*. 4:907-917.

Gingras, A.C., B. Raught, and N. Sonenberg. 1999. eIF4 initiation factors: effectors of mRNA recruitment to ribosomes and regulators of translation. *Annual review of biochemistry*. 68:913-963.

Git, A., H. Dvinge, M. Salmon-Divon, M. Osborne, C. Kutter, J. Hadfield, P. Bertone, and C. Caldas. 2010. Systematic comparison of microarray profiling, real-time PCR, and next-generation sequencing technologies for measuring differential microRNA expression. *RNA (New York, N.Y.)*. 16:991-1006.

Glinghammar, B., I. Rafter, A.K. Lindstrom, J.J. Hedberg, H.B. Andersson, P. Lindblom, A.L. Berg, and I. Cotgreave. 2009. Detection of the mitochondrial and catalytically active alanine aminotransferase in human tissues and plasma. *International journal of molecular medicine*. 23:621-631.

Golebiowski, F., I. Matic, M.H. Tatham, C. Cole, Y. Yin, A. Nakamura, J. Cox, G.J. Barton, M. Mann, and R.T. Hay. 2009. System-wide changes to SUMO modifications in response to heat shock. *Science signaling*. 2:ra24.

Gong, P., Y. Yang, W. Lei, Y. Feng, S. Li, X. Peng, and Y. Gong. 2012. SMARCE1 Promotes chicken embryonic gonad development by regulating ER alpha and AR expression. *Sexual development : genetics, molecular biology, evolution, endocrinology, embryology, and pathology of sex determination and differentiation*. 6:178-187.

Gray, N.K., and M.W. Hentze. 1994. Iron regulatory protein prevents binding of the 43S translation pre-initiation complex to ferritin and eALAS mRNAs. *The EMBO journal*. 13:3882-3891.

Greaves, P. 2012. Histopathology of Preclinical Toxicity Studies. Elsevier.

Greenman, I.C., E. Gomez, C.E. Moore, and T.P. Herbert. 2007. Distinct glucose-dependent stress responses revealed by translational profiling in pancreatic beta-cells. *The Journal of endocrinology*. 192:179-187.

Grolleau, A., J. Bowman, B. Pradet-Balade, E. Puravs, S. Hanash, J.A. Garcia-Sanz, and L. Beretta. 2002. Global and specific translational control by rapamycin in T cells uncovered by microarrays and proteomics. *The Journal of biological chemistry*. 277:22175-22184.

Guicciardi, M.E., H. Malhi, J.L. Mott, and G.J. Gores. 2013. Apoptosis and necrosis in the liver. *Comprehensive Physiology*. 3:977-1010.

Gunaratne, P.H., C.J. Creighton, M. Watson, and J.B. Tennakoon. 2010. Large-scale integration of MicroRNA and gene expression data for identification of enriched microRNA-mRNA associations in biological systems. *Methods in molecular biology (Clifton, N.J.)*. 667:297-315.

Guo, H., N.T. Ingolia, J.S. Weissman, and D.P. Bartel. 2010. Mammalian microRNAs predominantly act to decrease target mRNA levels. *Nature*. 466:835-840.

Gupta, A.K., D.N. Sauder, and N.H. Shear. 1994. Antifungal agents: an overview. Part I. *Journal of the American Academy of Dermatology*. 30:677-698; quiz 698-700.

Gupta, D.N. 1956. Acute changes in the liver after administration of thioacetamide. *The Journal of pathology and bacteriology*. 72:183-192.

Guthrie, J.L., C. Seah, S. Brown, P. Tang, F. Jamieson, and S.J. Drews. 2008. Use of Bordetella pertussis BP3385 to establish a cutoff value for an IS481-targeted real-time PCR assay. *Journal of clinical microbiology*. 46:3798-3799.

Guttman, M., I. Amit, M. Garber, C. French, M.F. Lin, D. Feldser, M. Huarte, O. Zuk, B.W. Carey, J.P. Cassady, M.N. Cabili, R. Jaenisch, T.S. Mikkelsen, T. Jacks, N. Hacohen, B.E. Bernstein, M. Kellis, A. Regev, J.L. Rinn, and E.S. Lander. 2009. Chromatin signature reveals over a thousand highly conserved large non-coding RNAs in mammals. *Nature*. 458:223-227.

Guttman, M., and J.L. Rinn. 2012. Modular regulatory principles of large non-coding RNAs. *Nature*. 482:339-346.

Habraken, Y., and J. Piette. 2006. NF-kappaB activation by double-strand breaks. *Biochemical pharmacology*. 72:1132-1141.

Haddow, J.E., G.E. Palomaki, W.C. Allan, J.R. Williams, G.J. Knight, J. Gagnon, C.E. O'Heir, M.L. Mitchell, R.J. Hermos, S.E. Waisbren, J.D. Faix, and R.Z. Klein. 1999. Maternal thyroid deficiency during pregnancy and subsequent neuropsychological development of the child. *N Engl J Med*. 341:549-555.

Hagiwara, S., P. Kantharidis, and M.E. Cooper. 2013. microRNA as Biomarkers and Regulator of Cardiovascular Development and Disease. *Current pharmaceutical design*.

Hah, N., A. Kolkman, D.D. Ruhl, W.W. Pijnappel, A.J. Heck, H.T. Timmers, and W.L. Kraus. 2010. A role for BAF57 in cell cycle-dependent transcriptional regulation by the SWI/SNF chromatin remodeling complex. *Cancer research*. 70:4402-4411.

Hames, B.D., and N.M. Hooper. 2000. Instant Notes Biochemistry. BIOS Scientific Publishers Ltd, Oxford, UK. 422 pp.

Hao, N., and M.L. Whitelaw. 2013. The emerging roles of AhR in physiology and immunity. *Biochemical pharmacology*. 86:561-570.

Hastings, M.L., H.A. Ingle, M.A. Lazar, and S.H. Munroe. 2000. Post-transcriptional regulation of thyroid hormone receptor expression by cis-acting sequences and a naturally occurring antisense RNA. *J. Biol. Chem.* 275:11507-11513.

Hastings, M.L., J. Palma, and D.M. Duelli. 2012. Sensitive PCR-based quantitation of cell-free circulating microRNAs. *Methods (San Diego, Calif.)*. 58:144-150.

Hay, N. 2008. p53 strikes mTORC1 by employing sestrins. *Cell metabolism*. 8:184-185.

Hayashi, S., E. Fujii, A. Kato, K. Kimura, K. Mizoguchi, M. Suzuki, T. Sugimoto, H. Takanashi, Z. Itoh, S. Omura, and H. Wanibuchi. 2008. Characterization of multinuclear hepatocytes induced in rats by mitemcinal (GM-611), an erythromycin derivative. *Toxicologic pathology*. 36:858-865.

Helmy, K., J. Halliday, E. Fomchenko, M. Setty, K. Pitter, C. Hafemeister, and E.C. Holland. 2012. Identification of global alteration of translational regulation in glioma in vivo. *PloS one*. 7:e46965.

Heneghan, H.M., N. Miller, and M.J. Kerin. 2010. Circulating miRNA signatures: promising prognostic tools for cancer. *Journal of clinical oncology : official journal of the American Society of Clinical Oncology*. 28:e573-574; author reply e575-576.

Hengen, P.N. 1996. Carriers for precipitating nucleic acids. *Trends in biochemical sciences*. 21:224-225.

Hernandez, A. 2005. Structure and function of the type 3 deiodinase gene. *Thyroid*. 15:865-874.

Hernandez, A., S. Fiering, E. Martinez, V.A. Galton, and D. St Germain. 2002. The gene locus encoding iodothyronine deiodinase type 3 (Dio3) is imprinted in the fetus and expresses antisense transcripts. *Endocrinology*. 143:4483-4486.

Hernandez, A., B. Garcia, and M.J. Obregon. 2007. Gene expression from the imprinted Dio3 locus is associated with cell proliferation of cultured brown adipocytes. *Endocrinology*. 148:3968-3976.

Hernandez, A., M.E. Martinez, W. Croteau, and D.L. St Germain. 2004. Complex organization and structure of sense and antisense transcripts expressed from the DIO3 gene imprinted locus. *Genomics*. 83:413-424.

Hernandez, A., M.E. Martinez, S. Fiering, V.A. Galton, and D. St Germain. 2006. Type 3 deiodinase is critical for the maturation and function of the thyroid axis. *J. Clin. Invest.* 116:476-484.

Hernandez, A., D.L. St Germain, and M.J. Obregon. 1998. Transcriptional activation of type III inner ring deiodinase by growth factors in cultured rat brown adipocytes. *Endocrinology*. 139:634-639.

Holden, P.R., and J.D. Tugwood. 1999. Peroxisome proliferator-activated receptor alpha: role in rodent liver cancer and species differences. *Journal of molecular endocrinology*. 22:1-8.

Hou, L., X. Zhang, D. Wang, and A. Baccarelli. 2012. Environmental chemical exposures and human epigenetics. *International journal of epidemiology*. 41:79-105.

Hsu, D.Z., P.Y. Chu, Y.H. Li, V.R. Chandrasekaran, and M.Y. Liu. 2012. Role of flavin-containing-monooxygenase-dependent neutrophil activation in thioacetamide-induced hepatic inflammation in rats. *Toxicology*. 298:52-58.

Hsu, S.H., and K. Ghoshal. 2013. MicroRNAs in Liver Health and Disease. *Current pathobiology reports*. 1:53-62.

Hu, Z., X. Chen, Y. Zhao, T. Tian, G. Jin, Y. Shu, Y. Chen, L. Xu, K. Zen, C. Zhang, and H. Shen. 2010. Serum microRNA signatures identified in a genome-wide serum microRNA expression profiling predict survival of non-small-cell lung cancer. *Journal of clinical oncology : official journal of the American Society of Clinical Oncology*. 28:1721-1726.

Huang, S.A., D.M. Dorfman, D.R. Genest, D. Salvatore, and P.R. Larsen. 2003. Type 3 iodothyronine deiodinase is highly expressed in the human uteroplacental unit and in fetal epithelium. *J. Clin. Endocrinol. Metab.* 88:1384-1388.

Huang, S.A., H.M. Tu, J.W. Harney, M. Venihaki, A.J. Butte, H.P. Kozakewich, S.J. Fishman, and P.R. Larsen. 2000. Severe hypothyroidism caused by type 3 iodothyronine deiodinase in infantile hemangiomas. *The New England journal of medicine*. 343:185-189.

Huang, Z., D. Huang, S. Ni, Z. Peng, W. Sheng, and X. Du. 2010. Plasma microRNAs are promising novel biomarkers for early detection of colorectal cancer. *International journal of cancer. Journal international du cancer*. 127:118-126.

Hui, A.Y., and S.L. Friedman. 2003. Molecular basis of hepatic fibrosis. *Expert reviews in molecular medicine*. 5:1-23.

Huntzinger, E., and E. Izaurralde. 2011. Gene silencing by microRNAs: contributions of translational repression and mRNA decay. *Nature reviews. Genetics*. 12:99-110.

Hutvagner, G., and P.D. Zamore. 2002. A microRNA in a multiple-turnover RNAi enzyme complex. *Science (New York, N.Y.)*. 297:2056-2060.

Hwang, C.S., A. Shemorry, and A. Varshavsky. 2010. N-terminal acetylation of cellular proteins creates specific degradation signals. *Science (New York, N.Y.)*. 327:973-977.

Iannuzzi, M.C., R.C. Stern, F.S. Collins, C.T. Hon, N. Hidaka, T. Strong, L. Becker, M.L. Drumm, M.B. White, B. Gerrard, and et al. 1991. Two frameshift mutations in the cystic fibrosis gene. *American journal of human genetics*. 48:227-231.

Iorio, M.V., and C.M. Croce. 2009. MicroRNAs in cancer: small molecules with a huge impact. *Journal of clinical oncology : official journal of the American Society of Clinical Oncology*. 27:5848-5856.

Ito, K., N. Kiyosawa, K. Kumagai, S. Manabe, N. Matsunuma, and T. Yamoto. 2006. Molecular mechanism investigation of cycloheximide-induced hepatocyte apoptosis in rat livers by morphological and microarray analysis. *Toxicology*. 219:175-186.

Jackson, A.L., J. Burchard, J. Schelter, B.N. Chau, M. Cleary, L. Lim, and P.S. Linsley. 2006. Widespread siRNA "off-target" transcript silencing mediated by seed region sequence complementarity. *RNA (New York, N.Y.)*. 12:1179-1187.

Jackson, R.J., C.U. Hellen, and T.V. Pestova. 2010. The mechanism of eukaryotic translation initiation and principles of its regulation. *Nature reviews. Molecular cell biology*. 11:113-127.

Jackson, R.J., A.J. Munro, and A. Korner. 1964. ERRORS IN THE USE OF 260-MU ABSORPTION FOR ESTIMATION OF RNPR PARTICLES. *Biochimica et biophysica acta*. 91:666-668.

Jaeschke, H., C.D. Williams, A. Ramachandran, and M.L. Bajt. 2012. Acetaminophen hepatotoxicity and repair: the role of sterile inflammation and innate immunity. *Liver international : official journal of the International Association for the Study of the Liver*. 32:8-20.

James, O., M. Lesna, S.H. Roberts, L. Pulman, A.P. Douglas, P.A. Smith, and A.J. Watson. 1975. Liver damage after paracetamol overdose. Comparison of liver-function tests, fasting serum bile acids, and liver histology. *Lancet*. 2:579-581.

Jeffery, E.H. 1991. Biochemical Basis of Toxicity. *In* Handbook of Toxicologic Pathology. W.M. Haschek and C.G. Rousseaux, editors. Academic Press Inc., London. 49-70.

Jensen, S.G., P. Lamy, M.H. Rasmussen, M.S. Ostenfeld, L. Dyrskjot, T.F. Orntoft, and C.L. Andersen. 2011. Evaluation of two commercial global miRNA expression profiling platforms for detection of less abundant miRNAs. *BMC genomics*. 12:435.

Jezequel, A.M., R. Mancini, M.L. Rinaldesi, G. Macarri, C. Venturini, and F. Orlandi. 1987. A morphological study of the early stages of hepatic fibrosis induced by low doses of dimethylnitrosamine in the rat. *Journal of hepatology*. 5:174-181.

Jiang, H., H. Schwertz, D.I. Schmid, B.B. Jones, J. Kriesel, M.L. Martinez, A.S. Weyrich, G.A. Zimmerman, and L.W. Kraiss. 2012. Different mechanisms preserve translation of programmed cell death 8 and JunB in virus-infected endothelial cells. *Arteriosclerosis, thrombosis, and vascular biology*. 32:997-1004.

Johannes, G., M.S. Carter, M.B. Eisen, P.O. Brown, and P. Sarnow. 1999. Identification of eukaryotic mRNAs that are translated at reduced cap binding complex eIF4F concentrations using a cDNA microarray. *Proceedings of the National Academy of Sciences of the United States of America*. 96:13118-13123.

Johannes, G., and P. Sarnow. 1998. Cap-independent polysomal association of natural mRNAs encoding c-myc, BiP, and eIF4G conferred by internal ribosome entry sites. *RNA (New York, N.Y.)*. 4:1500-1513.

Johnson, M.L., C. Navanukraw, A.T. Grazul-Bilska, L.P. Reynolds, and D.A. Redmer. 2003. Heparinase treatment of RNA before quantitative real-time RT-PCR. *BioTechniques*. 35:1140-1142, 1144.

Johnsson, P., A. Ackley, L. Vidarsdottir, W.O. Lui, M. Corcoran, D. Grander, and K.V. Morris. 2013. A pseudogene long-noncoding-RNA network regulates PTEN transcription and translation in human cells. *Nature structural & molecular biology*. 20:440-446.

Jones-Rhoades, M.W., D.P. Bartel, and B. Bartel. 2006. MicroRNAS and their regulatory roles in plants. *Annual review of plant biology*. 57:19-53.

Jones, H.B., N.A. Clarke, and N.C. Barrass. 1993. Phenobarbital-induced hepatocellular proliferation: anti-bromodeoxyuridine and anti-proliferating cell nuclear antigen immunocytochemistry. *The journal of histochemistry and cytochemistry : official journal of the Histochemistry Society*. 41:21-27.

Jonker, J.W., C.A. Stedman, C. Liddle, and M. Downes. 2009. Hepatobiliary ABC transporters: physiology, regulation and implications for disease. *Frontiers in bioscience (Landmark edition)*. 14:4904-4920.

Ju, C., T.P. Reilly, M. Bourdi, M.F. Radonovich, J.N. Brady, J.W. George, and L.R. Pohl. 2002. Protective role of Kupffer cells in acetaminophen-induced hepatic injury in mice. *Chemical research in toxicology*. 15:1504-1513.

Jung, T., and T. Grune. 2013. The proteasome and the degradation of oxidized proteins: Part I-structure of proteasomes. *Redox biology*. 1:178-182.

Kanemaru, H., S. Fukushima, J. Yamashita, N. Honda, R. Oyama, A. Kakimoto, S. Masuguchi, T. Ishihara, Y. Inoue, M. Jinnin, and H. Ihn. 2011. The circulating microRNA-221 level in patients with malignant melanoma as a new tumor marker. *Journal of dermatological science*. 61:187-193.

Kaplan, M.M., and K.A. Yaskoski. 1980. Phenolic and tyrosyl ring deiodination of iodothyronines in rat brain homogenates. *J. Clin. Invest.* 66:551-562.

Kertesz, M., N. Iovino, U. Unnerstall, U. Gaul, and E. Segal. 2007. The role of site accessibility in microRNA target recognition. *Nature genetics*. 39:1278-1284.

Kester, M.H., M.J. Toussaint, C.A. Punt, R. Matondo, A.M. Aarnio, V.M. Darras, M.E. Everts, A. de Bruin, and T.J. Visser. 2009. Large induction of type III deiodinase expression after partial hepatectomy in the regenerating mouse and rat liver. *Endocrinology*. 150:540-545.

Khella, H.W., M. Bakhet, G. Allo, M.A. Jewett, A.H. Girgis, A. Latif, H. Girgis, I. Von Both, G.A. Bjarnason, and G.M. Yousef. 2013. miR-192, miR-194 and miR-215: a convergent microRNA network suppressing tumor progression in renal cell carcinoma. *Carcinogenesis*. 34:2231-2239.

Kikkawa, R., M. Fujikawa, T. Yamamoto, Y. Hamada, H. Yamada, and I. Horii. 2006. In vivo hepatotoxicity study of rats in comparison with in vitro hepatotoxicity screening system. *The Journal of toxicological sciences*. 31:23-34.

Kim, D.J., S. Linnstaedt, J. Palma, J.C. Park, E. Ntrivalas, J.Y. Kwak-Kim, A. Gilman-Sachs, K. Beaman, M.L. Hastings, J.N. Martin, and D.M. Duelli. 2012. Plasma components affect accuracy of circulating cancer-related microRNA quantitation. *The Journal of molecular diagnostics : JMD*. 14:71-80.

Kim, W.R., S.L. Flamm, A.M. Di Bisceglie, and H.C. Bodenheimer. 2008. Serum activity of alanine aminotransferase (ALT) as an indicator of health and disease. *Hepatology (Baltimore, Md.)*. 47:1363-1370.

Kim, Y., P. Alpmann, S. Blaum-Feder, S. Kramer, T. Endo, D. Lu, D. Carson, and I.G. Schmidt-Wolf. 2011. In vivo efficacy of griseofulvin against multiple myeloma. *Leukemia research*. 35:1070-1073.

Kirchheiner, J., H. Schmidt, M. Tzvetkov, J.T. Keulen, J. Lotsch, I. Roots, and J. Brockmoller. 2007. Pharmacokinetics of codeine and its metabolite morphine in ultra-rapid metabolizers due to CYP2D6 duplication. *The pharmacogenomics journal*. 7:257-265.

Kirschner, M.B., J.J. Edelman, S.C. Kao, M.P. Vallely, N. van Zandwijk, and G. Reid. 2013. The Impact of Hemolysis on Cell-Free microRNA Biomarkers. *Frontiers in genetics*. 4:94.

Kirschner, M.B., S.C. Kao, J.J. Edelman, N.J. Armstrong, M.P. Vallely, N. van Zandwijk, and G. Reid. 2011. Haemolysis during sample preparation alters microRNA content of plasma. *PloS one*. 6:e24145.

Klose, R.J., and Y. Zhang. 2007. Regulation of histone methylation by demethylimination and demethylation. *Nature reviews. Molecular cell biology*. 8:307-318.

Knasmuller, S., W. Parzefall, C. Helma, F. Kassie, S. Ecker, and R. Schulte-Hermann. 1997. Toxic effects of griseofulvin: disease models, mechanisms, and risk assessment. *Critical reviews in toxicology*. 27:495-537.

Kong, X., Y. Du, G. Wang, J. Gao, Y. Gong, L. Li, Z. Zhang, J. Zhu, Q. Jing, Y. Qin, and Z. Li. 2011. Detection of differentially expressed microRNAs in serum of pancreatic ductal adenocarcinoma patients: miR-196a could be a potential marker for poor prognosis. *Digestive diseases and sciences*. 56:602-609.

Konno, Y., M. Negishi, and S. Kodama. 2008. The roles of nuclear receptors CAR and PXR in hepatic energy metabolism. *Drug metabolism and pharmacokinetics*. 23:8-13.

Kopnin, P.B., L.S. Agapova, B.P. Kopnin, and P.M. Chumakov. 2007. Repression of sestrin family genes contributes to oncogenic Ras-induced reactive oxygen species up-regulation and genetic instability. *Cancer research*. 67:4671-4678.

Kornberg, R.D. 1977. Structure of chromatin. *Annual review of biochemistry*. 46:931-954.

Kornberg, R.D., and Y. Lorch. 1992. Chromatin structure and transcription. *Annual review of cell biology*. 8:563-587.

Kosaka, N., H. Iguchi, and T. Ochiya. 2010. Circulating microRNA in body fluid: a new potential biomarker for cancer diagnosis and prognosis. *Cancer science*. 101:2087-2092.

Koufaris, C., and N.J. Gooderham. 2013. Are differences in microRNA regulation implicated in species-dependent response to toxicological exposures? *Toxicological sciences : an official journal of the Society of Toxicology*. 131:337-342.

Koufaris, C., J. Wright, R.A. Currie, and N.J. Gooderham. 2012. Hepatic microRNA profiles offer predictive and mechanistic insights after exposure to genotoxic and epigenetic hepatocarcinogens. *Toxicological sciences : an official journal of the Society of Toxicology*. 128:532-543.

Koutedakis, Y., A. Raafat, N.C. Sharp, M.N. Rosmarin, M.J. Beard, and S.W. Robbins. 1993. Serum enzyme activities in individuals with different levels of physical fitness. *The Journal of sports medicine and physical fitness*. 33:252-257.

Kozak, M. 1992. Regulation of translation in eukaryotic systems. *Annual review of cell biology*. 8:197-225.

Kozak, M. 2005. Regulation of translation via mRNA structure in prokaryotes and eukaryotes. *Gene*. 361:13-37.

Kroh, E.M., R.K. Parkin, P.S. Mitchell, and M. Tewari. 2010. Analysis of circulating microRNA biomarkers in plasma and serum using quantitative reverse transcription-PCR (qRT-PCR). *Methods (San Diego, Calif.)*. 50:298-301.

Krol, J., I. Loedige, and W. Filipowicz. 2010. The widespread regulation of microRNA biogenesis, function and decay. *Nature reviews. Genetics*. 11:597-610.

Krumova, P., E. Meulmeester, M. Garrido, M. Tirard, H.H. Hsiao, G. Bossis, H. Urlaub, M. Zweckstetter, S. Kugler, F. Melchior, M. Bahr, and J.H. Weishaupt. 2011. Sumoylation inhibits alpha-synuclein aggregation and toxicity. *The Journal of cell biology*. 194:49-60.

Kubota, N., S. Kado, M. Kano, N. Masuoka, Y. Nagata, T. Kobayashi, K. Miyazaki, and F. Ishikawa. 2013. A high-fat diet and multiple administration of carbon tetrachloride induces liver injury and pathological features associated with non-alcoholic steatohepatitis in mice. *Clinical and experimental pharmacology & physiology*. 40:422-430.

Kucera, O., H. Lotkova, P. Stankova, M. Podhola, T. Rousar, V. Mezera, and Z. Cervinkova. 2011. Is rat liver affected by non-alcoholic steatosis more susceptible to the acute toxic effect of thioacetamide? *International journal of experimental pathology*. 92:281-289.

Kudo, K., Y. Xi, Y. Wang, B. Song, E. Chu, J. Ju, and J.J. Russo. 2010. Translational control analysis by translationally active RNA capture/microarray analysis (TrIP-Chip). *Nucleic acids research*. 38:e104.

Kumar, P., Z. Dezso, C. Mackenzie, J. Oestreicher, S. Agoulnik, M. Byrne, F. Bernier, M. Yanagimachi, K. Aoshima, and Y. Oda. 2013. Circulating miRNA Biomarkers for Alzheimer's Disease. *PloS one*. 8:e69807.

Kyle, M.E., and J.L. Farber. 1991. Biochemical Mechanisms of Toxic Cell Injury. *In* Handbook of Toxicologic Pathology. W.M. Haschek and C.G. Rousseaux, editors. Academic Press Inc, London. 71-89.

Laleman, W., I. Vander Elst, M. Zeegers, R. Servaes, L. Libbrecht, T. Roskams, J. Fevery, and F. Nevens. 2006. A stable model of cirrhotic portal hypertension in the rat: thioacetamide revisited. *European journal of clinical investigation*. 36:242-249.

Lardizabal, M.N., A.L. Nocito, S.M. Daniele, L.A. Ornella, J.F. Palatnik, and L.M. Veggi. 2012. Reference genes for real-time PCR quantification of microRNAs and messenger RNAs in rat models of hepatotoxicity. *PloS one*. 7:e36323.

Larson, A.M., J. Polson, R.J. Fontana, T.J. Davern, E. Lalani, L.S. Hynan, J.S. Reisch, F.V. Schiodt, G. Ostapowicz, A.O. Shakil, and W.M. Lee. 2005. Acetaminophen-induced acute liver failure: results of a United States multicenter, prospective study. *Hepatology (Baltimore, Md.)*. 42:1364-1372.

Lautt, W.W., and C.V. Greenway. 1987. Conceptual review of the hepatic vascular bed. *Hepatology (Baltimore, Md.)*. 7:952-963.

Lawrie, C.H., S. Gal, H.M. Dunlop, B. Pushkaran, A.P. Liggins, K. Pulford, A.H. Banham, F. Pezzella, J. Boultwood, J.S. Wainscoat, C.S. Hatton, and A.L. Harris. 2008. Detection of elevated levels of tumour-associated microRNAs in serum of patients with diffuse large B-cell lymphoma. *British journal of haematology*. 141:672-675.

Le Quesne, J.P., K.A. Spriggs, M. Bushell, and A.E. Willis. 2010. Dysregulation of protein synthesis and disease. *J. Pathol.* 220:140-151.

Lee, R.C., R.L. Feinbaum, and V. Ambros. 1993. The C. elegans heterochronic gene lin-4 encodes small RNAs with antisense complementarity to lin-14. *Cell*. 75:843-854.

Lee, S., and F.T. Tsai. 2005. Molecular chaperones in protein quality control. *Journal of biochemistry and molecular biology*. 38:259-265.

Lee, Y., M. Kim, J. Han, K.H. Yeom, S. Lee, S.H. Baek, and V.N. Kim. 2004. MicroRNA genes are transcribed by RNA polymerase II. *The EMBO journal*. 23:4051-4060.

Lema, C., and M.J. Cunningham. 2010. MicroRNAs and their implications in toxicological research. *Toxicology letters*. 198:100-105.

Lema, S.C., and G.A. Nevitt. 2004. Evidence that thyroid hormone induces olfactory cellular proliferation in salmon during a sensitive period for imprinting. *J Exp Biol*. 207:3317-3327.

Leonard, J.L., C.A. Siegrist-Kaiser, and C.J. Zuckerman. 1990. Regulation of type II iodothyronine 5'-deiodinase by thyroid hormone. Inhibition of actin polymerization blocks enzyme inactivation in cAMP-stimulated glial cells. *J Biol Chem*. 265:940-946.

Lewis, B.P., C.B. Burge, and D.P. Bartel. 2005. Conserved seed pairing, often flanked by adenosines, indicates that thousands of human genes are microRNA targets. *Cell*. 120:15-20.

Li, J., P. Smyth, R. Flavin, S. Cahill, K. Denning, S. Aherne, S.M. Guenther, J.J. O'Leary, and O. Sheils. 2007. Comparison of miRNA expression patterns using total RNA extracted from matched samples of formalin-fixed paraffin-embedded (FFPE) cells and snap frozen cells. *BMC biotechnology*. 7:36.

Li, X., I.S. Benjamin, and B. Alexander. 2002. Reproducible production of thioacetamide-induced macronodular cirrhosis in the rat with no mortality. *Journal of hepatology*. 36:488-493.

Li, X., and R.W. Carthew. 2005. A microRNA mediates EGF receptor signaling and promotes photoreceptor differentiation in the Drosophila eye. *Cell*. 123:1267-1277.

Li, Y., X.R. Wu, X.F. Li, Suriguga, C.H. Yu, Y.R. Li, and Z.C. Yi. 2013. Changes in DNA methylation of erythroid-specific genes in K562 cells exposed to phenol and hydroquinone. *Toxicology*. 312C:108-114.

Liang, H., J. Zhang, K. Zen, C.Y. Zhang, and X. Chen. 2013. Nuclear microRNAs and their unconventional role in regulating non-coding RNAs. *Protein & cell*. 4:325-330.

Liang, Y., D. Ridzon, L. Wong, and C. Chen. 2007. Characterization of microRNA expression profiles in normal human tissues. *BMC genomics*. 8:166.

Libbrecht, L., L. Meerman, F. Kuipers, T. Roskams, V. Desmet, and P. Jansen. 2003. Liver pathology and hepatocarcinogenesis in a long-term mouse model of erythropoietic protoporphyria. *The Journal of pathology*. 199:191-200.

Lim, L.P., N.C. Lau, P. Garrett-Engele, A. Grimson, J.M. Schelter, J. Castle, D.P. Bartel, P.S. Linsley, and J.M. Johnson. 2005. Microarray analysis shows that some microRNAs downregulate large numbers of target mRNAs. *Nature*. 433:769-773.

Lindblom, P., I. Rafter, C. Copley, U. Andersson, J.J. Hedberg, A.L. Berg, A. Samuelsson, H. Hellmold, I. Cotgreave, and B. Glinghammar. 2007. Isoforms of alanine aminotransferases in human tissues and serum--differential tissue expression using novel antibodies. *Archives of biochemistry and biophysics*. 466:66-77.

Linsen, S.E., E. de Wit, E. de Bruijn, and E. Cuppen. 2010. Small RNA expression and strain specificity in the rat. *BMC genomics*. 11:249.

Lipshutz, R.J., D. Morris, M. Chee, E. Hubbell, M.J. Kozal, N. Shah, N. Shen, R. Yang, and S.P. Fodor. 1995. Using oligonucleotide probe arrays to access genetic diversity. *BioTechniques*. 19:442-447.

Liu, B., Y. Han, and S.B. Qian. 2013. Cotranslational response to proteotoxic stress by elongation pausing of ribosomes. *Molecular cell*. 49:453-463.

Liu, M.J., S.H. Wu, and H.M. Chen. 2012. Widespread translational control contributes to the regulation of Arabidopsis photomorphogenesis. *Molecular systems biology*. 8:566.

Liu, S.P., R.H. Fu, H.H. Yu, K.W. Li, C.H. Tsai, W.C. Shyu, and S.Z. Lin. 2009. MicroRNAs regulation modulated self-renewal and lineage differentiation of stem cells. *Cell transplantation*. 18:1039-1045.

Liu, Z.X., S. Govindarajan, and N. Kaplowitz. 2004. Innate immune system plays a critical role in determining the progression and severity of acetaminophen hepatotoxicity. *Gastroenterology*. 127:1760-1774.

Llorens, F., M. Hummel, L. Pantano, X. Pastor, A. Vivancos, E. Castillo, H. Matllin, A. Ferrer, M. Ingham, M. Noguera, R. Kofler, J.C. Dohm, R. Pluvinet, M. Bayes, H. Himmelbauer, J.A. Del Rio, E. Marti, and L. Sumoy. 2013. Microarray and deep sequencing cross-platform analysis of the mirRNome and isomiR variation in response to epidermal growth factor. *BMC genomics*. 14:371.

Lochmatter, P., A. Zawodniak, and W.J. Pichler. 2009. In vitro tests in drug hypersensitivity diagnosis. *Immunology and allergy clinics of North America*. 29:537-554.

Locke, W. 1982. Management of hyper & hypo thyroid conditions. *Postgraduate medicine*. 71:118-125, 128-119.

Lu, J., G. Getz, E.A. Miska, E. Alvarez-Saavedra, J. Lamb, D. Peck, A. Sweet-Cordero, B.L. Ebert, R.H. Mak, A.A. Ferrando, J.R. Downing, T. Jacks, H.R. Horvitz, and T.R. Golub. 2005. MicroRNA expression profiles classify human cancers. *Nature*. 435:834-838.

Lu, Z., M. Bourdi, J.H. Li, A.M. Aponte, Y. Chen, D.B. Lombard, M. Gucek, L.R. Pohl, and M.N. Sack. 2011. SIRT3-dependent deacetylation exacerbates acetaminophen hepatotoxicity. *EMBO reports*. 12:840-846.

Lujambio, A., A. Portela, J. Liz, S.A. Melo, S. Rossi, R. Spizzo, C.M. Croce, G.A. Calin, and M. Esteller. 2010. CpG island hypermethylation-associated silencing of non-coding RNAs transcribed from ultraconserved regions in human cancer. *Oncogene*. 29:6390-6401.

Maeda, N., T. Kasukawa, R. Oyama, J. Gough, M. Frith, P.G. Engstrom, B. Lenhard, R.N. Aturaliya, S. Batalov, K.W. Beisel, C.J. Bult, C.F. Fletcher, A.R. Forrest, M. Furuno, D. Hill, M. Itoh, M. Kanamori-Katayama, S. Katayama, M. Katoh, T. Kawashima, J. Quackenbush, T. Ravasi, B.Z. Ring, K. Shibata, K. Sugiura, Y. Takenaka, R.D. Teasdale, C.A. Wells, Y. Zhu, C. Kai, J. Kawai, D.A. Hume, P. Carninci, and Y. Hayashizaki. 2006. Transcript annotation in FANTOM3: mouse gene catalog based on physical cDNAs. *PLoS genetics*. 2:e62.

Mangipudy, R.S., S. Chanda, and H.M. Mehendale. 1995a. Tissue repair response as a function of dose in thioacetamide hepatotoxicity. *Environmental health perspectives*. 103:260-267.

Mangipudy, R.S., S. Chanda, and H.M. Mehendale. 1995b. Tissue repair response as a function of dose in thioacetamide hepatotoxicity. *Environ. Health Perspect.* 103:260-267.

Marczylo, E.L., A.A. Amoako, J.C. Konje, T.W. Gant, and T.H. Marczylo. 2012. Smoking induces differential miRNA expression in human spermatozoa: a potential transgenerational epigenetic concern? *Epigenetics : official journal of the DNA Methylation Society*. 7:432-439.

Matheis, K.A., E. Com, J.C. Gautier, N. Guerreiro, A. Brandenburg, H. Gmuender, A. Sposny, P. Hewitt, A. Amberg, O. Boernsen, B. Riefke, D. Hoffmann, A. Mally, A. Kalkuhl, L. Suter, F. Dieterle, and F. Staedtler. 2011a. Cross-study and cross-omics comparisons of three nephrotoxic compounds reveal mechanistic insights and new candidate biomarkers. *Toxicol. Appl. Pharmacol.* 252:112-122.

Matheis, K.A., E. Com, J.C. Gautier, N. Guerreiro, A. Brandenburg, H. Gmuender, A. Sposny, P. Hewitt, A. Amberg, O. Boernsen, B. Riefke, D. Hoffmann, A. Mally, A. Kalkuhl, L. Suter, F. Dieterle, and F. Staedtler. 2011b. Cross-study and cross-omics comparisons of three nephrotoxic compounds reveal mechanistic insights and new candidate biomarkers. *Toxicology and applied pharmacology*. 252:112-122.

Matsufuji, S., T. Matsufuji, Y. Miyazaki, Y. Murakami, J.F. Atkins, R.F. Gesteland, and S. Hayashi. 1995. Autoregulatory frameshifting in decoding mammalian ornithine decarboxylase antizyme. *Cell*. 80:51-60.

Mayorga, C., M.L. Sanz, P. Gamboa, M.C. Garcia-Aviles, J. Fernandez, and M.J. Torres. 2013. In vitro methods for diagnosing nonimmediate hypersensitivity reactions to drugs. *Journal of investigational allergology & clinical immunology*. 23:213-225; quiz precedeing 225.

McAlexander, M.A., M.J. Phillips, and K.W. Witwer. 2013. Comparison of Methods for miRNA Extraction from Plasma and Quantitative Recovery of RNA from Cerebrospinal Fluid. *Frontiers in genetics*. 4:83.

McCracken, S., N. Fong, E. Rosonina, K. Yankulov, G. Brothers, D. Siderovski, A. Hessel, S. Foster, S. Shuman, and D.L. Bentley. 1997. 5'-Capping enzymes are targeted to pre-mRNA by binding to the phosphorylated carboxy-terminal domain of RNA polymerase II. *Genes & development*. 11:3306-3318.

McDonald, J.S., D. Milosevic, H.V. Reddi, S.K. Grebe, and A. Algeciras-Schimnich. 2011. Analysis of circulating microRNA: preanalytical and analytical challenges. *Clinical chemistry*. 57:833-840.

Mehendale, H.M. 2005. Tissue repair: an important determinant of final outcome of toxicant-induced injury. *Toxicologic pathology*. 33:41-51.

Meijer, H.A., Y.W. Kong, W.T. Lu, A. Wilczynska, R.V. Spriggs, S.W. Robinson, J.D. Godfrey, A.E. Willis, and M. Bushell. 2013. Translational repression and eIF4A2 activity are critical for microRNA-mediated gene regulation. *Science (New York, N.Y.)*. 340:82-85.

Michalopoulos, G.K. 2007. Liver regeneration. *Journal of cellular physiology*. 213:286-300.

Miller, O.J., W. Schnedl, J. Allen, and B.F. Erlanger. 1974. 5-Methylcytosine localised in mammalian constitutive heterochromatin. *Nature*. 251:636-637.

Mitchell, P.S., R.K. Parkin, E.M. Kroh, B.R. Fritz, S.K. Wyman, E.L. Pogosova-Agadjanyan, A. Peterson, J. Noteboom, K.C. O'Briant, A. Allen, D.W. Lin, N. Urban, C.W. Drescher, B.S. Knudsen, D.L. Stirewalt, R. Gentleman, R.L. Vessella, P.S. Nelson, D.B. Martin, and M. Tewari. 2008. Circulating microRNAs as stable blood-based markers for cancer detection. *Proceedings of the National Academy of Sciences of the United States of America*. 105:10513-10518.

Mondol, V., and A.E. Pasquinelli. 2012. Let's make it happen: the role of let-7 microRNA in development. *Current topics in developmental biology*. 99:1-30.

Mor, E., Y. Cabilly, Y. Goldshmit, H. Zalts, S. Modai, L. Edry, O. Elroy-Stein, and N. Shomron. 2011. Species-specific microRNA roles elucidated following astrocyte activation. *Nucleic acids research*. 39:3710-3723.

Moreno, J.A., H. Radford, D. Peretti, J.R. Steinert, N. Verity, M.G. Martin, M. Halliday, J. Morgan, D. Dinsdale, C.A. Ortori, D.A. Barrett, P. Tsaytler, A. Bertolotti, A.E. Willis, M.

Bushell, and G.R. Mallucci. 2012. Sustained translational repression by eIF2alpha-P mediates prion neurodegeneration. *Nature*. 485:507-511.

Mori, K., K. Yoshida, H. Fukazawa, Y. Kiso, N. Sayama, K. Kikuchi, Y. Aizawa, and K. Abe. 1995. Thyroid hormone regulates rat placental type III iodothyronine deiodinase activity by inducing kinetic changes different from those in the same isozyme in rat brain. *Endocr. J.* 42:753-760.

Mota, L.C., C. Barfield, J.P. Hernandez, and W.S. Baldwin. 2011. Nonylphenol-mediated CYP induction is PXR-dependent: The use of humanized mice and human hepatocytes suggests that hPXR is less sensitive than mouse PXR to nonylphenol treatment. *Toxicology and applied pharmacology*. 252:259-267.

Muckenthaler, M., N.K. Gray, and M.W. Hentze. 1998. IRP-1 binding to ferritin mRNA prevents the recruitment of the small ribosomal subunit by the cap-binding complex eIF4F. *Molecular cell*. 2:383-388.

Murray, C.J., M.A. Richards, J.N. Newton, K.A. Fenton, H.R. Anderson, C. Atkinson, D. Bennett, E. Bernabe, H. Blencowe, R. Bourne, T. Braithwaite, C. Brayne, N.G. Bruce, T.S. Brugha, P. Burney, M. Dherani, H. Dolk, K. Edmond, M. Ezzati, A.D. Flaxman, T.D. Fleming, G. Freedman, D. Gunnell, R.J. Hay, S.J. Hutchings, S.L. Ohno, R. Lozano, R.A. Lyons, W. Marcenes, M. Naghavi, C.R. Newton, N. Pearce, D. Pope, L. Rushton, J.A. Salomon, K. Shibuya, T. Vos, H. Wang, H.C. Williams, A.D. Woolf, A.D. Lopez, and A. Davis. 2013. UK health performance: findings of the Global Burden of Disease Study 2010. *Lancet*. 381:997-1020.

Nachman, M.W. 2001. Single nucleotide polymorphisms and recombination rate in humans. *Trends in genetics : TIG*. 17:481-485.

Namy, O., J.P. Rousset, S. Napthine, and I. Brierley. 2004. Reprogrammed genetic decoding in cellular gene expression. *Molecular cell*. 13:157-168.

Nathwani, R.A., S. Pais, T.B. Reynolds, and N. Kaplowitz. 2005. Serum alanine aminotransferase in skeletal muscle diseases. *Hepatology (Baltimore, Md.)*. 41:380-382.

Nelson, D.R., D.C. Zeldin, S.M. Hoffman, L.J. Maltais, H.M. Wain, and D.W. Nebert. 2004. Comparison of cytochrome P450 (CYP) genes from the mouse and human genomes, including nomenclature recommendations for genes, pseudogenes and alternative-splice variants. *Pharmacogenetics*. 14:1-18.

Nelson, S.D. 1990. Molecular mechanisms of the hepatotoxicity caused by acetaminophen. *Seminars in liver disease*. 10:267-278.

Nobrega, M.A., I. Ovcharenko, V. Afzal, and E.M. Rubin. 2003. Scanning human gene deserts for long-range enhancers. *Science (New York, N.Y.)*. 302:413.

Nuber, R., H.F. Teutsch, and D. Sasse. 1980. Metabolic zonation in thioacetamide-induced liver cirrhosis. *Histochemistry*. 69:277-288.

Ockner, R.K., and R. Schmid. 1961. Acquired porphyria in man and rat due to hexachlorobenzene intoxication. *Nature*. 189:499.

Oerbeck, B., I. Reinvang, K. Sundet, and S. Heyerdahl. 2007. Young adults with severe congenital hypothyroidism: cognitive event related potentials (ERPs) and the significance of an early start of thyroxine treatment. *Scand J Psychol*. 48:61-67.

Okamura, K., and E.C. Lai. 2008. Endogenous small interfering RNAs in animals. *Nature reviews. Molecular cell biology*. 9:673-678.

Omer, A.D., M.M. Janas, and C.D. Novina. 2009. The chicken or the egg: microRNA-mediated regulation of mRNA translation or mRNA stability. *Molecular cell*. 35:739-740.

Oren, R., I. Dotan, M. Papa, Y. Marravi, H. Aeed, J. Barg, L. Zeidel, R. Bruck, and Z. Halpern. 1996. Inhibition of experimentally induced cirrhosis in rats by hypothyroidism. *Hepatology (Baltimore, Md.)*. 24:419-423.

Orom, U.A., and A.H. Lund. 2010. Experimental identification of microRNA targets. *Gene*. 451:1-5.

Orom, U.A., F.C. Nielsen, and A.H. Lund. 2008. MicroRNA-10a binds the 5'UTR of ribosomal protein mRNAs and enhances their translation. *Molecular cell*. 30:460-471.

Ozer, J., M. Ratner, M. Shaw, W. Bailey, and S. Schomaker. 2008. The current state of serum biomarkers of hepatotoxicity. *Toxicology*. 245:194-205.

Padda, M.S., M. Sanchez, A.J. Akhtar, and J.L. Boyer. 2011. Drug-induced cholestasis. *Hepatology (Baltimore, Md.)*. 53:1377-1387.

Pandya-Jones, A. 2011. Pre-mRNA splicing during transcription in the mammalian system. *Wiley interdisciplinary reviews. RNA*. 2:700-717.

Paquette, M.A., H. Dong, R. Gagne, A. Williams, M. Malowany, M.G. Wade, and C.L. Yauk. 2011. Thyroid Hormone-Regulated Gene Expression in Juvenile Mouse Liver: Identification of Thyroid Response Elements Using Microarray Profiling and In Silico Analyses. *BMC Genomics*. 12:634.

Park, B.K., A. Boobis, S. Clarke, C.E. Goldring, D. Jones, J.G. Kenna, C. Lambert, H.G. Laverty, D.J. Naisbitt, S. Nelson, D.A. Nicoll-Griffith, R.S. Obach, P. Routledge, D.A. Smith, D.J. Tweedie, N. Vermeulen, D.P. Williams, I.D. Wilson, and T.A. Baillie. 2011. Managing the challenge of chemically reactive metabolites in drug development. *Nature reviews. Drug discovery*. 10:292-306.

Park, B.K., M. Pirmohamed, and N.R. Kitteringham. 1998. Role of drug disposition in drug hypersensitivity: a chemical, molecular, and clinical perspective. *Chemical research in toxicology*. 11:969-988.

Paternostro, M.A., and E. Meisami. 1994. Quantitative [3H]thymidine autoradiography of neurogenesis in the olfactory epithelium of developing normal, hypothyroid and hypothyroid-rehabilitated rats. *Brain research. Developmental brain research*. 83:151-162.

Paul, S.M., D.S. Mytelka, C.T. Dunwiddie, C.C. Persinger, B.H. Munos, S.R. Lindborg, and A.L. Schacht. 2010. How to improve R&D productivity: the pharmaceutical industry's grand challenge. *Nature reviews. Drug discovery*. 9:203-214.

Peeters, R., C. Fekete, C. Goncalves, G. Legradi, H.M. Tu, J.W. Harney, A.C. Bianco, R.M. Lechan, and P.R. Larsen. 2001. Regional physiological adaptation of the central nervous system deiodinases to iodine deficiency. *American journal of physiology. Endocrinology and metabolism*. 281:E54-61.

Peeters, R.P., P.J. Wouters, E. Kaptein, H. van Toor, T.J. Visser, and G. Van den Berghe. 2003. Reduced activation and increased inactivation of thyroid hormone in tissues of critically ill patients. *J. Clin. Endocrinol. Metab.* 88:3202-3211.

Peters, J.M., R.C. Cattley, and F.J. Gonzalez. 1997. Role of PPAR alpha in the mechanism of action of the nongenotoxic carcinogen and peroxisome proliferator Wy-14,643. *Carcinogenesis*. 18:2029-2033.

Pogribny, I.P., A. Starlard-Davenport, V.P. Tryndyak, T. Han, S.A. Ross, I. Rusyn, and F.A. Beland. 2010. Difference in expression of hepatic microRNAs miR-29c, miR-34a, miR-155, and miR-200b is associated with strain-specific susceptibility to dietary nonalcoholic steatohepatitis in mice. *Laboratory investigation; a journal of technical methods and pathology*. 90:1437-1446.

Pogribny, I.P., V.P. Tryndyak, A. Boyko, R. Rodriguez-Juarez, F.A. Beland, and O. Kovalchuk. 2007. Induction of microRNAome deregulation in rat liver by long-term tamoxifen exposure. *Mutation research*. 619:30-37.

Polyak, K., Y. Xia, J.L. Zweier, K.W. Kinzler, and B. Vogelstein. 1997. A model for p53-induced apoptosis. *Nature*. 389:300-305.

Ponting, C.P., P.L. Oliver, and W. Reik. 2009. Evolution and functions of long noncoding RNAs. *Cell*. 136:629-641.

Popp, J.A., and R.C. Cattley. 1991. Hepatobiliary System. *In* Handbook of Toxicologic Pathology. W.M. Haschek and C.G. Rousseaux, editors. Academic Press Inc, London. 279-314.

Porter, W.R., M.J. Gudzinowicz, and R.A. Neal. 1979. Thioacetamide-induced hepatic necrosis. II. Pharmacokinetics of thioacetamide and thioacetamide-S-oxide in the rat. *The Journal of pharmacology and experimental therapeutics*. 208:386-391.

Powley, I.R., A. Kondrashov, L.A. Young, H.C. Dobbyn, K. Hill, I.G. Cannell, M. Stoneley, Y.W. Kong, J.A. Cotes, G.C. Smith, R. Wek, C. Hayes, T.W. Gant, K.A. Spriggs, M. Bushell, and A.E. Willis. 2009. Translational reprogramming following UVB irradiation is mediated by DNA-PKcs and allows selective recruitment to the polysomes of mRNAs encoding DNA repair enzymes. *Genes & development*. 23:1207-1220.

Pritchard, C.C., H.H. Cheng, and M. Tewari. 2012. MicroRNA profiling: approaches and considerations. *Nature reviews. Genetics*. 13:358-369.

Qin, J., M.J. Li, P. Wang, N.S. Wong, M.P. Wong, Z. Xia, G.S. Tsao, M.Q. Zhang, and J. Wang. 2013. ProteoMirExpress: inferring microRNA-centered regulatory networks from high throughput proteomic and mRNA expression data. *Molecular & cellular proteomics : MCP*. 12:3379-3387.

Quackenbush, J. 2002. Microarray data normalization and transformation. *Nature genetics*. 32 Suppl:496-501.

Radonic, A., S. Thulke, I.M. Mackay, O. Landt, W. Siegert, and A. Nitsche. 2004. Guideline to reference gene selection for quantitative real-time PCR. *Biochemical and biophysical research communications*. 313:856-862.

Rao, D.D., J.S. Vorhies, N. Senzer, and J. Nemunaitis. 2009. siRNA vs. shRNA: similarities and differences. *Advanced drug delivery reviews*. 61:746-759.

Rao, P.S., R.S. Mangipudy, and H.M. Mehendale. 1997. Tissue injury and repair as parallel and opposing responses to CCl4 hepatotoxicity: a novel dose-response. *Toxicology*. 118:181-193.

Rapicavoli, N.A., K. Qu, J. Zhang, M. Mikhail, R.M. Laberge, and H.Y. Chang. 2013. A mammalian pseudogene lncRNA at the interface of inflammation and anti-inflammatory therapeutics. *eLife*. 2:e00762.

Rathinasamy, K., B. Jindal, J. Asthana, P. Singh, P.V. Balaji, and D. Panda. 2010. Griseofulvin stabilizes microtubule dynamics, activates p53 and inhibits the proliferation of MCF-7 cells synergistically with vinblastine. *BMC cancer*. 10:213.

Rebacz, B., T.O. Larsen, M.H. Clausen, M.H. Ronnest, H. Loffler, A.D. Ho, and A. Kramer. 2007. Identification of griseofulvin as an inhibitor of centrosomal clustering in a phenotype-based screen. *Cancer research*. 67:6342-6350.

Reid, D.W., and C.V. Nicchitta. 2012. Primary role for endoplasmic reticulum-bound ribosomes in cellular translation identified by ribosome profiling. *The Journal of biological chemistry*. 287:5518-5527.

Reisman, D., S. Glaros, and E.A. Thompson. 2009. The SWI/SNF complex and cancer. *Oncogene*. 28:1653-1668.

Reynolds, T.B., R.L. Peters, and S. Yamada. 1971. Chronic active and lupoid hepatitis caused by a laxative, oxyphenisatin. *The New England journal of medicine*. 285:813-820.

Reyns, G.E., K.A. Janssens, J. Buyse, E.R. Kuhn, and V.M. Darras. 2002. Changes in thyroid hormone levels in chicken liver during fasting and refeeding. *Comparative biochemistry and physiology. Part B, Biochemistry & molecular biology*. 132:239-245.

Reznik-Schuller, H.M., and W. Lijinsky. 1983. Methaphenilene, an analogue of the antihistaminic methapyrilene, is a "peroxisome proliferator". *Archives of toxicology*. 52:165-166.

Rhoades, M.W., B.J. Reinhart, L.P. Lim, C.B. Burge, B. Bartel, and D.P. Bartel. 2002. Prediction of plant microRNA targets. *Cell*. 110:513-520.

Richards, W.L., Y. Tsukada, and V.R. Potter. 1982. gamma-Glutamyl transpeptidase and alpha-fetoprotein expression during alpha-naphthylisothiocyanate-induced hepatotoxicity in rats. *Cancer research*. 42:5133-5138.

Rinn, J.L., and H.Y. Chang. 2012. Genome regulation by long noncoding RNAs. *Annual review of biochemistry*. 81:145-166.

Rio, D.C., M. Ares, Jr., G.J. Hannon, and T.W. Nilsen. 2010. Purification of RNA using TRIzol (TRI reagent). *Cold Spring Harbor protocols*. 2010:pdb prot5439.

Ro, S., C. Park, D. Young, K.M. Sanders, and W. Yan. 2007. Tissue-dependent paired expression of miRNAs. *Nucleic acids research*. 35:5944-5953.

Roberts, C.W., and S.H. Orkin. 2004. The SWI/SNF complex--chromatin and cancer. *Nature reviews. Cancer*. 4:133-142.

Robertson, K.D., S. Ait-Si-Ali, T. Yokochi, P.A. Wade, P.L. Jones, and A.P. Wolffe. 2000. DNMT1 forms a complex with Rb, E2F1 and HDAC1 and represses transcription from E2F-responsive promoters. *Nature genetics*. 25:338-342.

Rocchi, P., G. Prodi, S. Grilli, and A.M. Ferreri. 1973. In vivo and in vitro binding of carbon tetrachloride with nucleic acids and proteins in rat and mouse liver. *International journal of cancer. Journal international du cancer*. 11:419-425.

Roeder, R.G., and W.J. Rutter. 1969. Multiple forms of DNA-dependent RNA polymerase in eukaryotic organisms. *Nature*. 224:234-237.

Rong, H., T.B. Liu, K.J. Yang, H.C. Yang, D.H. Wu, C.P. Liao, F. Hong, H.Z. Yang, F. Wan, X.Y. Ye, D. Xu, X. Zhang, C.A. Chao, and Q.J. Shen. 2011. MicroRNA-134 plasma levels before and after treatment for bipolar mania. *Journal of psychiatric research*. 45:92-95.

Roques, B.B., J. Leghait, M.Z. Lacroix, F. Lasserre, T. Pineau, C. Viguie, and P.G. Martin. 2013. The nuclear receptors pregnane X receptor and constitutive androstane receptor contribute to the impact of fipronil on hepatic gene expression linked to thyroid hormone metabolism. *Biochemical pharmacology*. 86:997-1039.

Roth, C., B. Rack, V. Muller, W. Janni, K. Pantel, and H. Schwarzenbach. 2010. Circulating microRNAs as blood-based markers for patients with primary and metastatic breast cancer. *Breast cancer research : BCR*. 12:R90.

Ruepp, S.U., R.P. Tonge, J. Shaw, N. Wallis, and F. Pognan. 2002. Genomics and proteomics analysis of acetaminophen toxicity in mouse liver. *Toxicological sciences : an official journal of the Society of Toxicology*. 65:135-150.

Russell, R.I., J.G. Allan, and R. Patrick. 1973. Active chronic hepatitis after chlorpromazine ingestion. *British medical journal*. 1:655-656.

Sah, S., M.N. McCall, D. Eveleigh, M. Wilson, and R.A. Irizarry. 2010. Performance evaluation of commercial miRNA expression array platforms. *BMC research notes*. 3:80.

Saini, P., D.E. Eyler, R. Green, and T.E. Dever. 2009. Hypusine-containing protein eIF5A promotes translation elongation. *Nature*. 459:118-121.

Sakamoto, K.M. 2002. Ubiquitin-dependent proteolysis: its role in human diseases and the design of therapeutic strategies. *Molecular genetics and metabolism*. 77:44-56.

Salditt-Georgieff, M., M. Harpold, S. Chen-Kiang, and J.E. Darnell, Jr. 1980. The addition of 5' cap structures occurs early in hnRNA synthesis and prematurely terminated molecules are capped. *Cell*. 19:69-78.

Saw, D., E. Pitman, M. Maung, P. Savasatit, D. Wasserman, and C.K. Yeung. 1996. Granulomatous hepatitis associated with glyburide. *Digestive diseases and sciences*. 41:322-325.

Schena, M., D. Shalon, R.W. Davis, and P.O. Brown. 1995. Quantitative monitoring of gene expression patterns with a complementary DNA microarray. *Science (New York, N.Y.)*. 270:467-470.

Schnabl, B., Y.O. Kweon, J.P. Frederick, X.F. Wang, R.A. Rippe, and D.A. Brenner. 2001. The role of Smad3 in mediating mouse hepatic stellate cell activation. *Hepatology (Baltimore, Md.)*. 34:89-100.

Schulze-Krebs, A., D. Preimel, Y. Popov, R. Bartenschlager, V. Lohmann, M. Pinzani, and D. Schuppan. 2005. Hepatitis C virus-replicating hepatocytes induce fibrogenic activation of hepatic stellate cells. *Gastroenterology*. 129:246-258.

Schwanhausser, B., D. Busse, N. Li, G. Dittmar, J. Schuchhardt, J. Wolf, W. Chen, and M. Selbach. 2011. Global quantification of mammalian gene expression control. *Nature*. 473:337-342.

Scornik, O.A. 1973. Improved sucrose gradient analysis of mouse liver polyribosomes. *Analytical biochemistry*. 52:56-62.

Seggerson, K., L. Tang, and E.G. Moss. 2002. Two genetic circuits repress the Caenorhabditis elegans heterochronic gene lin-28 after translation initiation. *Developmental biology*. 243:215-225.

Selkoe, D.J. 2003. Folding proteins in fatal ways. *Nature*. 426:900-904.

Shahbazian, M.D., and M. Grunstein. 2007. Functions of site-specific histone acetylation and deacetylation. *Annual review of biochemistry*. 76:75-100.

Shan, S.W., L. Fang, T. Shatseva, Z.J. Rutnam, X. Yang, W. Du, W.Y. Lu, J.W. Xuan, Z. Deng, and B.B. Yang. 2013. Mature miR-17-5p and passenger miR-17-3p induce hepatocellular carcinoma by targeting PTEN, GalNT7 and vimentin in different signal pathways. *Journal of cell science*. 126:1517-1530.

Shatkin, A.J. 1976. Capping of eucaryotic mRNAs. *Cell*. 9:645-653.

Shatkin, A.J., A.K. Banerjee, G.W. Both, Y. Furuichi, and S. Muthukrishnan. 1976. Dependence of translation on 5'-terminal methylation of mRNA. *Federation proceedings*. 35:2214-2217.

Shin, S.M., J.H. Yang, and S.H. Ki. 2013. Role of the Nrf2-ARE pathway in liver diseases. *Oxidative medicine and cellular longevity*. 2013:763257.

Shirai, M., S. Arakawa, H. Miida, T. Matsuyama, J. Kinoshita, T. Makino, K. Kai, and M. Teranishi. 2013. Thioacetamide-induced Hepatocellular Necrosis Is Attenuated in Diet-induced Obese Mice. *Journal of toxicologic pathology*. 26:175-186.

Shukla, G.C., J. Singh, and S. Barik. 2011a. MicroRNAs: Processing, Maturation, Target Recognition and Regulatory Functions. *Molecular and cellular pharmacology*. 3:83-92.

Shukla, P.K., L.J. Sittig, T.M. Ullmann, and E.E. Redei. 2011b. Candidate placental biomarkers for intrauterine alcohol exposure. *Alcohol Clin Exp Res*. 35:559-565.

Simonides, W.S., M.A. Mulcahey, E.M. Redout, A. Muller, M.J. Zuidwijk, T.J. Visser, F.W. Wassen, A. Crescenzi, W.S. da-Silva, J. Harney, F.B. Engel, M.J. Obregon, P.R. Larsen, A.C. Bianco, and S.A. Huang. 2008. Hypoxia-inducible factor induces local thyroid hormone inactivation during hypoxic-ischemic disease in rats. *J Clin Invest*. 118:975-983.

Simonides, W.S., and C. van Hardeveld. 2008. Thyroid hormone as a determinant of metabolic and contractile phenotype of skeletal muscle. *Thyroid*. 18:205-216.

Sittig, L.J., P.K. Shukla, L.B. Herzing, and E.E. Redei. 2011. Strain-specific vulnerability to alcohol exposure in utero via hippocampal parent-of-origin expression of deiodinase-III. *FASEB J.* 25:2313-2324.

Skenderi, K.P., S.A. Kavouras, C.A. Anastasiou, N. Yiannakouris, and A.L. Matalas. 2006. Exertional Rhabdomyolysis during a 246-km continuous running race. *Medicine and science in sports and exercise*. 38:1054-1057.

Skog, J., T. Wurdinger, S. van Rijn, D.H. Meijer, L. Gainche, M. Sena-Esteves, W.T. Curry, Jr., B.S. Carter, A.M. Krichevsky, and X.O. Breakefield. 2008. Glioblastoma microvesicles transport RNA and proteins that promote tumour growth and provide diagnostic biomarkers. *Nature cell biology*. 10:1470-1476.

Smirnova, J.B., J.N. Selley, F. Sanchez-Cabo, K. Carroll, A.A. Eddy, J.E. McCarthy, S.J. Hubbard, G.D. Pavitt, C.M. Grant, and M.P. Ashe. 2005. Global gene expression profiling reveals widespread yet distinctive translational responses to different eukaryotic translation initiation factor 2B-targeting stress pathways. *Molecular and cellular biology*. 25:9340-9349.

Snow, K.L., and R.H. Moseley. 2007. Effect of thiazolidinediones on bile acid transport in rat liver. *Life sciences*. 80:732-740.

Sonenberg, N., and A.G. Hinnebusch. 2009. Regulation of translation initiation in eukaryotes: mechanisms and biological targets. *Cell*. 136:731-745.

Song, B., Y. Wang, K. Kudo, E.J. Gavin, Y. Xi, and J. Ju. 2008. miR-192 Regulates dihydrofolate reductase and cellular proliferation through the p53-microRNA circuit. *Clinical cancer research : an official journal of the American Association for Cancer Research*. 14:8080-8086.

Spriggs, K.A., M. Bushell, and A.E. Willis. 2010. Translational regulation of gene expression during conditions of cell stress. *Molecular cell*. 40:228-237.

Spriggs, K.A., M. Stoneley, M. Bushell, and A.E. Willis. 2008. Re-programming of translation following cell stress allows IRES-mediated translation to predominate. *Biology of the cell / under the auspices of the European Cell Biology Organization*. 100:27-38.

St Germain, D.L., R.A. Schwartzman, W. Croteau, A. Kanamori, Z. Wang, D.D. Brown, and V.A. Galton. 1994. A thyroid hormone-regulated gene in Xenopus laevis encodes a type III iodothyronine 5-deiodinase. *Proc Natl Acad Sci U S A*. 91:11282.

Stachulski, A.V., T.A. Baillie, B.K. Park, R.S. Obach, D.K. Dalvie, D.P. Williams, A. Srivastava, S.L. Regan, D.J. Antoine, C.E. Goldring, A.J. Chia, N.R. Kitteringham, L.E. Randle, H. Callan, J.L. Castrejon, J. Farrell, D.J. Naisbitt, and M.S. Lennard. 2013. The generation, detection, and effects of reactive drug metabolites. *Medicinal research reviews*. 33:985-1080.

Starkey Lewis, P.J., J. Dear, V. Platt, K.J. Simpson, D.G. Craig, D.J. Antoine, N.S. French, N. Dhaun, D.J. Webb, E.M. Costello, J.P. Neoptolemos, J. Moggs, C.E. Goldring, and B.K. Park. 2011. Circulating microRNAs as potential markers of human drug-induced liver injury. *Hepatology (Baltimore, Md.)*. 54:1767-1776.

Starkey Lewis, P.J., M. Merz, P. Couttet, O. Grenet, J. Dear, D.J. Antoine, C. Goldring, B.K. Park, and J.G. Moggs. 2012. Serum microRNA biomarkers for drug-induced liver injury. *Clinical pharmacology and therapeutics*. 92:291-293.

Stefani, M., and S. Rigacci. 2013. Protein folding and aggregation into amyloid: the interference by natural phenolic compounds. *International journal of molecular sciences*. 14:12411-12457.

Steinsapir, J., A.C. Bianco, C. Buettner, J. Harney, and P.R. Larsen. 2000. Substrate-induced down-regulation of human type 2 deiodinase (hD2) is mediated through proteasomal degradation and requires interaction with the enzyme's active center. *Endocrinology*. 141:1127-1135.

Steinsapir, J., J. Harney, and P.R. Larsen. 1998. Type 2 iodothyronine deiodinase in rat pituitary tumor cells is inactivated in proteasomes. *J. Clin. Invest.* 102:1895-1899.

Stejskal, R., M. Itabashi, J. Stanek, and Z. Hruban. 1975. Experimental porphyria induced by 3-(2,4,6-trimethylphenyl)-thioethyl)-4 methylsydnone. *Virchows Archiv. B: Cell pathology*. 18:83-100.

Sterner, D.E., and S.L. Berger. 2000. Acetylation of histones and transcription-related factors. *Microbiology and molecular biology reviews : MMBR*. 64:435-459.

Su, Y.W., X. Chen, Z.Z. Jiang, T. Wang, C. Wang, Y. Zhang, J. Wen, M. Xue, D. Zhu, Y.J. Su, T.Y. Xing, C.Y. Zhang, and L.Y. Zhang. 2012. A panel of serum microRNAs as specific biomarkers for diagnosis of compound- and herb-induced liver injury in rats. *PloS one*. 7:e37395.

Suematsu, M., and S. Aiso. 2001. Professor Toshio Ito: a clairvoyant in pericyte biology. *The Keio journal of medicine*. 50:66-71.

Sukata, T., K. Sumida, M. Kushida, K. Ogata, K. Miyata, S. Yabushita, and S. Uwagawa. 2011. Circulating microRNAs, possible indicators of progress of rat hepatocarcinogenesis from early stages. *Toxicology letters*. 200:46-52.

Suter, L., S. Schroeder, K. Meyer, J.C. Gautier, A. Amberg, M. Wendt, H. Gmuender, A. Mally, E. Boitier, H. Ellinger-Ziegelbauer, K. Matheis, and F. Pfannkuch. 2011. EU framework 6

project: predictive toxicology (PredTox)--overview and outcome. *Toxicology and applied pharmacology*. 252:73-84.

Suzuki, M., and J.M. Greally. 2013. Genome-wide DNA methylation analysis using massively parallel sequencing technologies. *Seminars in hematology*. 50:70-77.

Taylor, E.L., and T.W. Gant. 2008. Emerging fundamental roles for non-coding RNA species in toxicology. *Toxicology*. 246:34-39.

Thomas, J.D., and G.J. Johannes. 2007. Identification of mRNAs that continue to associate with polysomes during hypoxia. *RNA (New York, N.Y.)*. 13:1116-1131.

Thomas, M.C., and C.M. Chiang. 2006. The general transcription machinery and general cofactors. *Critical reviews in biochemistry and molecular biology*. 41:105-178.

Tibbetts, R.S., D. Cortez, K.M. Brumbaugh, R. Scully, D. Livingston, S.J. Elledge, and R.T. Abraham. 2000. Functional interactions between BRCA1 and the checkpoint kinase ATR during genotoxic stress. *Genes & development*. 14:2989-3002.

Tikhanovich, I., J. Cox, and S.A. Weinman. 2013. Forkhead box class O transcription factors in liver function and disease. *Journal of gastroenterology and hepatology*. 28 Suppl 1:125-131.

Tonder, M., A. Nordoy, and Elgjo. 1974. Sulfonamide-induced chronic liver disease. *Scandinavian journal of gastroenterology*. 9:93-96.

Trotta, M.D., D.M. Cajaiba, O.M. Parra, M.L. Dagli, and F.J. Hernandez-Blazquez. 2013. Parenteral Solution of Nutritional Hepatotrophic Factors Improves Regeneration in Thioacetamide-induced Cirrhotic Livers after Partial Hepatectomy. *Toxicologic pathology*.

Tsai, M.C., R.C. Spitale, and H.Y. Chang. 2011. Long intergenic noncoding RNAs: new links in cancer progression. *Cancer research*. 71:3-7.

Tsai, N.P., Y.L. Lin, and L.N. Wei. 2009. MicroRNA mir-346 targets the 5'-untranslated region of receptor-interacting protein 140 (RIP140) mRNA and up-regulates its protein expression. *The Biochemical journal*. 424:411-418.

Tsui, N.B., E.K. Ng, and Y.M. Lo. 2002. Stability of endogenous and added RNA in blood specimens, serum, and plasma. *Clinical chemistry*. 48:1647-1653.

Turchinovich, A., T.R. Samatov, A.G. Tonevitsky, and B. Burwinkel. 2013. Circulating miRNAs: cell-cell communication function? *Frontiers in genetics*. 4:119.

Turchinovich, A., L. Weiz, A. Langheinz, and B. Burwinkel. 2011. Characterization of extracellular circulating microRNA. *Nucleic acids research*. 39:7223-7233.

Valadi, H., K. Ekstrom, A. Bossios, M. Sjostrand, J.J. Lee, and J.O. Lotvall. 2007. Exosome-mediated transfer of mRNAs and microRNAs is a novel mechanism of genetic exchange between cells. *Nature cell biology*. 9:654-659.

Van der Geyten, S., N. Buys, J.P. Sanders, E. Decuypere, T.J. Visser, E.R. Kuhn, and V.M. Darras. 1999. Acute pretranslational regulation of type III iodothyronine deiodinase by growth hormone and dexamethasone in chicken embryos. *Mol. Cell. Endocrinol.* 147:49-56.

Vasudevan, S., Y. Tong, and J.A. Steitz. 2007. Switching from repression to activation: microRNAs can up-regulate translation. *Science (New York, N.Y.)*. 318:1931-1934.

Vernon, G., A. Baranova, and Z.M. Younossi. 2011. Systematic review: the epidemiology and natural history of non-alcoholic fatty liver disease and non-alcoholic steatohepatitis in adults. *Alimentary pharmacology & therapeutics*. 34:274-285.

Vyas, K., S. Chaudhuri, D.W. Leaman, A.A. Komar, A. Musiyenko, S. Barik, and B. Mazumder. 2009. Genome-wide polysome profiling reveals an inflammation-responsive posttranscriptional operon in gamma interferon-activated monocytes. *Molecular and cellular biology*. 29:458-470.

Wahl, M.C., C.L. Will, and R. Luhrmann. 2009. The spliceosome: design principles of a dynamic RNP machine. *Cell*. 136:701-718.

Walker, R.M., Z.W. Wojcinski, A.H. Hofstra, L.M. King, J.E. Rogers, K.W. Baker, P.K. Chang, and G.S. Smith. 1996. Hepatotumorigenicity and peroxisome proliferation induced by the

hypolipidemic CI-924 in a two-year study in male and female B6C3F1 mice. *Toxicologic pathology*. 24:265-272.

Walsh, K.M., and C.E. Rothwell. 1999. Hepatic effects in beagle dogs administered atorvastatin, a 3-hydroxy-3-methylglutaryl coenzyme A reductase inhibitor, for 2 years. *Toxicologic pathology*. 27:395-401.

Wang, B. 2013. Base Composition Characteristics of Mammalian miRNAs. *Journal of nucleic acids*. 2013:951570.

Wang, K., H. Li, Y. Yuan, A. Etheridge, Y. Zhou, D. Huang, P. Wilmes, and D. Galas. 2012a. The complex exogenous RNA spectra in human plasma: an interface with human gut biota? *PloS one*. 7:e51009.

Wang, K., S. Zhang, B. Marzolf, P. Troisch, A. Brightman, Z. Hu, L.E. Hood, and D.J. Galas. 2009. Circulating microRNAs, potential biomarkers for drug-induced liver injury. *Proceedings of the National Academy of Sciences of the United States of America*. 106:4402-4407.

Wang, K.C., L.X. Garmire, A. Young, P. Nguyen, A. Trinh, S. Subramaniam, N. Wang, J.Y. Shyy, Y.S. Li, and S. Chien. 2010. Role of microRNA-23b in flow-regulation of Rb phosphorylation and endothelial cell growth. *Proceedings of the National Academy of Sciences of the United States of America*. 107:3234-3239.

Wang, Q., Z. Huang, S. Ni, X. Xiao, Q. Xu, L. Wang, D. Huang, C. Tan, W. Sheng, and X. Du. 2012b. Plasma miR-601 and miR-760 are novel biomarkers for the early detection of colorectal cancer. *PloS one*. 7:e44398.

Wang, X. 2008. miRDB: a microRNA target prediction and functional annotation database with a wiki interface. *RNA (New York, N.Y.)*. 14:1012-1017.

Wang, X., and I.M. El Naqa. 2008. Prediction of both conserved and nonconserved microRNA targets in animals. *Bioinformatics (Oxford, England)*. 24:325-332.

Wang, X.W., N.H. Heegaard, and H. Orum. 2012c. MicroRNAs in liver disease. *Gastroenterology*. 142:1431-1443.

Wang, Y., J. Li, X. Wang, M. Sang, and W. Ho. 2013a. Hepatic stellate cells, liver innate immunity, and hepatitis C virus. *Journal of gastroenterology and hepatology*. 28 Suppl 1:112-115.

Wang, Y., N. Tang, T. Hui, S. Wang, X. Zeng, H. Li, and J. Ma. 2013b. Identification of endogenous reference genes for RT-qPCR analysis of plasma microRNAs levels in rats with acetaminophen-induced hepatotoxicity. *Journal of applied toxicology : JAT*.

Wark, A.W., H.J. Lee, and R.M. Corn. 2008. Multiplexed detection methods for profiling microRNA expression in biological samples. *Angewandte Chemie (International ed. in English)*. 47:644-652.

Warner, J.R., M. Girard, H. Latham, and J.E. Darnell. 1966. Ribosome formation in HeLa cells in the absence of protein synthesis. *Journal of molecular biology*. 19:373-382.

Wassen, F.W., A.E. Schiel, G.G. Kuiper, E. Kaptein, O. Bakker, T.J. Visser, and W.S. Simonides. 2002. Induction of thyroid hormone-degrading deiodinase in cardiac hypertrophy and failure. *Endocrinology*. 143:2812-2815.

Watanabe, Y., M. Tomita, and A. Kanai. 2007. Computational methods for microRNA target prediction. *Methods in enzymology*. 427:65-86.

Weber, B., C. Stresemann, B. Brueckner, and F. Lyko. 2007. Methylation of human microRNA genes in normal and neoplastic cells. *Cell cycle (Georgetown, Tex.)*. 6:1001-1005.

Weber, J.A., D.H. Baxter, S. Zhang, D.Y. Huang, K.H. Huang, M.J. Lee, D.J. Galas, and K. Wang. 2010. The microRNA spectrum in 12 body fluids. *Clinical chemistry*. 56:1733-1741.

Weibel, E.R., W. Staubli, H.R. Gnagi, and F.A. Hess. 1969. Correlated morphometric and biochemical studies on the liver cell. I. Morphometric model, stereologic methods, and normal morphometric data for rat liver. *The Journal of cell biology*. 42:68-91.

Wells, S.E., P.E. Hillner, R.D. Vale, and A.B. Sachs. 1998. Circularization of mRNA by eukaryotic translation initiation factors. *Molecular cell*. 2:135-140.

West, A.G., and P. Fraser. 2005. Remote control of gene transcription. *Human molecular genetics*. 14 Spec No 1:R101-111.

WHO. 1972. International drug monitoring: the role of national centres. Report of a WHO meeting. *World Health Organization technical report series*. 498:1-25.

Wightman, B., I. Ha, and G. Ruvkun. 1993. Posttranscriptional regulation of the heterochronic gene lin-14 by lin-4 mediates temporal pattern formation in C. elegans. *Cell*. 75:855-862.

Williams, D.P. 2006. Toxicophores: investigations in drug safety. *Toxicology*. 226:1-11.

Williams, D.P., C. Garcia-Allan, G. Hanton, J.L. LeNet, J.P. Provost, P. Brain, R. Walsh, G.I. Johnston, D.A. Smith, and B.K. Park. 2004. Time course toxicogenomic profiles in CD-1 mice after nontoxic and nonlethal hepatotoxic paracetamol administration. *Chemical research in toxicology*. 17:1551-1561.

Wong, T.S., X.B. Liu, B.Y. Wong, R.W. Ng, A.P. Yuen, and W.I. Wei. 2008. Mature miR-184 as Potential Oncogenic microRNA of Squamous Cell Carcinoma of Tongue. *Clinical cancer research : an official journal of the American Association for Cancer Research*. 14:2588-2592.

Xia, J., C.E. Joyce, A.M. Bowcock, and W. Zhang. 2013. Noncanonical microRNAs and endogenous siRNAs in normal and psoriatic human skin. *Human molecular genetics*. 22:737-748.

Xu, X., K. Zhu, F. Liu, Y. Wang, J. Shen, J. Jin, Z. Wang, L. Chen, J. Li, and M. Xu. 2013. Identification of somatic mutations in human prostate cancer by RNA-Seq. *Gene*. 519:343-347.

Yamada, H., K. Suzuki, N. Ichino, Y. Ando, A. Sawada, K. Osakabe, K. Sugimoto, K. Ohashi, R. Teradaira, T. Inoue, N. Hamajima, and S. Hashimoto. 2013. Associations between circulating microRNAs (miR-21, miR-34a, miR-122 and miR-451) and non-alcoholic fatty liver. *Clinica chimica acta; international journal of clinical chemistry*. 424C:99-103.

Yang, X., W.W. Du, H. Li, F. Liu, A. Khorshidi, Z.J. Rutnam, and B.B. Yang. 2013. Both mature miR-17-5p and passenger strand miR-17-3p target TIMP3 and induce prostate tumor growth and invasion. *Nucleic acids research*. 41:9688-9704.

Yang, X., J. Greenhaw, Q. Shi, Z. Su, F. Qian, K. Davis, D.L. Mendrick, and W.F. Salminen. 2012. Identification of urinary microRNA profiles in rats that may diagnose hepatotoxicity. *Toxicological sciences : an official journal of the Society of Toxicology*. 125:335-344.

Yang, Y.H., S. Dudoit, P. Luu, D.M. Lin, V. Peng, J. Ngai, and T.P. Speed. 2002. Normalization for cDNA microarray data: a robust composite method addressing single and multiple slide systematic variation. *Nucleic acids research*. 30:e15.

Yin, S., H. Wang, O. Park, W. Wei, J. Shen, and B. Gao. 2011. Enhanced liver regeneration in IL-10-deficient mice after partial hepatectomy via stimulating inflammatory response and activating hepatocyte STAT3. *The American journal of pathology*. 178:1614-1621.

Young, A.M., K.M. Archibald, L.A. Tookman, A. Pool, K. Dudek, C. Jones, S.L. Williams, K.J. Pirlo, A.E. Willis, M. Lockley, and I.A. McNeish. 2012. Failure of translation of human adenovirus mRNA in murine cancer cells can be partially overcome by L4-100K expression in vitro and in vivo. *Molecular therapy : the journal of the American Society of Gene Therapy*. 20:1676-1688.

Zafra-Ceres, M., T. de Haro, E. Farez-Vidal, I. Blancas, F. Bandres, E.M. de Duenas, E. Ochoa-Aranda, J.A. Gomez-Capilla, and C. Gomez-Llorente. 2013. Influence of CYP2D6 polymorphisms on serum levels of tamoxifen metabolites in Spanish women with breast cancer. *International journal of medical sciences*. 10:932-937.

Zampetaki, A., and M. Mayr. 2012. Analytical challenges and technical limitations in assessing circulating miRNAs. *Thrombosis and haemostasis*. 108:592-598.

Zatloukal, K., S.W. French, C. Stumptner, P. Strnad, M. Harada, D.M. Toivola, M. Cadrin, and M.B. Omary. 2007. From Mallory to Mallory-Denk bodies: what, how and why? *Experimental cell research*. 313:2033-2049.

Zen, K., and C.Y. Zhang. 2012. Circulating microRNAs: a novel class of biomarkers to diagnose and monitor human cancers. *Medicinal research reviews*. 32:326-348.

Zhang, B., S. Kirov, and J. Snoddy. 2005. WebGestalt: an integrated system for exploring gene sets in various biological contexts. *Nucleic acids research*. 33:W741-748.

Zhang, B., and X. Pan. 2009. RDX induces aberrant expression of microRNAs in mouse brain and liver. *Environmental health perspectives*. 117:231-240.

Zhang, B., X. Pan, G.P. Cobb, and T.A. Anderson. 2007. microRNAs as oncogenes and tumor suppressors. *Developmental biology*. 302:1-12.

Zhang, L., D. Hou, X. Chen, D. Li, L. Zhu, Y. Zhang, J. Li, Z. Bian, X. Liang, X. Cai, Y. Yin, C. Wang, T. Zhang, D. Zhu, D. Zhang, J. Xu, Q. Chen, Y. Ba, J. Liu, Q. Wang, J. Chen, J. Wang, M. Wang, Q. Zhang, J. Zhang, K. Zen, and C.Y. Zhang. 2012. Exogenous plant MIR168a specifically targets mammalian LDLRAP1: evidence of cross-kingdom regulation by microRNA. *Cell research*. 22:107-126.

Zhang, S.D. 2011. Towards accurate estimation of the proportion of true null hypotheses in multiple testing. *PloS one*. 6:e18874.

Zhang, S.D., and T.W. Gant. 2004. A statistical framework for the design of microarray experiments and effective detection of differential gene expression. *Bioinformatics (Oxford, England)*. 20:2821-2828.

Zhang, Y., Y. Jia, R. Zheng, Y. Guo, Y. Wang, H. Guo, M. Fei, and S. Sun. 2010. Plasma microRNA-122 as a biomarker for viral-, alcohol-, and chemical-related hepatic diseases. *Clinical chemistry*. 56:1830-1838.

Zhou, S.F. 2009. Polymorphism of human cytochrome P450 2D6 and its clinical significance: Part I. *Clinical pharmacokinetics*. 48:689-723.

Zhou, W., J.J. Ryan, and H. Zhou. 2004. Global analyses of sumoylated proteins in Saccharomyces cerevisiae. Induction of protein sumoylation by cellular stresses. *The Journal of biological chemistry*. 279:32262-32268.

Zhouravleva, G., L. Frolova, X. Le Goff, R. Le Guellec, S. Inge-Vechtomov, L. Kisselev, and M. Philippe. 1995. Termination of translation in eukaryotes is governed by two interacting polypeptide chain release factors, eRF1 and eRF3. *The EMBO journal*. 14:4065-4072.

Zhu, R., Y. Wang, L. Zhang, and Q. Guo. 2012. Oxidative stress and liver disease. *Hepatology research : the official journal of the Japan Society of Hepatology*. 42:741-749.